Identification of organophosphorus simulants for the development of next-generation detection technologies

Rebecca J. Ellaby,[a] Ewan R. Clark,*[a] Nyasha Allen,[b] Faith R. Taylor,[a] Kendrick K. L. Ng,[a] Dominique F. Chu,[c] Milan Dimitrovski,[a] Daniel P. Mulvihill [b] and Jennifer R. Hiscock *[a]

[a.] *School of Physical Sciences, University of Kent, Park Wood Road, Canterbury, Kent, CT2 7NH, UK. E-mail: J.R.Hiscock@Kent.ac.uk; Tel: +44(0) 1227 816467. E-mail: J.R.Hiscock@Kent.ac.uk; Tel: +44(0) 1227 816467. E-mail: E.R.Clark@Kent.ac.uk; Tel: +44(0) 1227 816152.*
[b.] *School of Biosciences, University of Kent, Park Wood Road, Canterbury, Kent, CT2 7NH, UK.*
[c.] *School of Computing, University of Kent, Darwin Road, Canterbury, CT2 7NF.*

Table of contents

Chemical structures

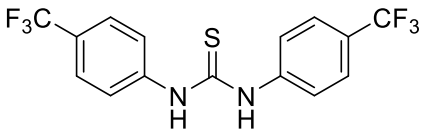

1

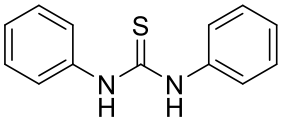

2

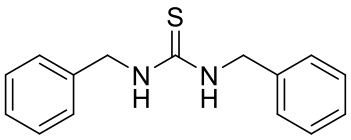

3

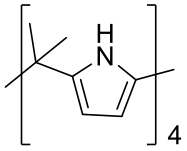

4

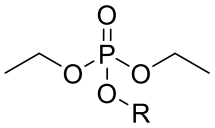

5 R = a; **6** R = b
7 R = c; **8** R = d
9 R = e; **10** R = f

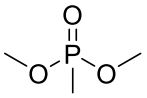

11
(DMMP)

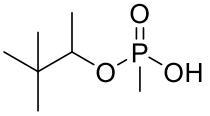

12
(PMP)

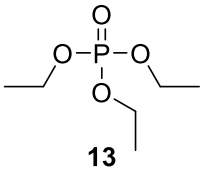

13
(TEP)

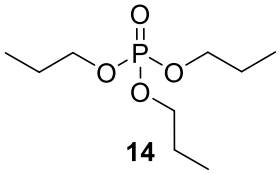

14
(TnPP)

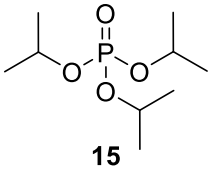

15
(TiPP)

R Group

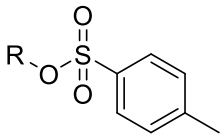

16 R = b; **17** R = c
18 R = d; **19** R = e
20 R = f

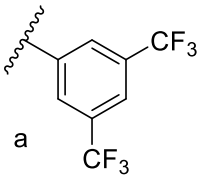

a

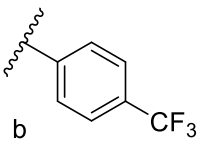

b

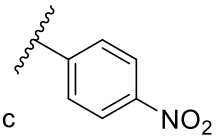

c

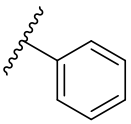

d

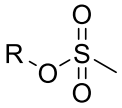

21 R = a; **22** R = b
23 R = c; **24** R = d
25 R = e; **26** R = f

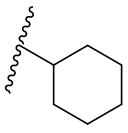

e

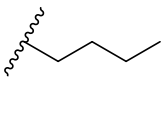

f

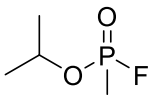

sarin

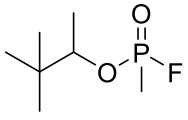

soman

Experimental

General remarks: All reactions were performed under slight positive pressure of nitrogen using oven dried glassware. NMR spectra were determined using a Bruker AV II or NEO 400 MHz spectrometer with chemical shifts reported in parts per million (ppm) and calibrated to the centre of the solvent peak set. Herein: br = broad; s = singlet; d = doublet; t = triplet; q = quartet, sept = septet and; m = multiplet. All solvents and starting materials were purchased from commercial sources or chemical stores where available and, used as purchased unless stated otherwise. High resolution mass spectra were collected using a Bruker microTOF-Q mass spectrometer or a SYNAPT G2-S Mass Spectrometer. Infrared spectra were recorded on a Shimadzu IR-Affinity 1 and reported in wavenumbers (cm^{-1}). The melting point for each compound was determined using Stuart SMP10 melting point apparatus. *Schizosaccharomyces pombe* screening was carried out using 96 well plates and the Thermo Scientific™, Multiskan™ GO Microplate Spectrophotometer or CLARIOstar high performance plate reader with optical density reading taken at 600 nm every 15 minutes for 45 hours. A Neubauer Improved Bright-Line Cell Counting Chamber Hemocytometer was used in all cell density measurements. Tensiometry measurements were undertaken using the Biolin Scientific Theta Attension optical tensiometer.

Proton NMR titration method: Firstly, a solution of receptor **1-4** (1.5 mL, 0.01 M) was prepared. Of this solution 0.5 mL was placed in an NMR tube. The remaining 1 mL of the receptor solution was used to prepare a 0.15 M solution of the guest (**5-26**). The guest-receptor stock solution was titrated into the NMR tube and a ^{1}H NMR taken before/after each addition of the stock solution.

Association constant determination: All association constants were calculated using Bindfit v0.5 (http://app.supramolecular.org/bindfit/). All data relating to the calculation of the association constants can be accessed online, through the links given for each association event.

Job Plot analysis method: Two solutions were produced; the first solution was a 3 mL, 0.01 M solution of the receptor and the second was a 3 mL, 0.01 M solution of the simulant. Of the receptor solution 0.5 mL was added to a NMR tube. The amount of receptor solution was then decreased by 0.05 mL and the amount of simulant solution increased by 0.05 mL for each successive NMR tubes until a 9:1 simulant:receptor ratio was reached. A ^{1}H NMR spectra was taken for each of the ten NMR tubes and calibrated to the solvent peak. The data was then used to produce a job plot, in accordance with the methods described by Job.[1]

Experimental for compounds 1-26

Compound 1: A solution of 4-(trifluoromethyl)phenyl isothiocyanate (1.57 g, 7.16 mmol) and 4-(trifluoromethyl)aniline (0.90 mL, 7.16 mmol) in pyridine (4 mL) was stirred at room temperature overnight. The pyridine solution was then added to water (30 mL) to precipitate a white solid. This solid was collected by filtration and washed with water and then dried to give the final product as a white solid (1.92 g, 5.26 mmol) in a yield of 73.5 %. ^{1}H NMR: (400 MHz, 298 K, DMSO-d_6): δ: 7.72 (dd, J_1= 8.80 Hz, J_2 = 16.40 Hz, 8H), 10.37 (s, 2NH).

This compound has been previously synthesised by Gale and co-workers.[1] The ^{1}H NMR data provided was found to match these previously published data.

Compound 2: A solution of phenyl isothiocyanate (1.45 g, 10.74 mmol) and aniline (0.98 mL, 10.74 mmol) in pyridine (4 mL) was stirred at room temperature overnight. The pyridine solution was then added to water (30 mL) to precipitate a white solid. This solid was collected by filtration and washed with water and dried to give the final product as a white solid (2.07 g, 9.06 mmol) in a yield of 84.4 %. ^{1}H NMR: (400 MHz, 298 K, DMSO-d_6): δ: 7.12 (t, J = 7.40 Hz, 2H), 7.33 (t, J_1 = 8.28 Hz , 4H), 7.47 (d, J = 7.52 Hz, 4H), 9.80 (s, 2NH).

This compound has been previously synthesised by Gale and co-workers.[1] The ^{1}H NMR data provided was found to match these previously published data.

Compound 3: A solution of benzyl isothiocyanate (1.24 mL, 9.33 mmol) and benzylamine (1 mL, 9.33 mmol) in pyridine (4 mL) was stirred at room temperature overnight. The pyridine solution was then added to water (30 mL) to precipitate a white solid. The white solid was then collected by filtration and washed with water and dried to give the pure product (1.74 g, 6.79 mmol) in a yield of 72.8 %. ^{1}H NMR: (400 MHz, 298 K, $CDCl_3$): δ: 4.66 (s, 4H), 7.25-7.34 (m, 12H).^{1}H NMR: (400 MHz, 298 K, CD_3CN): δ: 4.69 (br s, 2H), 6.77 (br s, 2NH), 7.24-7.35 (m, 10H).

This compound has been previously synthesised by Lui and co-workers.[2] The ^{1}H NMR data provided was found to match previously these published data. Proton NMR was also obtained in CD_3CN (Figure S4) to allow accurate integration.

Compound 4: Acetone (5.00 mL, 67.15 mmol) was added to pyrrole (1.00 mL, 14.04 mmol), followed with a few drops of HCl. The solution was left to stir for 30 minutes. A yellow precipitate formed which was collected by filtration, washed with methanol and then dried to give the final product as a white solid (0.858 g, 2.00 mmol) in a yield of 57.1 %. ^{1}H NMR: (400 MHz, 298 K, $CDCl_3$): δ: 7.00 (s, 4NH), 5.90 (d, J = 2.72 Hz, 8H), 1.51 (s, 24H).

This compound has been previously synthesised by Chauhan and co-workers.[3] The ^{1}H NMR data provided was found to match these previously published data.

Compound 5: Diethyl chlorophosphate (0.45 mL, 3.08 mmol) was added to a stirring solution of 3,5-(trifluoromethyl)phenol (0.47 mL, 3.08 mmol) and triethylamine (0.43 mL, 3.08 mmol) in chloroform (10 mL). The mixture was then allowed to stir at room temperature overnight. The organic phase was then washed with an aqueous 0.3M NaOH solution (30 mL). The organic layer was then taken to dryness to give this final product as a colourless oil (0.73 g, 2.00 mmol) with a yield of 64.9 %. ^{1}H{^{31}P} NMR: (400 MHz, 298 K, $CDCl_3$): δ: 1.32 (t, J= 7.08 Hz, 6H), 4.22 (q, J = 7.12 Hz, 4H), 7.64 (br s, 3H); ^{13}C{^{1}H} NMR: (100 MHz, 298 K, $CDCl_3$): δ: 16.0 (d, J = 6.49 Hz, CH_3), 65.3 (d, J = 6.12 Hz, CH_2), 118.7 (sept, J = 3.61 Hz, ArCH), 120.8 (m, ArCH), 122.6 (q, J = 271.42 Hz, CF_3), 133.3 (q, J = 33.94 Hz, ArC), 151.4

(d, J = 6.31 Hz, ArC). IR (film): ν = (cm^{-1}): 831 (P-O stretch), 1275 (P=O stretch); HRMS ($C_{12}H_{13}F_6O_4P$) (ESI^+): m/z: act: 367.0652 $[M + H]^+$, cal: 367.0534 $[M + H]^+$.

Compound 6: Diethyl chlorophosphate (0.59 g, 3.08 mmol) was added to a stirring solution of 4-(trifluoromethyl)phenol (0.50 g, 3.08 mmol) and triethylamine (0.43 mL, 3.08 mmol) in chloroform (10 mL). The mixture was then allowed to stir at room temperature overnight. The organic phase was then washed with an aqueous 0.3M NaOH solution (30 mL). The organic layer was then taken to dryness to give the final product as a colourless oil (0.83 g, 2.78 mmol) in a yield of 90.3 %. $^1H\{^{31}P\}$ NMR: (400 MHz, 298 K, $CDCl_3$): δ: 1.39 (t, J= 7.08 Hz, 6H), 4.26 (q, J = 7.08 Hz, 4H), 7.36 (d, J = 8.56 Hz, 2H), 7.64 (d, J = 8.64 Hz, 2H); $^{13}C\{^1H\}$ NMR: (100 MHz, 298 K, $CDCl_3$): δ: 16.0 (d, J = 7.22 Hz, CH_3), 64.9 (d, J = 5.77 Hz, CH_2), 120.2 (d, J = 5.05, ArCH), 122.5 (q, J = 270.08 Hz, CF_3), 127.1 (q, J = 3.61 Hz, ArCH), 127.2 (q, J = 33.22 Hz, ArC), 153.2 (dd, J_1 = 1.59 Hz, J_2 = 6.50 Hz, ArC); IR (film): ν = (cm^{-1}): 820 (P-O stretch), 1277 (P=O stretch). HRMS ($C_{11}H_{14}F_3O_4P$) (ESI^+): m/z: act: 299.0762 $[M + H]^+$, cal: 299.0660 $[M + H]^+$.

Compound 7: Diethyl chlorophosphate (0.52 mL, 3.59 mmol) was added to a stirring solution of 4-nitrophenol (0.50 g, 3.59 mmol) and triethylamine (0.50 mL, 3.59 mmol) in chloroform (10 mL). This mixture was then allowed to stir at room temperature overnight. The organic phase was then washed with an aqueous 0.3M NaOH solution (30 mL). The organic layer was then taken to dryness to give the pure product as a clear yellow oil (0.86 g, 2.86 mmol) in a yield of 79.7 %. ^1H NMR: (400 MHz, 298 K, $CDCl_3$): δ: 1.31 (t, J = 7.08 Hz, 6H), 4.19 (q, J = 7.08, 4H), 7.31 (d, J = 9.20 Hz, 2H), 8.18 (d, J = 9.16, 2H).

This compound has been previously synthesised by Kuei and co-workers.[4] The ^1H NMR data provided was found to match previously these published data.

Compound 8: Diethyl chlorophosphate (0.77 mL, 5.31 mmol) was added to a stirring solution of phenol (0.5 g, 5.31 mmol) and triethylamine (0.74 mL, 5.31 mmol) in chloroform (10 mL). The mixture was then allowed to stir at room temperature overnight. The mixture was then allowed to stir at room temperature overnight. The organic phase was then washed with an aqueous 0.3M NaOH solution (30 mL). The organic layer was then taken to dryness to give the pure product as a colourless oil (0.77 g, 3.37 mmol) with a yield of 63.5 %. $^1H\{^{31}P\}$ NMR: (400 MHz, 298 K, $CDCl_3$): δ: 1.34 (t, J = 7.08 Hz, 6H), 4.20 (q, J = 7.08 Hz, 4H), 7.14 – 7.22 (m, 3H), 7.33 (t, J = 8.58 Hz, 2H).

This compound has been previously synthesised by Katritzky and co-workers.[5] The ^1H NMR data provided was found to match previously these published data.

Compound 9: Diethyl chlorophosphate (2.20 mL, 15.0 mmol) in pyridine (1.20 mL, 15.0 mmol) was added to a stirring solution of cyclohexanol (1.00 g, 9.98 mmol) in dichloromethane (10 mL).The solution was stirred at 0 ℃ then allowed to warm up to room temperature overnight. The reaction was then quenched with methanol (50 mL) and concentrated in vaccu. The resulting white solid was then dissolved in ethyl acetate (50 mL) and washed with 1M HCl (50 mL), saturated $NaHCO_3$ solution (50 mL). The organic layer was then taken to dryness to give a colourless oil (1.93 g, 8.17 mmol) with a yield of 81.7 %. $^1H\{^{31}P\}$ NMR (298 K, $CDCl_3$, 400 MHz): δ; 1.24-1.99 (m, 18H), 4.11 (q, J = 7.08, 4H), 4.34-4.41 (m, 1H).

This compound has been previously synthesised by Kang et al.[6] The ^1H NMR data provided was found to match previously these published data.

Compound 10: Diethyl chlorophosphate (0.97 mL, 6.74 mmol) was added to a stirring solution of butanol (0.50 g, 6.74 mmol) and triethylamine (0.94 mL, 6.74 mmol) in chloroform (10 mL). The mixture was then allowed to stir at room temperature overnight. The organic phase was then washed with an aqueous 0.3M NaOH solution (30 mL). The organic layer was then taken to dryness to give the pure product as a colourless oil (1.21 g, 5.74 mmol) in a yield of 85.2 %. $^{1}H\{^{31}P\}$ NMR: (400 MHz, 298 K, $CDCl_3$): δ: 0.93 (t, J = 7.36 Hz, 3H), 1.32 – 1.46 (m, 8H), 1.63 – 1.70 (m, 2H), 4.02 – 4.13 (m, 6H); $^{13}C\{^{1}H\}$ NMR: (100 MHz, 298 K, DMSO-d_6): δ: 13.9 (CH_3), 16.4 (CH_2), 18.6 (CH_2), 32.2 (d, J = 6.54 Hz, CH_3), 63.5 (d, J = 5.80 Hz, CH_2), 67.0 (d, J = 5.95 Hz, CH_2); IR (film): ν = (cm-1): 802 (P-O stretch), 1275 (P=O stretch); HRMS ($C_8H_{19}O_4P$) (ESI^+): m/z: act: 211.1142 $[M + H]^+$, cal: 211.1099 $[M + H]^+$.

Compound 16: *p*-Toluene sulfonylchloride (0.588 g, 3.08 mmol) was added to a stirring solution of 4-(trifluoromethyl)phenol (0.75 g, 4.62 mmol) and triethylamine (0.43 mL, 4.62 mmol) in chloroform (10 mL). The mixture was then allowed to stir at room temperature overnight and then washed with an aqueous 0.3M NaOH solution (30 mL). The organic layer was then taken to dryness under reduced pressure to give the pure product as a white solid (0.58 g, 1.82 mmol) in a yield of 59.1 %. ^{1}H NMR: (400 MHz, 298 K, $CDCl_3$): δ: 2.44 (s, 3H), 7.10 (d, J = 8.36 Hz, 2H), 7.32 (d, J = 8.00 Hz, 2H), 7.55 (d, J = 8.52 Hz, 2H), 7.70 (d, J = 8.40 Hz, 2H). $^{13}C\{^{1}H\}$ NMR: (100 MHz, 298 K, $CDCl_3$): δ: 21.7 (CH_3), 122.9 (ArCH), 122.2 (q, J = 270.81 Hz, CF_3), 127.0 (q, J = 3.61 Hz, ArCH), 128.5 (ArC), 129.2 (q, J = 33.22 Hz, ArC), 129.9 (ArCH), 132.0 (ArC), 145.8 (ArC), 151.9 (ArC); IR (film): ν = (cm^{-1}): 849 (S-O stretch), 1184 and 1352 (S=O stretch); HRMS ($C_{14}H_{11}F_3O_3S$) (ESI^+): m/z: act: 339.0286 $[M + Na]^+$, cal: 339.0279 $[M + Na]^+$.

Compound 17: *p*-Toluene sulfonylchloride (0.69 g, 3.59 mmol) was added to a stirring solution of 4-nitrophenol (0.50 g, 3.59 mmol) and triethylamine (0.50 mL, 3.59 mmol) in chloroform (10 mL). This mixture was allowed to stir at room temperature overnight, then washed with an aqueous 0.3M NaOH solution (30 mL), and the organic layer was then taken to dryness to give the pure product as a pale yellow solid (0.84 g, 2.88 mmol) in a yield of 80.2 %. ^{1}H NMR: (400 MHz, 298 K, $CDCl_3$): δ: 2.50 (s, 3H), 7.21 (d, J = 9.20 Hz, 2H), 7.38 (d, J = 8.04 Hz, 2H), 7.76 (d, J = 8.40 Hz, 2H), 8.22 (d, J = 9.20 Hz, 2H).

This compound has been previously synthesised by Wei and co-workers.[7] The ^{1}H NMR data provided was found to match these previously published data.

Compound 18: *p*-Toluene sulfonylchloride (1.01 g, 5.31 mmol) was added to a stirring solution of phenol (0.50 g, 5.31 mmol) and triethylamine (0.74 mL, 5.31 mmol) in chloroform (10 mL) and, stirred at room temperature overnight. The solution was then washed with an aqueous 0.3M NaOH solution (30 mL), and the organic layer was then taken to dryness to give the pure product as a white solid (1.27 g, 5.10 mmol) in a yield of 96.0 %. ^{1}H NMR: (400 MHz, 298 K, $CDCl_3$): δ: 2.42 (s, 3H), 7.00 (d, J = 8.16 Hz, 2H), 7.31 (t, J = 7.36 Hz, 1H), 7.38 (t, J = 7.12 Hz, 2H), 7.46 (d, J = 7.96 Hz, 2H), 7.72 (d, J = 8.32 Hz, 2H).

This compound has been previously synthesised by Gibson and co-workers.[8] The ^{1}H NMR data provided was found to match these previously published data.

Compound 19: *p*-Toluenesulfonyl chloride (2.85 g, 15.00 mmol) in pyridine (1.20 mL, 15.00 mmol) was added to a stirring solution of cyclohexanol (1.00 g, 9.98 mmol) in dichloromethane (10 mL). The solution was stirred at 0 °C and allowed to warm to room temperature overnight. The reaction was then quenched with methanol (50 mL) and concentrated in vaccu. The resulting white solid was then dissolved in ethyl acetate (50 mL) and washed with 1M HCl (50

mL), saturated $NaHCO_3$ solution (50 mL). The organic layer was taken to dryness to give a colourless oil (1.82 g, 7.16 mmol) with a yield 71.6 %. ^{1}H NMR (298 K, $CDCl_3$, 400 MHz): δ; 0.85-1.81 (m, 12H), 2.46 (s, 3H), 4.49 – 4.55 (m, 1H), 7.34 (d, J = 7.96 Hz, 2H), 7.34 (d, J = 8.32 Hz, 2H).

This compound has been previously synthesised by Wei and co-workers.[7] The ^{1}H NMR data provided was found to match those previously published data.

Compound 20: *p*-Toluene sulfonylchloride (1.29 g, 6.74 mmol) was added to a stirring solution of butanol (0.62 mL, 6.74 mmol) and triethylamine (0.94 mL, 6.74 mmol) in chloroform (10 mL). This mixture was allowed to stir at room temperature overnight, then washed with an aqueous 0.3M NaOH solution (30 mL), and the organic layer was then taken to dryness to give the pure product as a colourless oil (1.32 g, 5.78 mmol) in a yield of 85.8 %. ^{1}H NMR: (400 MHz, 298 K, $CDCl_3$): δ: 0.85 (t, J = 7.40 Hz, 3H), 1.29-1.39 (m, 2H), 1.59-1.66 (m, 2H), 2.45 (s, CH_3), 4.03 (t, J = 6.74 Hz, 2H), 7.35 (d, J = 8.00 Hz, 2H), 7.79 (d, J = 7.79 Hz, 2H).

This compound has been previously synthesised by Wei and co-workers.[7] The ^{1}H NMR data provided was found to match these previously published data.

Compound 21: To a stirring solution of 3,5-bis(trifluoromethyl) phenol (1.00 g, 4.34 mmol) in chloroform (10 mL) and trimethylamine (0.86 ml, 6.17 mmol), was added methylsulfonyl chloride (0.34 mL, 4.34 mmol). The solution was stirred at room temperature for three hours, washed with an aqueous 0.3M NaOH solution (30 mL), and the organic layer taken to dryness to give a white solid (1.31 g, 4.25 mmol) with a yield of 98.5 % . ^{1}H NMR (298 K, $CDCl_3$, 400 MHz): δ; 3.31 (s, 3H), 7.79 (s, 2H), 7.89 (s, 2H).

This compound has been previously synthesised by Seayad and co-workers.[9] The ^{1}H NMR data provided was found to match previously these published data.

Compound 22: Methylsulfonyl chloride (0.13 mL, 1.58 mmol) was added to a stirring solution of 4-trifluoromethyl phenol (0.26 g, 1.58 mmol) in chloroform (10 mL) and trimethylamine (0.22 ml, 1.58 mmol). The solution was stirred at room temperature for three hours, washed with an aqueous 0.3M NaOH solution (30 mL), and the organic layer taken to dryness to give a pale yellow solid (0.35 g, 1.44 mmol) with a yield of 91.2 %, mp 49-51 °C. ^{1}H NMR (298 K, $CDCl_3$, 400 MHz): δ; 3.23 (s, 3H), 7.44 (d, J = 8.52 Hz, 2H), 7.73 (d, J = 8.52 Hz, 2H); ^{13}C{^{1}H} NMR: (100 MHz, 298 K, $CDCl_3$): δ: 37.8 (CH_3), 122.2 (q, J = 270.84 Hz, CF_3), 122.6 (ArCH), 127.5 (q, J = 3.69 Hz, ArCH), 129.37 (q, J = 32.93 Hz, ArC), 151.3 (ArC). IR (film): ν = (cm^{-1}): 851 (S-O stretch), 1175 and 1364 (S=O stretch).

Compound 23: Methylsulfonyl chloride (0.56 mL, 7.19 mmol) was added to a stirring solution of 4-nitrophenol (1.00 g, 7.19 mmol) in chloroform (10 mL) and trimethylamine (0.50 ml, 3.56 mmol). The solution was stirred at room temperature for three hours, washed with an aqueous 0.3M NaOH solution (30 mL), and the organic layer taken to dryness to give a white solid (0.94 g, 4.35 mmol) with a yield of 60.5 %**.** ^{1}H NMR (298 K, $CDCl_3$, 400 MHz): δ; 3.23 (s, 3H), 7.50 (d, J = 9.20 Hz, 2H), 8.34 (d, J = 9.16 Hz, 2H).

This compound has been previously synthesised by Tokuyama and co-workers.[10] The ^{1}H NMR data provided was found to match previously these published data.

Compound 24: Methylsulfonyl chloride (0.82 mL, 10.63 mmol) was added to a stirring solution of phenol (1.00 g, 10.63 mmol) in chloroform (10 mL) and trimethylamine (0.50 ml, 3.56 mmol). The solution was stirred at room temperature for three hours, washed with an aqueous 0.3M NaOH solution (30 mL), and the organic layer taken to dryness to give a white solid (0.96 g, 5.56 mmol) with a yield of 52.3 %**.** ^{1}H NMR (298 K, $CDCl_3$, 400 MHz): δ; 3.16 (s, 3H), 7.31 – 7.38 (m, 3H), 7.45 (t, J = 7.28 Hz, 2H).

This compound has been previously synthesised by Seayad and co-workers.[9] The ^{1}H NMR data provided was found to match previously these published data.

Compound 25: Methylsulfonyl chloride (0.78 mL, 10.10 mmol) in pyridine (0.82 mL, 10.10 mmol) was added to a stirring solution of cyclohexanol (1.00 g, 9.98 mmol) in dichloromethane (10 mL). The solution was stirred at 0 ℃ and allowed to warm to room temperature. The reaction was then quenched with methanol (50 mL) and concentrated in vaccu. The resulting white solid was then dissolved in ethyl acetate (50 mL) and washed with 1M HCl (50 mL), saturated $NaHCO_3$ solution (50 mL). The organic layer was then taken to dryness to give a yellow oil (1.68 g, 9.42 mmol) with a yield of 94.4 %. ^{1}H NMR (298 K, $CDCl_3$, 400 MHz): δ; 1.29-2.03 (m, 10H), 3.02 (s, 3H), 4.72 (m, 1H).

This compound has been previously synthesised by Martín and co-workers.[11] The ^{1}H NMR data provided was found to match previously these published data.

Compound 26: Methylsulfonyl chloride (1.56 mL, 20.20 mmol) in pyridine (1.64 mL, 20.20 mmol) was added to a stirring solution of butanol (1.00 g, 13.4 mmol) in dichloromethane (10 mL). The solution was stirred at 0 ℃ and allowed to warm to room temperature. The reaction was then quenched with methanol (50 mL) and concentrated in vaccu. The resulting white solid was then dissolved in ethyl acetate (50 mL) and washed with 1M HCl (50 mL), saturated $NaHCO_3$ solution (50 mL) organic layer taken to dryness to give a yellow oil (1.43 g, 9.39 mmol) with a yield of 70.1 %. ^{1}H NMR (298 K, $CDCl_3$, 400 MHz): δ; 0.89 (t, J = 7.36 Hz, 3H), 1.37 (m, 2H), 1.67 (m, 2H), 2.93 (s, 3H), 4.17 (t, J = 6.56 Hz, 2H).

This compound has been previously synthesised by Li and co-workers.[12] The ^{1}H NMR data provided was found to match previously these published data.

NMR characterisation

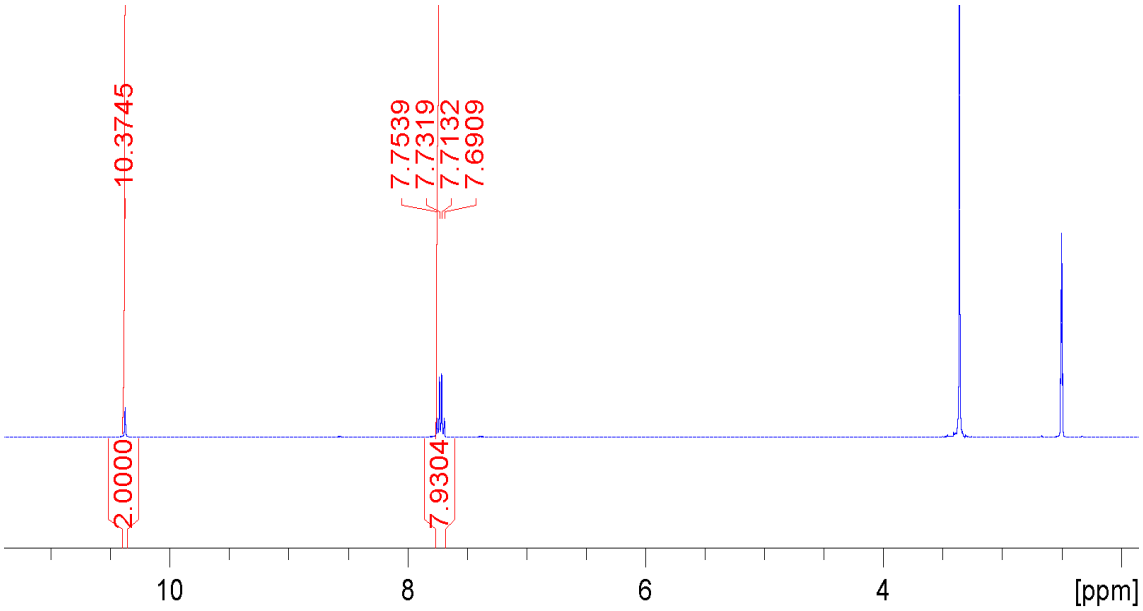

Figure S1: ^{1}H NMR spectra of compound **1** in DMSO-d_6 conducted at 298 K.

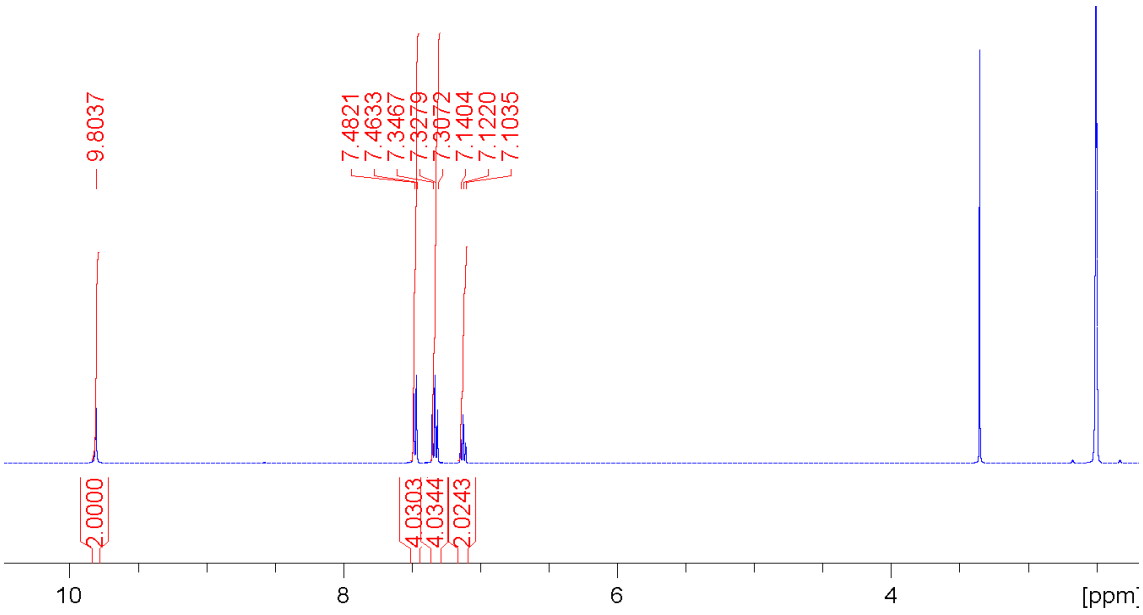

Figure S2: ^{1}H NMR spectra of compound **2** in DMSO-d_6 conducted at 298 K.

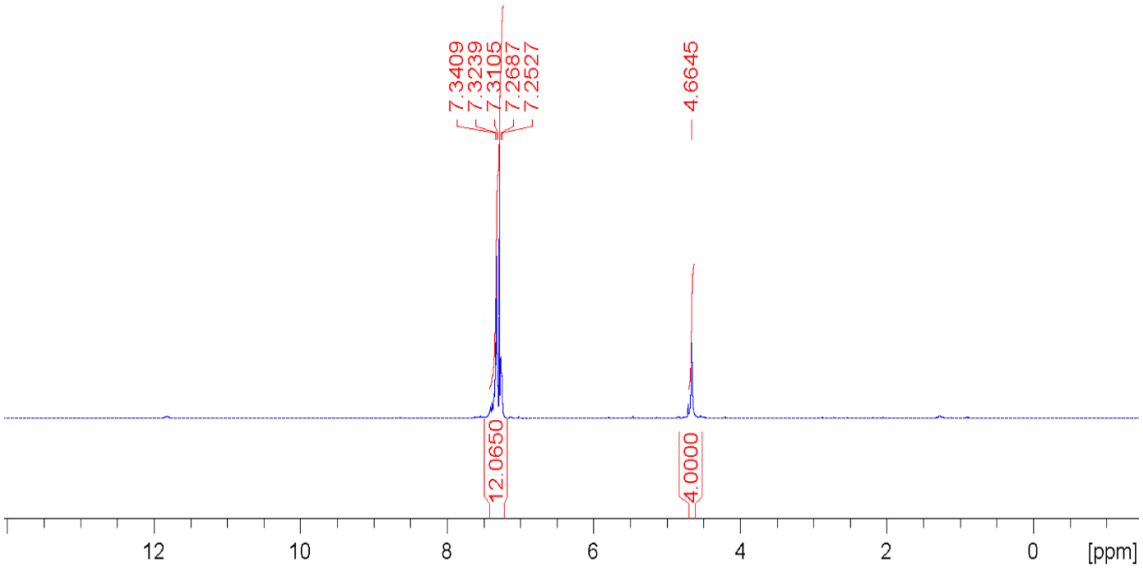

Figure S3: ^{1}H NMR spectra of compound **3** in $CDCl_3$ conducted at 298 K.

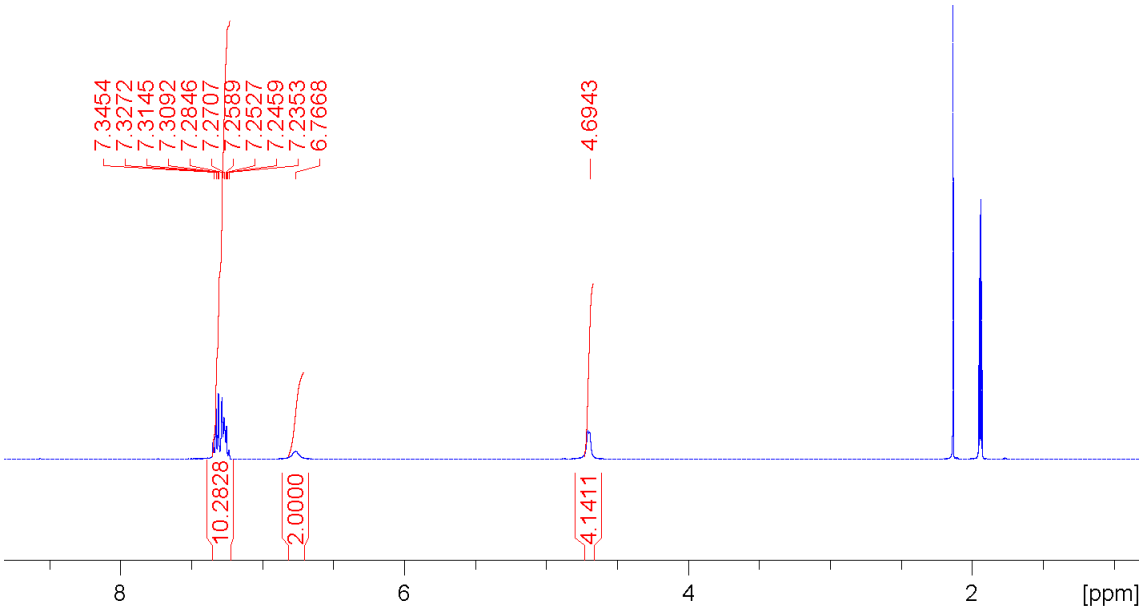

Figure S4: ^{1}H NMR spectra of compound **3** in CD_3CN conducted at 298 K.

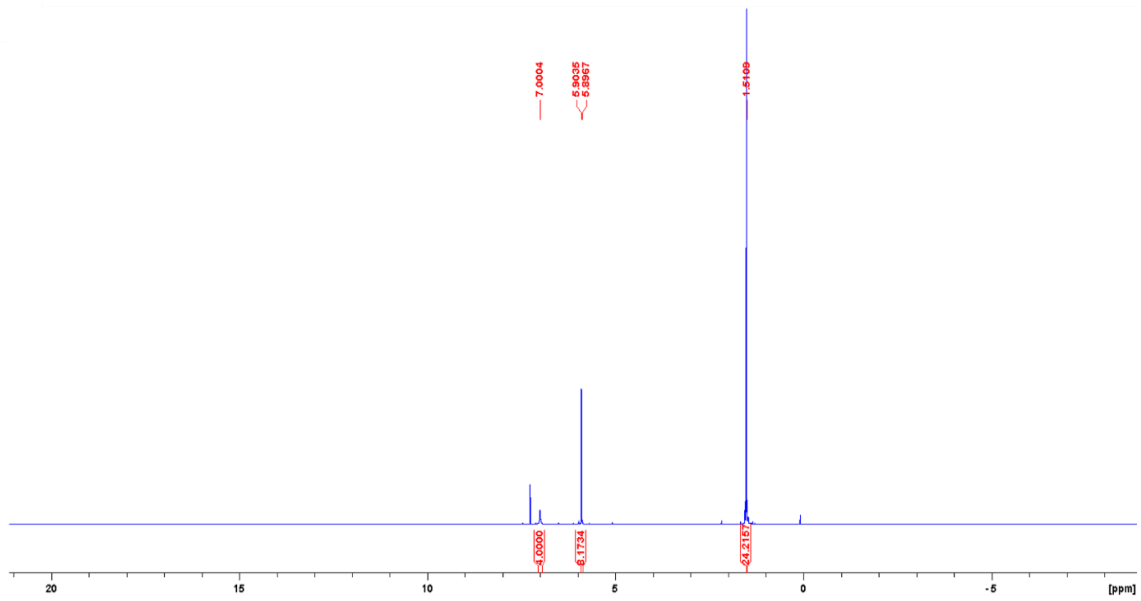

Figure S5: ^{1}H NMR spectra of compound **4** in $CDCl_3$ conducted at 298 K.

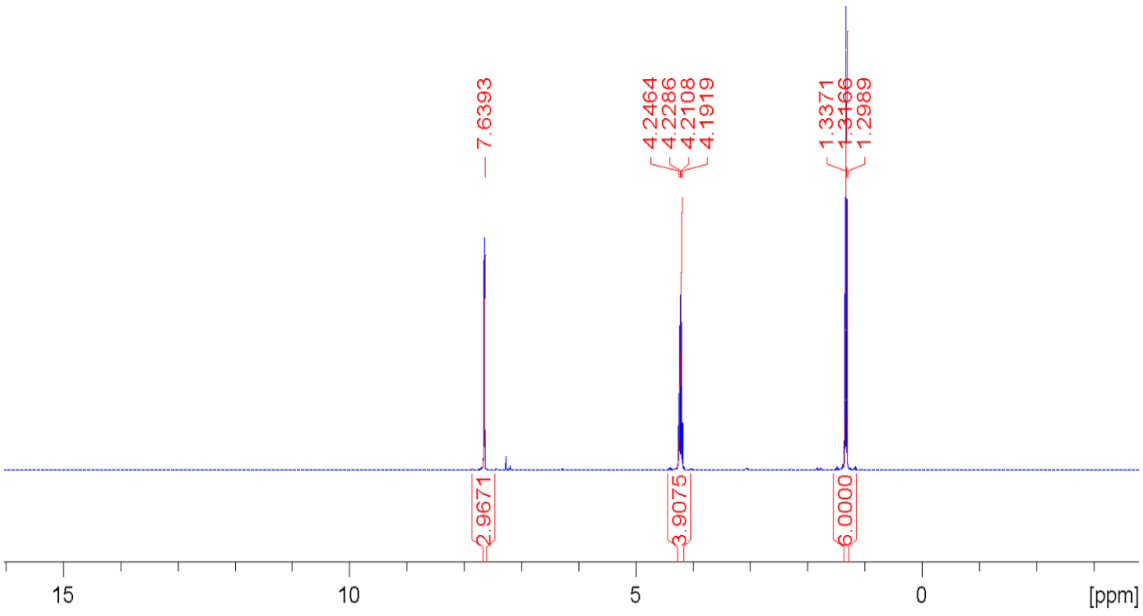

Figure S6: $^{1}H\{^{31}P\}$ NMR spectra of compound **5** in $CDCl_3$ conducted at 298 K.

.

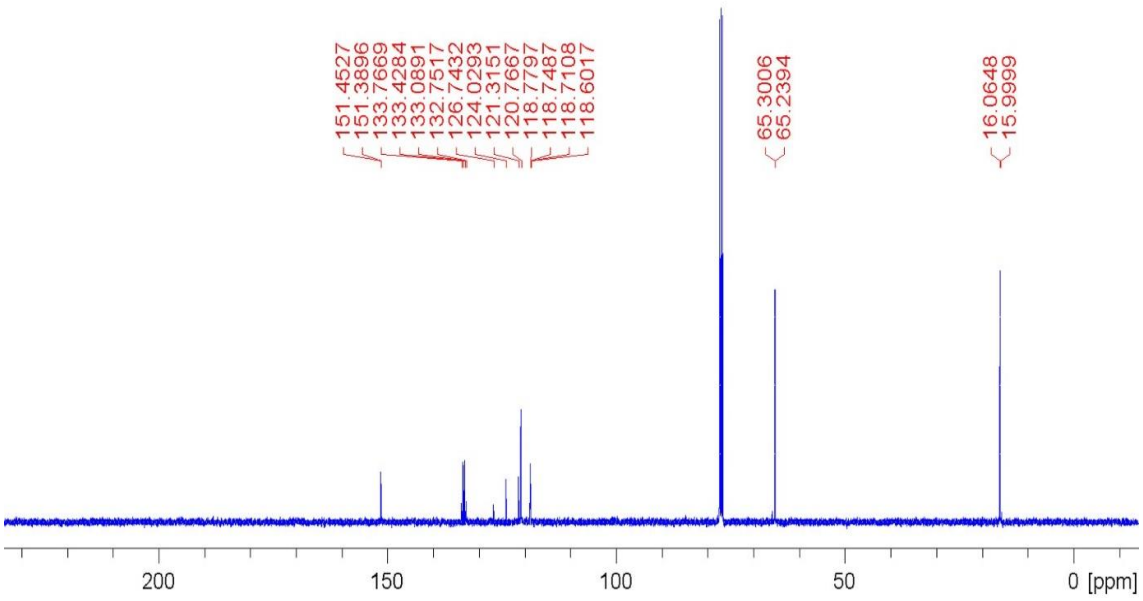

Figure S7: $^{13}C\{^{1}H\}$ NMR spectra of compound **5** in $CDCl_3$ conducted at 298 K.

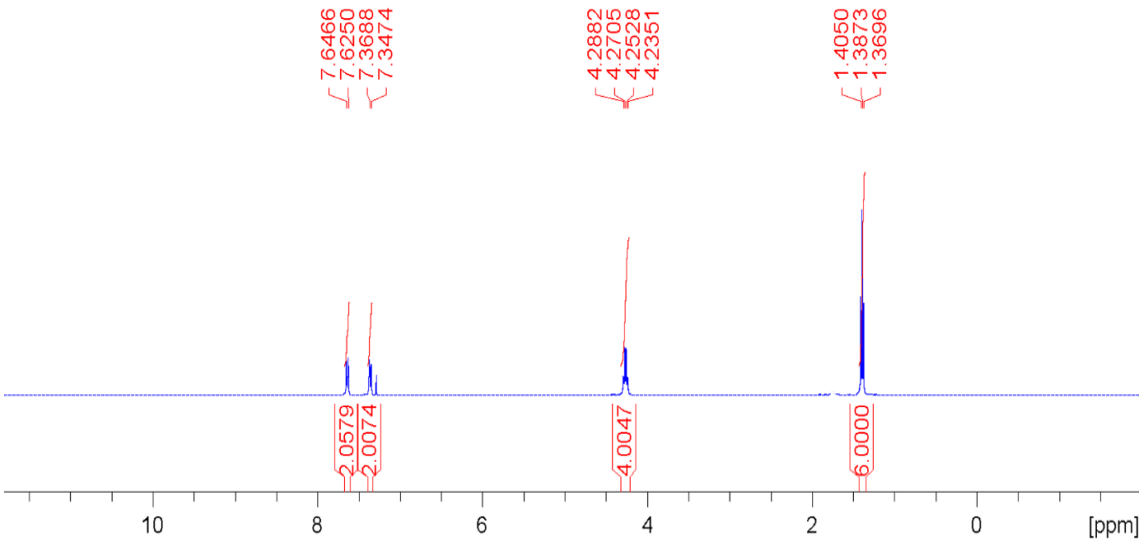

Figure S8: $^{1}H\{^{31}P\}$ NMR spectra of compound **6** in $CDCl_3$ conducted at 298 K.

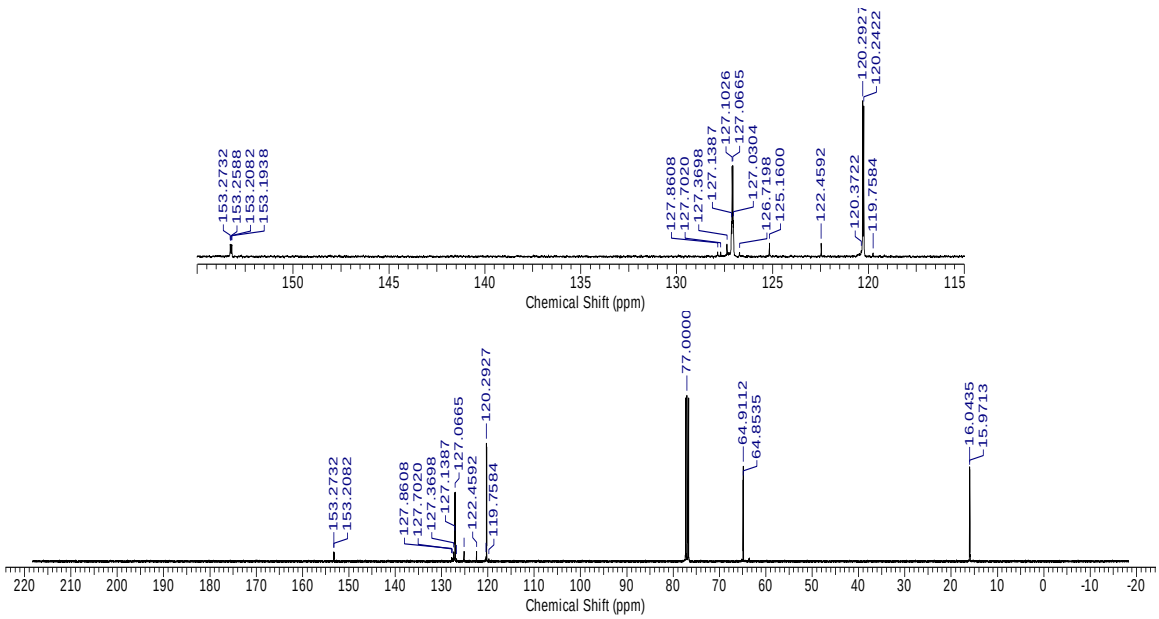

Figure S9: $^{13}C\{^{1}H\}$ NMR spectra of compound **6** in $CDCl_3$ conducted at 298 K.

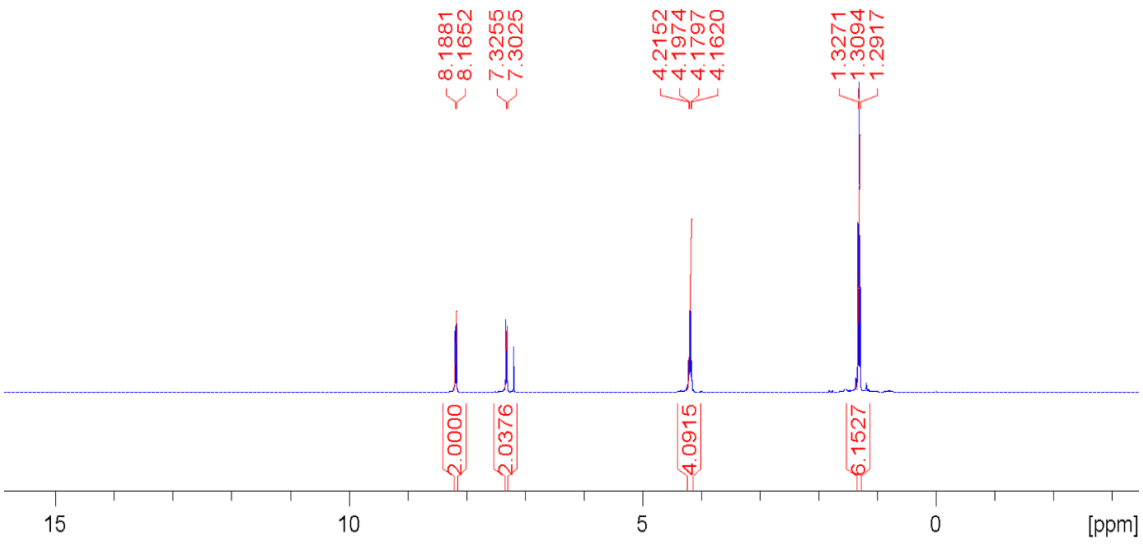

Figure S10: $^{1}H\{^{31}P\}$ NMR spectra of compound **7** in $CDCl_3$ conducted at 298 K.

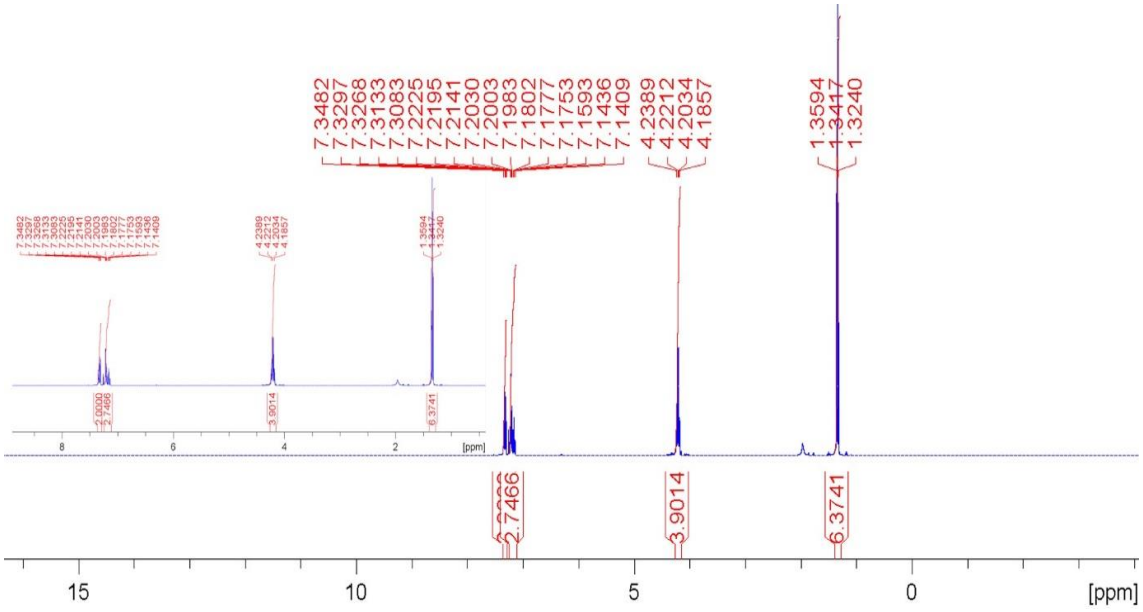

Figure S11: $^{1}H\{^{31}P\}$ NMR spectra of compound **8** in $CDCl_3$ conducted at 298 K.

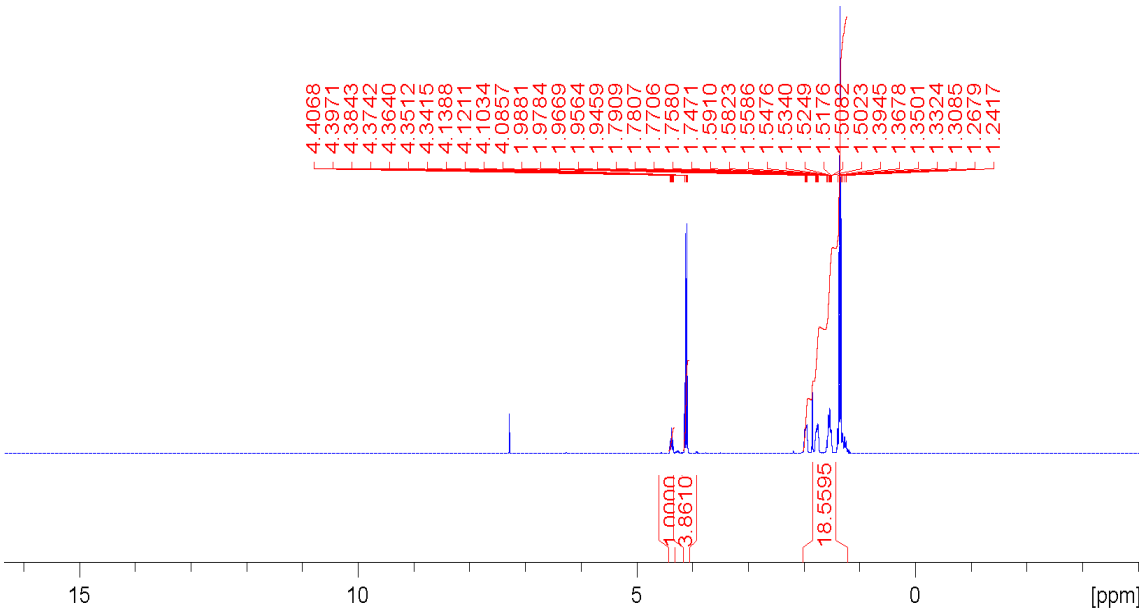

Figure S12: ^{1}H NMR spectra of **9** in $CDCl_3$ at 298 K. Residual H_2O present within the aliphatic region increasing the expected integration by two.

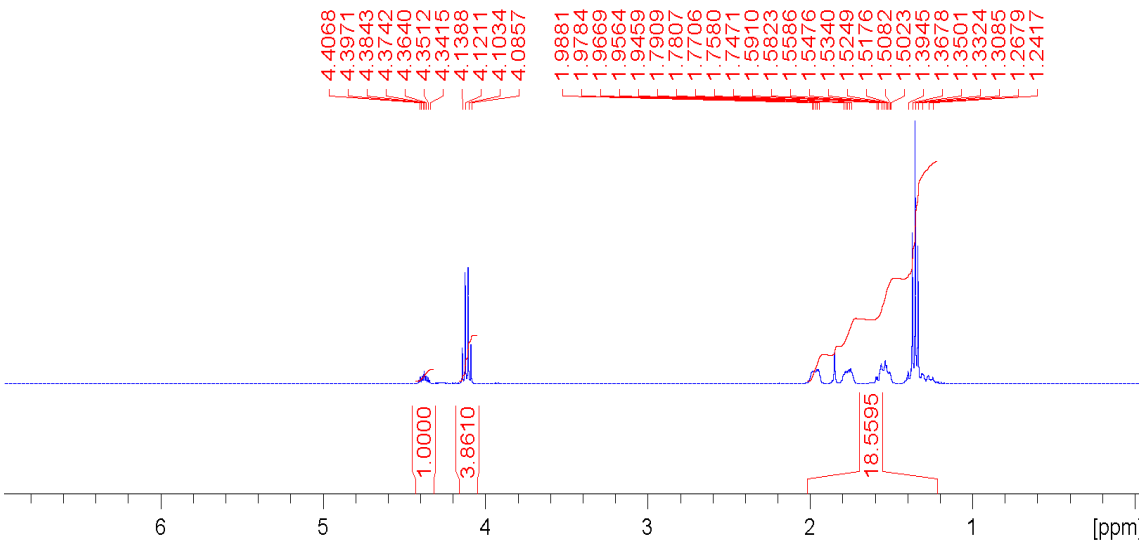

Figure S13: Zoomed in ^{1}H NMR spectra of **9** in $CDCl_3$ at 298 K. Residual H_2O present within the aliphatic region increasing the expected integration by two.

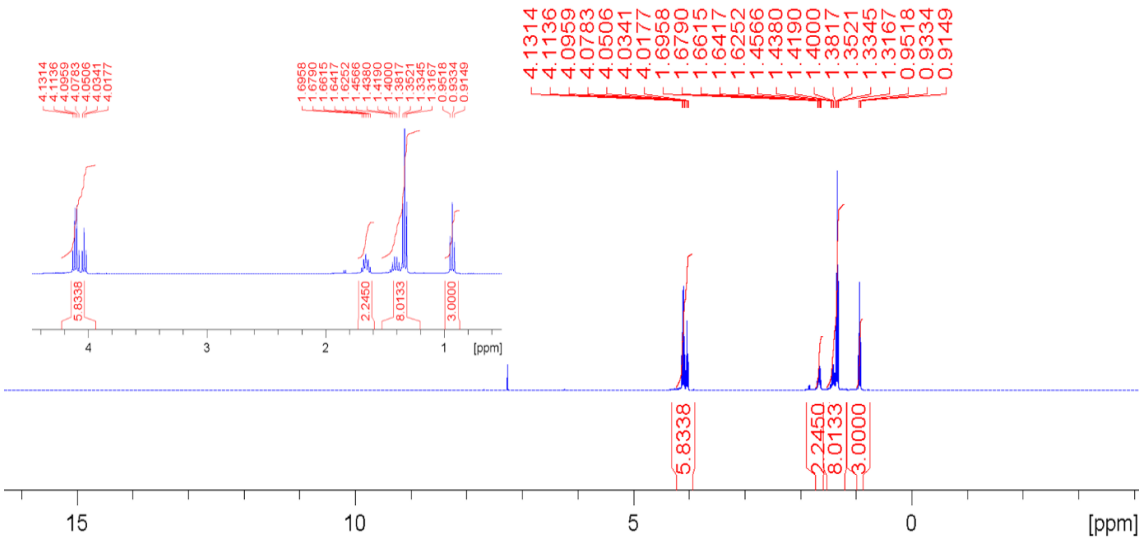

Figure S14: $^{1}H\{^{31}P\}$ NMR spectra of compound **10** in $CDCl_3$ conducted at 298 K.

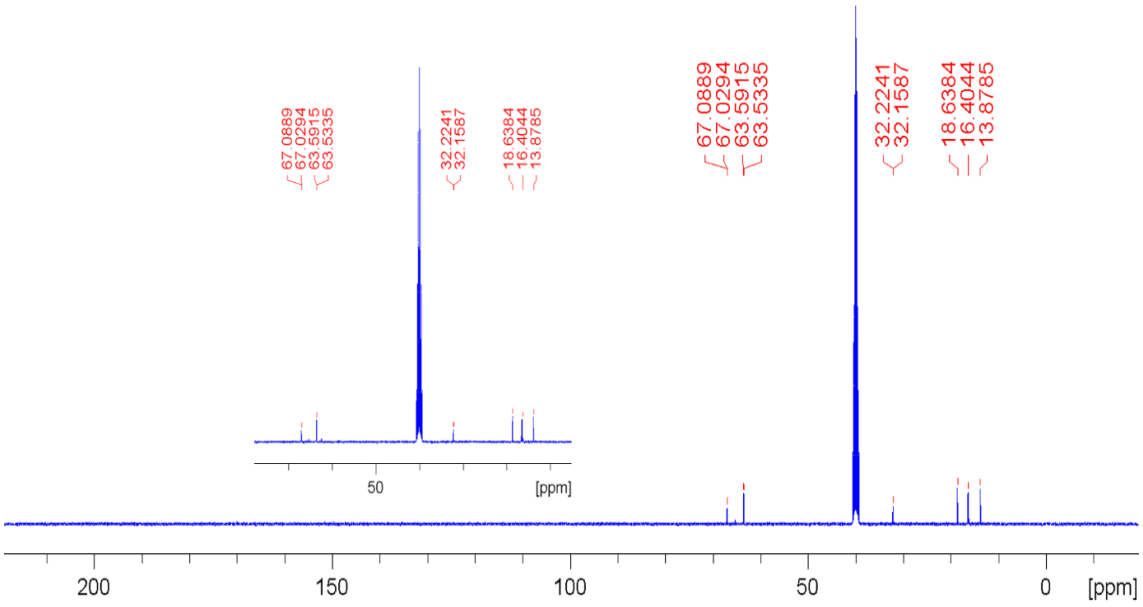

Figure S15: $^{13}C\{^{1}H\}$ NMR spectra of compound **10** in DMSO-d_6 conducted at 298 K.

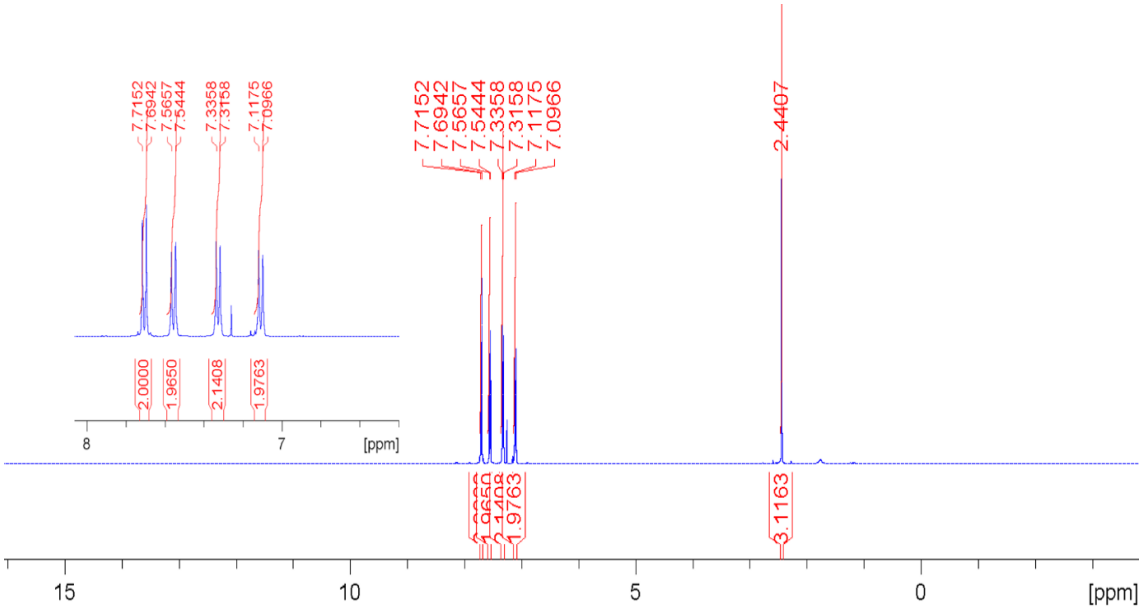

Figure S16: ^{1}H NMR spectra of compound **16** in $CDCl_3$ conducted at 298 K.

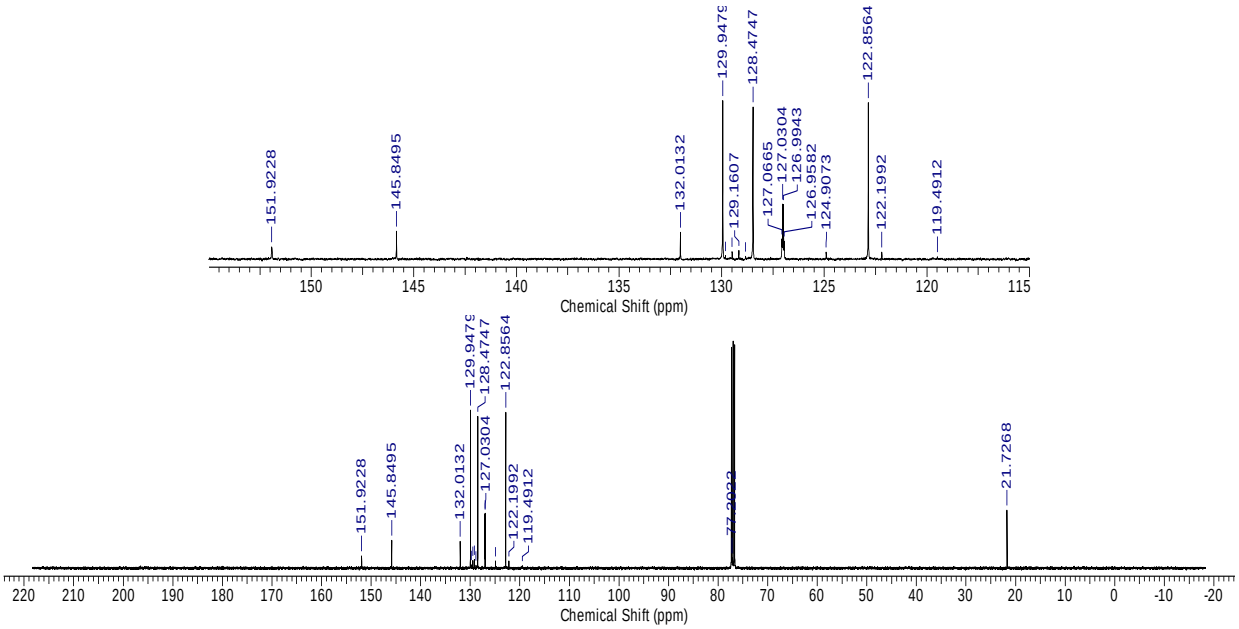

Figure S17: $^{13}C\{^{1}H\}$ NMR spectra of compound **16** in $CDCl_3$ conducted at 298 K.

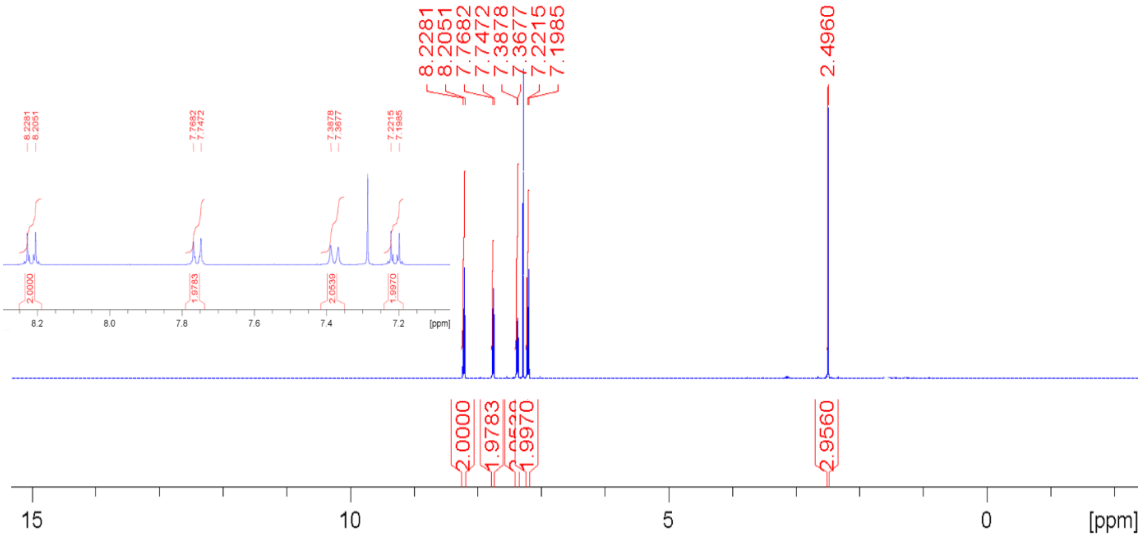

Figure S18*:* ^{1}H NMR spectra of compound **17** in $CDCl_3$ conducted at 298 K.

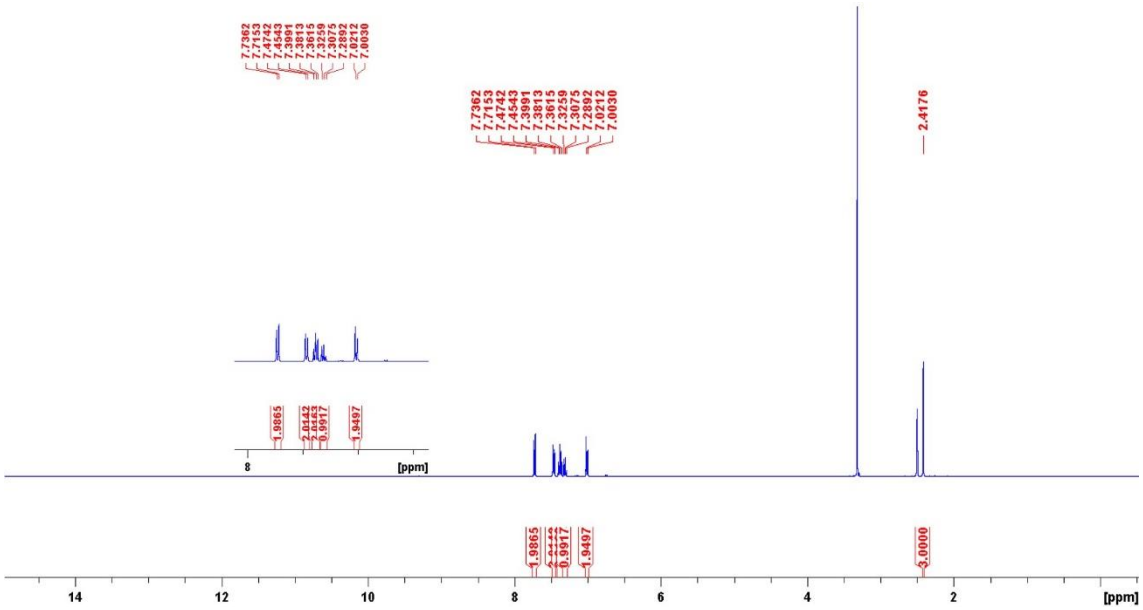

Figure S19: ^{1}H NMR spectra of compound **18** in DMSO-d_6 conducted at 298 K.

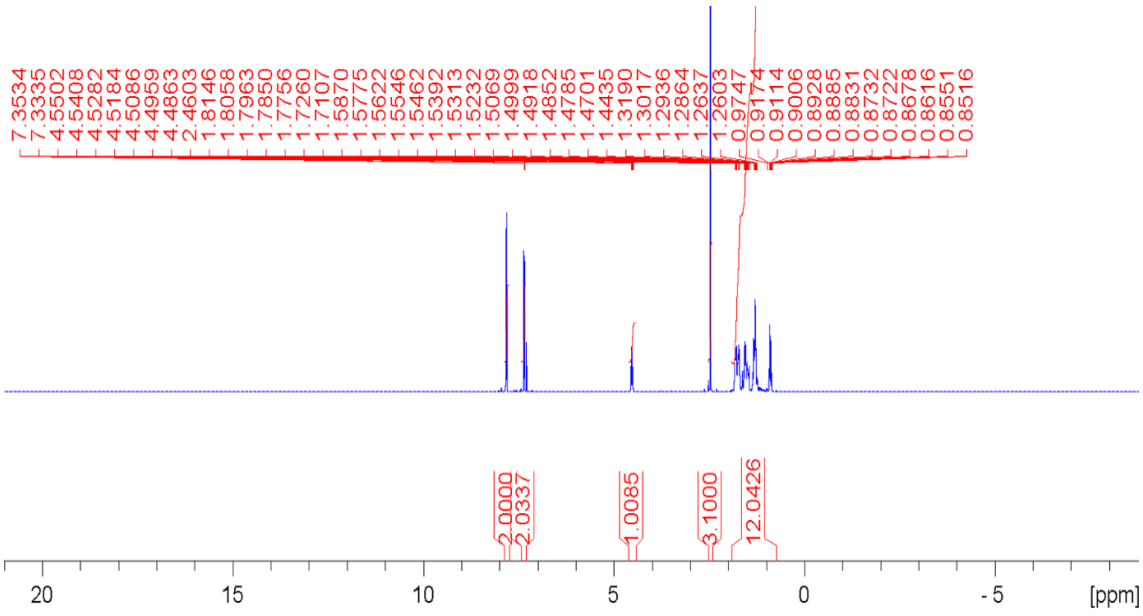

Figure S20: ^{1}H NMR spectra of **19** in $CDCl_3$ at 298 K.

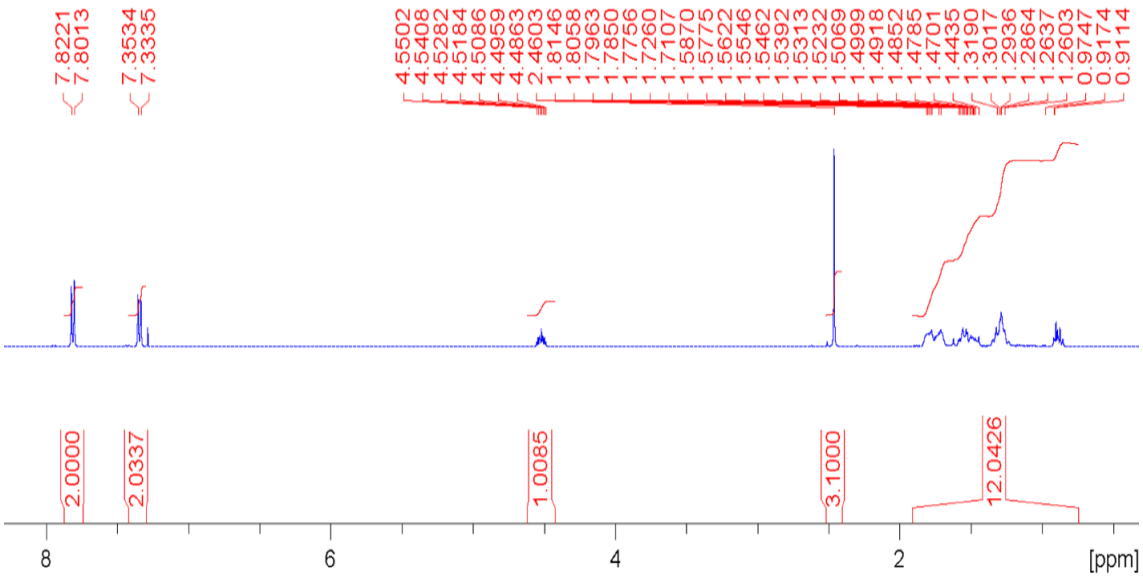

Figure S21: Zoomed in ^{1}H NMR spectra of **19** in $CDCl_3$ at 298 K.

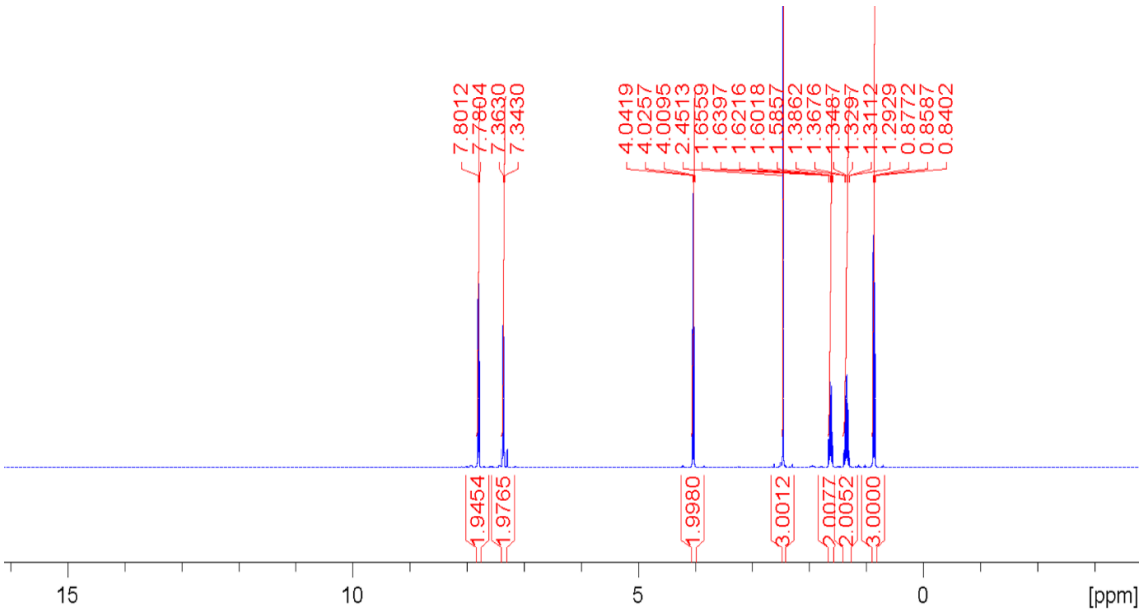

Figure S22: ^{1}H NMR spectra of compound **20** in $CDCl_3$ conducted at 298 K.

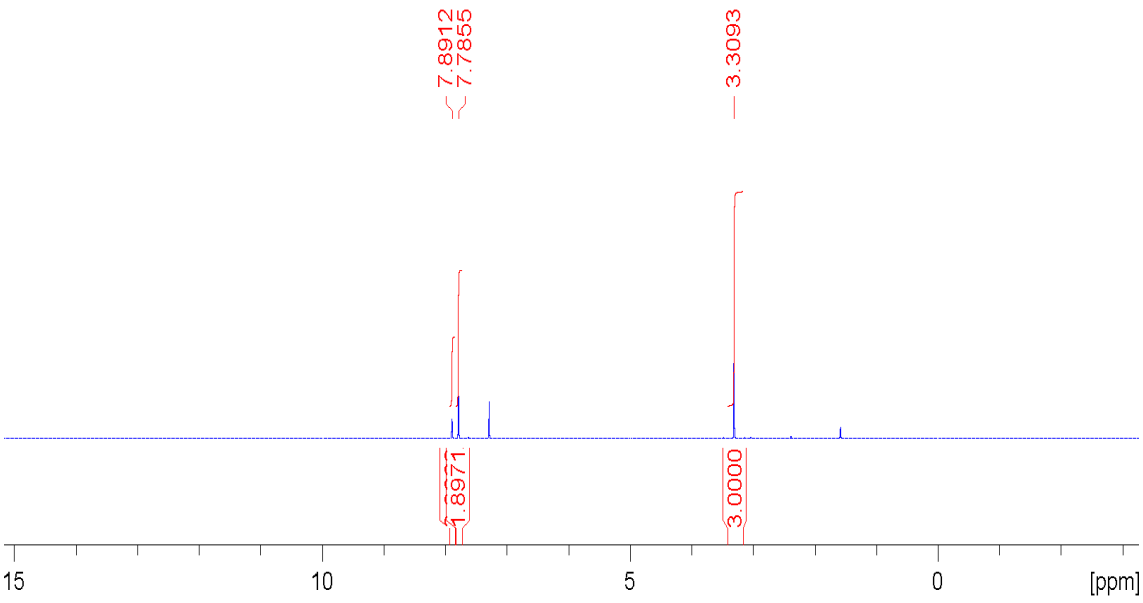

Figure S23: ^{1}H NMR spectra of **21** in $CDCl_3$ at 298 K.

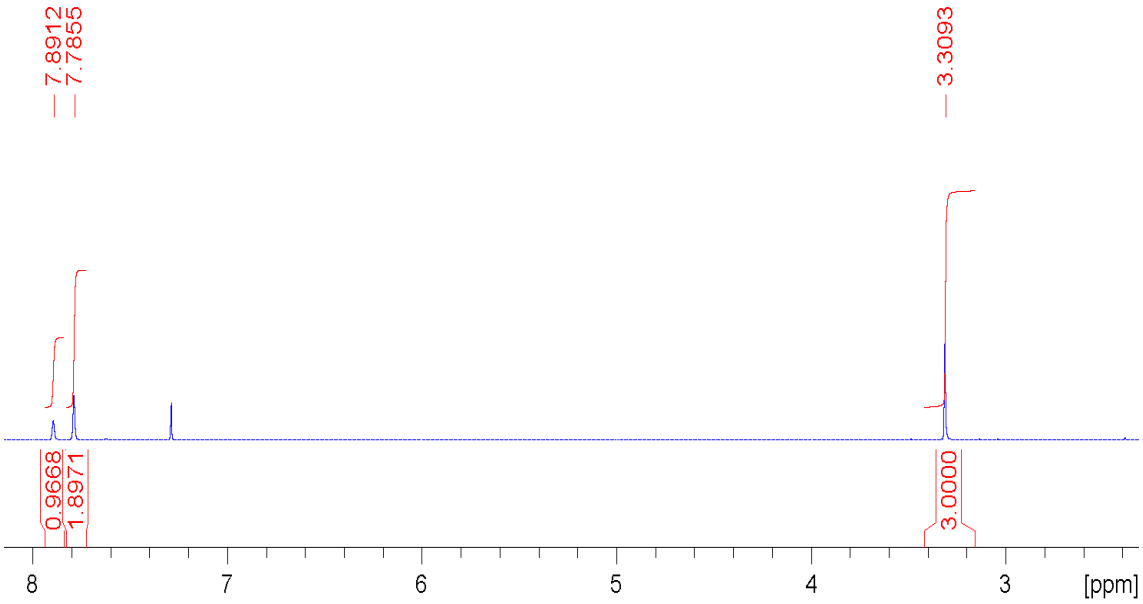

Figure S24: Zoomed in ^{1}H NMR spectra of **21** in $CDCl_3$ at 298 K.

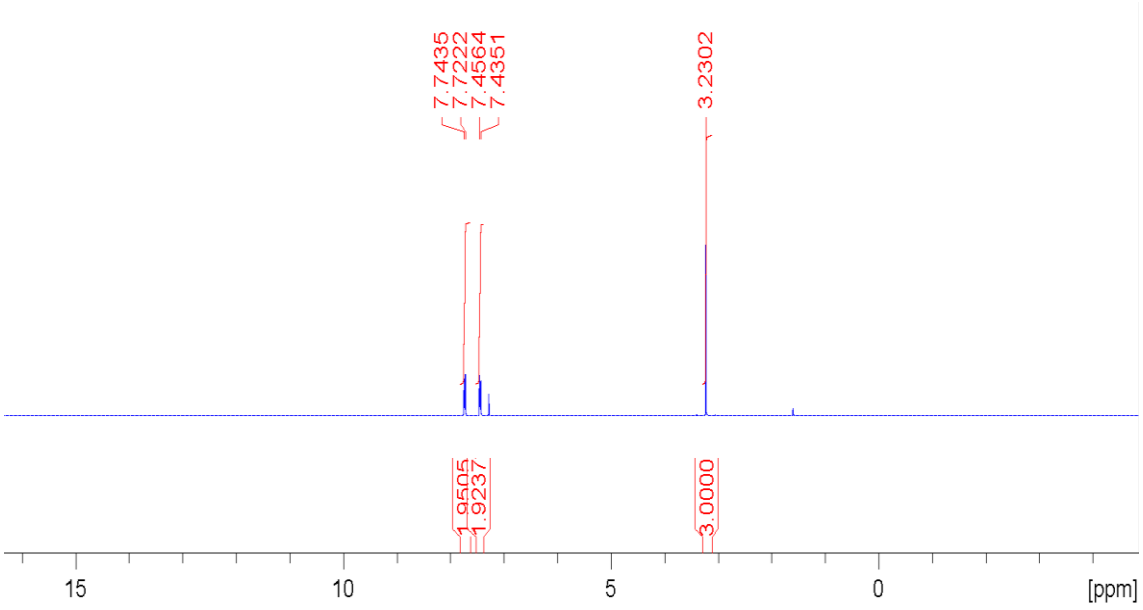

Figure S25: ^{1}H NMR spectra of **22** in $CDCl_3$ at 298 K.

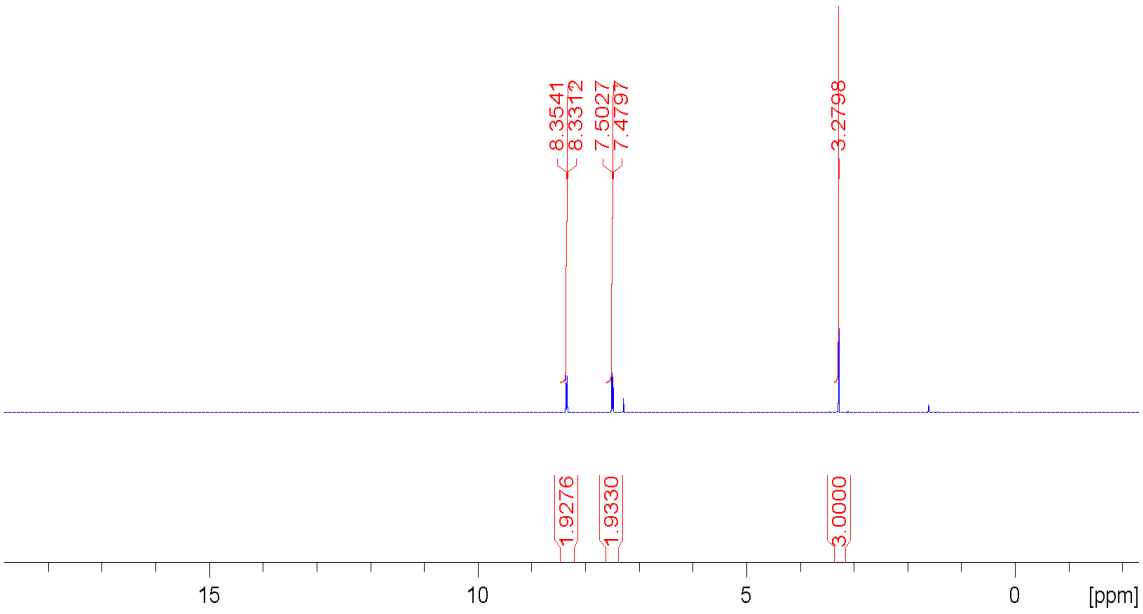

Figure S26: ^{1}H NMR spectra of **23** in $CDCl_3$ at 298 K.

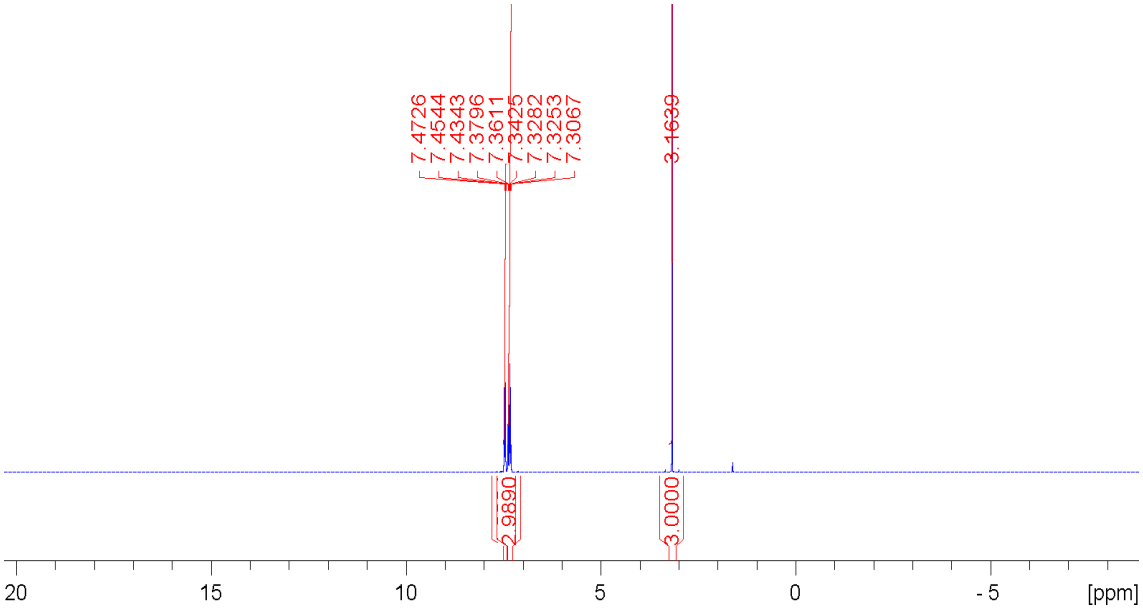

Figure S27: ^{1}H NMR spectra of **24** in $CDCl_3$ at 298 K.

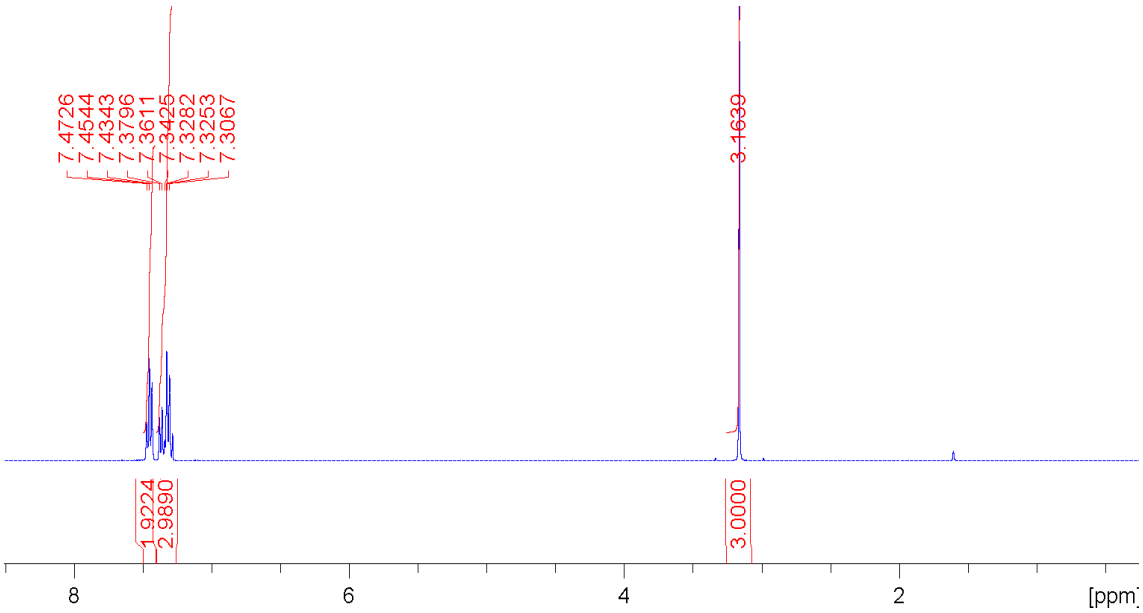

Figure S28: Zoomed in ^{1}H NMR spectra of **24** in $CDCl_3$ at 298 K.

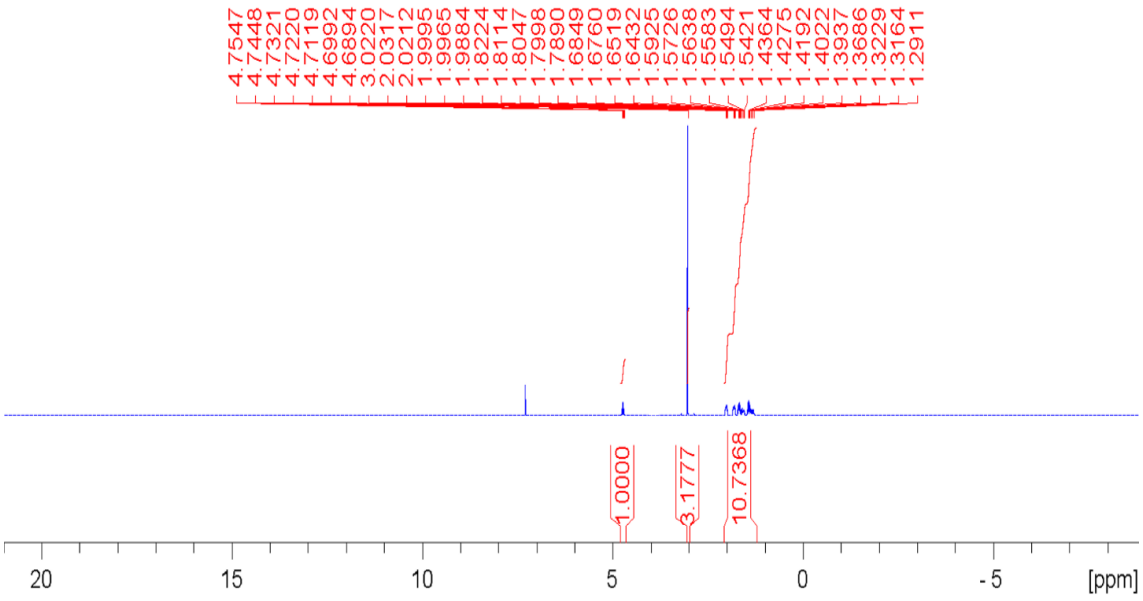

Figure S29: ^{1}H NMR spectra of **25** in $CDCl_3$ at 298 K.

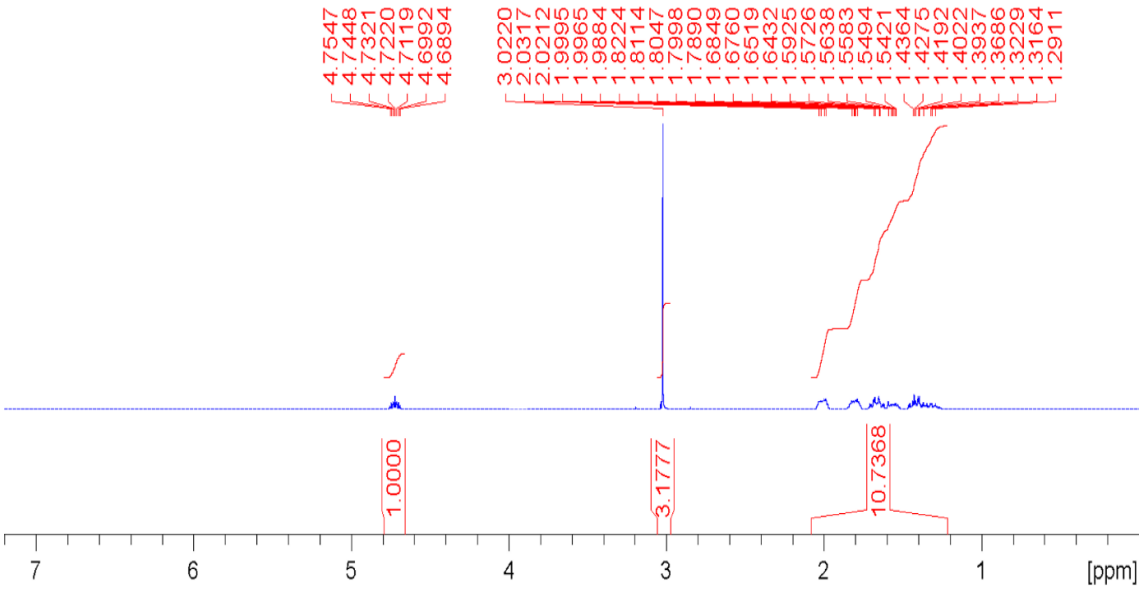

Figure S30: Zoomed in ^{1}H NMR spectra of **25** in $CDCl_3$ at 298 K.

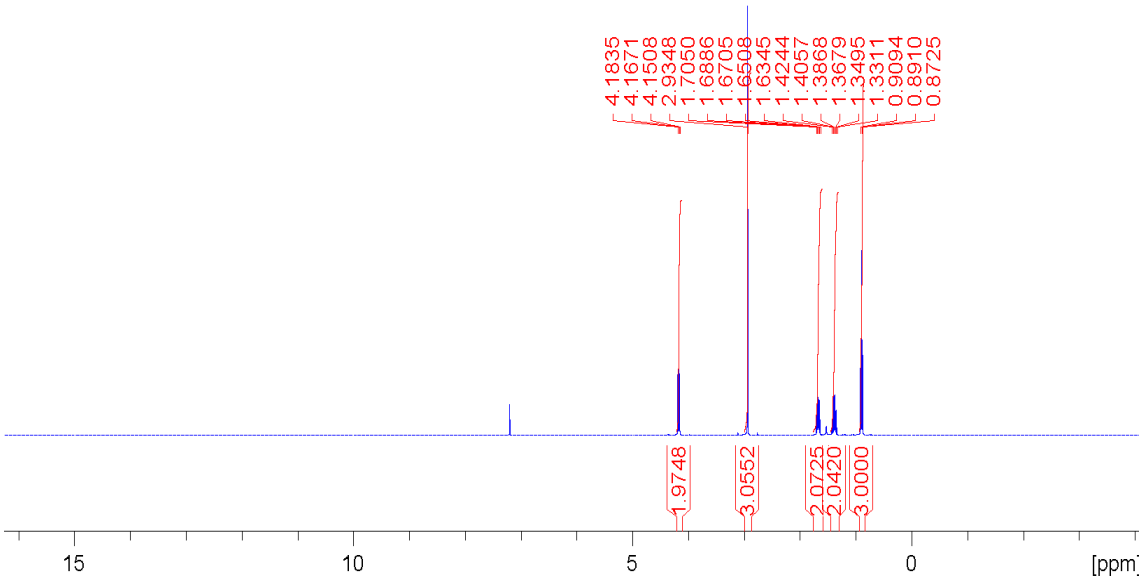

Figure S31: ^{1}H NMR spectra of **26** in $CDCl_3$ at 298 K.

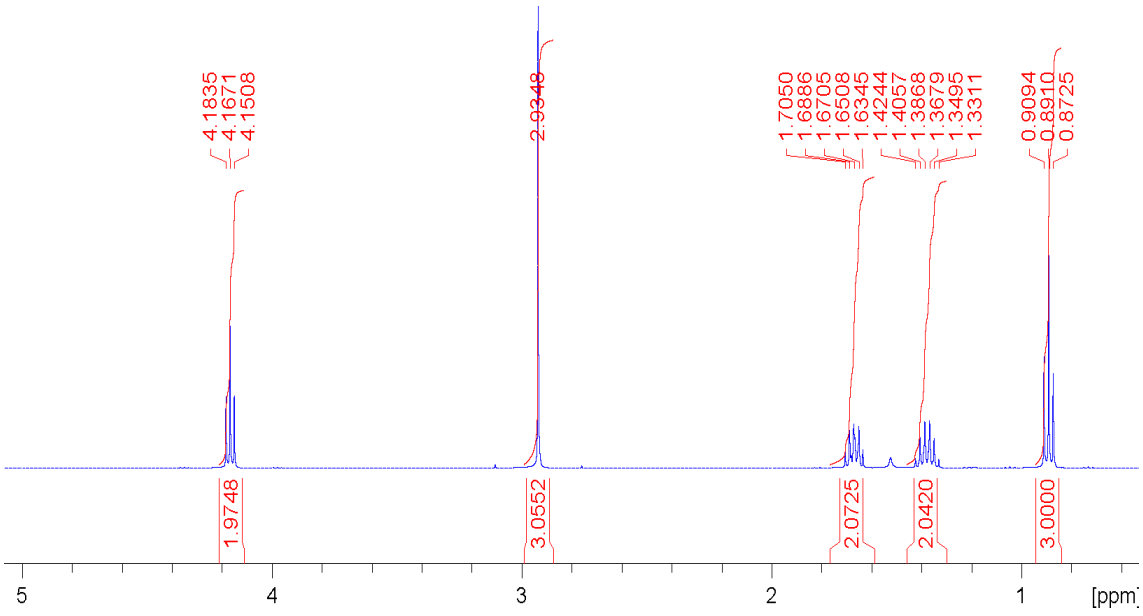

Figure S32: Zoomed in ^{1}H NMR spectra of **26** in $CDCl_3$ at 298 K.

^{1}H NMR titration results

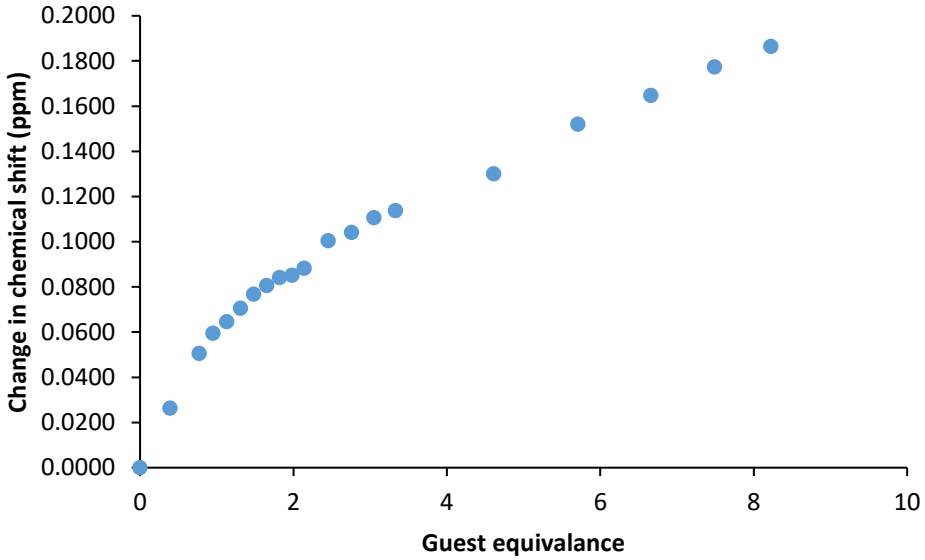

Figure S33: Change in chemical shift for the NH resonance of **1** (host) upon the addition of **5** (guest) in CD_3CN at 298 K. K_{ass} = 36.23 M^{-1} ± 6.27 %.

Bindfit link: http://app.supramolecular.org/bindfit/view/d3e53f5f-0820-41cb-bce8-157734b6a3c6

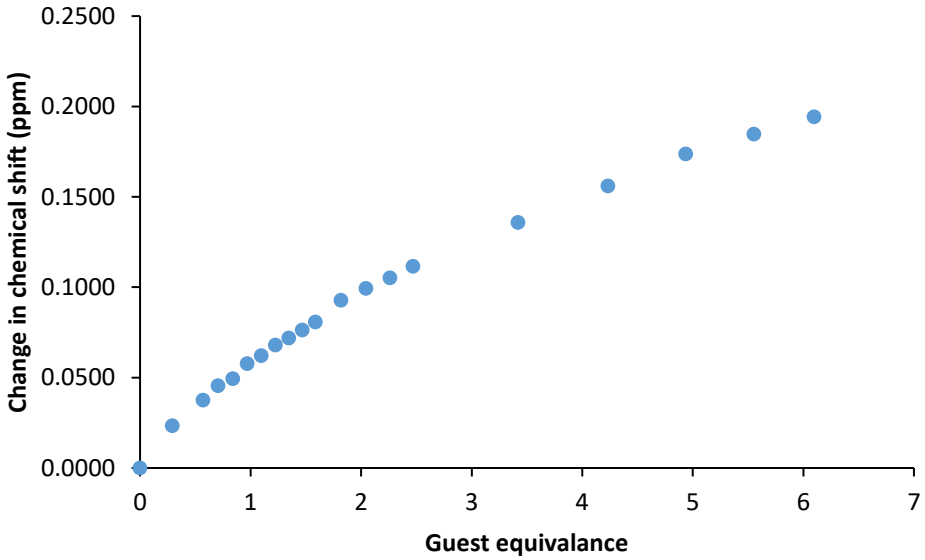

Figure S34: Change in chemical shift for the NH resonance of **1** (host) upon the addition of **6** (guest) in CD_3CN at 298 K. K_{ass} = 17.05 M^{-1} ± 1.18 %.

Bindfit link: http://app.supramolecular.org/bindfit/view/ce076885-b08d-447a-a86d-170d30bff745

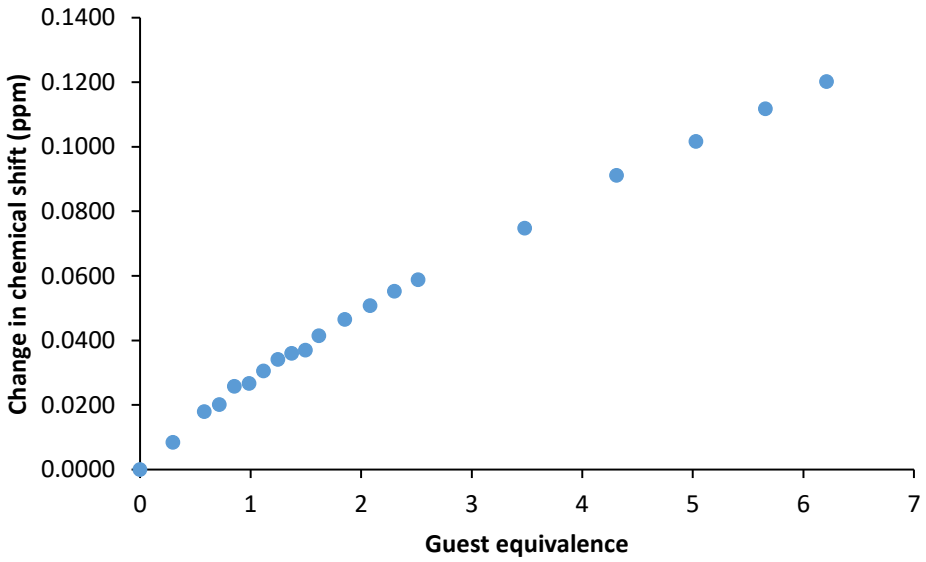

Figure S35: Change in chemical shift for the NH resonance of **1** (host) upon the addition of **7** (guest) in CD_3CN at 298 K. K_{ass} = 7.65 M^{-1} ± 1.41 %.

Bindfit link: http://app.supramolecular.org/bindfit/view/0b460b86-0754-4ce5-88f9-49c7e2df295c

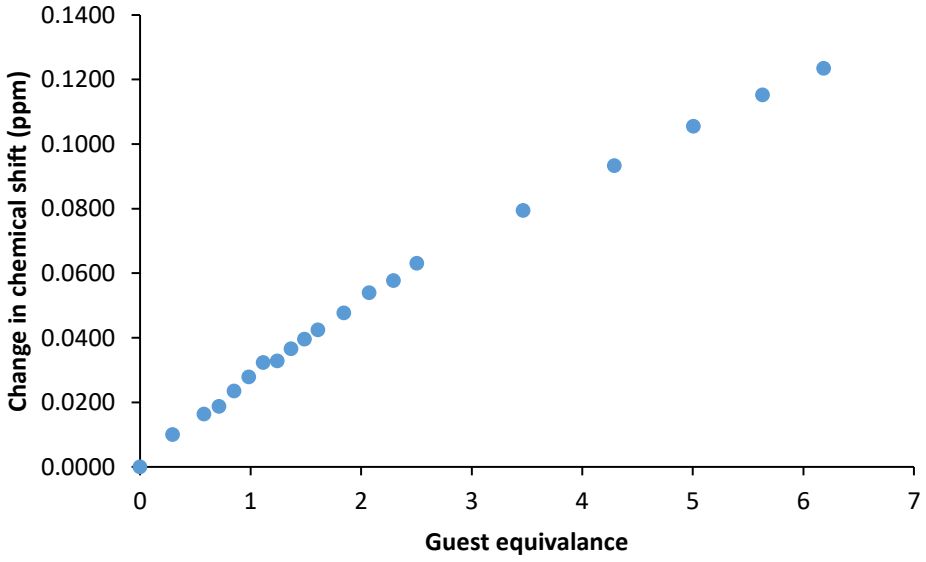

Figure S36: Change in chemical shift for the NH resonance of **1** (host) upon the addition of **8** (guest) in CD_3CN at 298 K. K_{ass} = 9.01 M^{-1} ± 1.07 %.

Bindfit link: http://app.supramolecular.org/bindfit/view/0c5b133c-b224-4a73-8c31-e604d6ecd956

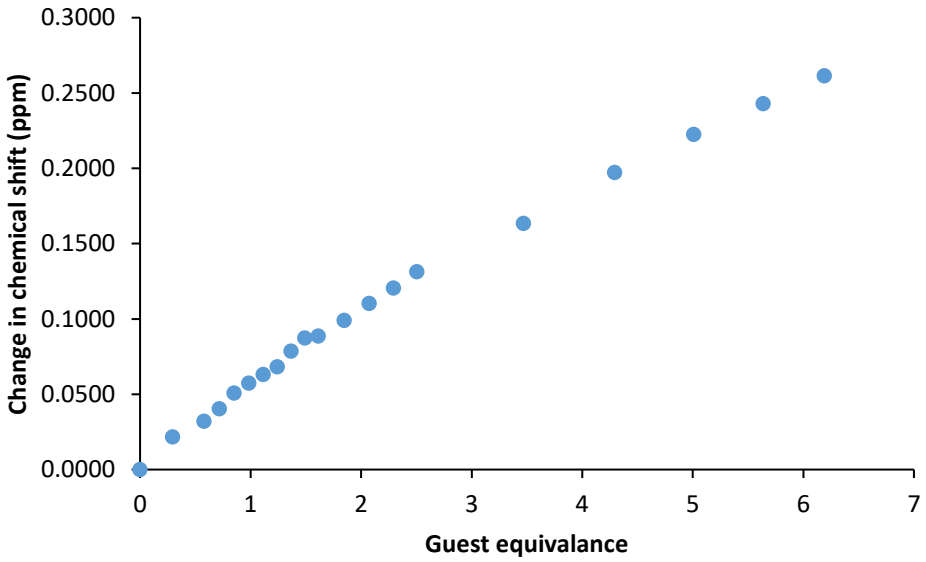

Figure S37: Change in chemical shift for the NH resonance of **1** (host) upon the addition of **9** (guest) in CD_3CN at 298 K. K_{ass} = 8.06 M^{-1} ± 1.26 %.

Bindfit link: http://app.supramolecular.org/bindfit/view/38ae6a9a-f202-459e-934d-9525ea1eafe6

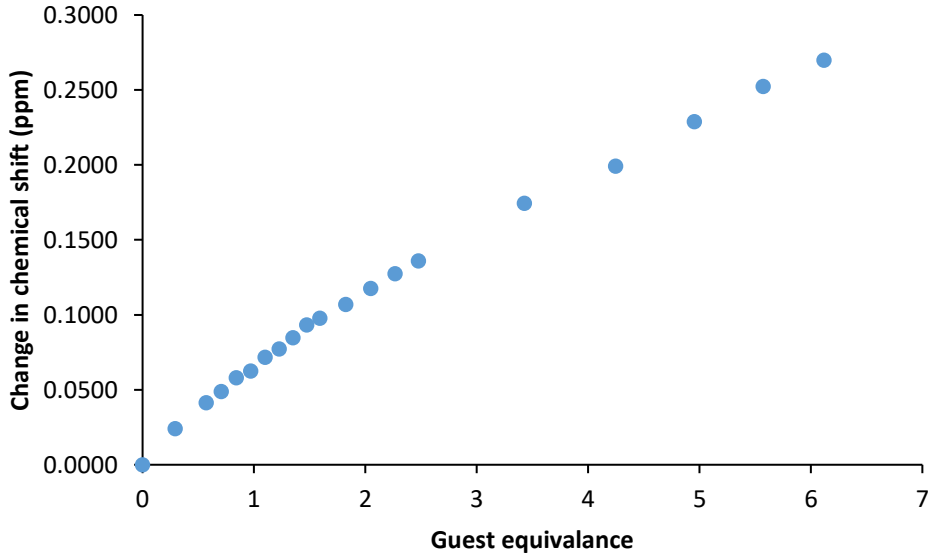

Figure S38: Change in chemical shift for the NH resonance of **1** (host) upon the addition of **10** (guest) in CD_3CN at 298 K. K_{ass} = 9.40 M^{-1} ± 1.58 %.

Bindfit link: http://app.supramolecular.org/bindfit/view/763f2ac2-6c56-4fea-8f1a-95a01b6206b2

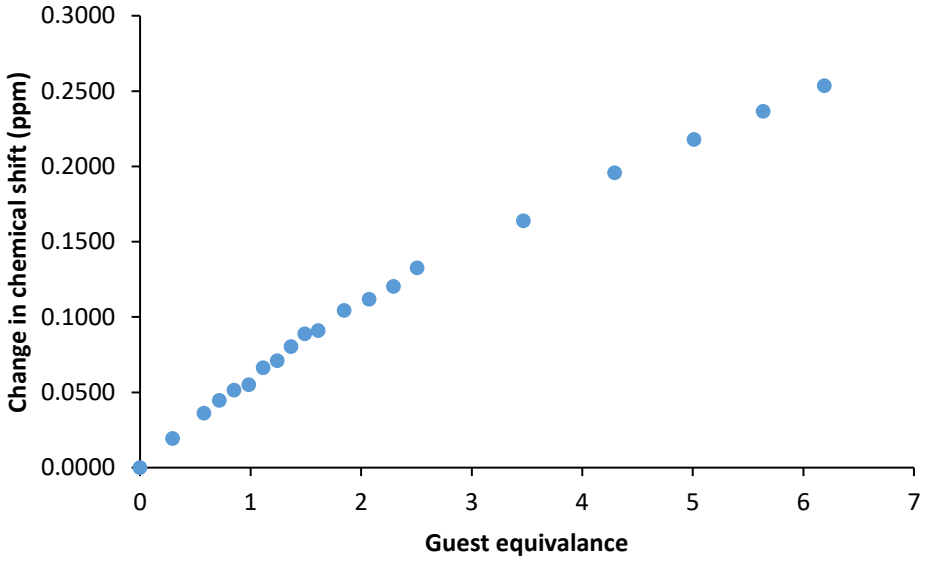

Figure S39: Change in chemical shift for the NH resonance for **1** (host) upon the addition of **11** (guest) in CD_3CN at 298 K. K_{ass} = 10.99 M^{-1} ± 1.23 %.

Bindfit link: http://app.supramolecular.org/bindfit/view/11cabb05-29a8-423b-afd8-f5842f895a29

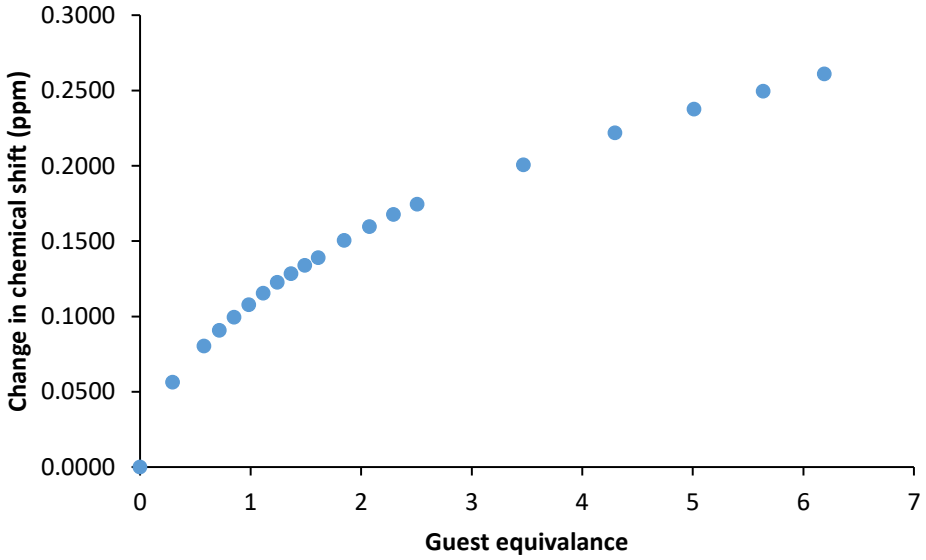

Figure S40: Change in chemical shift for the NH resonance for **1** (host) upon the addition of **12** (guest) in CD_3CN at 298 K. K_{ass} = 51.82 M^{-1} ± 5.73 %.

Bindfit link: http://app.supramolecular.org/bindfit/view/3caad220-a2c3-4733-8d8f-1f69889d2fd0

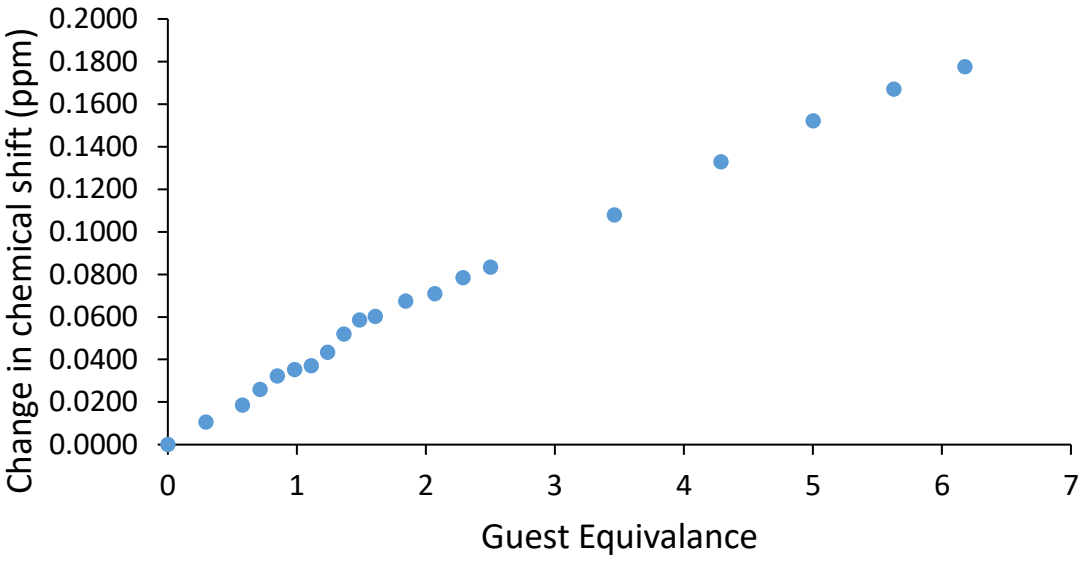

Figure S41: Change in chemical shift for the NH resonance of **1** (host) upon the addition of **13** (guest) in CD_3CN at 298 K. K_{ass} = 5.52 M^{-1} ± 1.8257%.

Bindfit link: http://app.supramolecular.org/bindfit/view/512087b6-a539-452f-a9ba-2f4ddd672556

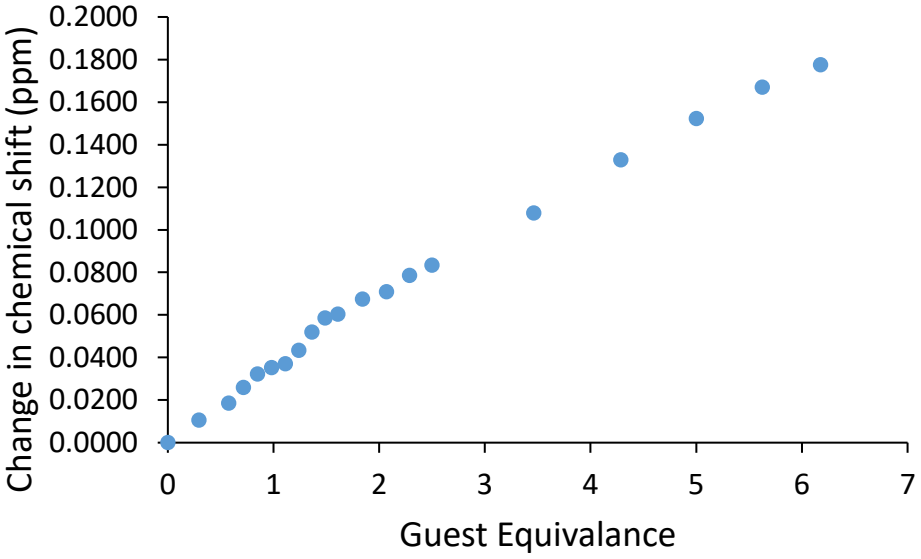

Figure S42: Change in chemical shift for the NH resonance of **1** (host) upon the addition of **14** (guest) in CD_3CN at 298 K. K_{ass} = 6.42 M^{-1} ± 1.8261%.

Bindfit link: http://app.supramolecular.org/bindfit/view/78d2596d-6e0a-4c8d-928f-fb27a33d9e48

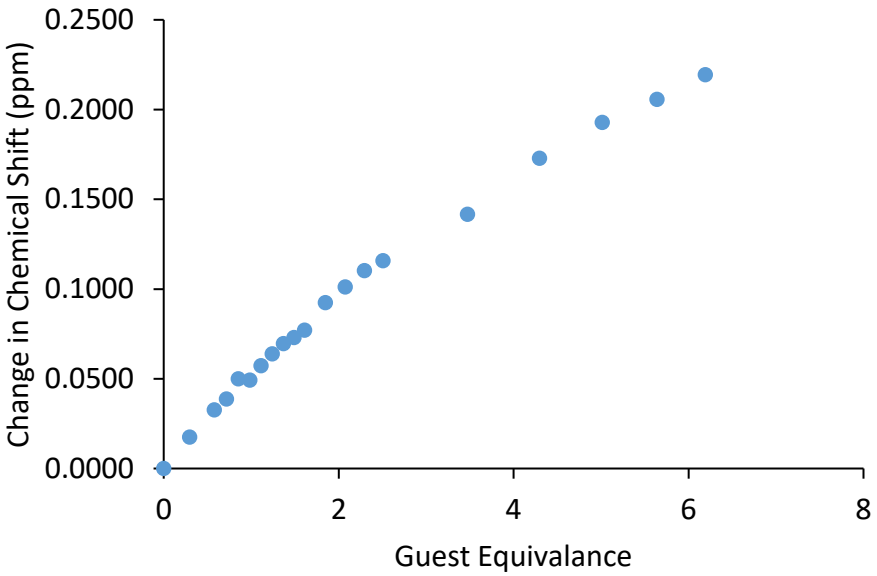

Figure S43: Change in chemical shift for the NH resonance of **1** (host) upon the addition of **15** (guest) in CD_3CN at 298 K. K_{ass} = 11.73 M^{-1} ± 1.6087%.

Bindfit link: http://app.supramolecular.org/bindfit/view/aa2cacf0-ce0a-4c3f-a4f0-8f355b318757

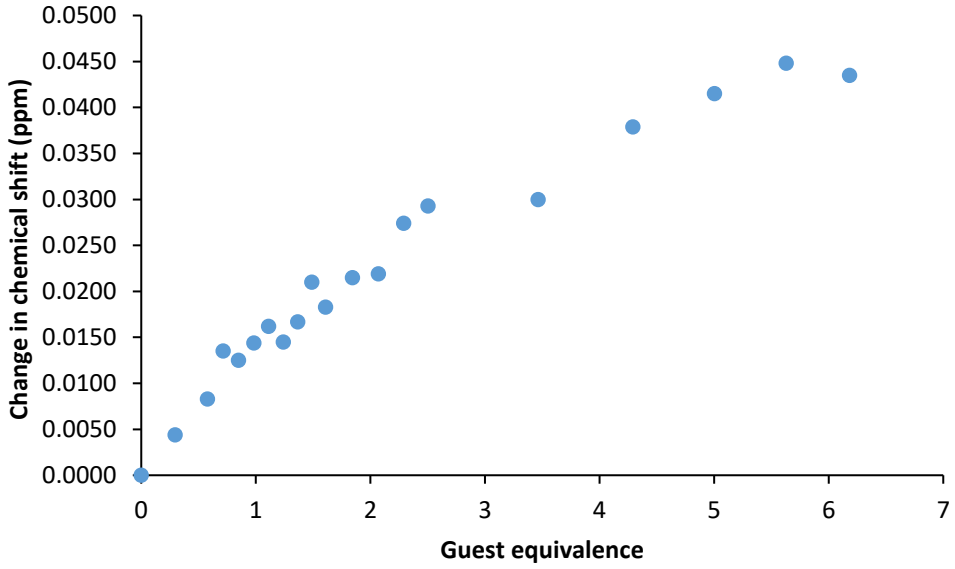

Figure S44: Change in chemical shift for the NH resonance for **1** (host) upon the addition of **16** (guest) in CD_3CN at 298 K. K_{ass} = 25.48 M^{-1} ± 6.7612 %.

Bindfit link: http://app.supramolecular.org/bindfit/view/f15d44d5-ae97-426d-a6c2-0c354641444c

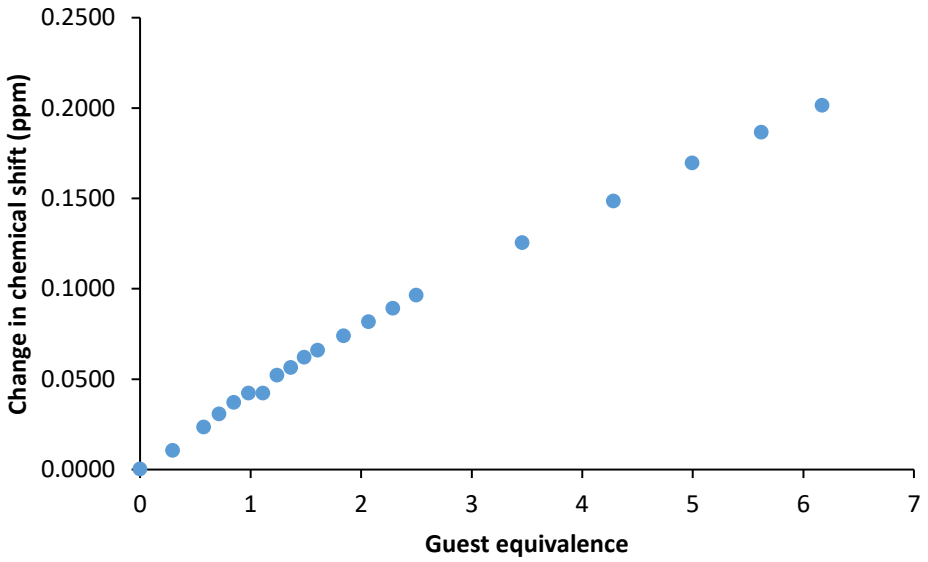

Figure S45: Change in chemical shift for the NH resonance for **1** (host) upon the addition of **17** (guest) in CD_3CN at 298 K. K_{ass} = 6.62 M^{-1} ± 1.05 %.

Bindfit link: http://app.supramolecular.org/bindfit/view/0c7ec2db-9812-4b5e-b2ee-d0cc6e5509ff

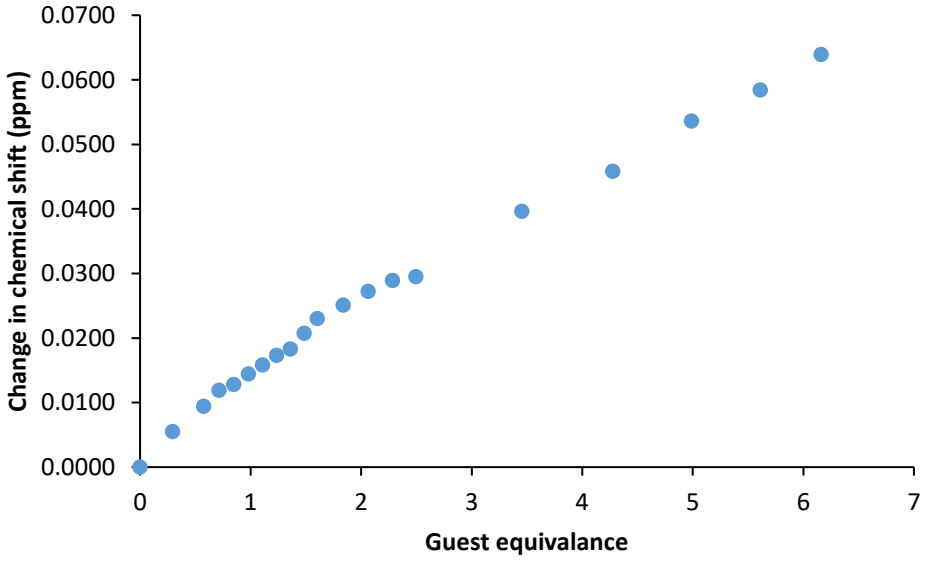

Figure S46: Change in chemical shift for the NH resonance for **1** (host) upon the addition of **18** (guest) in CD_3CN at 298 K. K_{ass} = 6.68 M^{-1} ± 2.14 %.

Bindfit link: http://app.supramolecular.org/bindfit/view/14708252-2d56-468a-a787-b9ce2633f96a

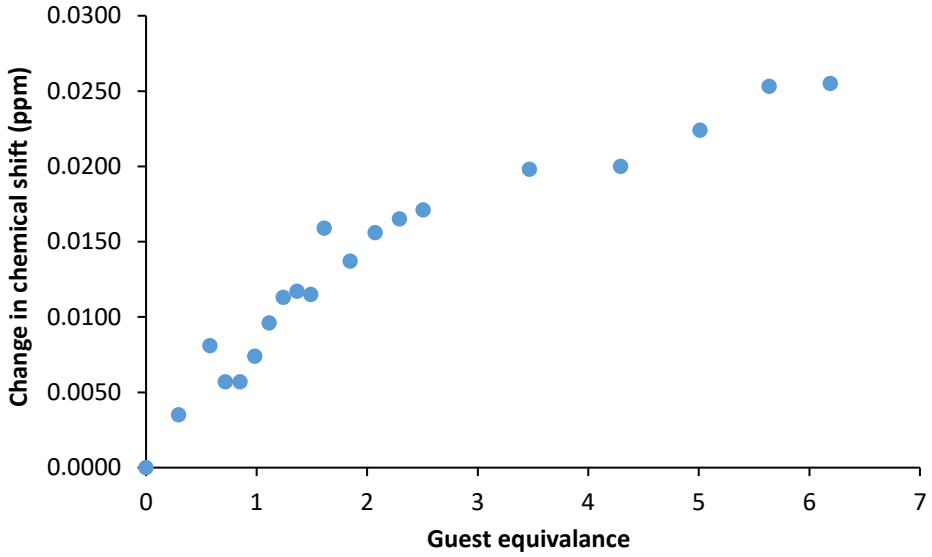

Figure S47: Change in chemical shift for the NH resonance of **1** (host) upon the addition of **19** (guest) in CD_3CN at 298 K. K_{ass} = 48.16 M^{-1} ± 10.77 %.

Bindfit link: http://app.supramolecular.org/bindfit/view/36b5a7a0-f745-4184-86b3-8d9cefd66414

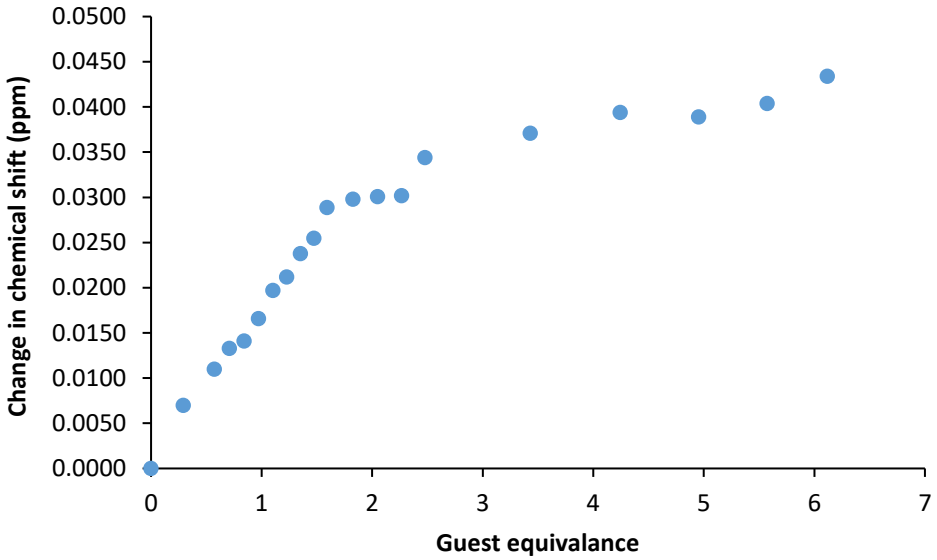

Figure S48: Change in chemical shift for the NH resonance for **1** (host) upon the addition of **20** (guest) in CD_3CN at 298 K. K_{ass} = 106.25 M^{-1} ± 8.39 %.

Bindfit link: http://app.supramolecular.org/bindfit/view/a305aa1a-78d0-40bb-9a4d-329131551e8c

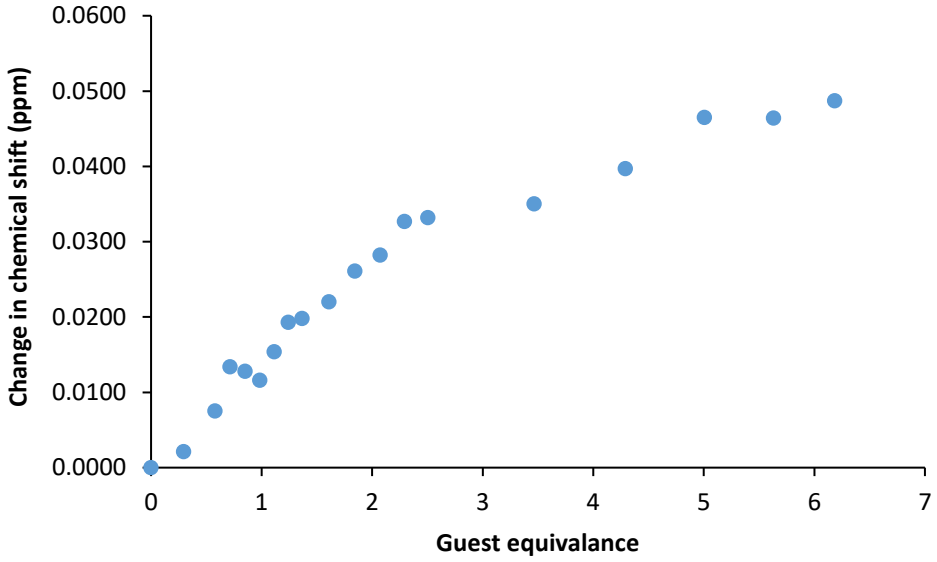

Figure S49: Change in chemical shift for the NH resonance of **1** (host) upon the addition of **21** (guest) in CD_3CN at 298 K. K_{ass} = 40.71 M^{-1} ± 7.49 %.

BindFit link: http://app.supramolecular.org/bindfit/view/8188c0f2-93d6-467d-acda-460dd2cba42d

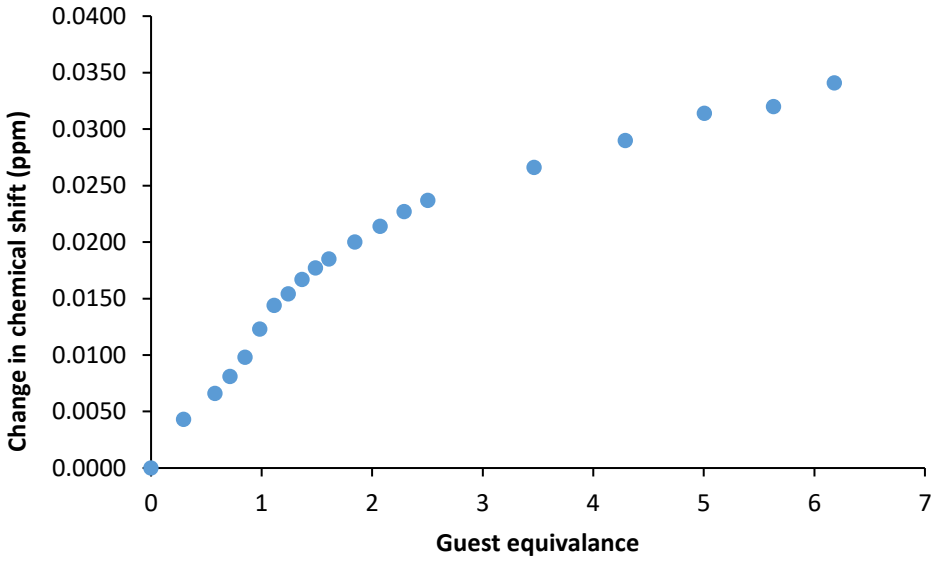

Figure S50: Change in chemical shift for the NH resonance of **1** (host) upon the addition of **22** (guest) in CD_3CN at 298 K. K_{ass} = 63.85 M^{-1} ± 4.71 %.

BindFit link: http://app.supramolecular.org/bindfit/view/7b3ab354-e64d-4402-a617-6b079312a03d

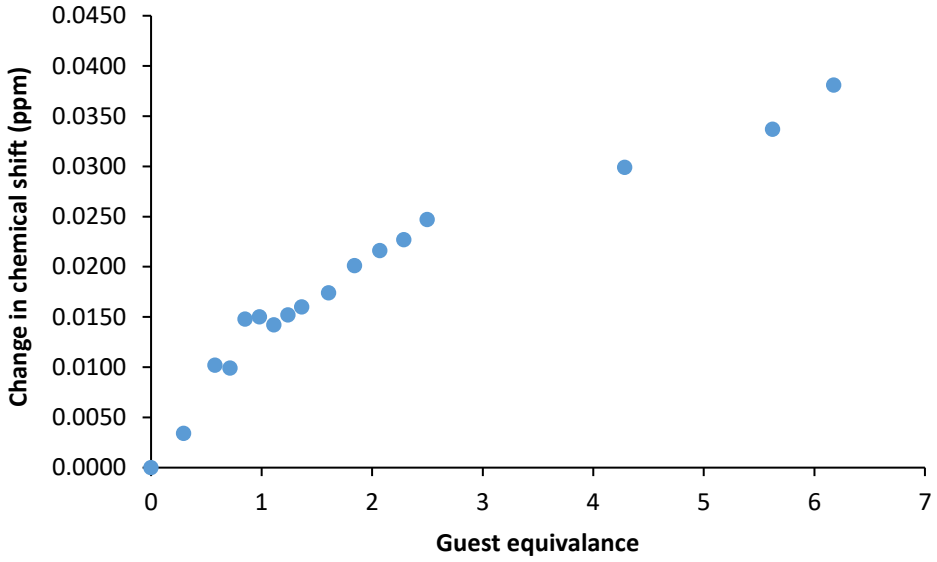

Figure S51: Change in chemical shift for the NH resonance of **1** (host) upon the addition of **23** (guest) in CD_3CN at 298 K. K_{ass} = 45.92 M^{-1} ± 9.40 %.

BindFit link: http://app.supramolecular.org/bindfit/view/735b8368-12d3-448e-bd48-b88ae4b2706f

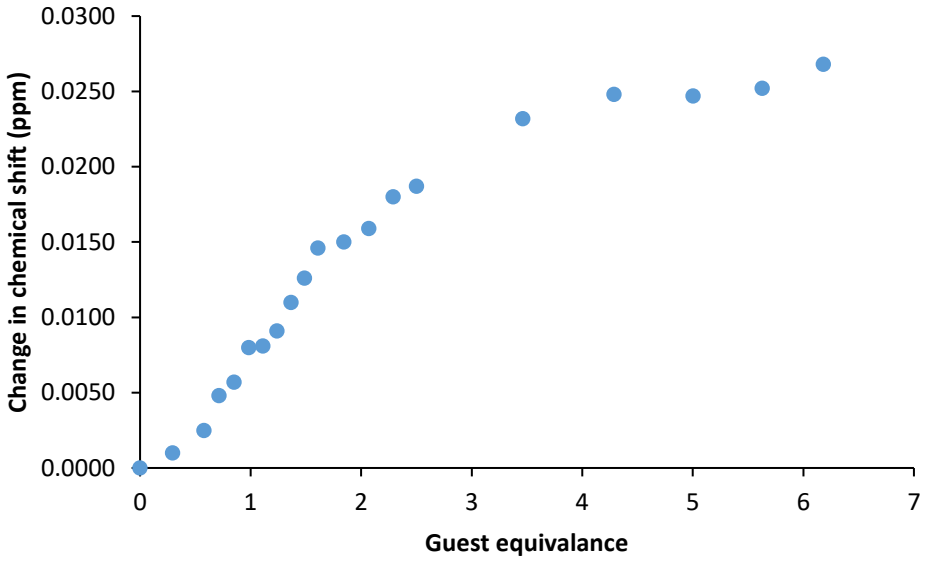

Figure S52: Change in chemical shift for the NH resonance of **1** (host) upon the addition of **24** (guest) in CD_3CN at 298 K. K_{ass} = 75.61 M^{-1} ± 6.28 %.

BindFit link: http://app.supramolecular.org/bindfit/view/c58dce05-522a-47ad-8fac-f282d82ea662

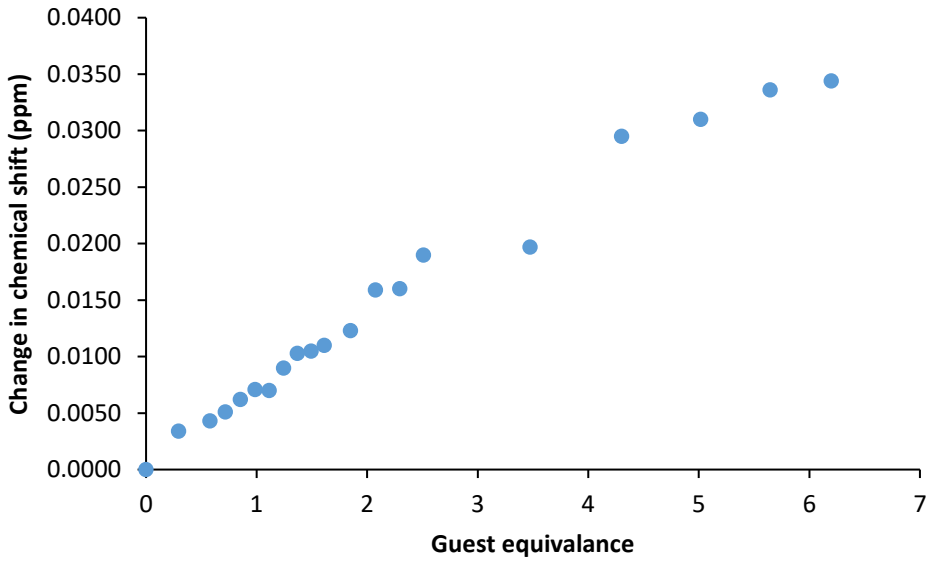

Figure S53: Change in chemical shift for the NH resonance of **1** (host) upon the addition of **25** (guest) in CD_3CN at 298 K. K_{ass} = 7.00 M^{-1} ± 4.56 %.

Bindfit link: http://app.supramolecular.org/bindfit/view/f31130c3-bf58-44f3-9b61-d32412f719d6

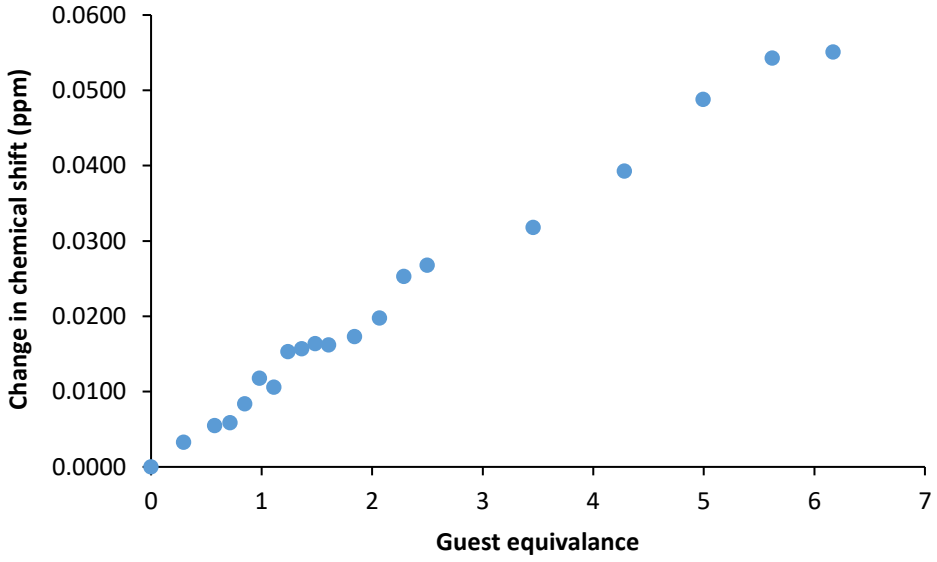

Figure S54: Change in chemical shift for the NH resonance of **1** (host) upon the addition of **26** (guest) in CD_3CN at 298 K. K_{ass} = 3.42 M^{-1} ± 3.54 %.

Bindfit link: http://app.supramolecular.org/bindfit/view/91a3c6af-f387-4bea-a131-ce52c0330a2c

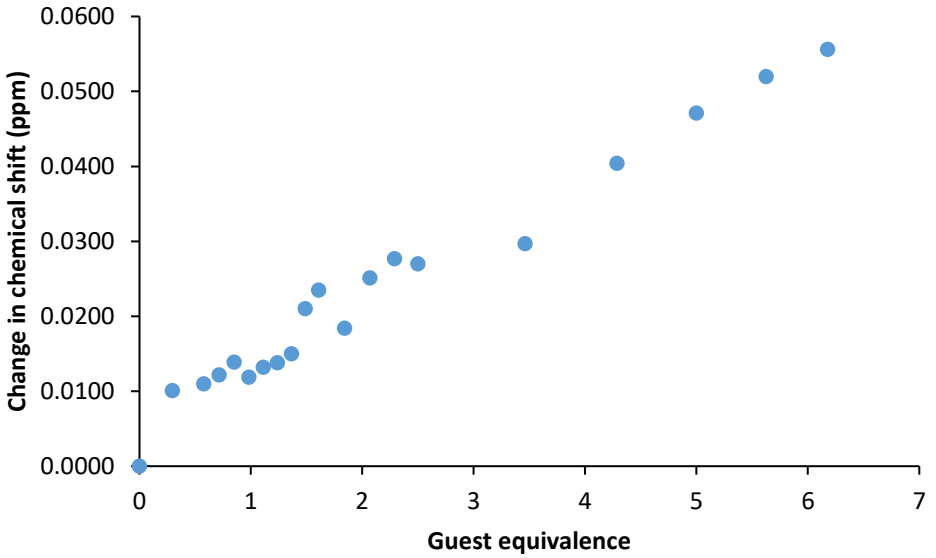

Figure S55: Change in chemical shift for the NH resonance for **2** (host) upon the addition of **5** (guest) in CD_3CN at 298 K. K_{ass} = 3.10 M^{-1} ± 6.22 %.

Bindfit link: http://app.supramolecular.org/bindfit/view/f45551ee-0a63-47bf-8032-0672ef69cca9

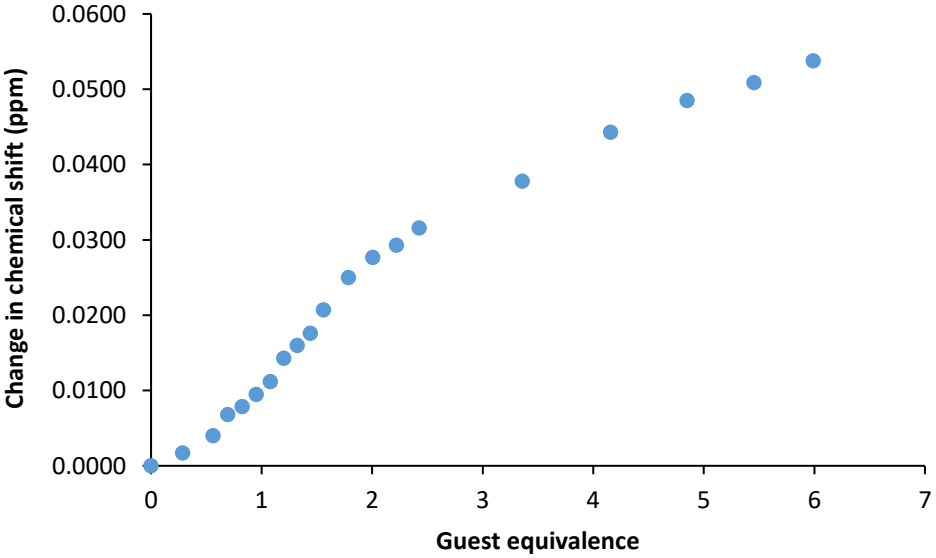

Figure S56: Change in chemical shift for the NH resonance for **2** (host) upon the addition of **6** (guest) in CD_3CN at 298 K. K_{ass} = 20.03 M^{-1} ± 5.08 %.

Bindfit link: http://app.supramolecular.org/bindfit/view/42016e96-e306-4b94-b283-1656839596d6

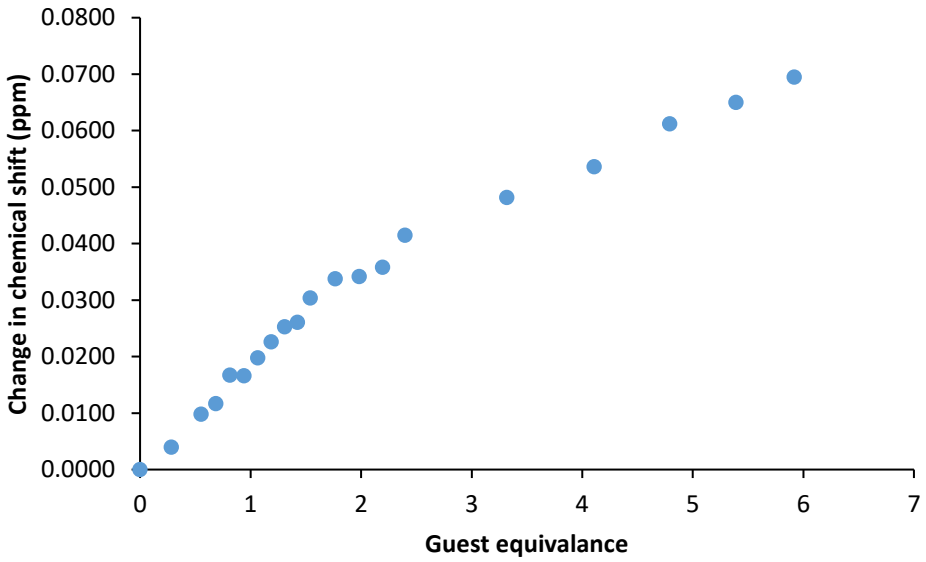

Figure S57: Change in chemical shift for the NH resonance for **2** (host) upon the addition of **8** (guest) in CD_3CN at 298 K. K_{ass} = 23.46 M^{-1} ± 3.58 %.

Bindfit link: http://app.supramolecular.org/bindfit/view/53fdddce-f2b3-450d-be29-b28429b45d41

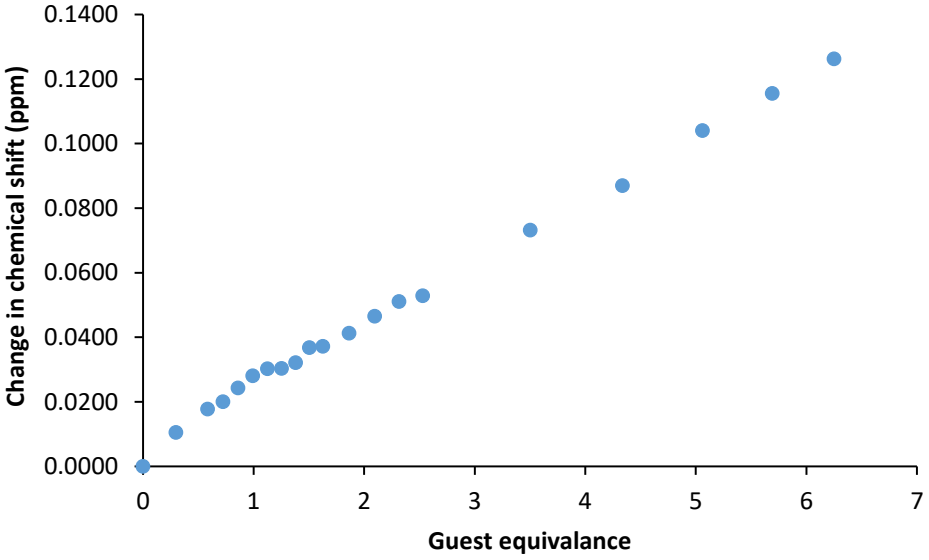

Figure S58: Change in chemical shift for the NH resonance for **2** (host) upon the addition of **10** (guest) in CD_3CN at 298 K. K_{ass} = 32.01 M^{-1} ± 7.48 %.

Bindfit link: http://app.supramolecular.org/bindfit/view/6e90f221-199d-4eff-aa7c-7b860a44307a

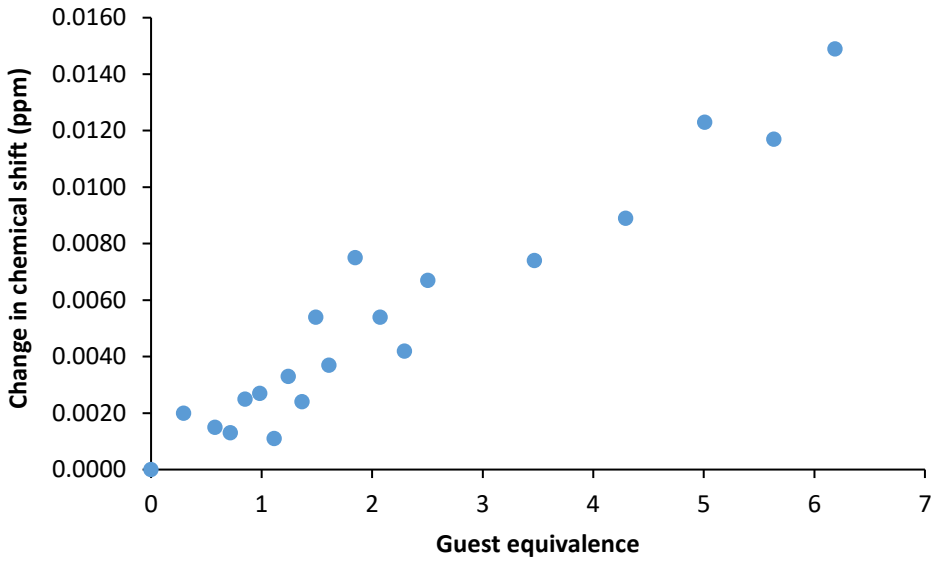

Figure S59: Change in chemical shift for the NH resonance for **2** (host) upon the addition of **16** (guest) in CD_3CN at 298 K. This data could not be fitted to a 1:1, 2:1 or 1:2 binding isotherm.

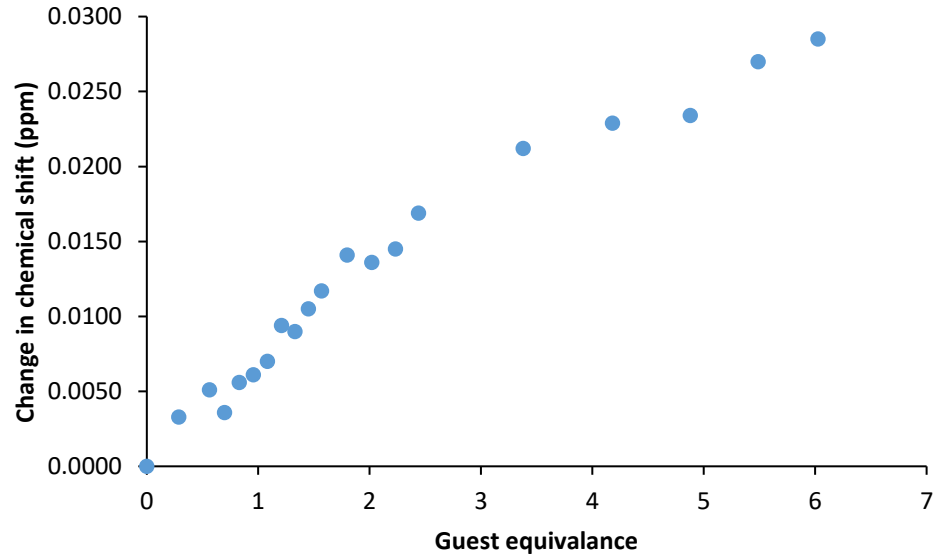

Figure S60: Change in chemical shift for the NH resonance for **2** (host) upon the addition of **18** (guest) in CD_3CN at 298 K. K_{ass} = 19.35 M^{-1} ± 5.62 %.

Bindfit link: http://app.supramolecular.org/bindfit/view/71b379ff-c9b0-43c6-9bd6-fddca0148f09

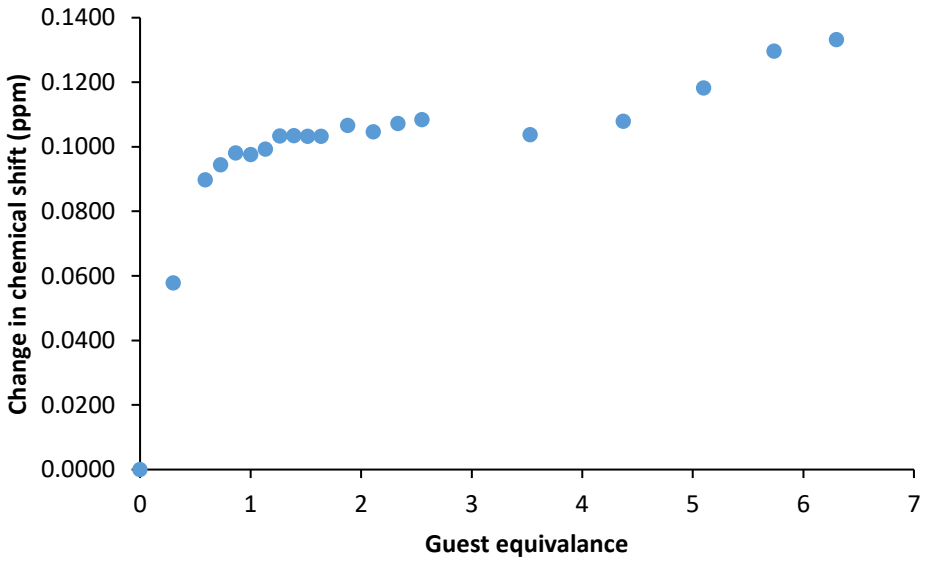

Figure S61: Change in chemical shift for the NH resonance for **2** (host) upon the addition of **20** (guest) in CD_3CN at 298 K. This data could not be fitted to a 1:1, 2:1 or 1:2 binding isotherm.

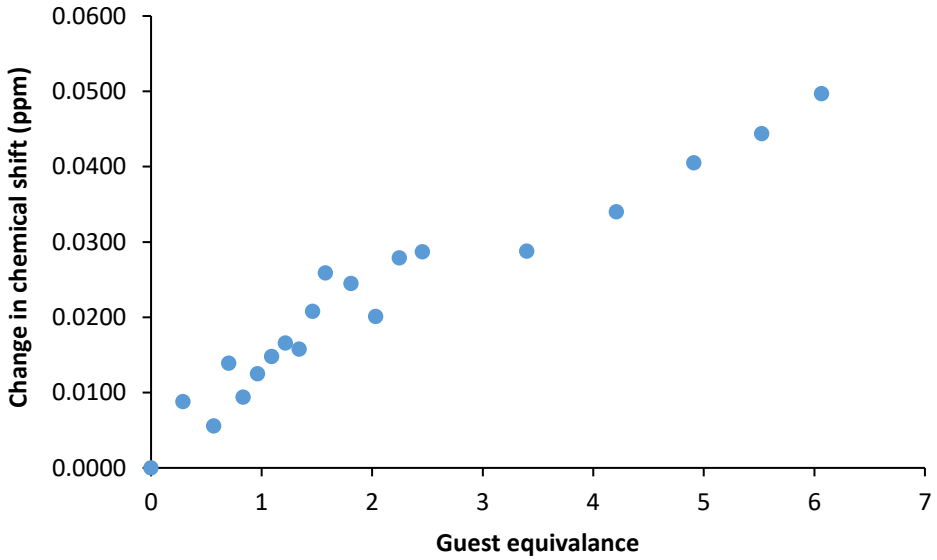

Figure S62: Change in chemical shift for the NH resonance for **3** (host) upon the addition of **5** (guest) in CD_3CN at 298 K. K_{ass} = 19.32 M^{-1} ± 11.33 %.

Bindfit link: http://app.supramolecular.org/bindfit/view/1de2d3e9-4f52-4511-950d-da5b76976e7b

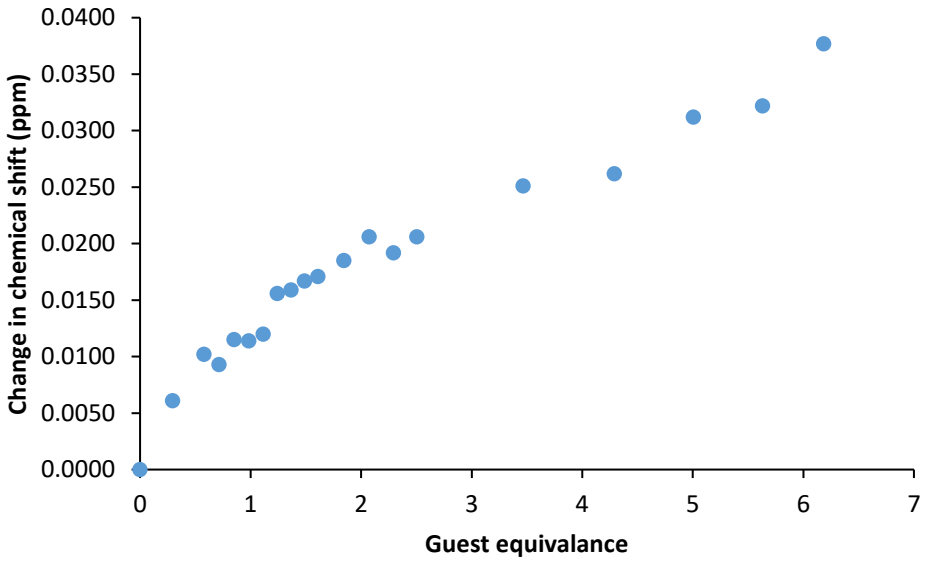

Figure S63: Change in chemical shift for the NH resonance for **3** (host) upon the addition of **6** (guest) in CD_3CN at 298 K. K_{ass} = 27.28 M^{-1} ± 8.69 %.

Bindfit link: http://app.supramolecular.org/bindfit/view/1f70a889-a047-406c-b11f-0d866a5898f8

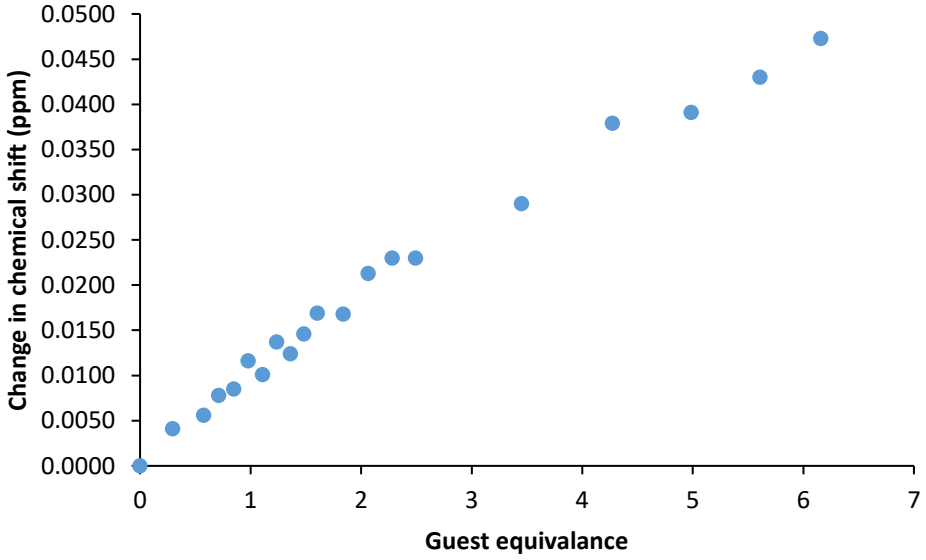

Figure S64: Change in chemical shift for the NH resonance for **3** (host) upon the addition of **8** (guest) in CD_3CN at 298 K. K_{ass} = 8.76 M^{-1} ± 3.37 %.

Bindfit link: http://app.supramolecular.org/bindfit/view/e17ebb8e-4bfd-4e99-b1e6-f2f640c1da32

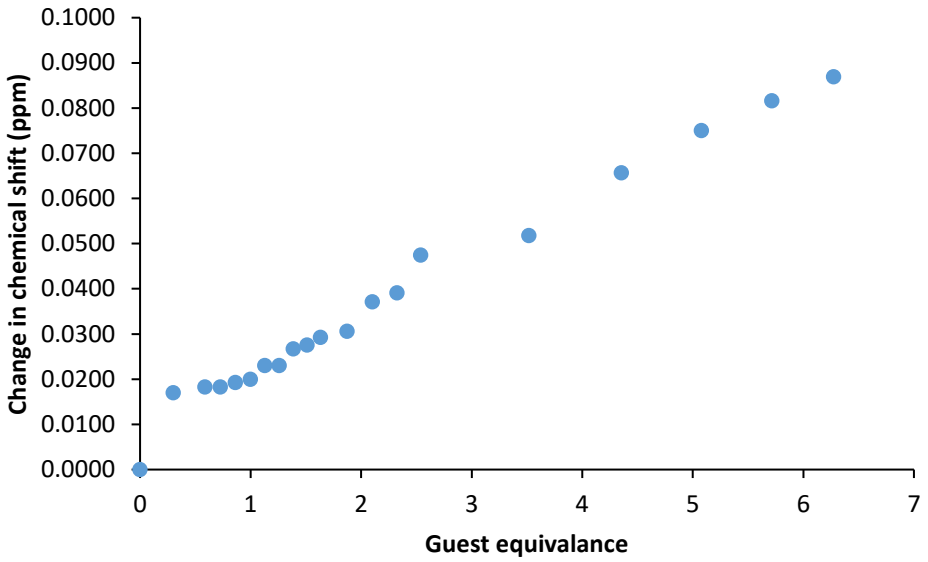

Figure S65: Change in chemical shift for the NH resonance for **3** (host) upon the addition of **10** (guest) in CD_3CN at 298 K. K_{ass} = 3.16 M^{-1} ± 4.25 %.

Bindfit link: http://app.supramolecular.org/bindfit/view/1d99c38f-3cf1-43af-a322-8f4a8415f495

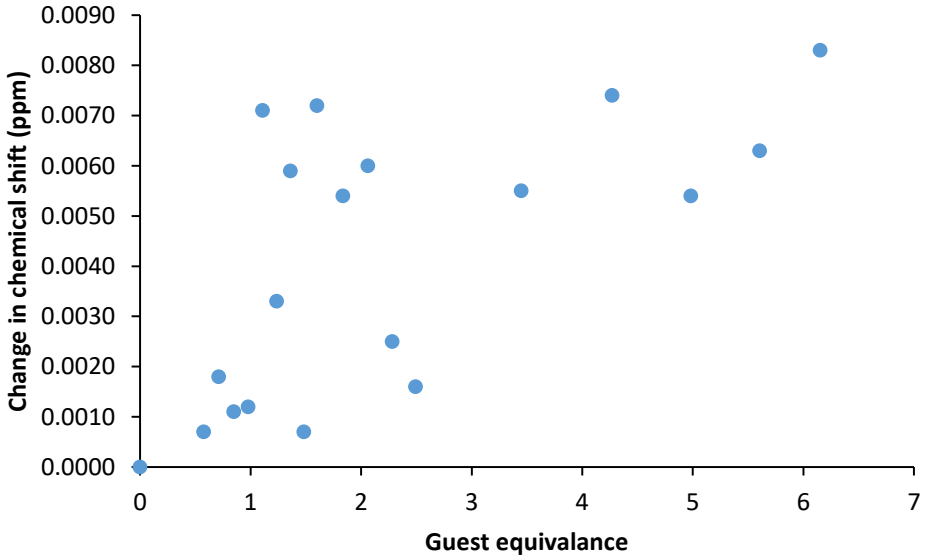

Figure S66: Change in chemical shift for the NH resonance for **3** (host) upon the addition of **16** (guest) in CD_3CN at 298 K. This data could not be fitted to a 1:1, 2:1 or 1:2 binding isotherm.

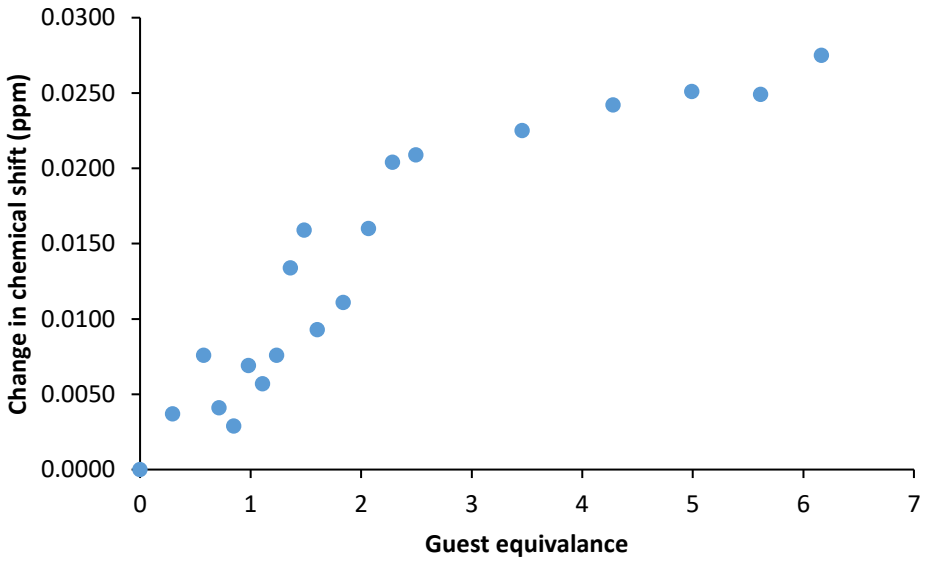

Figure S67: Change in chemical shift for the NH resonance for **3** (host) upon the addition of **18** (guest) in CD_3CN at 298 K. This data could not be fitted to a 1:1, 2:1 or 1:2 binding isotherm.

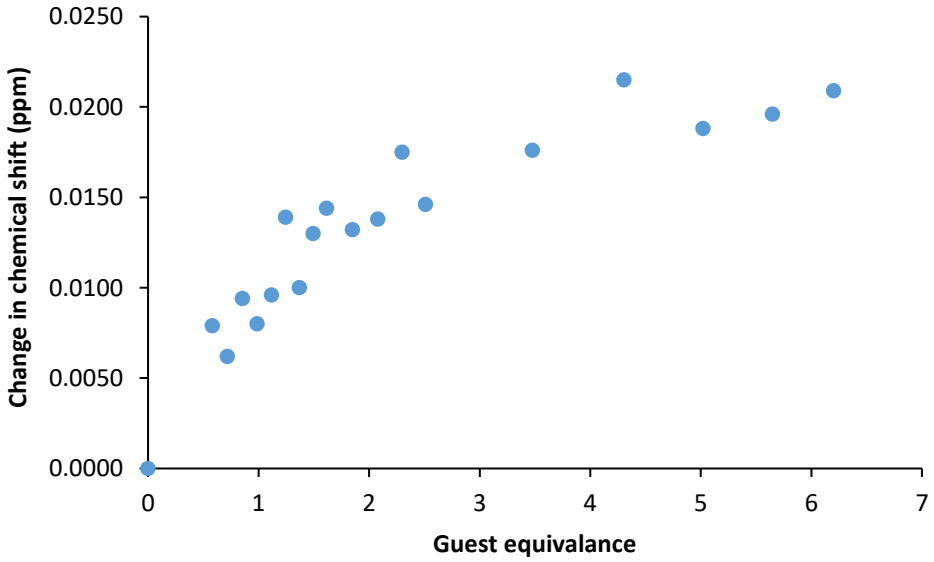

Figure S68: Change in chemical shift for the NH resonance for **3** (host) upon the addition of **20** (guest) in CD_3CN at 298 K. This data could not be fitted to a 1:1, 2:1 or 1:2 binding isotherm.

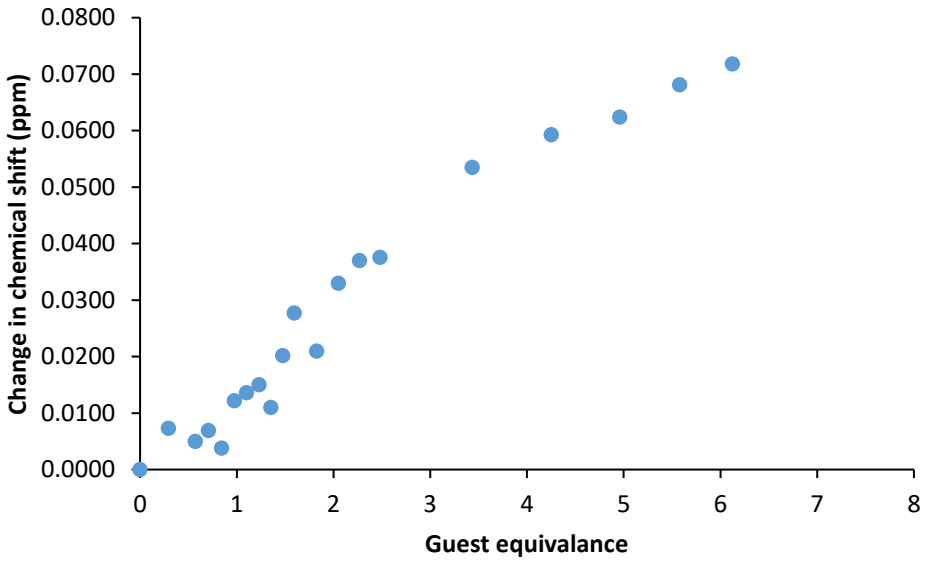

Figure S69: Change in chemical shift for the NH resonance for **4** (host) upon the addition of **5** (guest) in CD_3CN at 298 K. K_{ass} = 9.80 M^{-1} ± 7.71 %.

Bindfit link: http://app.supramolecular.org/bindfit/view/5841178c-5c2c-463a-83a4-2f9bd97dad7c

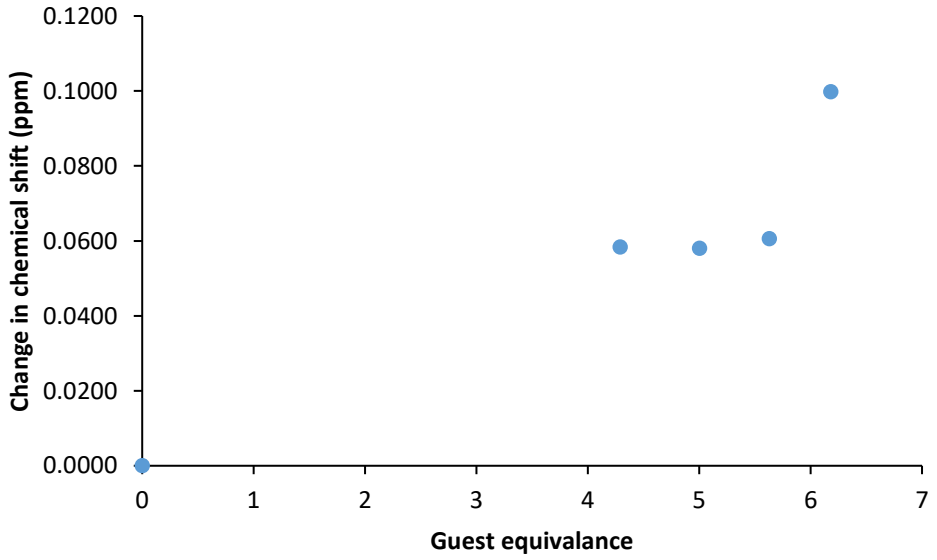

Figure S70: Change in chemical shift for the NH resonance for **4** (host) upon the addition of **6** (guest) in CD_3CN at 298 K. Due to peak overlap, the chemical shift for the NH resonance could not be followed accurately.

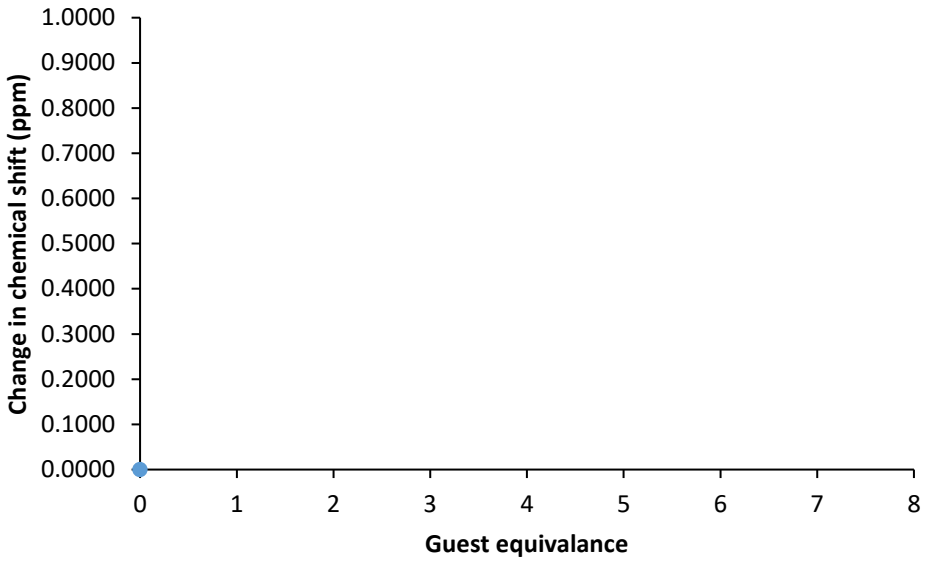

Figure S71: Change in chemical shift for the NH resonance for **4** (host) upon the addition of **8** (guest) in CD_3CN at 298 K. Due to peak overlap, the chemical shift for the NH resonance could not be followed accurately.

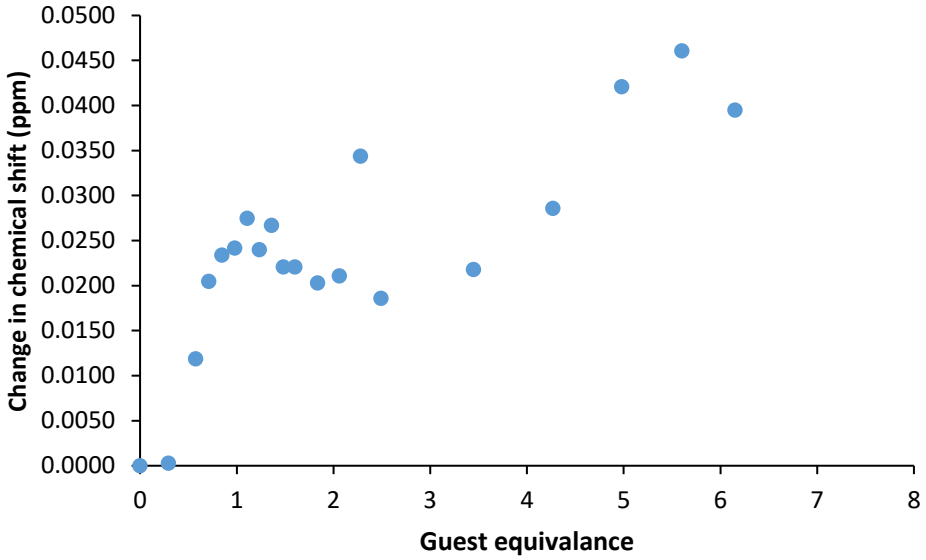

Figure S72: Change in chemical shift for the NH resonance for **4** (host) upon the addition of **10** (guest) in CD_3CN at 298 K. This data could not be fitted to a 1:1, 2:1 or 1:2 binding isotherm.

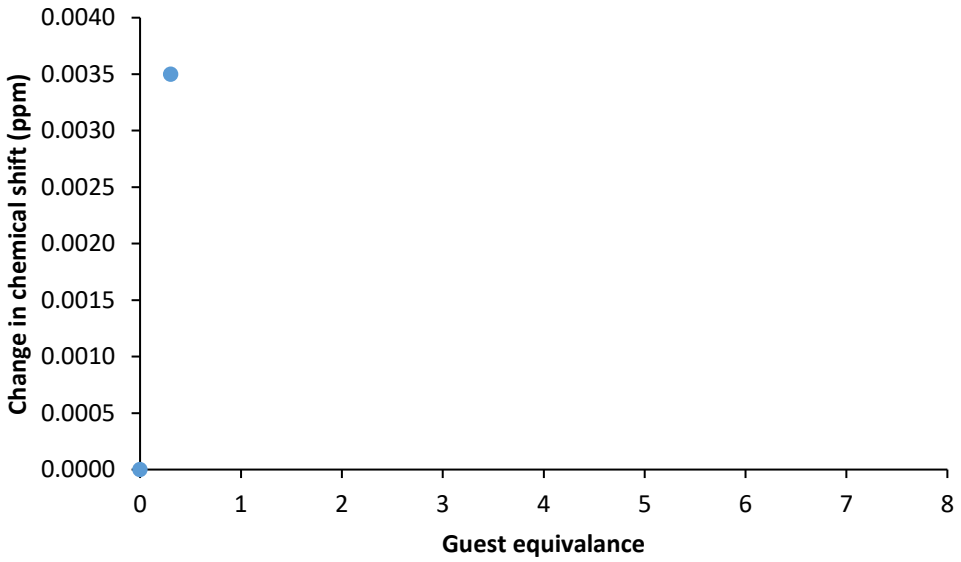

Figure S73: Change in chemical shift for the NH resonance for **4** (host) upon the addition of **16** (guest) in CD_3CN at 298 K. Due to peak overlap, the chemical shift for the NH resonance could not be followed accurately.

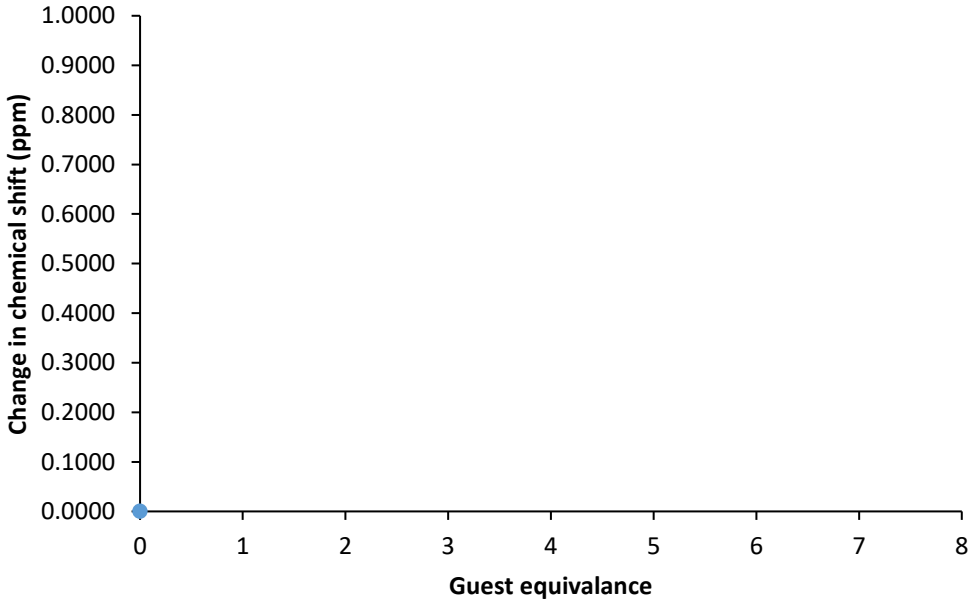

Figure S74: Change in chemical shift for the NH resonance for **4** (host) upon the addition of **18** (guest) in CD_3CN at 298 K. Due to peak overlap, the chemical shift for the NH resonance could not be followed accurately.

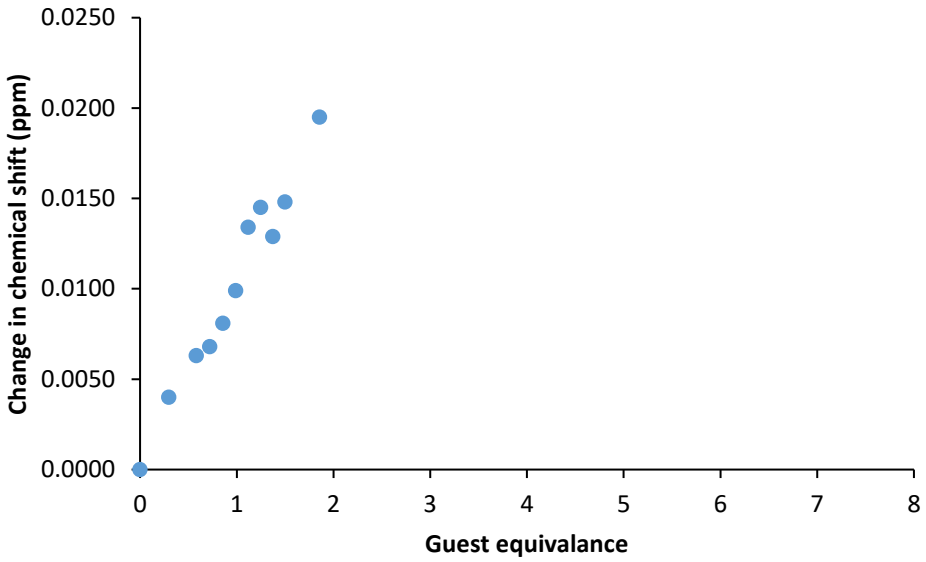

Figure S75: Change in chemical shift for the NH resonance for **4** (host) upon the addition of **20** (guest) in CD_3CN at 298 K. Due to peak overlap, the chemical shift for the NH resonance could not be followed accurately.

Job Plot analysis

Two solutions were produced; the first solution was a 3 mL, 0.01 M solution of the receptor and the second was a 3 mL, 0.01 M solution of the simulant. Of the receptor solution 0.5 mL was added to a NMR tube. The amount of receptor solution was then decreased by 0.05 mL and the amount of simulant solution increased by 0.05 mL for each successive NMR tubes until a 9:1 simulant:receptor ratio was reached. A ^{1}H NMR spectra was taken for each of the ten NMR tubes and calibrated to the solvent peak. The data was then used to produce a job plot, in accordance with the methods described by Job. Plotting the molar fraction of the receptor against the values given in the formula:

$$\frac{\boldsymbol{\delta obs} - \boldsymbol{\delta int}}{\boldsymbol{\delta fin} - \boldsymbol{\delta int}} \boldsymbol{x\, \chi r}$$

Where $\boldsymbol{\delta obs}$ is the observed chemical shift, $\boldsymbol{\delta int}$ is the initial chemical shift, $\boldsymbol{\delta fin}$ is the final chemical shift and $\boldsymbol{\chi r}$ is the molar fraction of the receptor

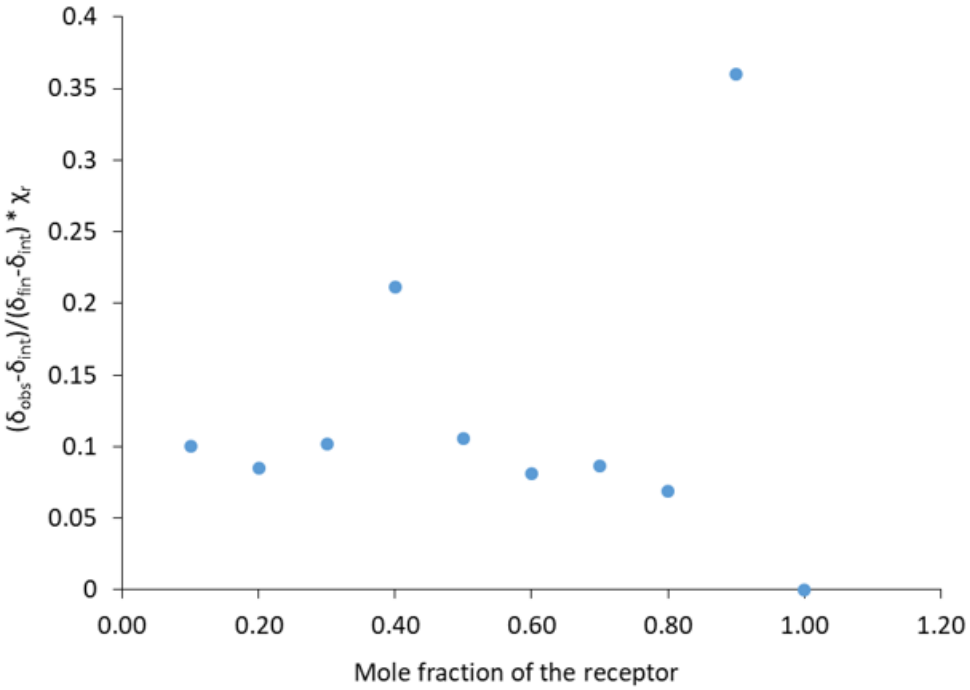

Figure S76: Job plot analysis for receptor **1** and compound **16**.

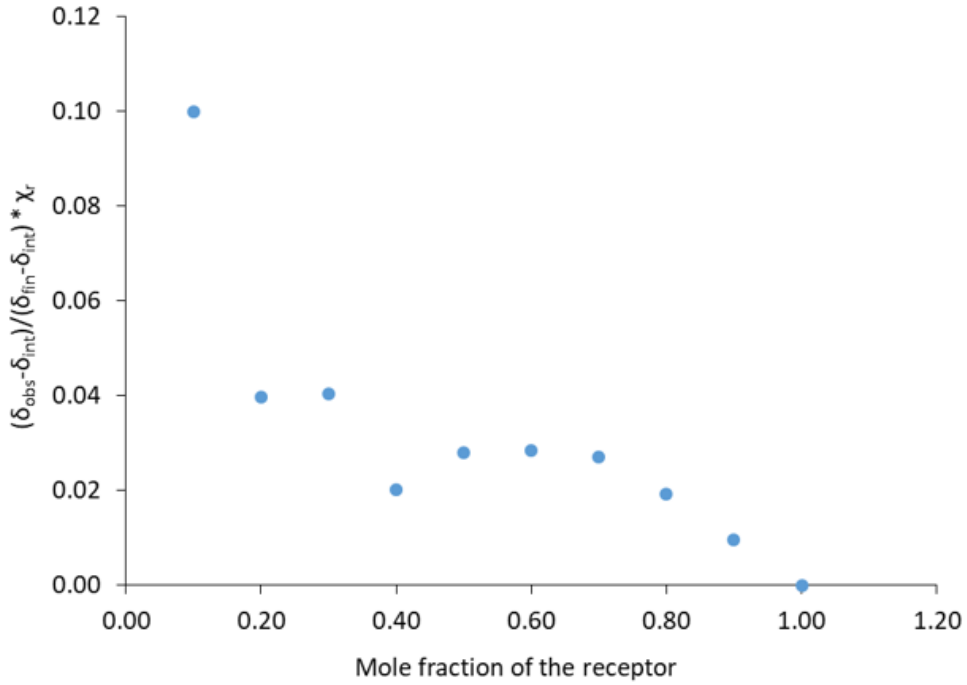

Figure S77: Job plot analysis for receptor **1** and compound **20**.

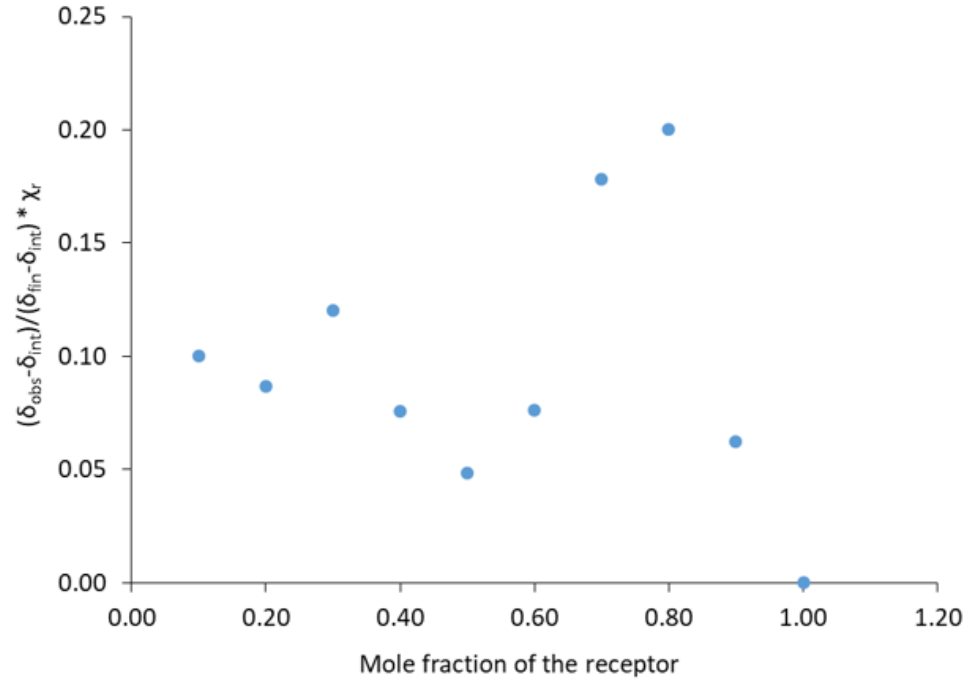

Figure S78: Job plot analysis for receptor **1** and compound **22**.

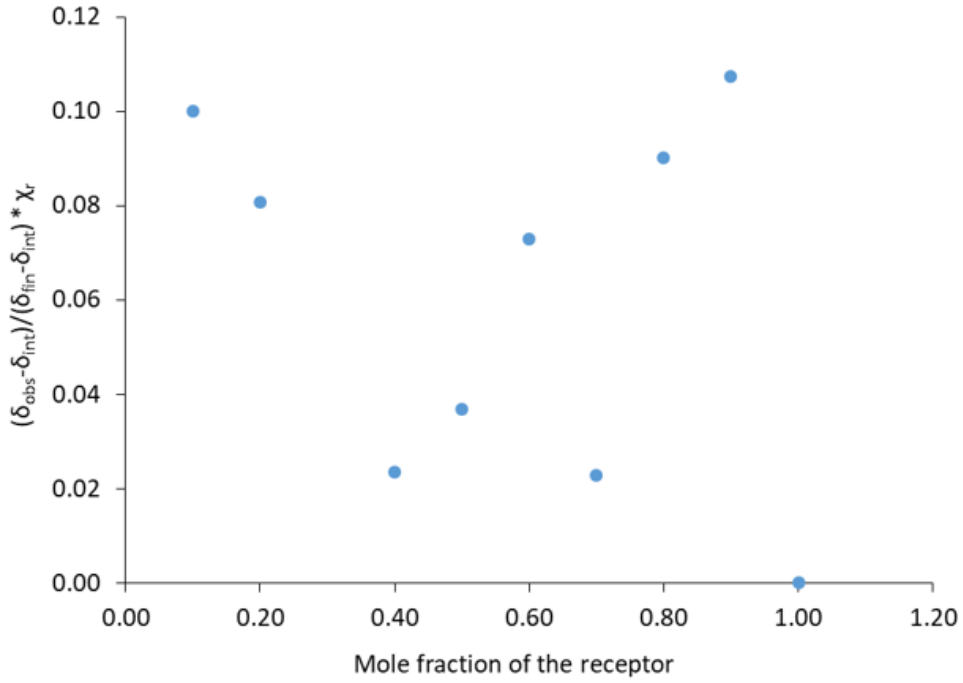

Figure S79: Job plot analysis for receptor **1** and compound **23**.

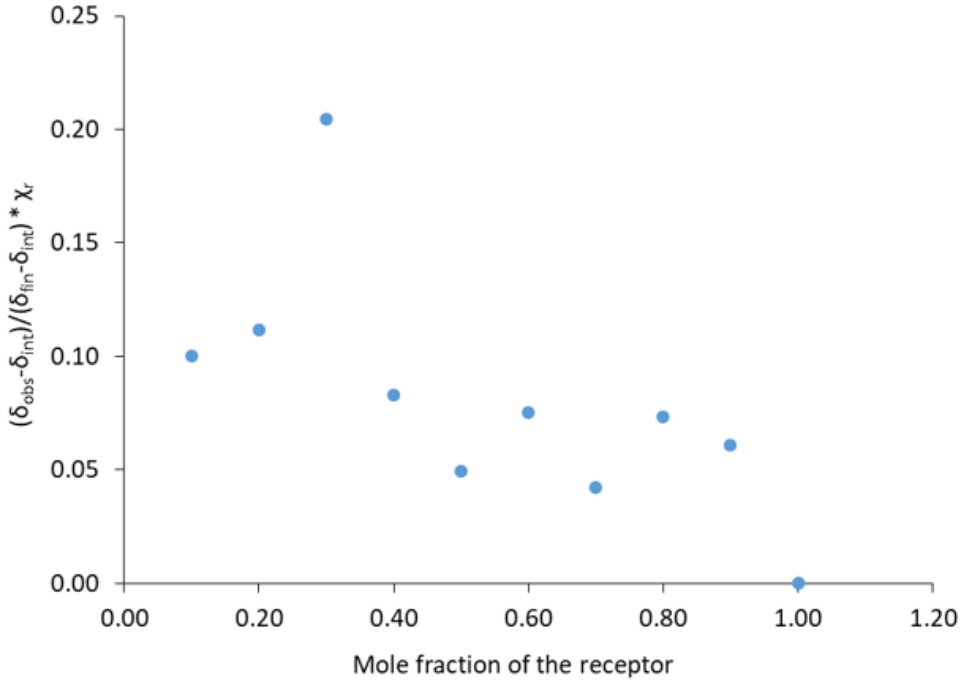

Figure S80: Job plot analysis for receptor **1** and compound **24**.

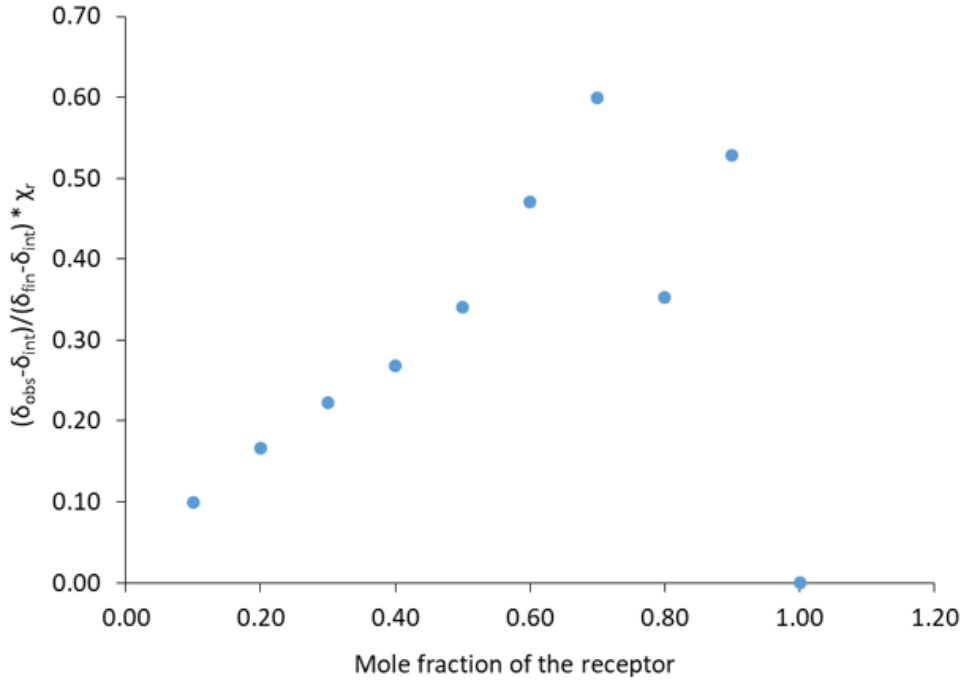

Figure S81: Job plot analysis for receptor **2** and compound **6**.

Single crystal X-ray structure information

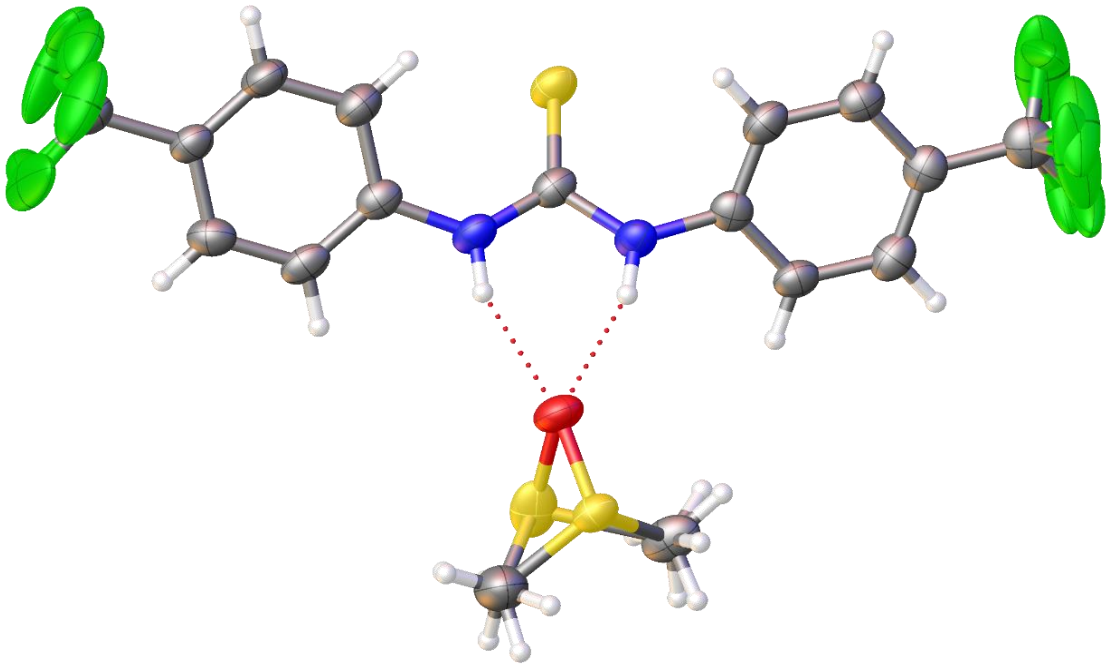

Figure S82: Crystal data for compound **1**: red = oxygen; yellow = sulfur; blue = nitrogen; white = hydrogen; grey = carbon; green = fluorine. CCDC 1855728, $C_{17}H_{16}F_6N_2OS_2$ (M =442.44): monoclinic, space group P 21/c, a = 9.5039(12) Å, b = 8.281(2) Å, c = 24.124(8) Å, α = 90°, β = 96.83(2)°, γ = 90°, V = 1885.1(8) $Å^3$, Z = 4, T = 100(1) K, CuK\α = 1.5418 Å, Dcalc = 1.559 g/cm^3, 11491 reflections measured ($7.382 \leq 2\Theta \leq 133.200$), 3331 unique ($R_{int}$ = 0.1420, R_{sigma} = 0.1376) which were used in all calculations. The final R_1 was 0.0709 ($I > 2\sigma(I)$) and wR_2 was 0.1800 (all data).

Hydrogen bonding table from single crystal X-ray structure

Table S1: Hydrogen bond distances and angles observed for hydrogen bonded complex formation, calculated from single crystal X-ray structure, Figure S95.

Compound	Hydrogen bond donor	Hydrogen atom	Hydrogen bond acceptor	Hydrogen bond length (D•••A) (Å)	Hydrogen bond angle (D-H•••A) (°)
1	N1	H1	O1	2.875 (6)	156.8 (3)
1	N2	H2	O1	2.808 (6)	164.6 (2)

Biological testing

Schizosaccharomyces pombe toxicity screening experimental

Preparation of amino acid solution: Adenine (5.63 g, 41.66 mmol), leucine (5.63 g, 41.00 mmol), histidine (5.63 g, 36.26 mmol) and uracil (5.63 g, 46.07 mmol) were dissolved into distilled H_2O (500 mL), autoclaved then allowed to cool to room temperature.

Preparation of agar plates and initial cell growth: Yeast extract (10 g) and glucose (60.0 g, 333.03 mmol) were dissolved in distilled H_2O (2000 mL). This stock solution was then divided equally into five bottles. Agar (6 g) was then dissolved into each 400 mL YES media stock solution. The bottles were autoclaved then allowed to cool to room temperature and to each stock solution was added the pre-prepared amino acid solution (8 mL). This solution was then immediately poured into sterile Petri dishes under sterile conditions. The plates were then left to set and stored at 4 °C. Prototroph *Schizosaccharomyces pombe* cells were then streaked onto the agar plates under sterile conditions, sealed using Parafilm then grown at 25 °C for two days.

EMMG (Edinburg minimal media with glutamic acid) media preparation: EMM powder without nitrogen (27.30 g) and *L*-glutamic acid monosodium salt hydrate (3.38 g, 19.99 mmol) were dissolved in distilled H_2O (1000 mL). The EMMG media was then poured into bottles, autoclaved and allowed to cool to room temperature before use.

Preparation of 96 well plates for *S. pombe* toxicity screening: EMMG media (20 mL) was inoculated in a sterile Falcon using single colonies from the YES plate and incubated overnight at 25 °C with shaking. The cell density was calculated using a haemocytometer on the following day and the number of generation times were calculated using equation 1. The cell suspension was then diluted using equation 2 to reach a cell density of $2x10^6$ cells/mL when grown for a further 20 hours. After 20 hours a final dilution with EMMG media was carried out to produce a cell suspension with a density of $0.5x10^6$ cells/mL when grown for a further 20 hours. Once the suspension had reached a cell density of $0.5x10^6$ cells/mL, an aliquot of the suspension (120 µL) was added to each well of the 96 well plate.

$$\text{Number of generation times} = \frac{\text{Incubation Time}}{\text{Generation time}}$$

Equation 1: Equation to calculate the number of generation times, calculated by dividing the time the culture is growing in EMMG media by the number generation time. Our cell suspensions were grown over 20 hours (incubation time) and the generation time was 4.

$$\text{Volume of Suspension needed for dilution} = 1000 \times \left[\left(\frac{\text{Desired volume (mL)} \times \text{Desired Cell Density (cells/mL)}}{2^{\text{Number of Generation times}}} \right) \div \text{Current Density} \right]$$

Equation 2: The dilution equation to calculate the volume of suspension needed to inoculate a specific volume to a specific concentration after a specific period of time. The desired volume used was 20 mL, the desired cell density as stated in text and the number of generation times was calculated using Equation 1.

A 10mM stock solution of each compound (**5-26**) to be tested was prepared in a sterile 1:19 Ethanol: Distilled water mixture no longer than 2 hours before the start of the toxicity screening

experiment. An aliquot (60 µL) of an appropriate compound stock solution was then added to a single well on the pre-prepared 96 well plate. Each experiment was repeated three times. A baseline for cell growth in the absence of compounds **5**-**26** was obtained through the addition of an aliquot of a sterile 1:19 Ethanol: Distilled water mixture (60 µL) to twelve wells of the 96 well plate, to ensure stable growth. The 96 well plates were then sealed using Parafilm and incubated in a plate reader at 25°C with shaking. An absorbance reading at 600 nm was taken every 15 minutes for 45 hours.

***S. Pombe* screening Results**

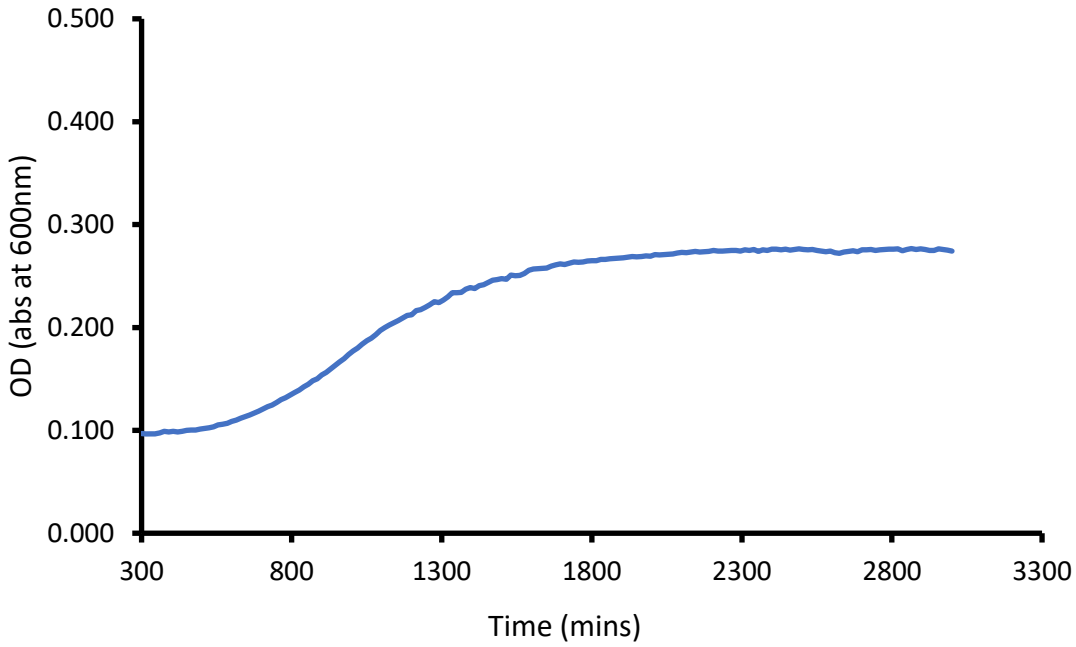

Figure S83: *S. pombe* growth curve. Data shown represents an average of six experiments. Graph shows the addition of a 1:19 EtOH:H_2O **control** solution (60 µL) to a suspension of cells (density = $0.5x10^6$ cells/mL) in EMMG media (120 µL). Data displayed from 300 minutes due to initial plate reader calibration.

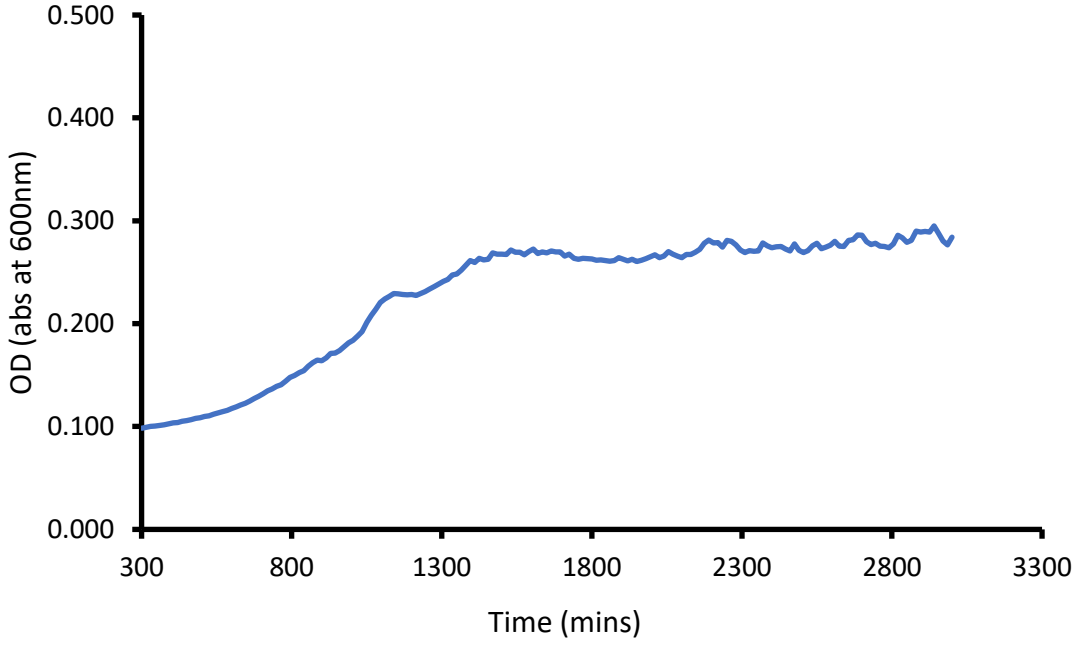

Figure S84: *S. pombe* growth curve. Data shown represents an average of three experiments. Graph shows the addition of 1:19 EtOH:H_2O solution of **5** (10 mM, 60 µL) to a suspension of cells (density = $0.5x10^6$ cells/mL) in EMMG media (120 µL). Data displayed from 300 minutes due to initial plate reader calibration.

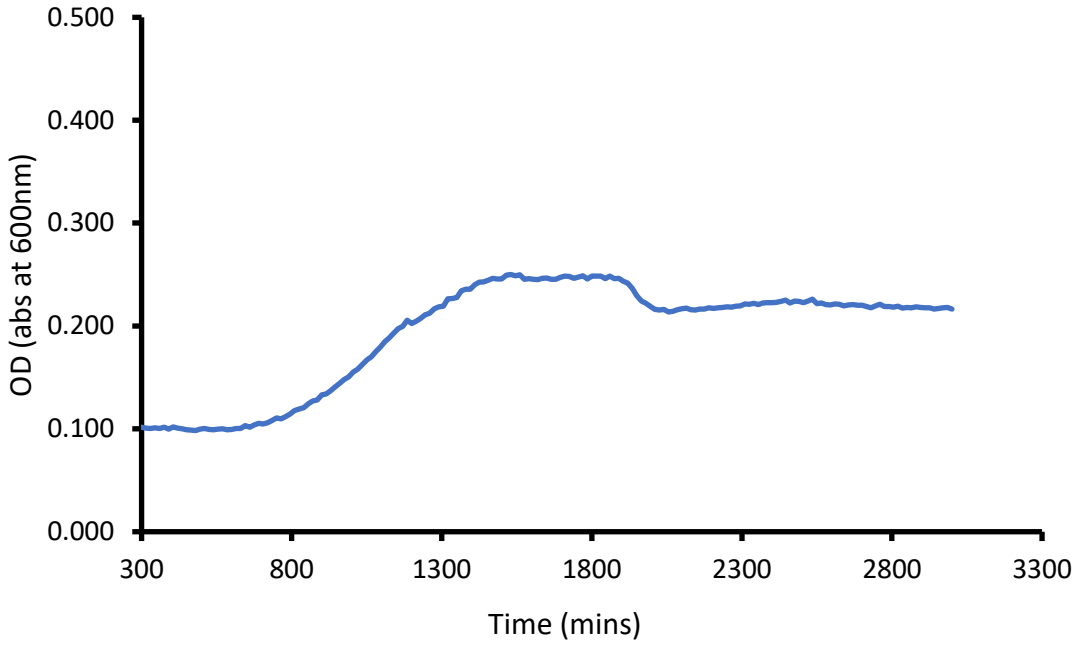

Figure S85: *S. pombe* growth curve. Data shown represents an average of three experiments. Graph shows the addition of 1:19 EtOH:H_2O solution of **6** (10 mM, 60 µL) to a suspension of cells (density = $0.5x10^6$ cells/mL) in EMMG media (120 µL). Data displayed from 300 minutes due to initial plate reader calibration.

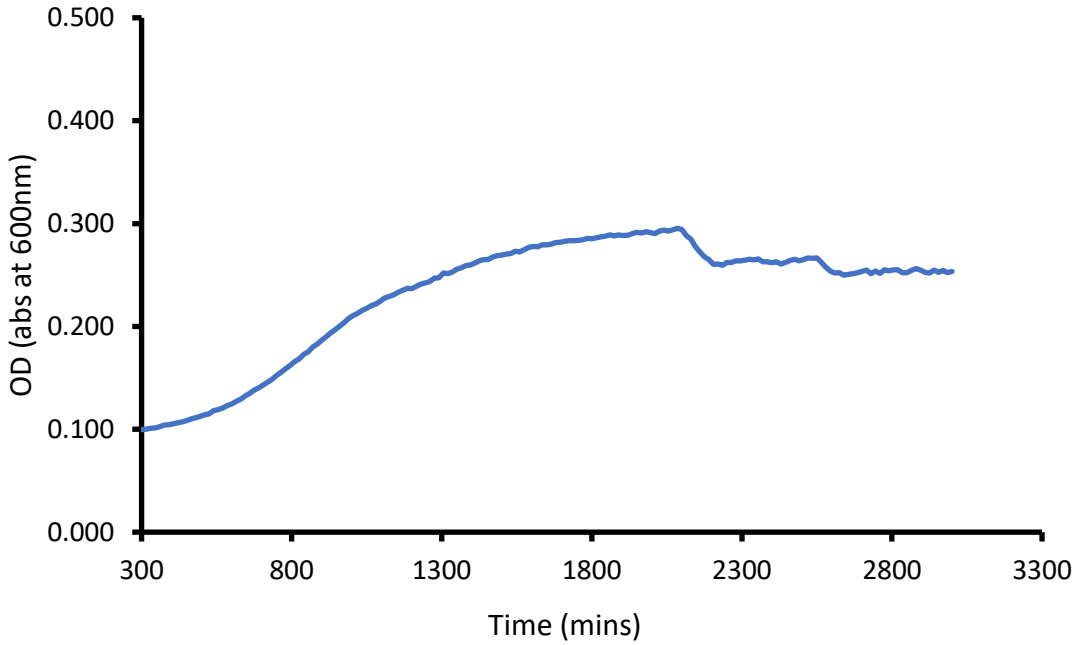

Figure S86: *S. pombe* growth curve. Data shown represents an average of three experiments. Graph shows the addition of 1:19 EtOH:H_2O solution of **7** (10 mM, 60 µL) to a suspension of cells (density = $0.5x10^6$ cells/mL) in EMMG media (120 µL). Data displayed from 200 minutes due to initial plate reader calibration.

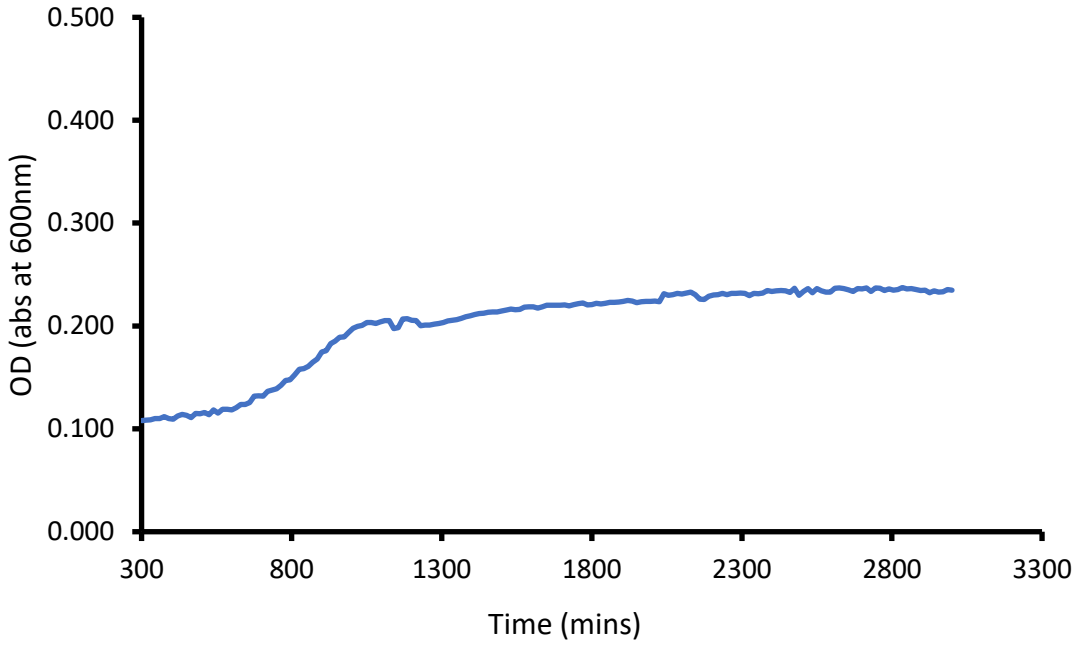

Figure S87: *S. pombe* growth curve. Data shown represents an average of three experiments. Graph shows the addition of 1:19 EtOH:H_2O solution of **8** (10 mM, 60 µL) to a suspension of cells (density = $0.5x10^6$ cells/mL) in EMMG media (120 µL). Data displayed from 300 minutes due to initial plate reader calibration.

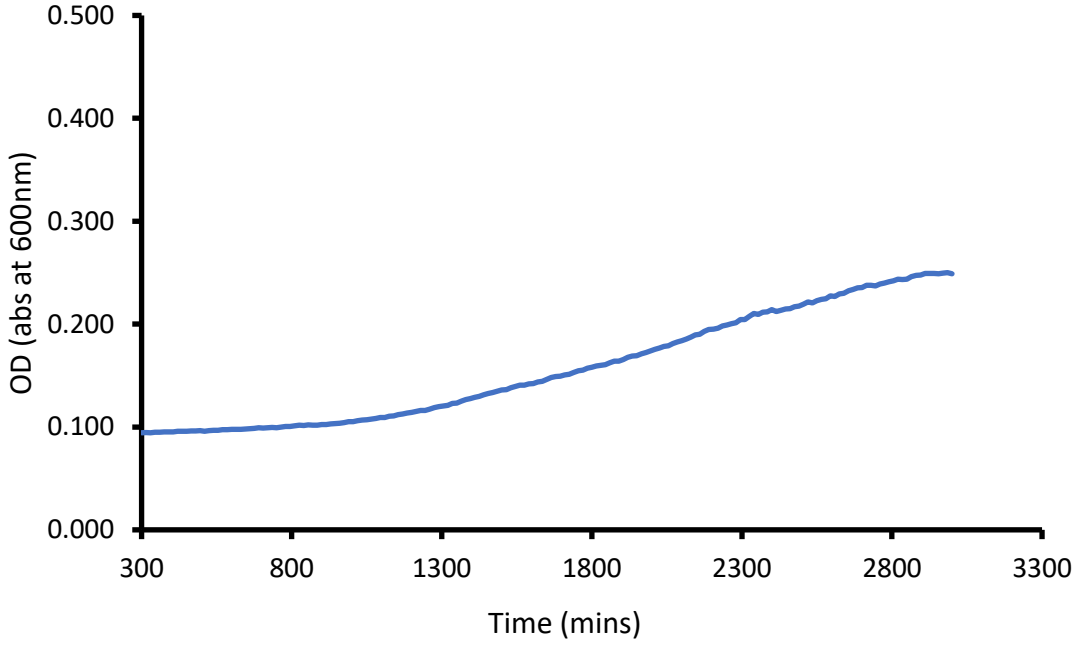

Figure S88: *S. pombe* growth curve. Data shown represents an average of three experiments. Graph shows the addition of 1:19 EtOH:H_2O solution of **9** (10 mM, 60 µL) to a suspension of cells (density = $0.5x10^6$ cells/mL) in EMMG media (120 µL). Data displayed from 300 minutes due to initial plate reader calibration.

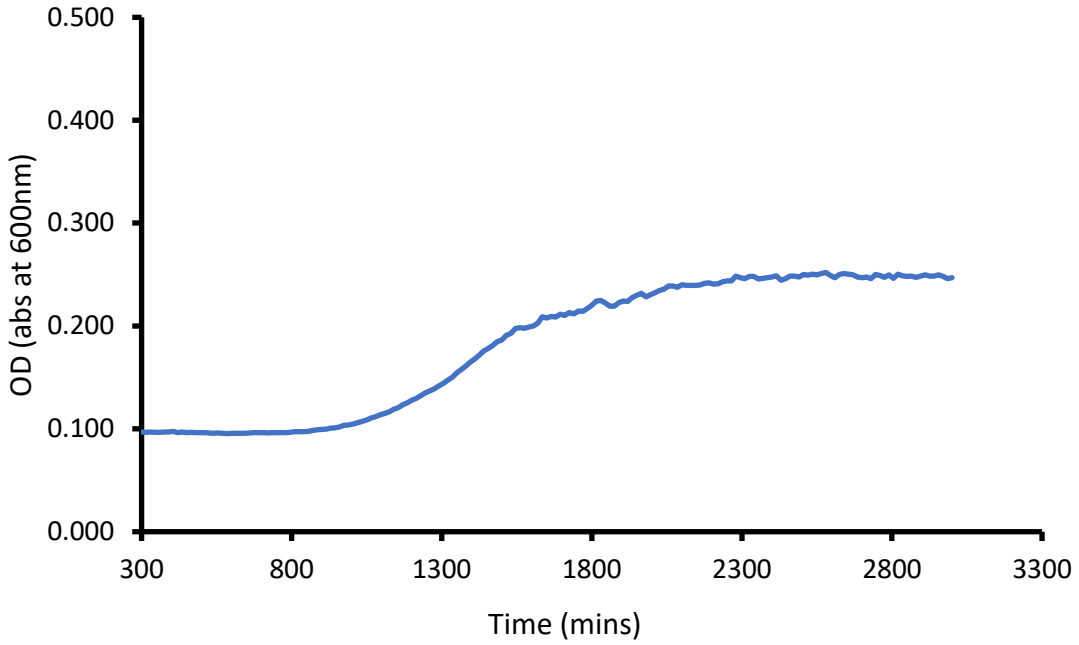

Figure S89: *S. pombe* toxicity screening study. Data shown represents an average of three experiments. Graph shows the addition of 1:19 EtOH:H_2O solution of **10** (10 mM, 60 µL) to a suspension of cells (density = $0.5x10^6$ cells/mL) in EMMG media (120 µL). Data displayed from 300 minutes due to initial plate reader calibration.

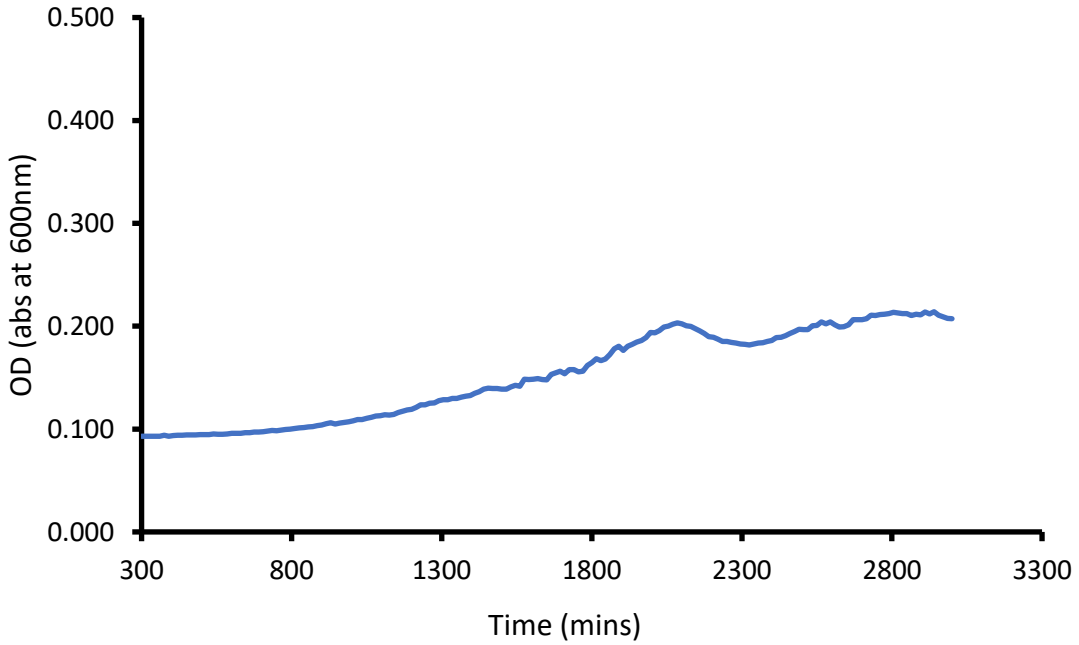

Figure S90: *S. pombe* growth curve. Data shown represents an average of three experiments. Graph shows the addition of 1:19 EtOH:H_2O solution of **11** (10 mM, 60 µL) to a suspension of cells (density = $0.5x10^6$ cells/mL) in EMMG media (120 µL). Data displayed from 300 minutes due to initial plate reader calibration.

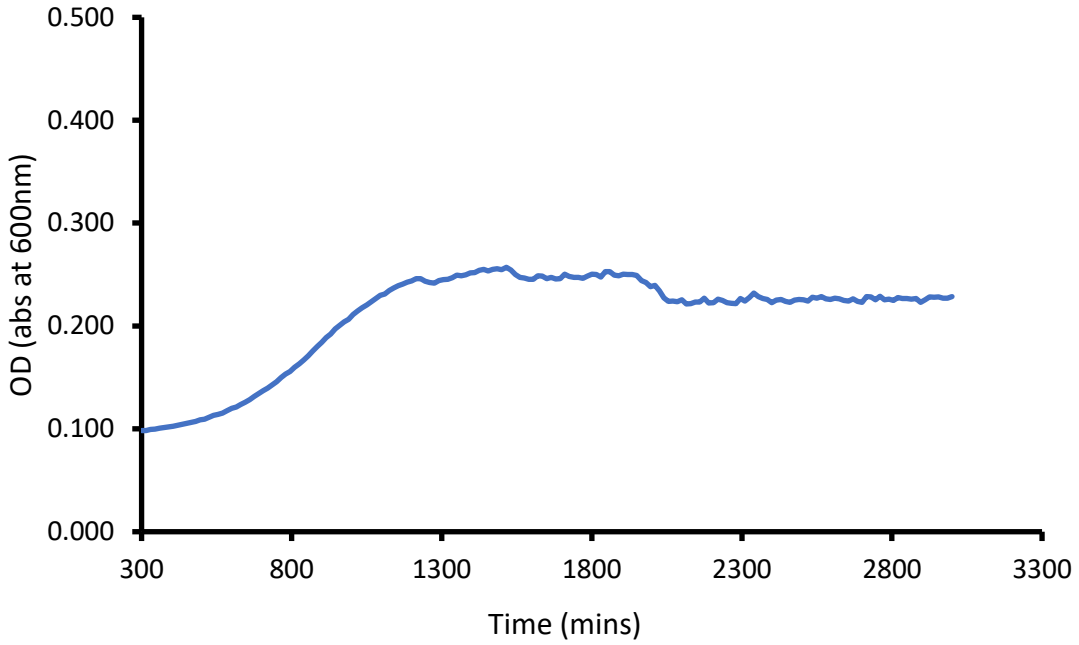

Figure S91: *S. pombe* growth curve. Data shown represents an average of three experiments. Graph shows the addition of 1:19 EtOH:H_2O solution of **12** (10 mM, 60 µL) to a suspension of cells (density = $0.5x10^6$ cells/mL) in EMMG media (120 µL). Data displayed from 300 minutes due to initial plate reader calibration.

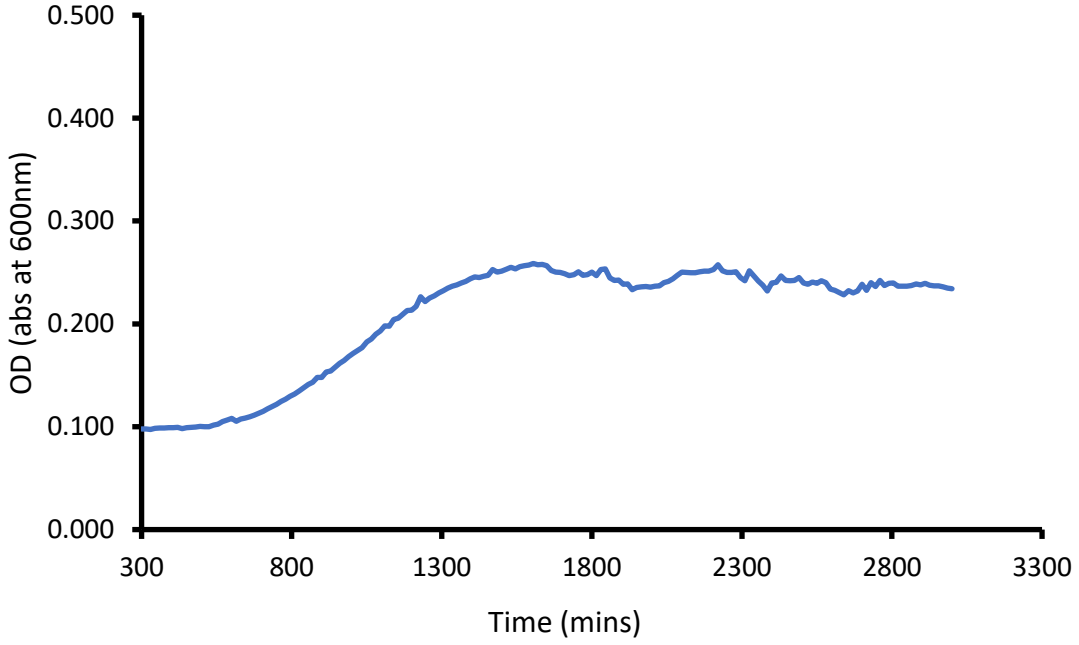

Figure S92: *S. pombe* growth curve. Data shown represents an average of three experiments. Graph shows the addition of 1:19 EtOH:H_2O solution of **16** (10 mM, 60 µL) to a suspension of cells (density = $0.5x10^6$ cells/mL) in EMMG media (120 µL). Data displayed from 300 minutes due to initial plate reader calibration.

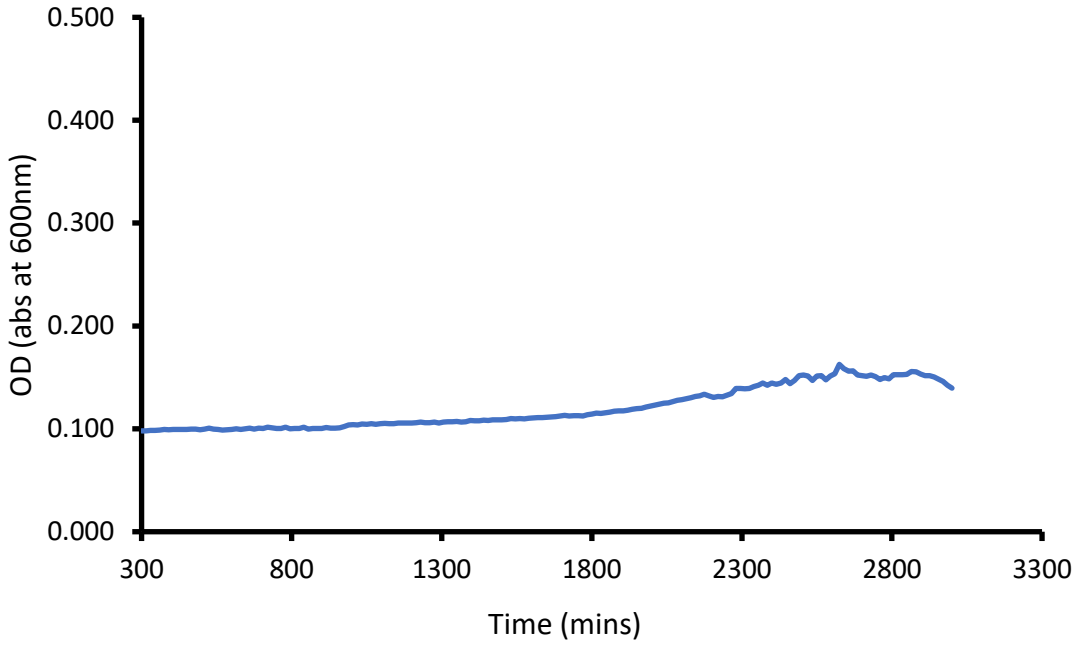

Figure S93: *S. pombe* growth curve. Data shown represents an average of three experiments. Graph shows the addition of 1:19 EtOH:H_2O solution of **17** (10 mM, 60 µL) to a suspension of cells (density = $0.5x10^6$ cells/mL) in EMMG media (120 µL). Data displayed from 300 minutes due to initial plate reader calibration.

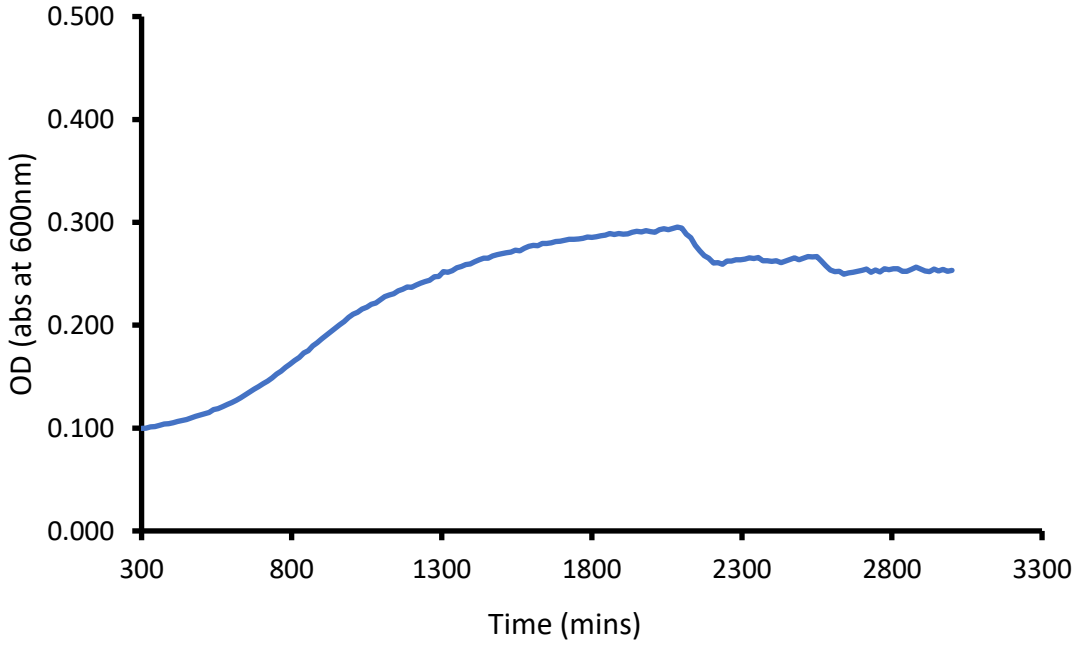

Figure S94: *S. pombe* growth curve. Data shown represents an average of three experiments. Graph shows the addition of 1:19 EtOH:H_2O solution of **18** (10 mM, 60 µL) to a suspension of cells (density = $0.5x10^6$ cells/mL) in EMMG media (120 µL). Data displayed from 300 minutes due to initial plate reader calibration.

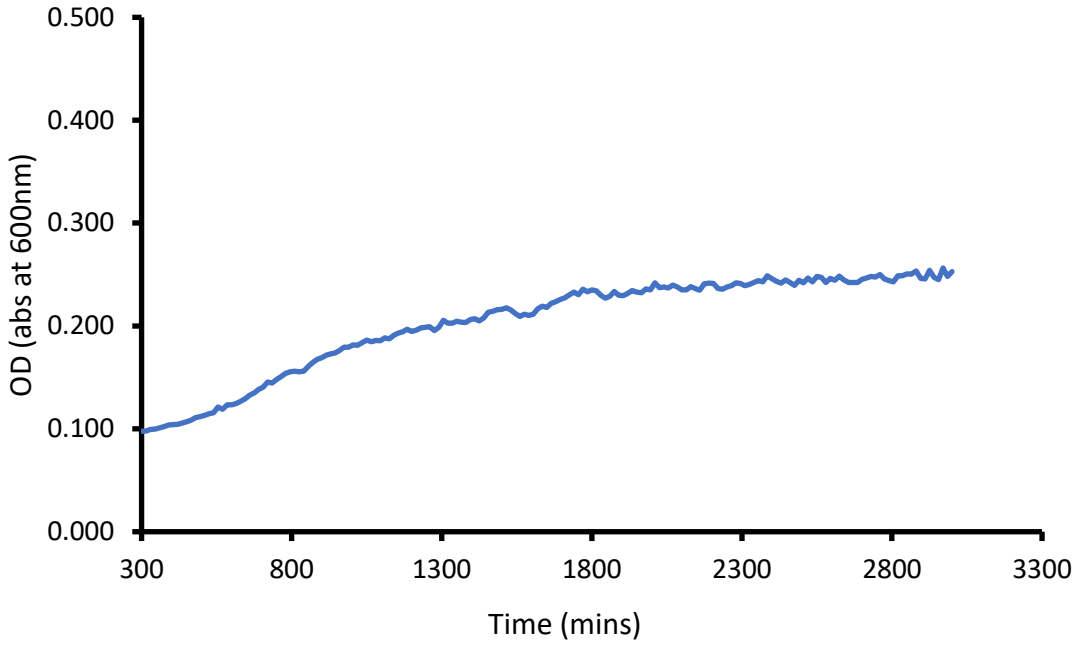

Figure S95: *S. pombe* growth curve. Data shown represents an average of three experiments. Graph shows the addition of 1:19 EtOH:H_2O solution of **19** (10 mM, 60 µL) to a suspension of cells (density = $0.5x10^6$ cells/mL) in EMMG media (120 µL). Data displayed from 300 minutes due to initial plate reader calibration.

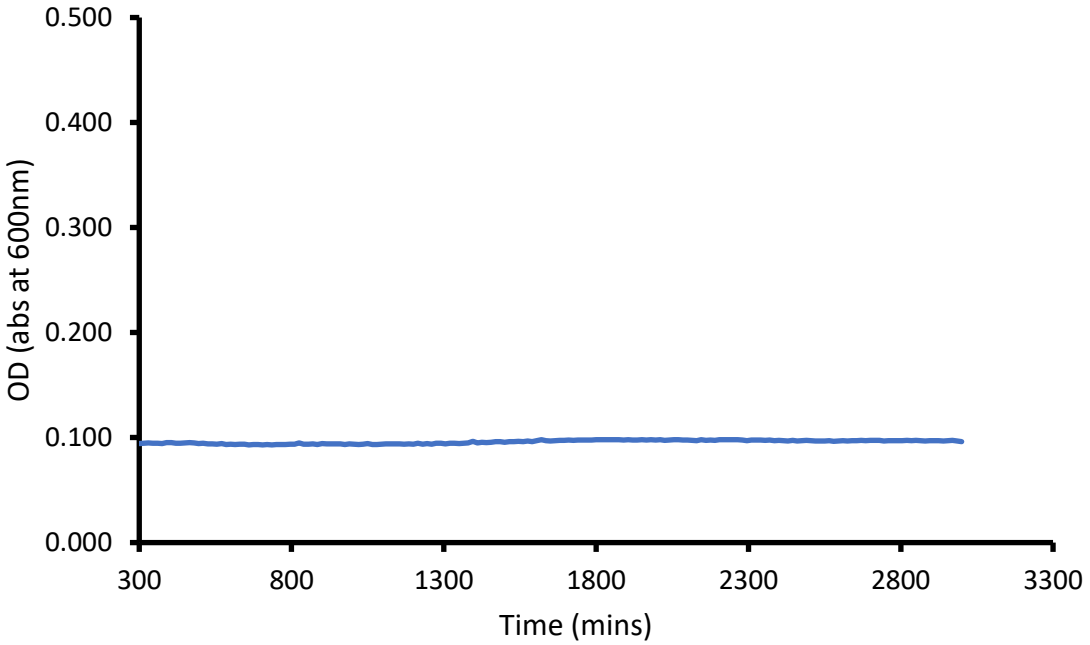

Figure S96: *S. pombe* growth curve. Data shown represents an average of three experiments. Graph shows the addition of 1:19 EtOH:H_2O solution of **20** (10 mM, 60 µL) to a suspension of cells (density = $0.5x10^6$ cells/mL) in EMMG media (120 µL). Data displayed from 300 minutes due to initial plate reader calibration.

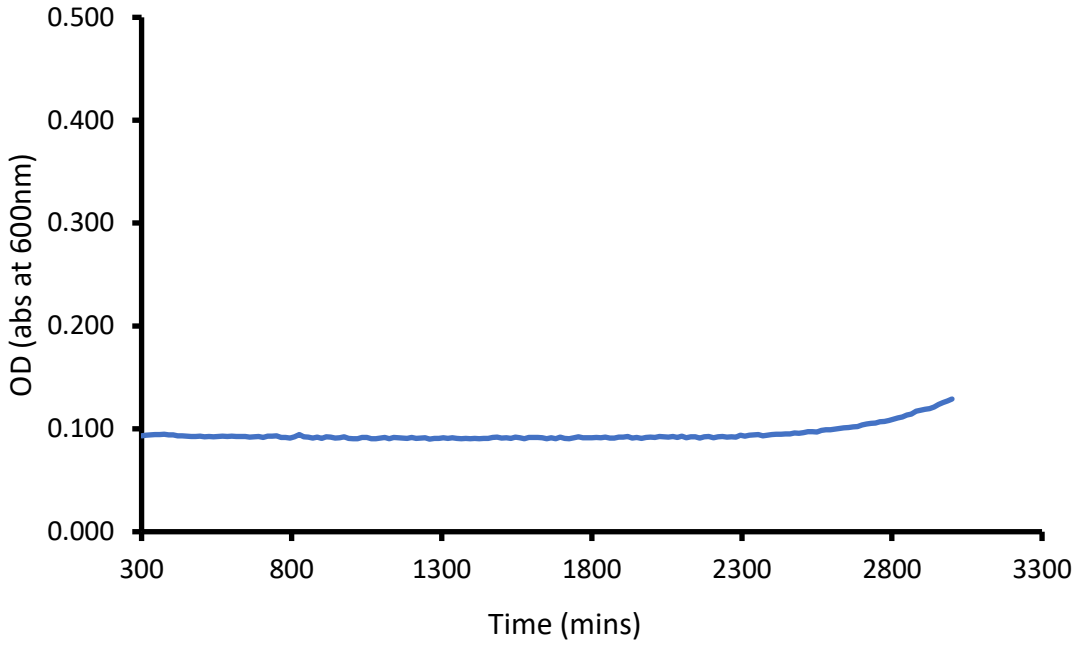

Figure S97: *S. pombe* growth curve. Data shown represents an average of three experiments. Graph shows the addition of 1:19 EtOH:H_2O solution of **21** (10 mM, 60 µL) to a suspension of cells (density = $0.5x10^6$ cells/mL) in EMMG media (120 µL). Data displayed from 300 minutes due to initial plate reader calibration.

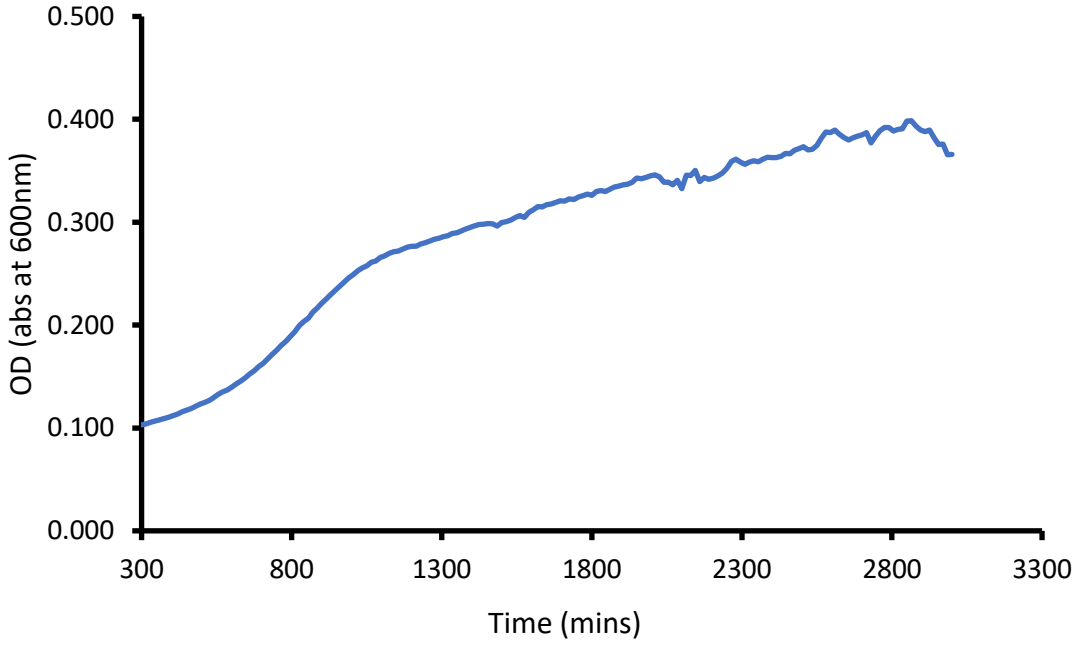

Figure S98: *S. pombe* growth curve. Data shown represents an average of three experiments. Graph shows the addition of 1:19 EtOH:H_2O solution of **22** (10 mM, 60 µL) to a suspension of cells (density = $0.5x10^6$ cells/mL) in EMMG media (120 µL). Data displayed from 300 minutes due to initial plate reader calibration.

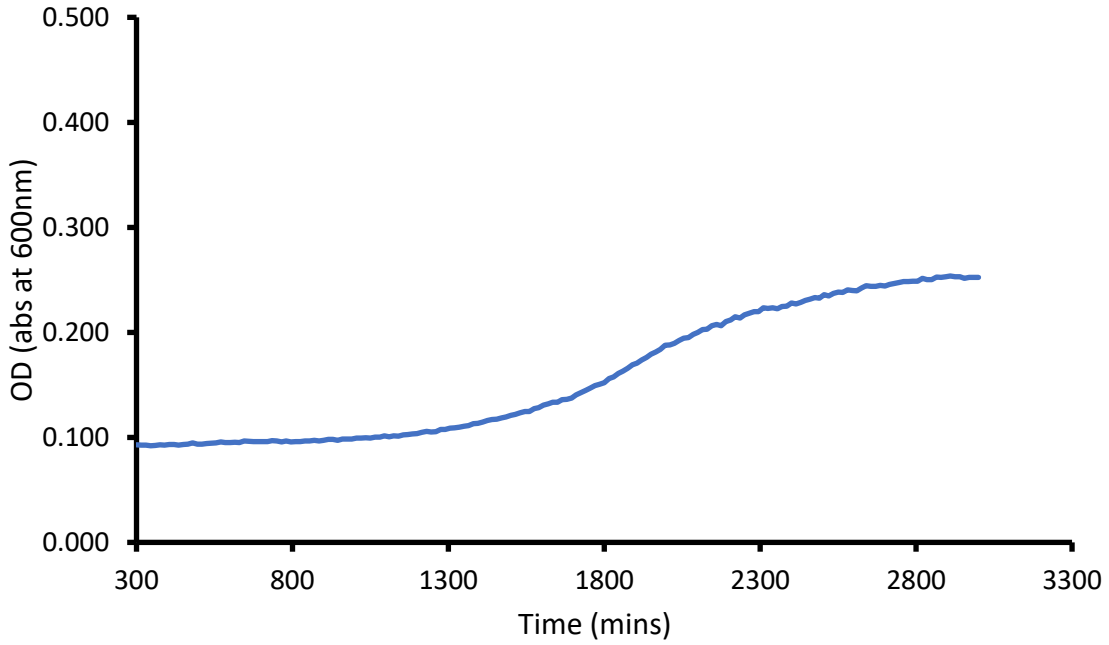

Figure S99: *S. pombe* growth curve. Data shown represents an average of three experiments. Graph shows the addition of 1:19 EtOH:H_2O solution of **23** (10 mM, 60 µL) to a suspension of cells (density = $0.5x10^6$ cells/mL) in EMMG media (120 µL). Data displayed from 300 minutes due to initial plate reader calibration.

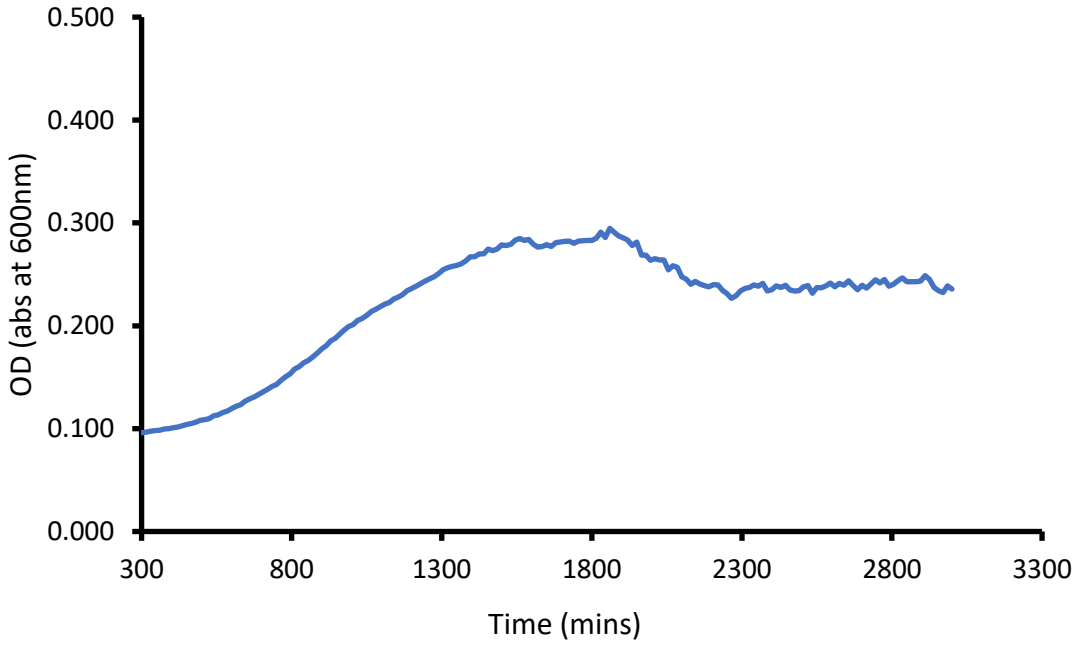

Figure S100: *S. pombe* growth curve. Data shown represents an average of three experiments. Graph shows the addition of 1:19 EtOH:H_2O solution of **24** (10 mM, 60 µL) to a suspension of cells (density = $0.5x10^6$ cells/mL) in EMMG media (120 µL). Data displayed from 300 minutes due to initial plate reader calibration.

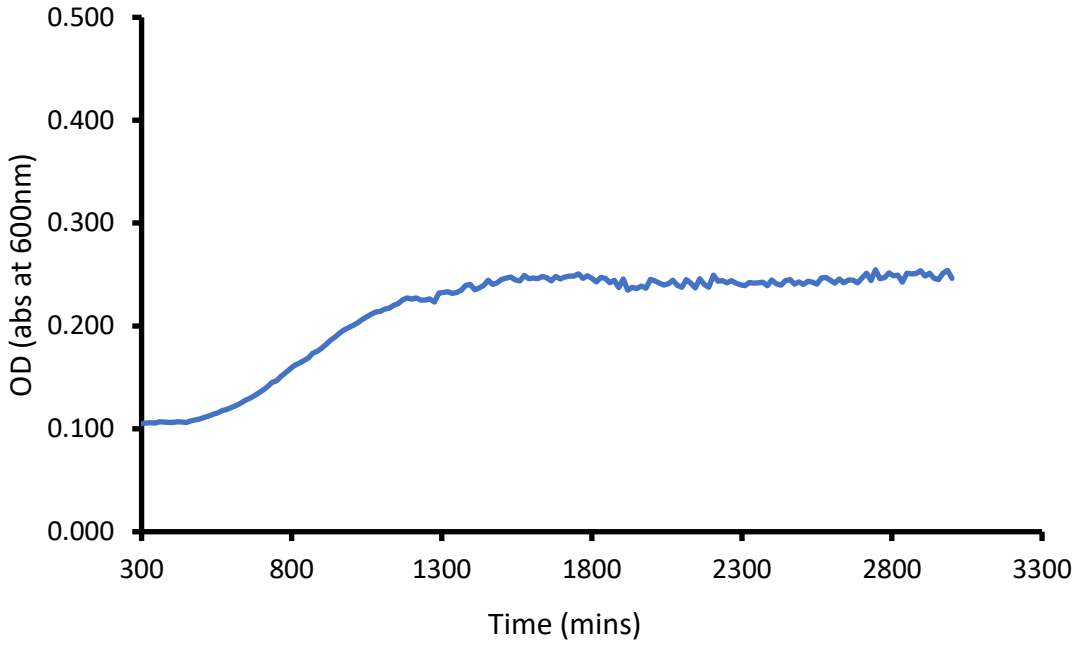

Figure S101: *S. pombe* growth curve. Data shown represents an average of three experiments. Graph shows the addition of 1:19 EtOH:H_2O solution of **25** (10 mM, 60 µL) to a suspension of cells (density = $0.5x10^6$ cells/mL) in EMMG media (120 µL). Data displayed from 300 minutes due to initial plate reader calibration.

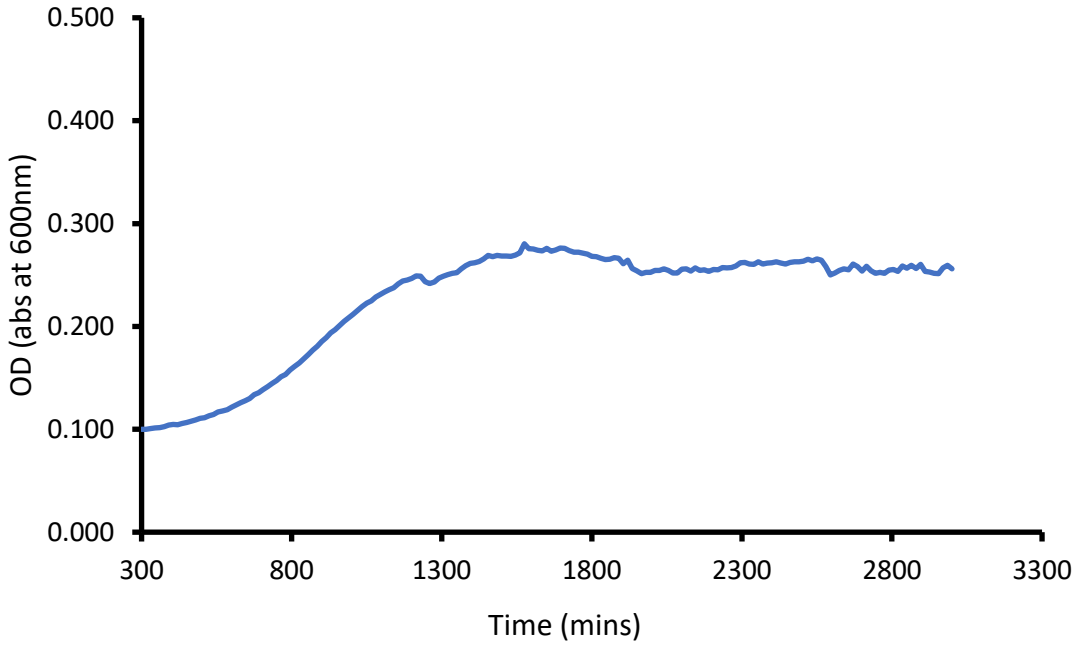

Figure S102: *S. pombe* growth curve. Data shown represents an average of three experiments. Graph shows the addition of 1:19 EtOH:H_2O solution of **26** (10 mM, 60 µL) to a suspension of cells (density = $0.5x10^6$ cells/mL) in EMMG media (120 µL). Data displayed from 300 minutes due to initial plate reader calibration.

Table S2: Summary of the *S. pombe* growth curve results showing the percentage cellular growth in comparison to a control solution after 45 hours.

No	%	No	%	No	%	No	%
5	92.5	**11**	77.7	**20**	95.4	**26**	92.9
6	77.9	**12**	83.5	**21**	49.2		
7	79.1	**16**	93.5	**22**	131.7		
8	82.2	**17**	101	**23**	94.1		
9	92.4	**18**	92.0	**24**	86.9		
10	90.7	**19**	103.6	**25**	87.5		

Low level PM6 modelling

Computational calculations to identify primary hydrogen bond donating and accepting sites were conducted in line with studies reported by Hunter using Spartan 16'.[13] Calculations were performed using semi-empirical PM6 methods, after energy minimisation calculations, to identify E_{min} and polarizability values. PM6 was used over AM1 in line with research conducted by Stewart.[14] To estimate the accessibility of the principle HBA site towards supramolecular coordination, the area of the ESPM within 1/8th of the E_{min} for the principle HBA group, and has been termed the 'steric weighting factor' (SWF) for ease of reference. The SWF was considered for either one or two sulfonate oxygen atoms for **16**-**26**.

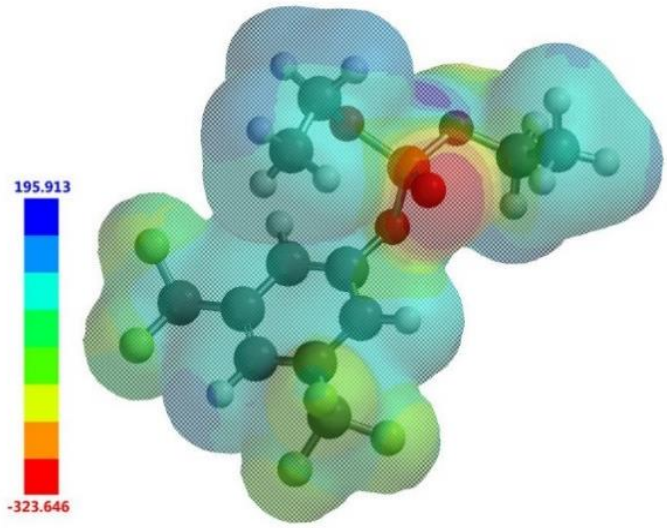

Figure S103: Electrostatic potential map calculated for compound **5**. E_{max} (deep blue) and E_{min} (bright red) values depicted in the Figure legends are given in kJ/mol. The area of the electrostatic potential map displayed in red is within 1/8th of the E_{min} and is termed the 'steric weighting factor' (SWF). The area of the electrostatic potential map displayed in deep blue is within 1/8th of the E_{max} and is termed the 'steric accessibility factor' (SAF).

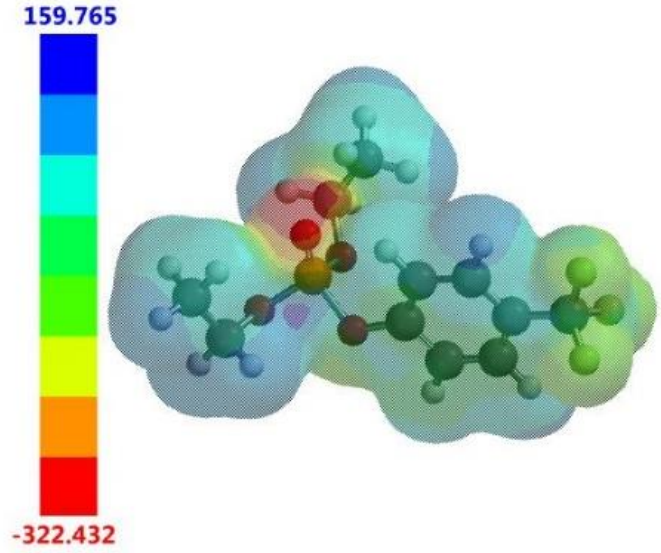

Figure S104: Electrostatic potential map calculated for compound **6**. E_{max} and E_{min} values depicted in the Figure legends are given in kJ/mol. The area of the electrostatic potential map displayed in red is within 1/8th of the E_{min} and is termed the 'steric weighting factor' (SWF). The area of the electrostatic potential map displayed in deep blue is within 1/8th of the E_{max} and is termed the 'steric accessibility factor' (SAF).

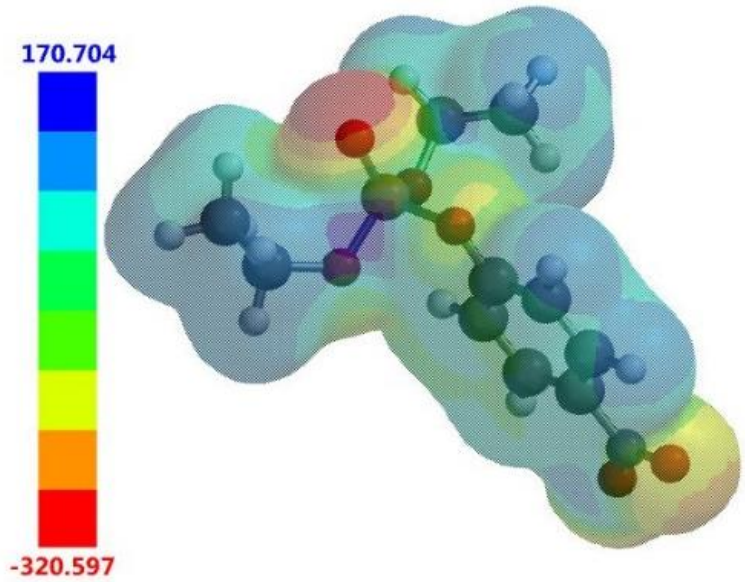

Figure S105: Electrostatic potential map calculated for compound **7**. E_{max} and E_{min} values depicted in the Figure legends are given in kJ/mol. The area of the electrostatic potential map displayed in red is within $1/8^{th}$ of the E_{min} and is termed the 'steric weighting factor' (SWF). The area of the electrostatic potential map displayed in deep blue is within $1/8^{th}$ of the E_{max} and is termed the 'steric accessibility factor' (SAF).

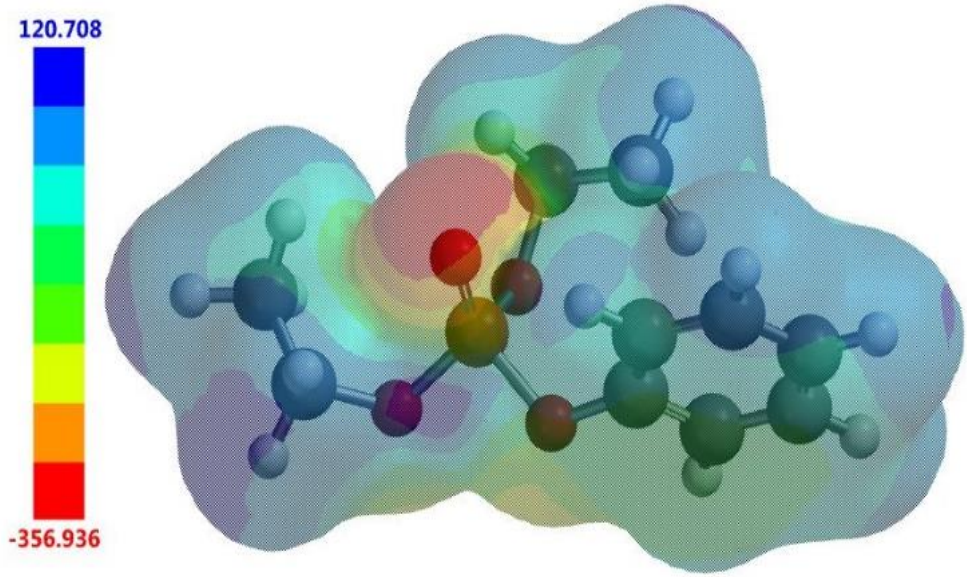

Figure S106: Electrostatic potential map calculated for compound **8**. E_{max} and E_{min} values depicted in the Figure legends are given in kJ/mol. The area of the electrostatic potential map displayed in red is within $1/8^{th}$ of the E_{min} and is termed the 'steric weighting factor' (SWF). The area of the electrostatic potential map displayed in deep blue is within $1/8^{th}$ of the E_{max} and is termed the 'steric accessibility factor' (SAF).

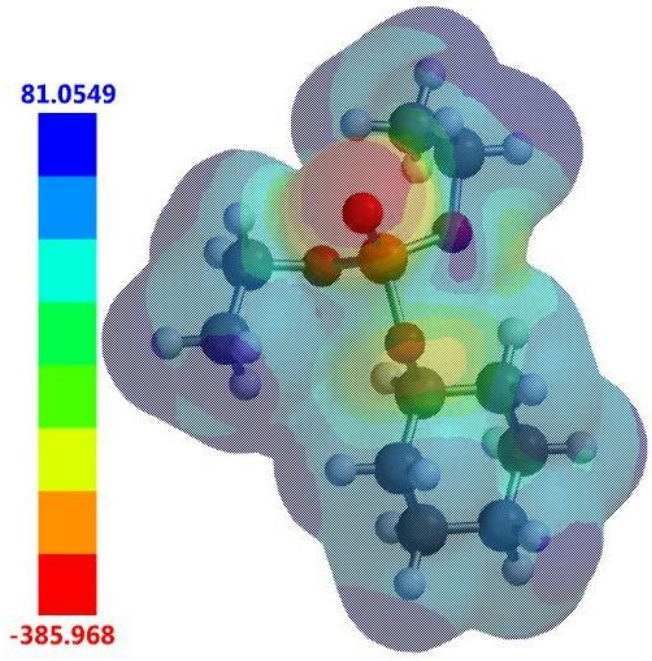

Figure S107: Electrostatic potential map calculated for compound **9**. E_{max} and E_{min} values depicted in the Figure legends are given in kJ/mol. The area of the electrostatic potential map displayed in red is within 1/8th of the E_{min} and is termed the 'steric weighting factor' (SWF). The area of the electrostatic potential map displayed in deep blue is within 1/8th of the E_{max} and is termed the 'steric accessibility factor' (SAF).

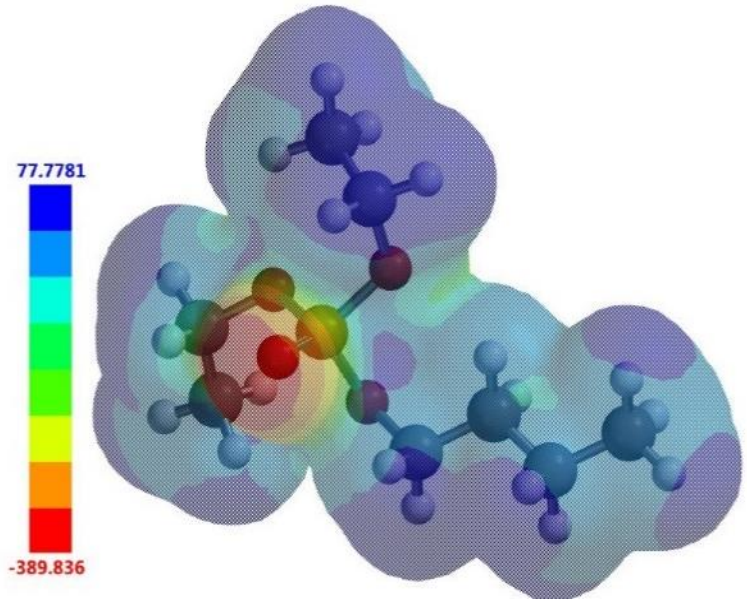

Figure S108: Electrostatic potential map calculated for compound **10**. E_{max} and E_{min} values depicted in the Figure legends are given in kJ/mol. The area of the electrostatic potential map displayed in red is within 1/8th of the E_{min} and is termed the 'steric weighting factor' (SWF). The area of the electrostatic potential map displayed in deep blue is within 1/8th of the E_{max} and is termed the 'steric accessibility factor' (SAF).

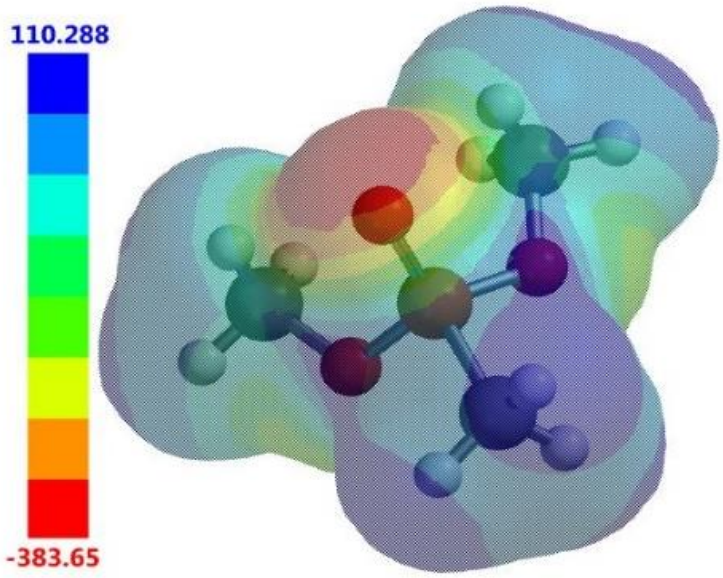

Figure S109: Electrostatic potential map calculated for compound **11**. E_{max} and E_{min} values depicted in the Figure legends are given in kJ/mol. The area of the electrostatic potential map displayed in red is within 1/8th of the E_{min} and is termed the 'steric weighting factor' (SWF). The area of the electrostatic potential map displayed in deep blue is within 1/8th of the E_{max} and is termed the 'steric accessibility factor' (SAF).

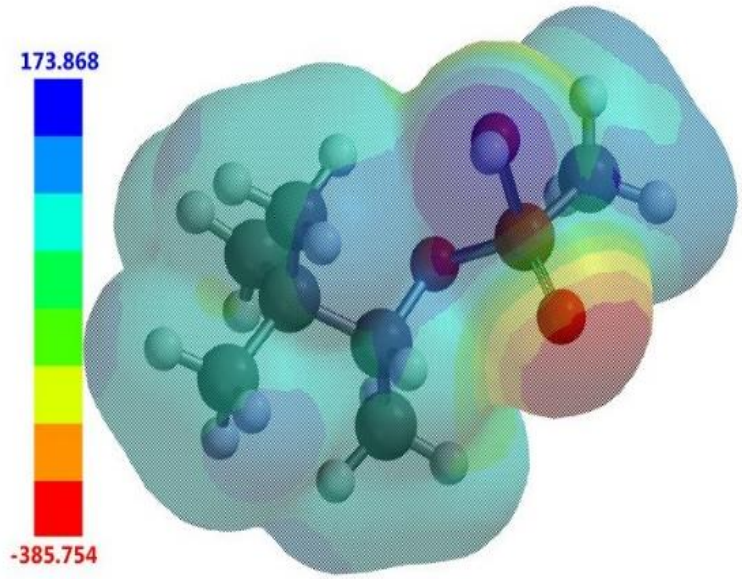

Figure S110: Electrostatic potential map calculated for compound **12**. E_{max} and E_{min} values depicted in the Figure legends are given in kJ/mol. The area of the electrostatic potential map displayed in red is within 1/8th of the E_{min} and is termed the 'steric weighting factor' (SWF). The area of the electrostatic potential map displayed in deep blue is within 1/8th of the E_{max} and is termed the 'steric accessibility factor' (SAF).

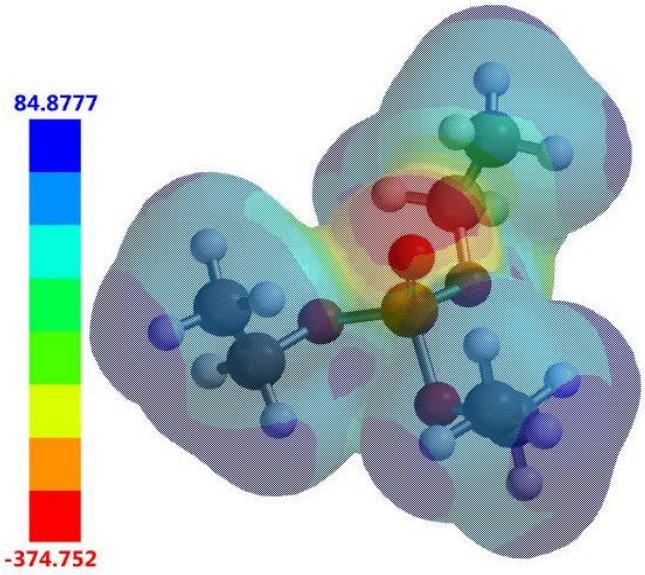

Figure S111: Electrostatic potential map calculated for compound **13**. E_{max} and E_{min} values depicted in the Figure legends are given in kJ/mol. The area of the electrostatic potential map displayed in red is within 1/8th of the E_{min} and is termed the 'steric weighting factor' (SWF). The area of the electrostatic potential map displayed in deep blue is within 1/8th of the E_{max} and is termed the 'steric accessibility factor' (SAF).

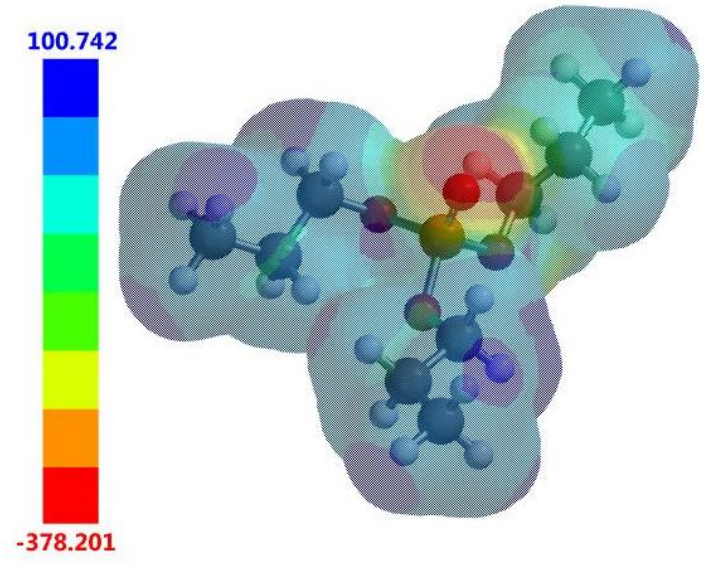

Figure S112: Electrostatic potential map calculated for compound **14**. E_{max} and E_{min} values depicted in the Figure legends are given in kJ/mol. The area of the electrostatic potential map displayed in red is within 1/8th of the E_{min} and is termed the 'steric weighting factor' (SWF). The area of the electrostatic potential map displayed in deep blue is within 1/8th of the E_{max} and is termed the 'steric accessibility factor' (SAF).

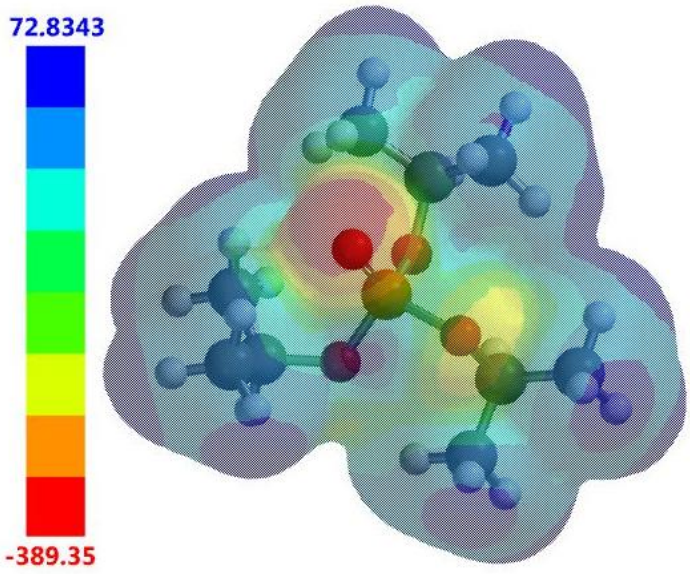

Figure S113: Electrostatic potential map calculated for compound **15**. E_{max} and E_{min} values depicted in the Figure legends are given in kJ/mol. The area of the electrostatic potential map displayed in red is within 1/8th of the E_{min} and is termed the 'steric weighting factor' (SWF). The area of the electrostatic potential map displayed in deep blue is within 1/8th of the E_{max} and is termed the 'steric accessibility factor' (SAF).

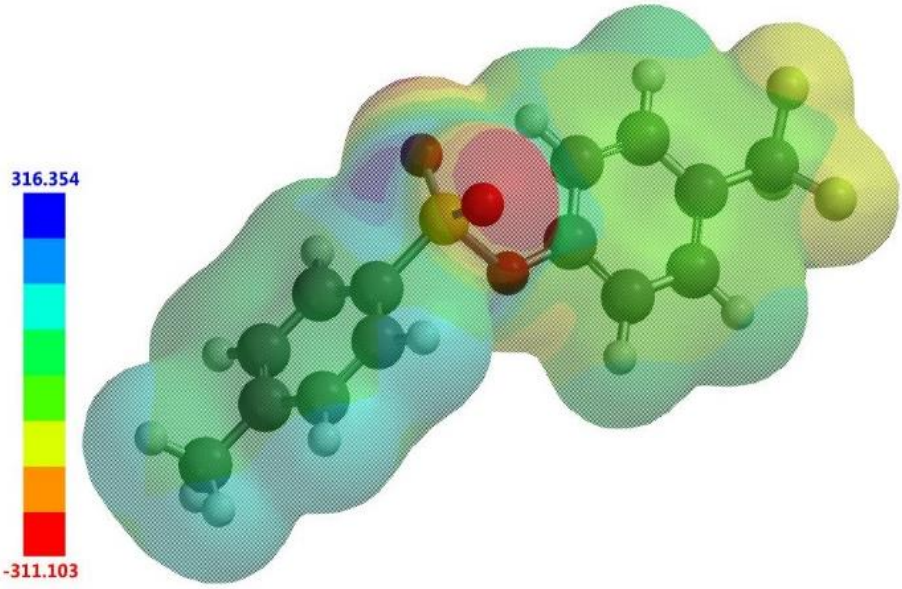

Figure S114: Electrostatic potential map calculated for compound **16**. E_{max} and E_{min} values depicted in the Figure legends are given in kJ/mol. The area of the electrostatic potential map displayed in red is within 1/8th of the E_{min} and is termed the 'steric weighting factor' (SWF). The area of the electrostatic potential map displayed in deep blue is within 1/8th of the E_{max} and is termed the 'steric accessibility factor' (SAF).

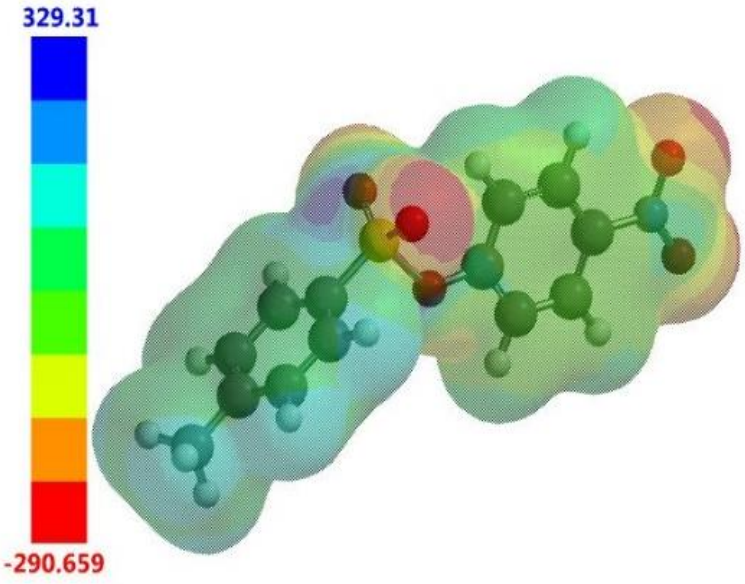

Figure S115: Electrostatic potential map calculated for compound **17**. E_{max} and E_{min} values depicted in the Figure legends are given in kJ/mol. The area of the electrostatic potential map displayed in red is within 1/8th of the E_{min} and is termed the 'steric weighting factor' (SWF). The area of the electrostatic potential map displayed in deep blue is within 1/8th of the E_{max} and is termed the 'steric accessibility factor' (SAF).

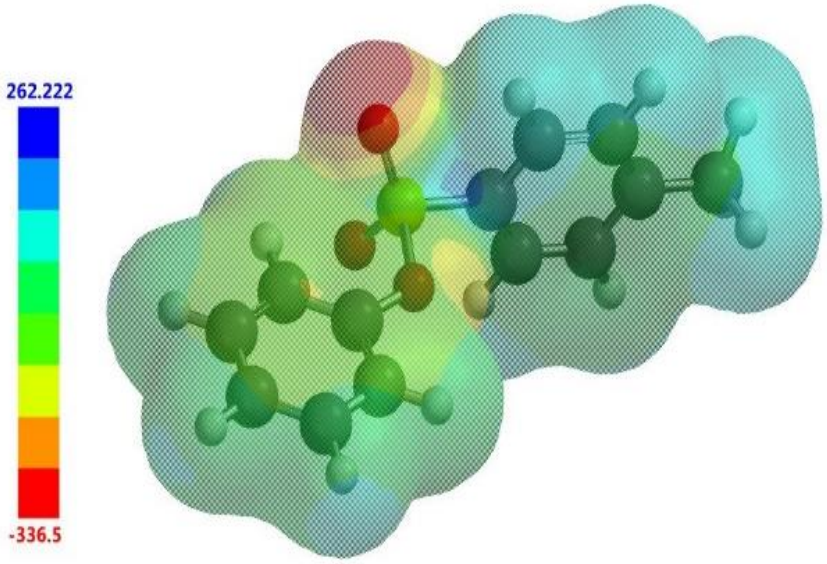

Figure S116: Electrostatic potential map calculated for compound **18**. E_{max} and E_{min} values depicted in the Figure legends are given in kJ/mol. The area of the electrostatic potential map displayed in red is within 1/8th of the E_{min} and is termed the 'steric weighting factor' (SWF). The area of the electrostatic potential map displayed in deep blue is within 1/8th of the E_{max} and is termed the 'steric accessibility factor' (SAF).

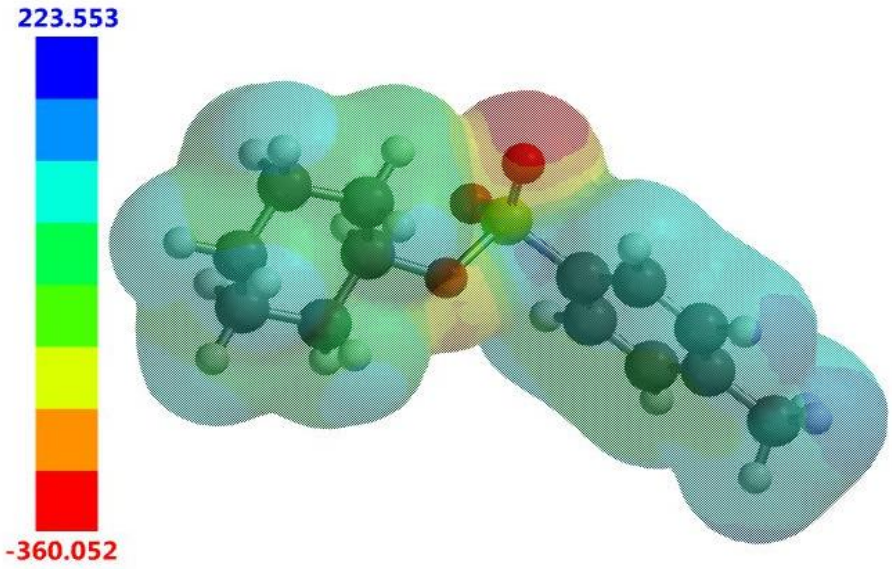

Figure S117: Electrostatic potential map calculated for compound **19**. E_{max} and E_{min} values depicted in the Figure legends are given in kJ/mol. The area of the electrostatic potential map displayed in red is within 1/8th of the E_{min} and is termed the 'steric weighting factor' (SWF). The area of the electrostatic potential map displayed in deep blue is within 1/8th of the E_{max} and is termed the 'steric accessibility factor' (SAF).

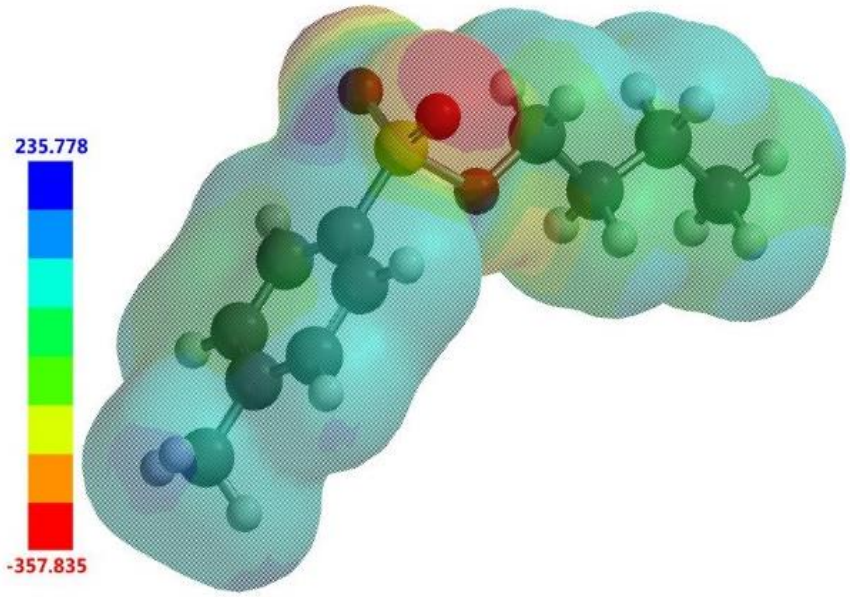

Figure S118: Electrostatic potential map calculated for compound **20**. E_{max} and E_{min} values depicted in the Figure legends are given in kJ/mol. The area of the electrostatic potential map displayed in red is within 1/8th of the E_{min} and is termed the 'steric weighting factor' (SWF). The area of the electrostatic potential map displayed in deep blue is within 1/8th of the E_{max} and is termed the 'steric accessibility factor' (SAF).

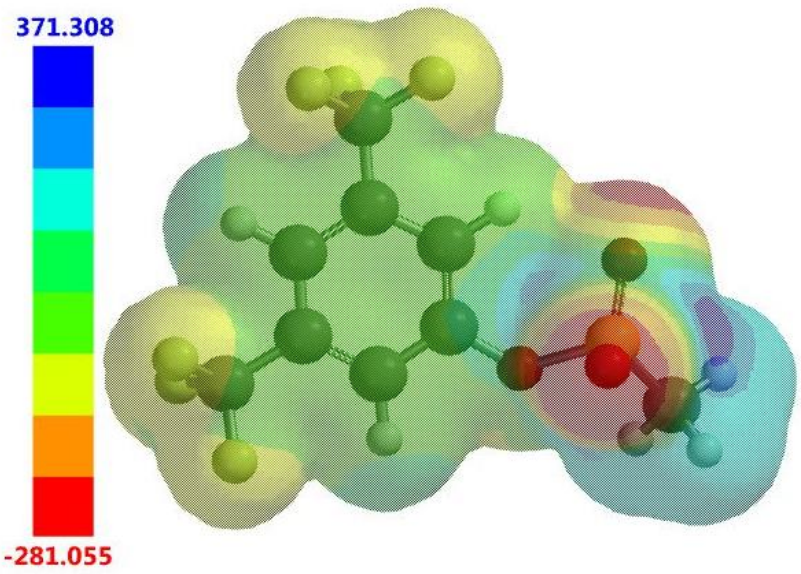

Figure S119: Electrostatic potential map calculated for compound **21**. E_{max} and E_{min} values depicted in the Figure legends are given in kJ/mol. The area of the electrostatic potential map displayed in red is within 1/8th of the E_{min} and is termed the 'steric weighting factor' (SWF). The area of the electrostatic potential map displayed in deep blue is within 1/8th of the E_{max} and is termed the 'steric accessibility factor' (SAF).

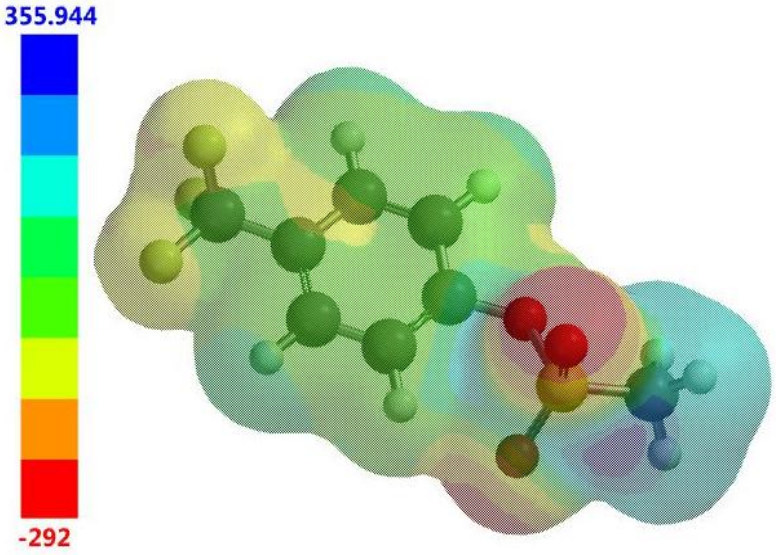

Figure S120: Electrostatic potential map calculated for compound **22**. E_{max} and E_{min} values depicted in the Figure legends are given in kJ/mol. The area of the electrostatic potential map displayed in red is within 1/8th of the E_{min} and is termed the 'steric weighting factor' (SWF). The area of the electrostatic potential map displayed in deep blue is within 1/8th of the E_{max} and is termed the 'steric accessibility factor' (SAF).

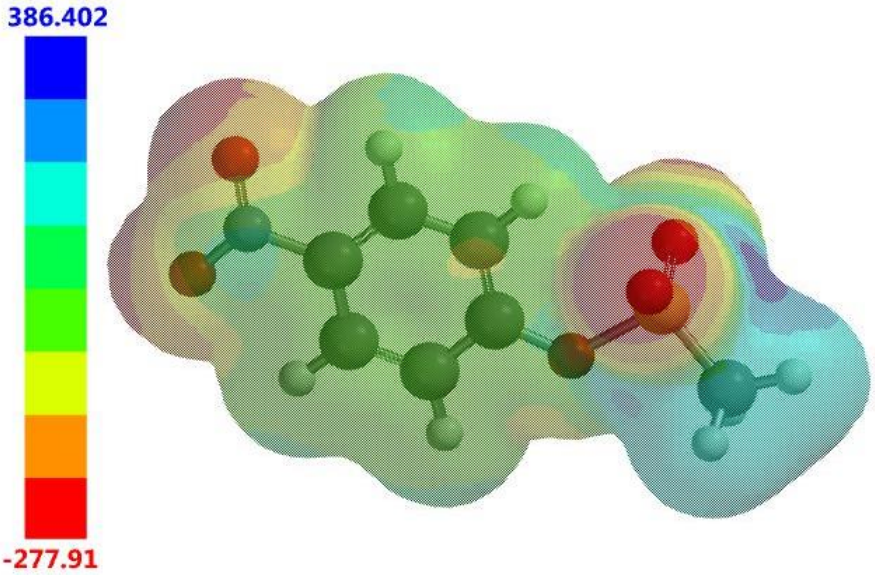

Figure S121: Electrostatic potential map calculated for compound **23**. E_{max} and E_{min} values depicted in the Figure legends are given in kJ/mol. The area of the electrostatic potential map displayed in red is within 1/8th of the E_{min} and is termed the 'steric weighting factor' (SWF). The area of the electrostatic potential map displayed in deep blue is within 1/8th of the E_{max} and is termed the 'steric accessibility factor' (SAF).

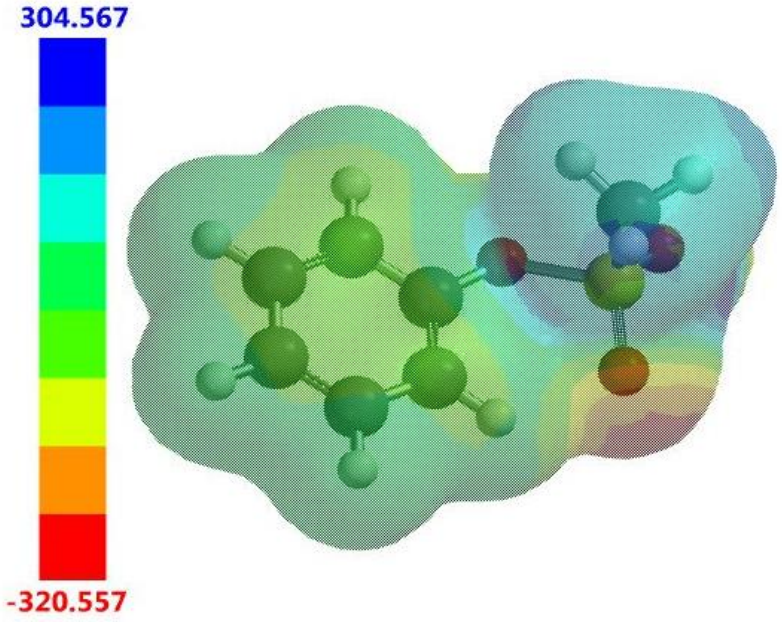

Figure S122: Electrostatic potential map calculated for compound **24**. E_{max} and E_{min} values depicted in the Figure legends are given in kJ/mol. The area of the electrostatic potential map displayed in red is within 1/8th of the E_{min} and is termed the 'steric weighting factor' (SWF). The area of the electrostatic potential map displayed in deep blue is within 1/8th of the E_{max} and is termed the 'steric accessibility factor' (SAF).

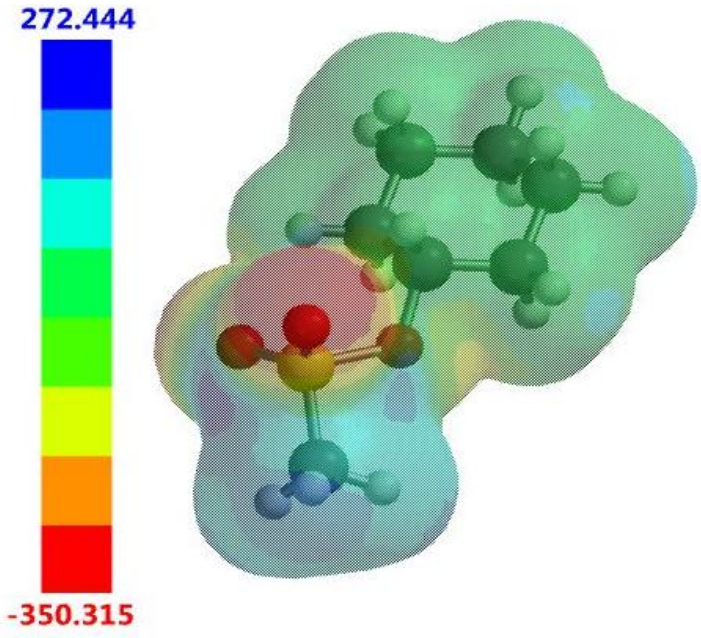

Figure S123: Electrostatic potential map calculated for compound **25**. E_{max} and E_{min} values depicted in the Figure legends are given in kJ/mol. The area of the electrostatic potential map displayed in red is within 1/8th of the E_{min} and is termed the 'steric weighting factor' (SWF). The area of the electrostatic potential map displayed in deep blue is within 1/8th of the E_{max} and is termed the 'steric accessibility factor' (SAF).

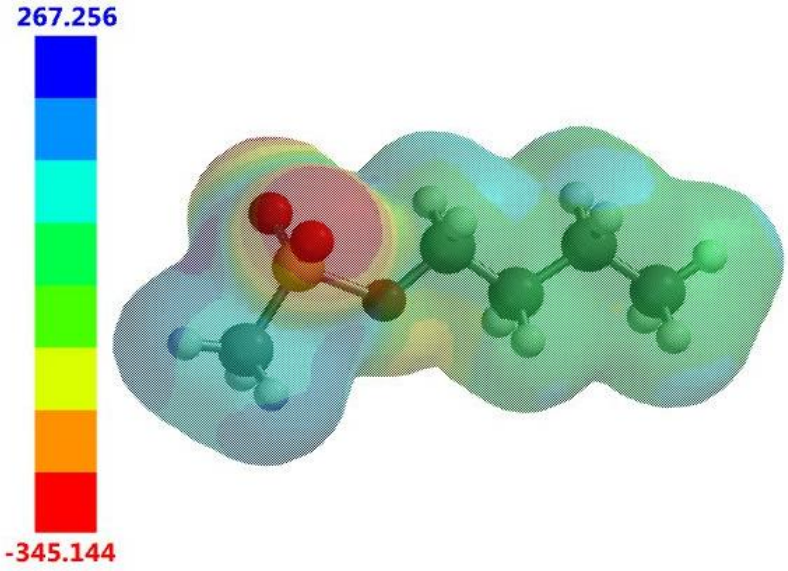

Figure S124: Electrostatic potential map calculated for compound **26**. E_{max} and E_{min} values depicted in the Figure legends are given in kJ/mol. The area of the electrostatic potential map displayed in red is within 1/8th of the E_{min} and is termed the 'steric weighting factor' (SWF). The area of the electrostatic potential map displayed in deep blue is within 1/8th of the E_{max} and is termed the 'steric accessibility factor' (SAF).

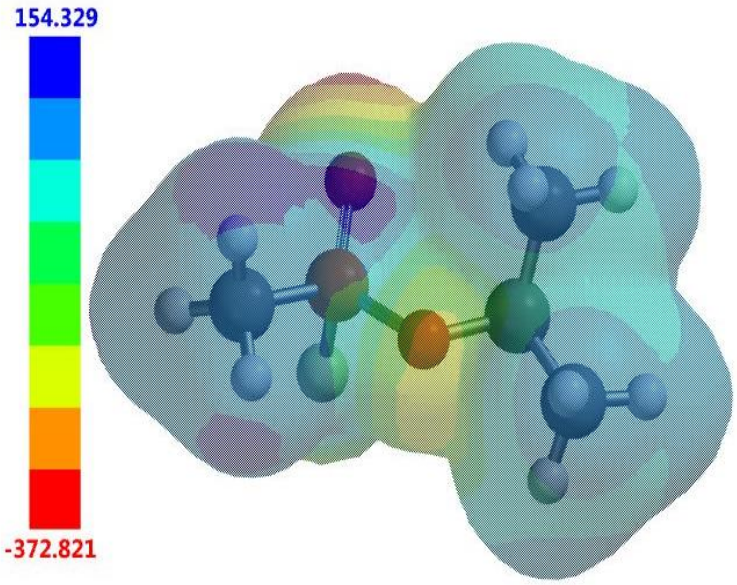

Figure S125: Electrostatic potential map calculated for sarin. E_{max} and E_{min} values depicted in the Figure legends are given in kJ/mol. The area of the electrostatic potential map displayed in red is within 1/8th of the E_{min} and is termed the 'steric weighting factor' (SWF). The area of the electrostatic potential map displayed in deep blue is within 1/8th of the E_{max} and is termed the 'steric accessibility factor' (SAF).

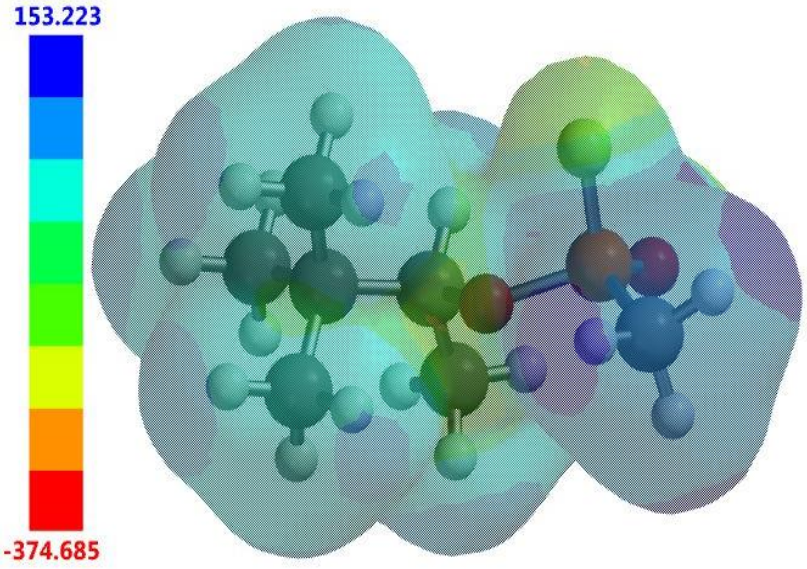

Figure S126: Electrostatic potential map calculated for soman. E_{max} and E_{min} values depicted in the Figure legends are given in kJ/mol. The area of the electrostatic potential map displayed in red is within 1/8th of the E_{min} and is termed the 'steric weighting factor' (SWF). The area of the electrostatic potential map displayed in deep blue is within 1/8th of the E_{max} and is termed the 'steric accessibility factor' (SAF).

Table S3: Summary of calculated parameters derived from the electrostatic potential maps calculated by Spartan '16 for compounds **5-27**, sarin and soman.

Simulant	E_{max} (kJmol^{-1})	E_{min} (kJmol^{-1})
5	195.91	-323.65
6	159.77	-322.43
7	170.70	-320.59
8	120.71	-356.94
9	81.05	-385.97
10	77.78	-389.84
11	110.29	-383.65
12	173.87	-385.75
16	316.35	-311.10
17	329.31	-290.66
18	262.22	-336.50
19	223.55	-360.05
20	235.78	-357.85
21	371.31	-281.06
22	355.94	-292.00
23	304.57	-320.56
24	386.40	-277.91
25	272.44	-350.32
26	267.26	-343.14
sarin	154.00	-373.00
soman	153.00	-375.00

Low level DFT (B3LYP/6-31G*) modelling

Calculations were performed using low level DFT (B3LYP/6-31G*), after energy minimisation calculations for compounds **5**-**26**, sarin and soman, along with complexes of **1** and compounds **5**-**26**, sarin and soman, in the gas phase using Spartan '16. Data from these calculations were compared to that of the semi-empirical PM6 calculations to determine which calculation method should be used for each parameter.

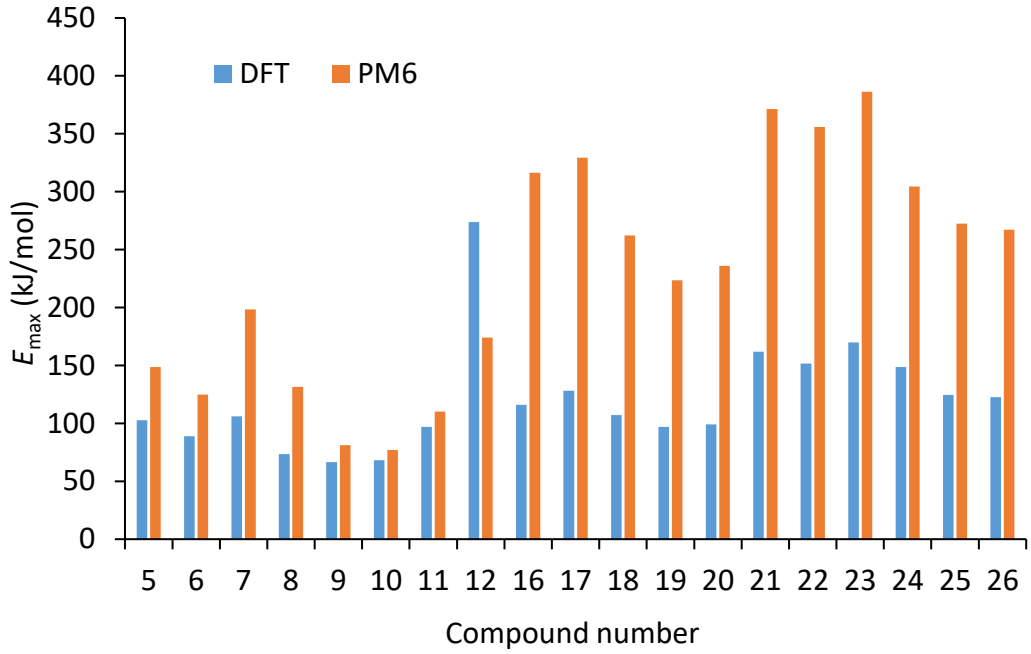

Figure S127: Comparison of data attained from DFT (B3LYP/6-31G*) and semi-empirical PM6 modelling methods for the parameter E_{max}.

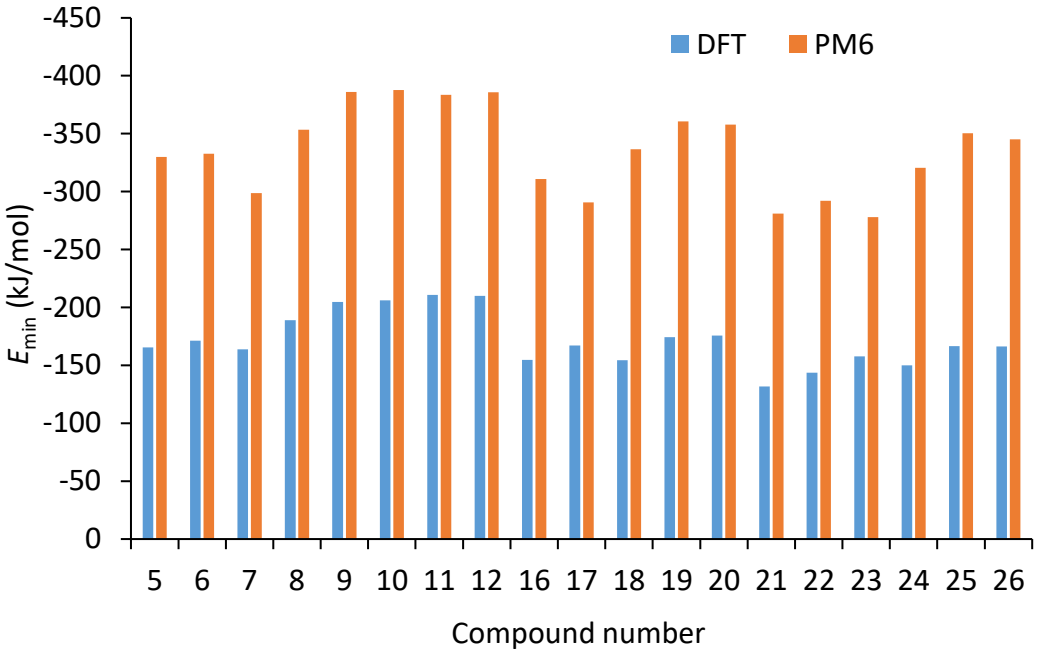

Figure S128: Comparison of data attained from DFT (B3LYP/6-31G*) and semi-empirical PM6 modelling methods for the parameter E_{min}.

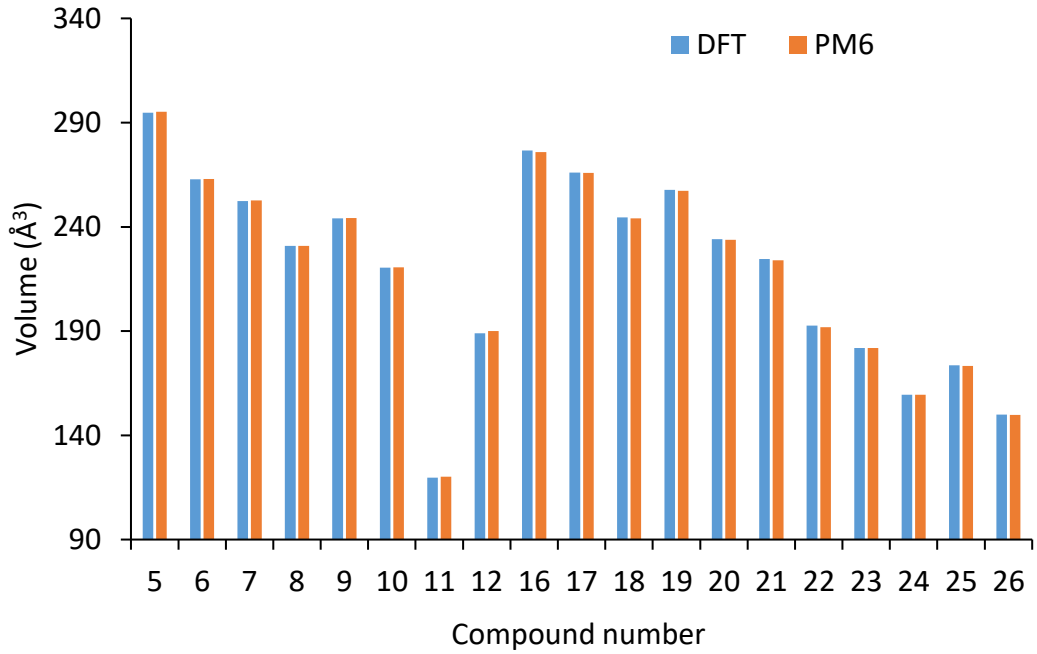

Figure S129: Comparison of data attained from DFT (B3LYP/6-31G*) and semi-empirical PM6 modelling methods for the parameter volume.

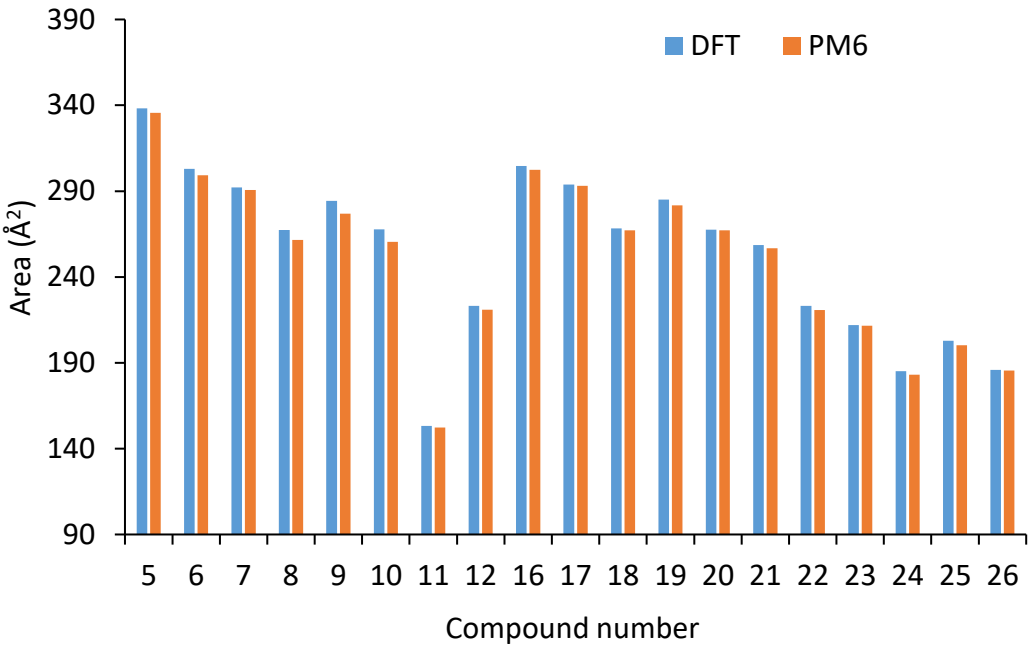

Figure S130: Comparison of data attained from DFT (B3LYP/6-31G*) and semi-empirical PM6 modelling methods for the parameter area.

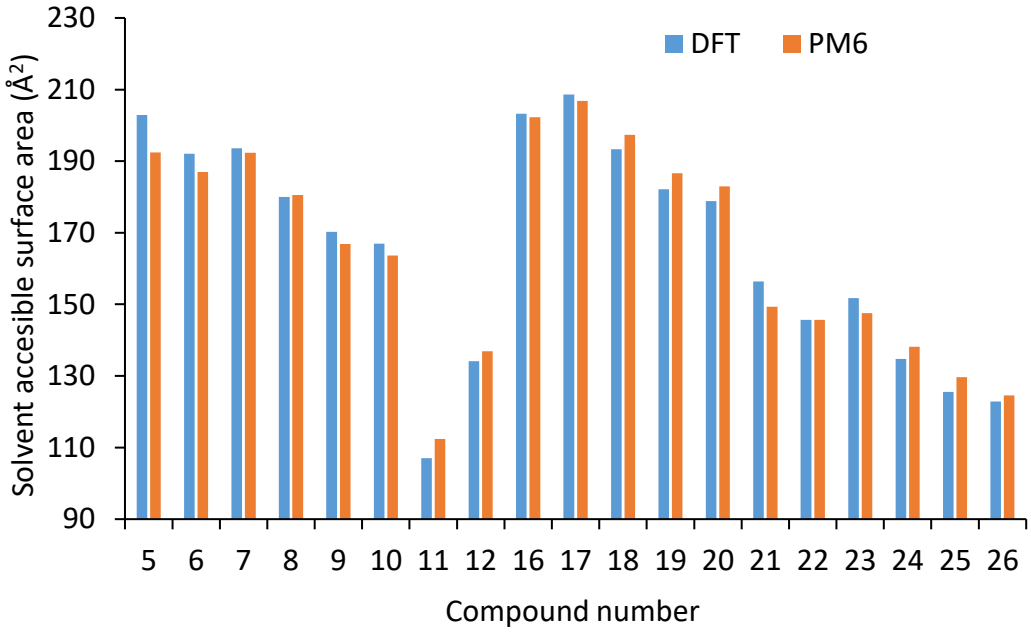

Figure S131: Comparison of data attained from DFT (B3LYP/6-31G*) and semi-empirical PM6 modelling methods for the parameter solvent accessible surface area.

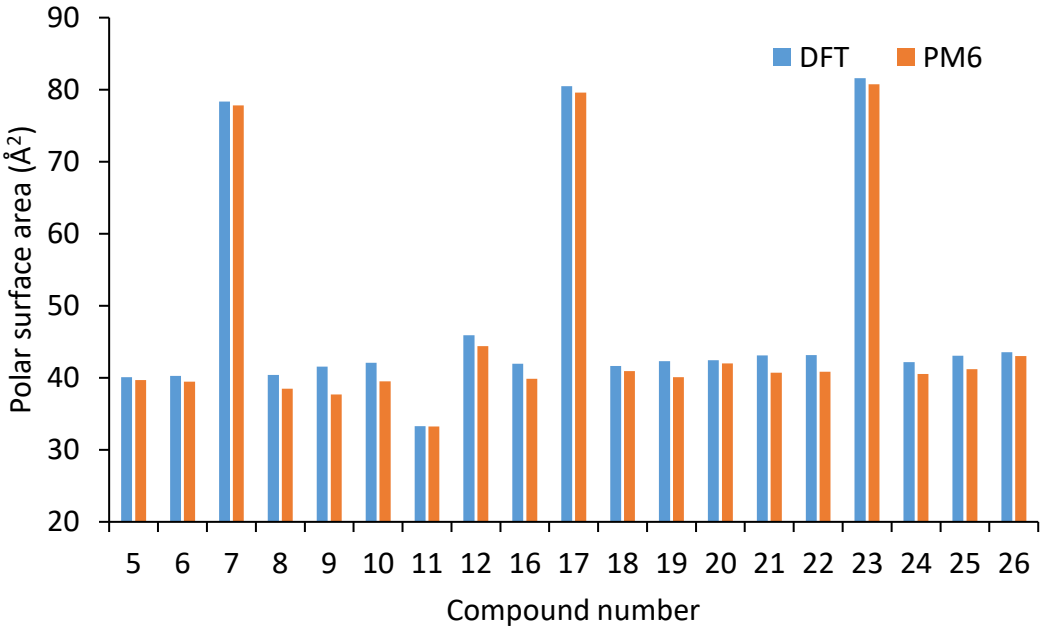

Figure S132: Comparison of data attained from DFT (B3LYP/6-31G*) and semi-empirical PM6 modelling methods for the parameter polar surface area.

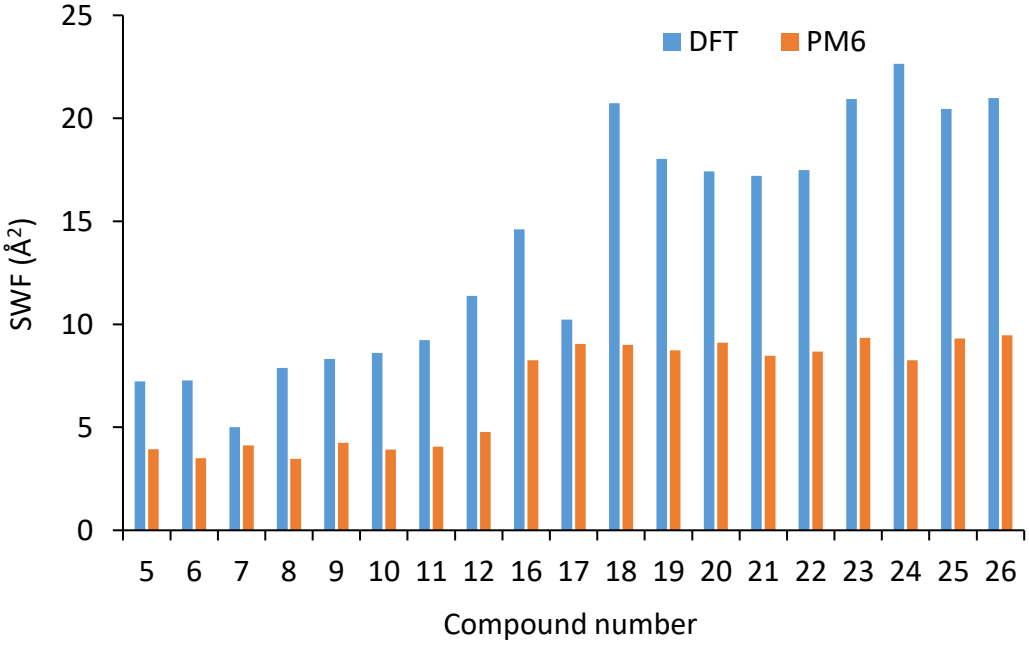

Figure S133: Comparison of data attained from DFT (B3LYP/6-31G*) and semi-empirical PM6 modelling methods for the parameter steric weighting factor (SWF).

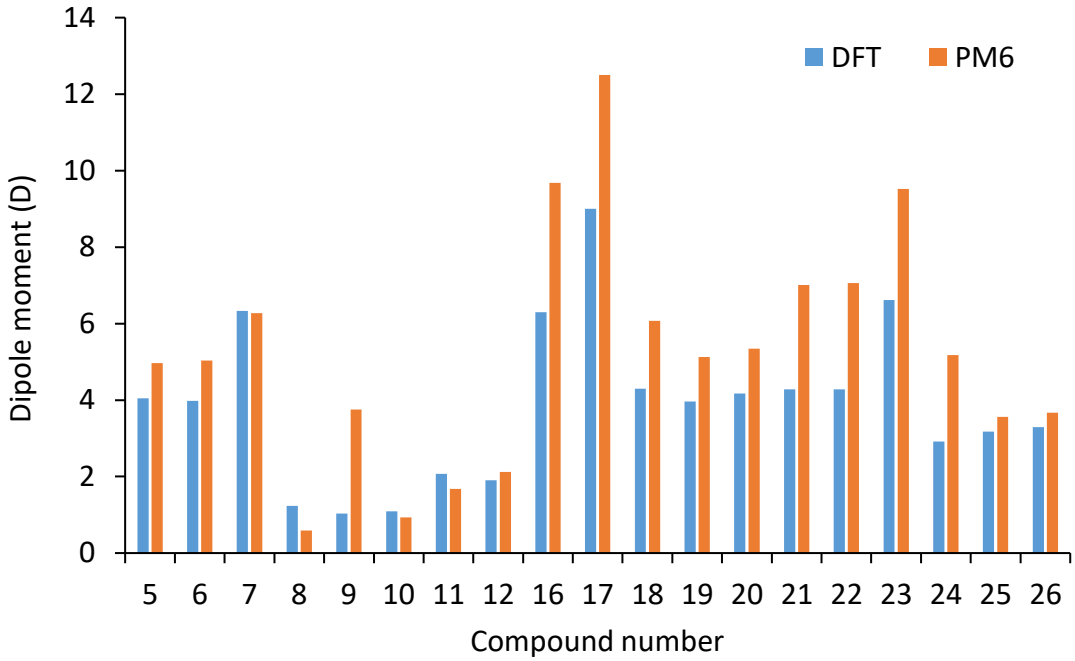

Figure S134: Comparison of data attained from DFT (B3LYP/6-31G*) and semi-empirical PM6 modelling methods for the parameter dipole moment.

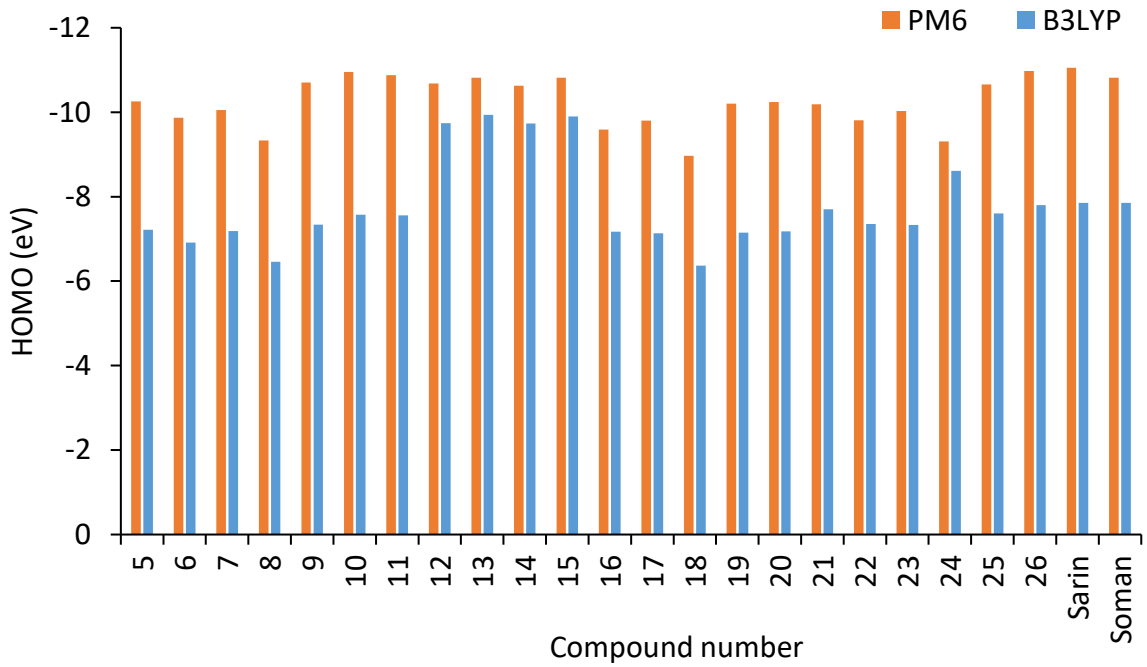

Figure S135: Comparison of data attained from DFT (B3LYP/6-31G*) and semi-empirical PM6 modelling methods for the parameter HOMO.

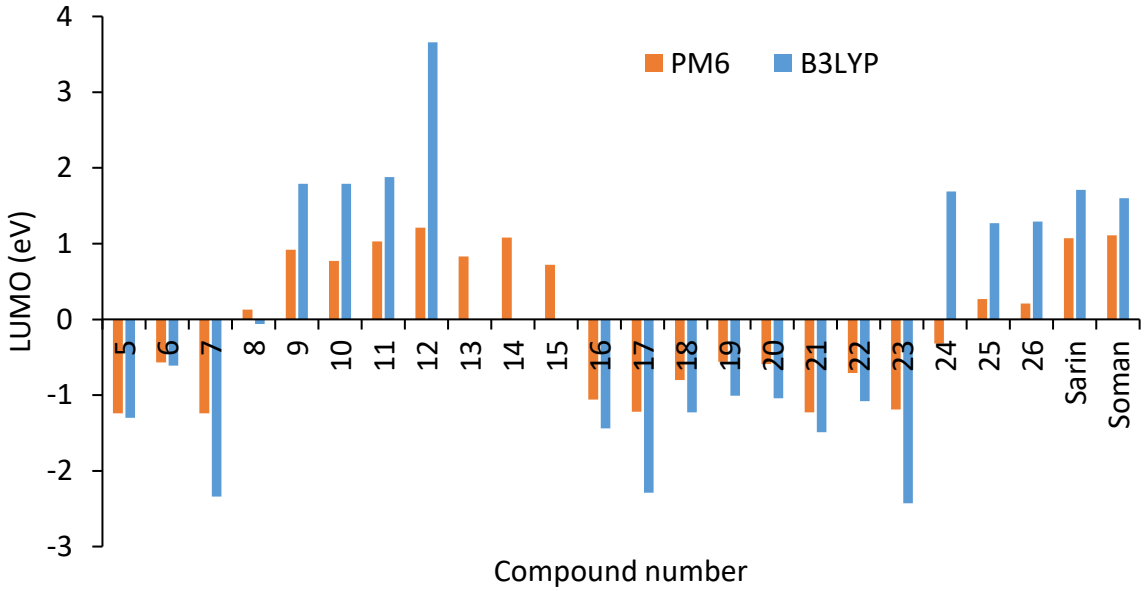

Figure S136: Comparison of data attained from DFT (B3LYP/6-31G*) and semi-empirical PM6 modelling methods for the parameter LUMO.

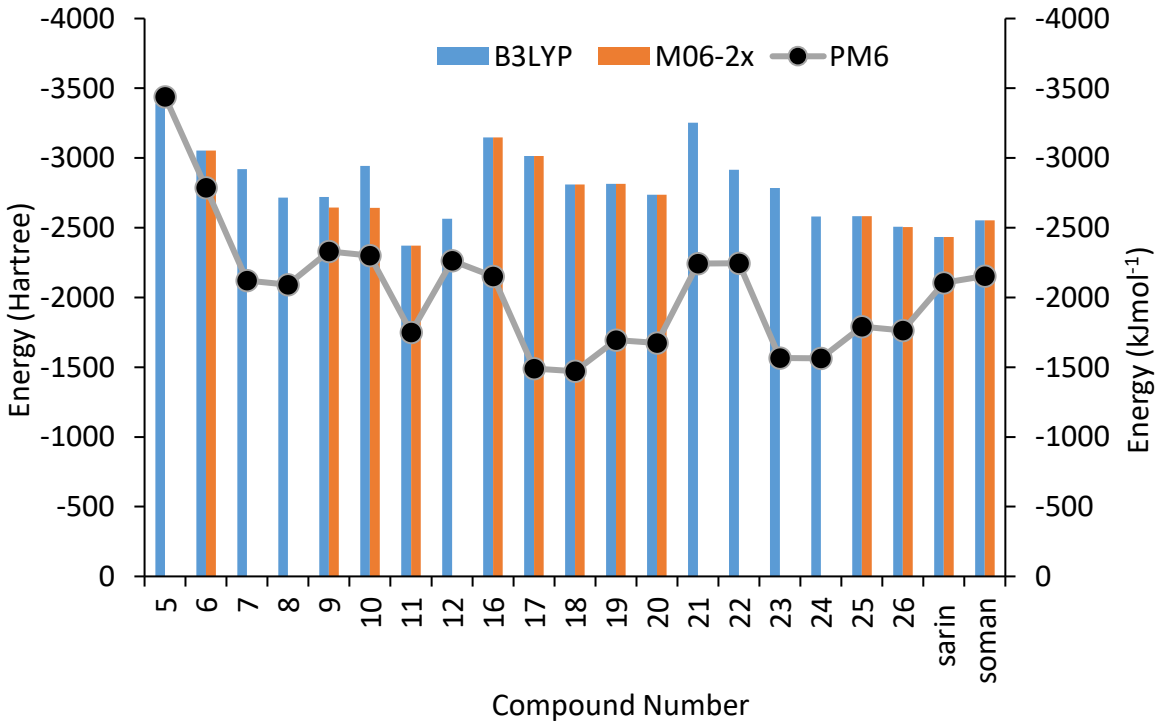

Figure S137: Comparison of data attained from DFT (B3LYP/6-31G*), semi-empirical PM6 and DFT (M06-2X/6-311g(d,p)) modelling methods for the parameter energy.

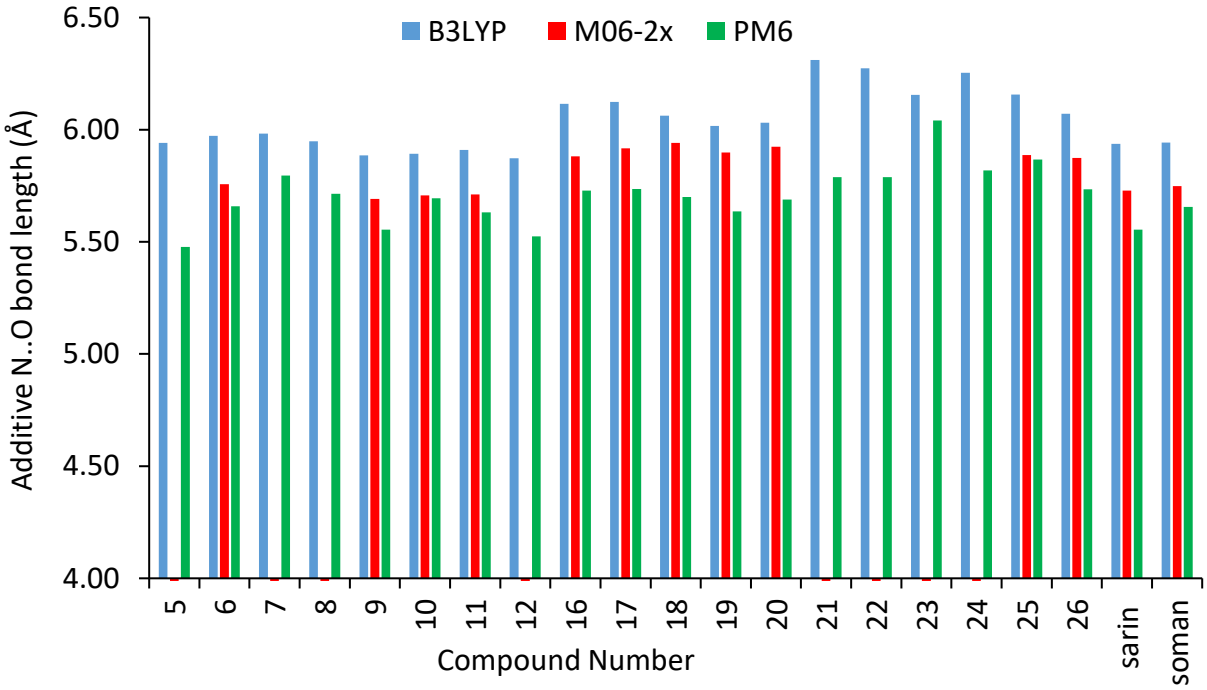

Figure S138: Comparison of data attained from DFT (B3LYP/6-31G*), semi-empirical PM6 and DFT (M06-2X/6-311g(d,p)) modelling methods for the additive N..O bond length.

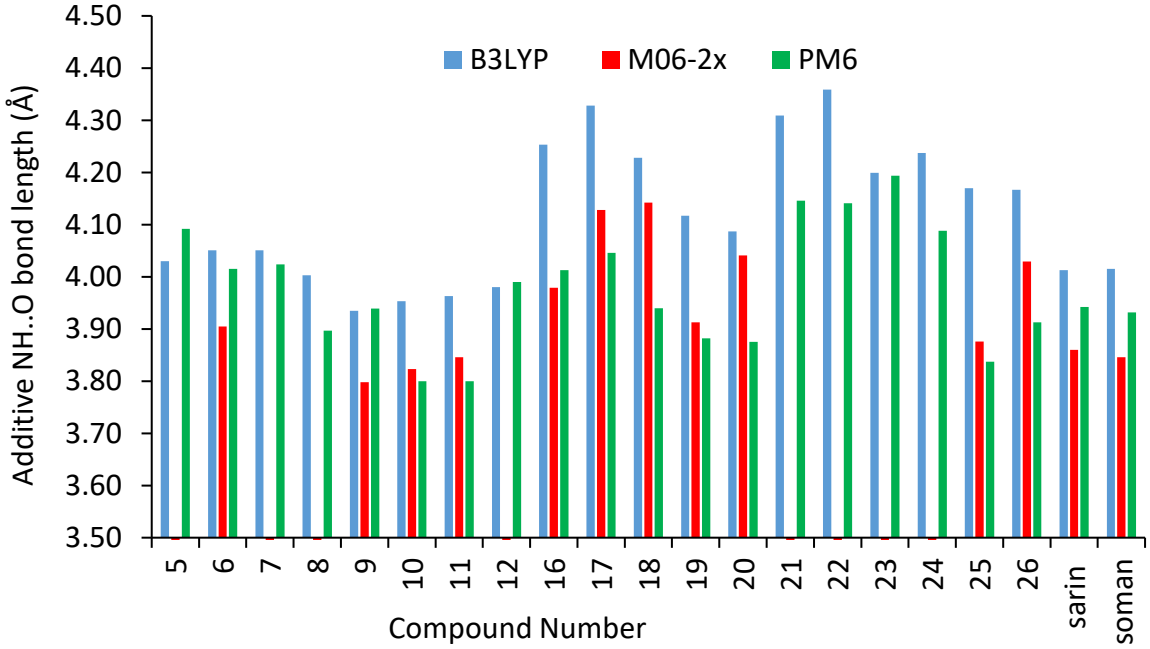

Figure S139: Comparison of data attained from DFT (B3LYP/6-31G*), semi-empirical PM6 and DFT (M06-2X/6-311g(d,p)) modelling methods for the additive NH..O bond length.

High-level DFT modelling

Each individual compound was pre-optimised in the gas phase at the PM6 level[15] using Spartan '16[18] before further geometry optimisation at the M06-2X level[16] and the 6-311g(d,p) basis set[15] using Gaussian16[17] with a PCM solvent model for acetonitrile. This functional was chosen as it is known to provide good results for main group elements and systems where hydrogen bonding is important and includes dispersion corrections to account for cumulative weak forces of interaction.[18] All structures were confirmed as energy minima by frequency analysis. Adducts were modelled by combining the appropriate M06-2X geometries. For each compound, initial geometries for appropriate coordination modes to **1** were chosen and allowed to freely optimise. Initial geometries for coordination via single oxygen atom (P=O or S=O), or via two oxygen atoms simultaneously (RO-P=O or O=S=O) were considered for **6**, **9**, **10**, **11**, **16-20**, **25**, **26**, sarin, soman; for **9**, the optimised geometry precluded a 2-oxygen coordination mode and so only the 1-oxygen mode was considered. Given the potential for the partial negative charge on fluorine in sarin and soman to engage in hydrogen bonding, an additional mode of association with the receptor via both the fluorine and P=O simultaneously (F-P=O association mode) was allowed to optimise for these systems. For sulfonates, stable binding modes were located utilising both S=O groups, but for all other compounds, the geometries instead converged on alternative binding modes involving only a single E=O (E = P, S) indicating that the RO-P=O or F-P=O binding modes are less favoured in these cases. In some cases, stable binding modes were located which utilised not only hydrogen bonding but also additional π-stacking interactions. In the images provided, dotted bonds are shown to indicate close contacts between relevant hydrogen bond donor and acceptor species; these are indicative only and should not be interpreted as in inferring bond strengths.

From these results, energies of complex formation could be determined by assessing the energy change for the reaction:

$$Receptor\ 1 + Binder \rightarrow Complex$$

These energies are found to be broadly comparable (see Table S4) but are not suitable for evaluating binding constants as solvation effects are not fully modelled and these are known to be significant in such hydrogen-bonded arrays.

It can clearly be seen that two binding modes are anomalously stable (**6**, Mode 2) and (**17**, Mode 1), with forming complexes ~ 84 kJmol^{-1} more stable than the free substrate and receptor, whilst the remaining structures fall in a narrow range of 49 to 66 kJmol^{-1} more stable. Notable, both the anomalously stable modes are those in which π-stacking is observed in addition to hydrogen-bonding interactions.

Table S4: Relative energies of binding modes compared to free species. [a] Mode 1 is binding through the single, primary H-bond acceptor atom. Mode 2 is bonding through two O acceptor atoms. Mode 3 is binding via fluoride. Mode 4 binding through the nitro functionality. [b] Oxygen except where otherwise specified [c] Fluorine [d] Sulfur.

Guest	Mode[a]	Total Energy Binding / kJmol^{-1}	NBO Charges on H-Bond Acceptors[b]					Evidence of Pi Stacking
			1	2	3	4	5	
sarin	1	-51.2	-1.107	-0.876	-0.582[c]			No
	2	-56.3						No
	3	-57.9						No
soman	1	-53.0	-1.109	-0.878	-0.582[c]			No
	2	-58.0						No
	3	-62.8						No
6	1	-58.0	-1.116	-0.860	-0.859	-0.823		No
	2	-84.6						Yes
9	1	-67.8	-1.138	-0.880	-0.866			No
10	1	-59.6	-1.130	-0.862	-0.862	-0.858		Yes
	2	-53.7						No
11	1	-63.0	-1.127	-0.860	-0.848			No
	2	-59.0						No
16	1	-81.5	-0.939	-0.939	-0.735			Yes
	2	-69.2						Yes
17	1	-74.4	-0.937	-0.936	-0.734	-0.413	-0.413	Yes
	2	-70.5						Yes
	4	-37.1						No
18	1	-84.2	-0.942	-0.942	-0.737			Yes
	2	-65.8						No
19	1	-57.8	-0.962	-0.961	-0.767			No
	2	-59.0						No
20	1	-49.2	-0.959	-0.959	-0.755			No
	2	-52.8						Yes
25	1	-41.1	-0.962	-0.961	-0.771			No
	2	-61.0						No
26	1	-58.9	-0.959	-0.958	-0.759			No
	2	-55.5						No

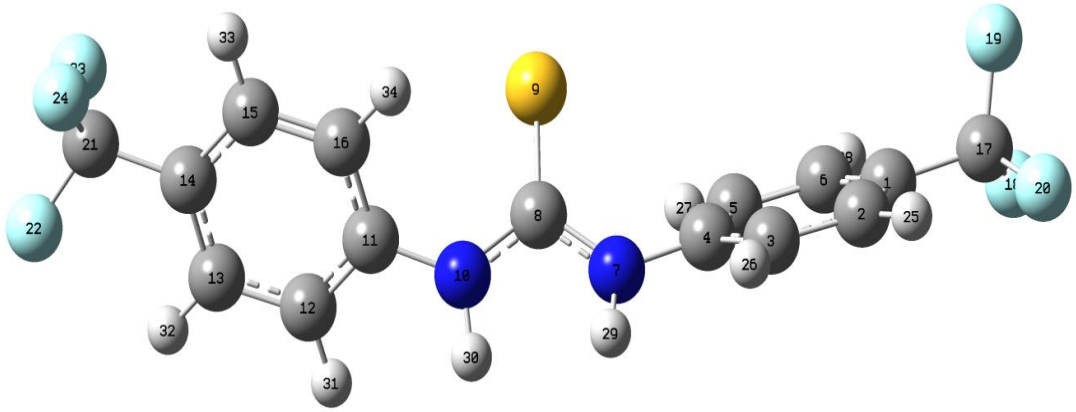

Figure S140: Output from the DFT modelling of **1** only. Total electronic energy (E(RM062X)):-1684.302146 Hartree. NBO Charges at Sulphur: S9 = -0.320 (see Table S5).

Table S5: Output from the DFT modelling of **1** only.

Center Number	Atomic Number	Atomic Type	Coordinates (Angstroms) X	Y	Z
1	6	0	5.128749	-0.064558	-0.263283
2	6	0	4.691981	0.951323	0.576343
3	6	0	3.355510	1.003248	0.951195
4	6	0	2.465816	0.036024	0.491200
5	6	0	2.912135	-0.995778	-0.335707
6	6	0	4.241929	-1.037866	-0.719094
7	7	0	1.125497	0.085992	0.941412
8	6	0	-0.001501	0.001189	0.183006
9	16	0	-0.005021	-0.033966	-1.495251
10	7	0	-1.126500	-0.051586	0.946989
11	6	0	-2.467001	-0.019210	0.494180
12	6	0	-3.353617	-0.978905	0.974364
13	6	0	-4.689653	-0.940421	0.595378
14	6	0	-5.127897	0.054210	-0.268308
15	6	0	-4.243537	1.019792	-0.745358
16	6	0	-2.914674	0.991144	-0.358056
17	6	0	6.552739	-0.104334	-0.724534
18	9	0	7.023559	-1.359179	-0.794036
19	9	0	6.695877	0.421530	-1.954171
20	9	0	7.370742	0.582272	0.084454
21	6	0	-6.551244	0.080441	-0.732746
22	9	0	-7.366280	-0.605705	0.079407
23	9	0	-6.687816	-0.454871	-1.958981
24	9	0	-7.030417	1.331599	-0.812338
25	1	0	5.385514	1.700782	0.935156
26	1	0	2.999966	1.795882	1.598415
27	1	0	2.221377	-1.759872	-0.663121
28	1	0	4.595858	-1.839397	-1.355788
29	1	0	1.005951	0.380323	1.903055
30	1	0	-1.006293	-0.304772	1.920215
31	1	0	-2.996476	-1.755362	1.639988
32	1	0	-5.381406	-1.683871	0.969697
33	1	0	-4.598815	1.804686	-1.401773
34	1	0	-2.225053	1.749216	-0.701908

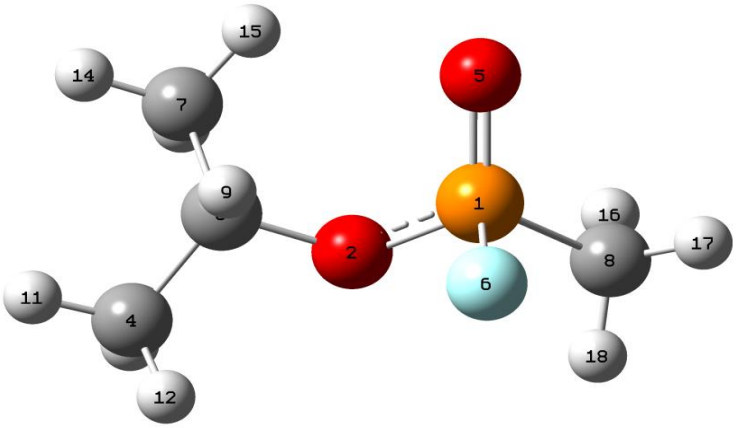

Figure S141: Output from the DFT modelling of sarin only. Total electronic energy (E(RM062X)):-750.131232 Hartree. NBO Charges at Selected Atoms: O2 = -0.876, O5 = -1.107, F6 = -0.582 (see Table S6).

Table S6: Output from the DFT modelling of sarin only.

Center Number	Atomic Number	Atomic Type	Coordinates (Angstroms) X	Y	Z
1	15	0	-0.812702	1.423205	-0.153104
2	8	0	0.212000	0.289626	0.252582
3	6	0	-0.135609	-1.125854	0.105888
4	6	0	0.557633	-1.848021	1.240314
5	8	0	-1.593217	1.201822	-1.381294
6	9	0	-1.785124	1.462393	1.109958
7	6	0	0.302882	-1.589442	-1.268449
8	6	0	0.119704	2.926719	0.014925
9	1	0	-1.220452	-1.219594	0.209435
10	1	0	1.638665	-1.716751	1.159039
11	1	0	0.329783	-2.914047	1.192105
12	1	0	0.224611	-1.459712	2.203119
13	1	0	1.380772	-1.451470	-1.377608
14	1	0	0.071016	-2.648837	-1.392124
15	1	0	-0.211584	-1.022974	-2.044862
16	1	0	0.871692	2.964249	-0.772254
17	1	0	-0.554742	3.776097	-0.087237
18	1	0	0.604672	2.952591	0.989567

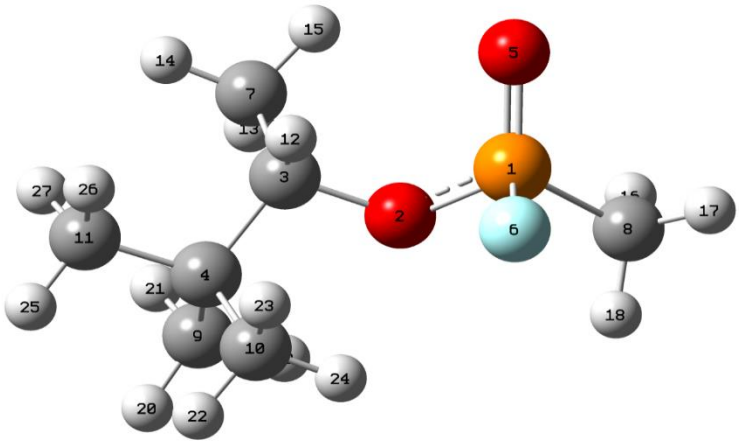

Figure S142: Output from the DFT modelling of soman only. Total electronic energy (E(RM062X)): -868.047449 Hartree. NBO Charges at Selected Atoms: O2 = -0.878, O5 = -1.109, F6 = -0.582 (see Table S7).

Table S7: Output from the DFT modelling of soman only.

Center Number	Atomic Number	Atomic Type	Coordinates (Angstroms) X	Y	Z
1	15	0	-0.937024	2.299793	-0.270997
2	8	0	-0.051833	1.003078	-0.442576
3	6	0	-0.631737	-0.330935	-0.276363
4	6	0	0.372704	-1.158151	0.541279
5	8	0	-2.298321	2.245495	-0.829289
6	9	0	-1.006541	2.459323	1.314264
7	6	0	-0.981037	-0.845973	-1.659328
8	6	0	0.142925	3.625328	-0.756809
9	6	0	1.711968	-1.282894	-0.191263
10	6	0	0.589450	-0.462872	1.890770
11	6	0	-0.220636	-2.550671	0.785799
12	1	0	-1.547221	-0.230529	0.318047
13	1	0	-0.090751	-0.898929	-2.287717
14	1	0	-1.435817	-1.835238	-1.600839
15	1	0	-1.696637	-0.166426	-2.123913
16	1	0	0.314932	3.562784	-1.830647
17	1	0	-0.332178	4.576587	-0.519834
18	1	0	1.090325	3.541219	-0.226283
19	1	0	2.118313	-0.297638	-0.429517
20	1	0	2.430783	-1.804555	0.445546
21	1	0	1.613961	-1.853324	-1.117632
22	1	0	1.248741	-1.065520	2.519891
23	1	0	-0.359741	-0.332126	2.419185
24	1	0	1.045394	0.519736	1.758176
25	1	0	0.429399	-3.110749	1.462111
26	1	0	-1.210153	-2.484124	1.247854
27	1	0	-0.309269	-3.122690	-0.139915

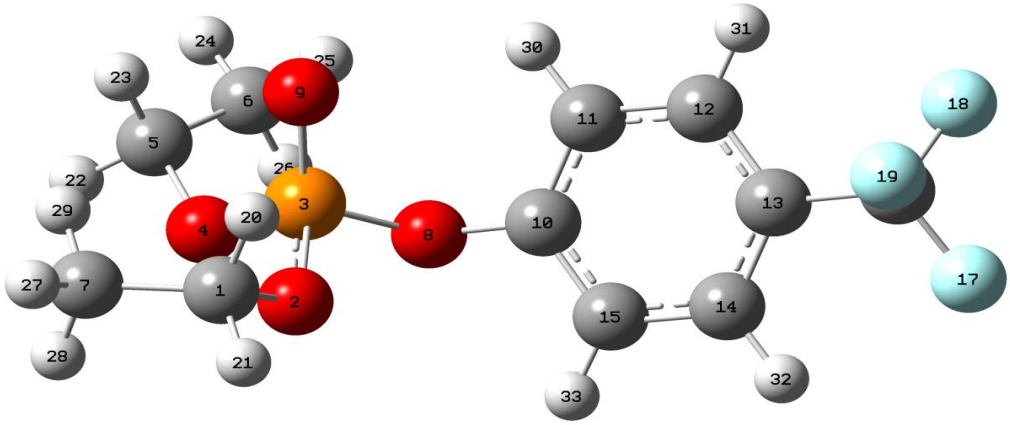

Figure S143: Output from the DFT modelling of **6** only. Total electronic energy (E(RM062X)):-1369.376406 Hartree. NBO Charges at Selected Atoms: O2 = -0.859, O4 = -0.860, O8 = -0.823, O9 = -1.116 (see Table S8).

Table S8: Output from the DFT modelling of **6** only.

Center Number	Atomic Number	Atomic Type	Coordinates (Angstroms) X	Y	Z
1	6	0	2.234140	2.285560	0.273295
2	8	0	1.049410	1.730069	-0.357797
3	15	0	1.047475	0.235577	-0.870934
4	8	0	1.415444	0.335459	-2.403231
5	6	0	1.973992	-0.809758	-3.101535
6	6	0	0.943151	-1.903123	-3.283630
7	6	0	3.365974	2.449186	-0.718692
8	8	0	-0.529389	-0.073761	-0.944153
9	8	0	1.844606	-0.719439	-0.082062
10	6	0	-1.273206	-0.252981	0.213422
11	6	0	-1.068773	-1.377741	1.003843
12	6	0	-1.861110	-1.556117	2.128159
13	6	0	-2.840946	-0.617756	2.441023
14	6	0	-3.035362	0.503362	1.641980
15	6	0	-2.243817	0.690030	0.516365
16	6	0	-3.656187	-0.806566	3.683576
17	9	0	-4.804035	-0.116898	3.649700
18	9	0	-3.971659	-2.094816	3.886174
19	9	0	-2.994752	-0.401566	4.782218
20	1	0	2.515504	1.634177	1.101710
21	1	0	1.904119	3.243741	0.667457
22	1	0	2.305797	-0.406866	-4.055459
23	1	0	2.840015	-1.162978	-2.540096
24	1	0	1.370145	-2.705178	-3.887762
25	1	0	0.642895	-2.324481	-2.321902
26	1	0	0.059118	-1.514673	-3.790872
27	1	0	4.200037	2.958557	-0.233527
28	1	0	3.041841	3.043278	-1.574031
29	1	0	3.721869	1.480256	-1.075589
30	1	0	-0.300093	-2.090227	0.735021
31	1	0	-1.723783	-2.429103	2.754295
32	1	0	-3.802102	1.225189	1.891860
33	1	0	-2.370326	1.549586	-0.128825

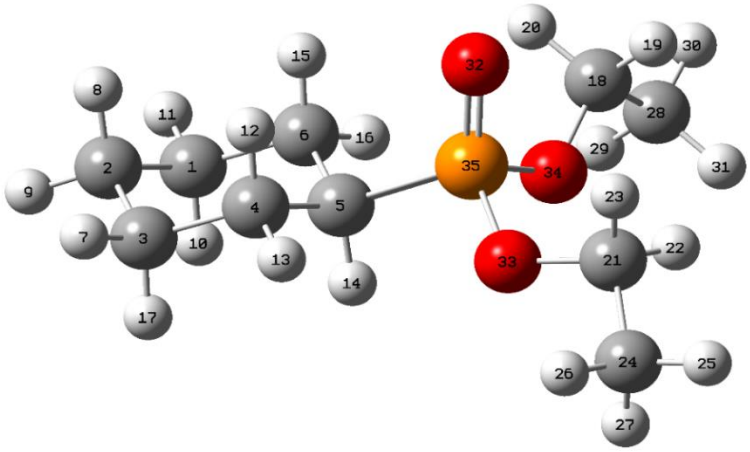

Figure S144: Output from the DFT modelling of **9** only. Total electronic energy (E(RM062X)):- -960.715367 Hartree. NBO Charges at Oxygen: O32 = -1.138, O33 = -0.866, O34 = -0.880 (see Table S9).

Table S9: Output from the DFT modelling of **9** only.

Center Number	Atomic Number	Atomic Type	Coordinates (Angstroms) X	Y	Z
1	6	0	-1.878251	-2.491138	-0.487328
2	6	0	-0.370967	-2.746561	-0.544167
3	6	0	0.410302	-1.432649	-0.484041
4	6	0	0.047290	-0.630391	0.767886
5	6	0	-1.467630	-0.378378	0.830317
6	6	0	-2.259563	-1.695391	0.763337
7	1	0	1.485448	-1.626808	-0.496512
8	1	0	-0.080622	-3.376555	0.304932
9	1	0	-0.115947	-3.296497	-1.453290
10	1	0	-2.183207	-1.926776	-1.376129
11	1	0	-2.427085	-3.435710	-0.502474
12	1	0	0.347627	-1.191654	1.659960
13	1	0	0.585639	0.320373	0.783992
14	1	0	-1.765995	0.261337	-0.008921
15	1	0	-2.036761	-2.293011	1.655453
16	1	0	-3.333112	-1.486933	0.766408
17	1	0	0.180825	-0.834097	-1.373224
18	6	0	-4.409000	0.107936	3.118699
19	1	0	-4.248951	0.480540	4.131720
20	1	0	-4.200318	-0.964649	3.108727
21	6	0	-1.501563	3.028402	3.005099
22	1	0	-2.573947	3.137535	3.186335
23	1	0	-1.012939	2.734732	3.936365
24	6	0	-0.905984	4.296825	2.441452
25	1	0	-1.035297	5.113622	3.153143
26	1	0	0.160115	4.164660	2.252485
27	1	0	-1.399535	4.566344	1.506955
28	6	0	-5.809202	0.398510	2.631812
29	1	0	-5.946105	0.019526	1.617869
30	1	0	-6.536002	-0.084488	3.286826
31	1	0	-5.997500	1.473020	2.634150
32	8	0	-1.496159	-0.088926	3.609548
33	8	0	-1.306675	1.979233	2.030108
34	8	0	-3.492522	0.781809	2.228451
35	15	0	-1.906836	0.525559	2.321321

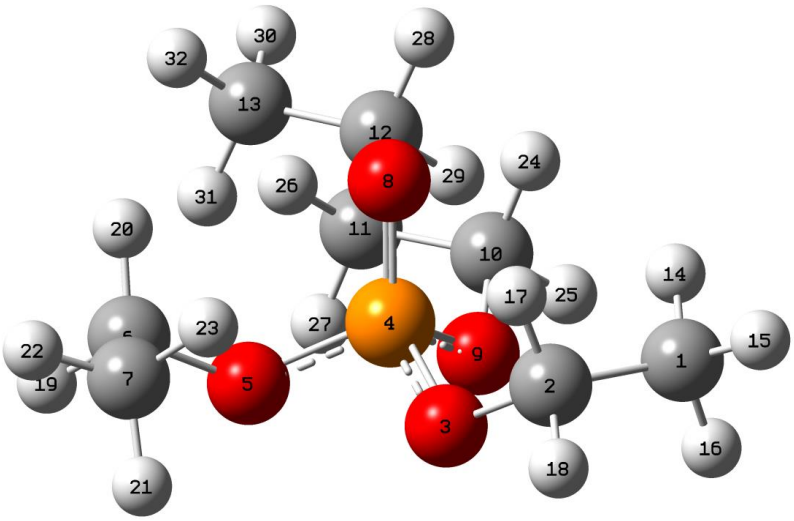

Figure S145: Output from the DFT modelling of **10** only. Total electronic energy (E(RM062X)): -958.536196 Hartree. NBO Charges at Selected Atoms: O3 = -0.862, O5 = -0.862, O8 = -1.130, O9 = -0.858 (see Table S10).

Table S10: Output from the DFT modelling of **10** only.

Center Number	Atomic Number	Atomic Type	Coordinates (Angstroms) X	Y	Z
1	6	0	-1.160942	3.370078	1.527378
2	6	0	-0.969550	3.435646	0.026156
3	8	0	-1.256444	2.166352	-0.611048
4	15	0	-0.310149	0.917993	-0.355421
5	8	0	-0.613960	-0.020894	-1.598343
6	6	0	0.222478	0.046829	-2.779573
7	6	0	0.071349	1.368861	-3.503495
8	8	0	1.115028	1.240328	-0.139128
9	8	0	-1.026762	0.166220	0.844959
10	6	0	-0.273992	-0.747337	1.677782
11	6	0	0.163673	-1.989392	0.924257
12	6	0	0.837946	-2.993480	1.857773
13	6	0	1.302385	-4.243484	1.114631
14	1	0	-0.426253	2.707744	1.989839
15	1	0	-1.034358	4.367636	1.951227
16	1	0	-2.161689	3.010276	1.769984
17	1	0	0.049973	3.726415	-0.233187
18	1	0	-1.665848	4.133593	-0.433618
19	1	0	-0.111075	-0.784976	-3.396138
20	1	0	1.256857	-0.126028	-2.477359
21	1	0	-0.977025	1.560058	-3.736210
22	1	0	0.637662	1.336876	-4.435712
23	1	0	0.454938	2.194118	-2.900045
24	1	0	0.587312	-0.213674	2.086983
25	1	0	-0.952672	-1.001929	2.490817
26	1	0	0.860240	-1.708104	0.126647
27	1	0	-0.710313	-2.444519	0.447991
28	1	0	1.693124	-2.516079	2.346904
29	1	0	0.138693	-3.274111	2.651845
30	1	0	1.780325	-4.953234	1.791929
31	1	0	0.457385	-4.746935	0.638525
32	1	0	2.021648	-3.984845	0.333649

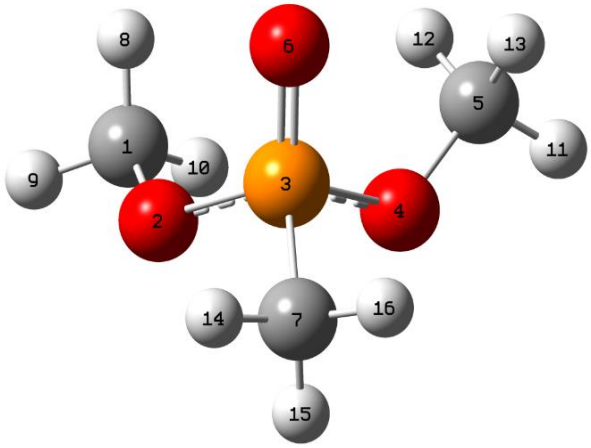

Figure S146: Output from the DFT modelling of **11** only. Total electronic energy (E(RM062X)): -686.773578 Hartree. NBO Charges at Selected Atoms: O2 = -0.848, O4 = -0.860, O6 = -1.127 (see Table S11).

Table S11: Output from the DFT modelling of **11** only.

Center Number	Atomic Number	Atomic Type	Coordinates (Angstroms) X	Y	Z
1	6	0	-0.966108	1.997798	-0.139257
2	8	0	-0.478245	1.136913	0.901082
3	15	0	0.518119	-0.054042	0.506522
4	8	0	-0.346257	-0.959794	-0.499608
5	6	0	0.040439	-1.114483	-1.874229
6	8	0	1.809250	0.379859	-0.078066
7	6	0	0.572405	-0.994906	2.020513
8	1	0	-0.134242	2.429399	-0.698228
9	1	0	-1.531502	2.787952	0.346505
10	1	0	-1.618214	1.434456	-0.809136
11	1	0	-0.581280	-1.908934	-2.278393
12	1	0	-0.137857	-0.190086	-2.425298
13	1	0	1.092931	-1.385595	-1.947074
14	1	0	1.000153	-0.381147	2.812503
15	1	0	-0.435170	-1.302496	2.296963
16	1	0	1.195577	-1.874894	1.865203

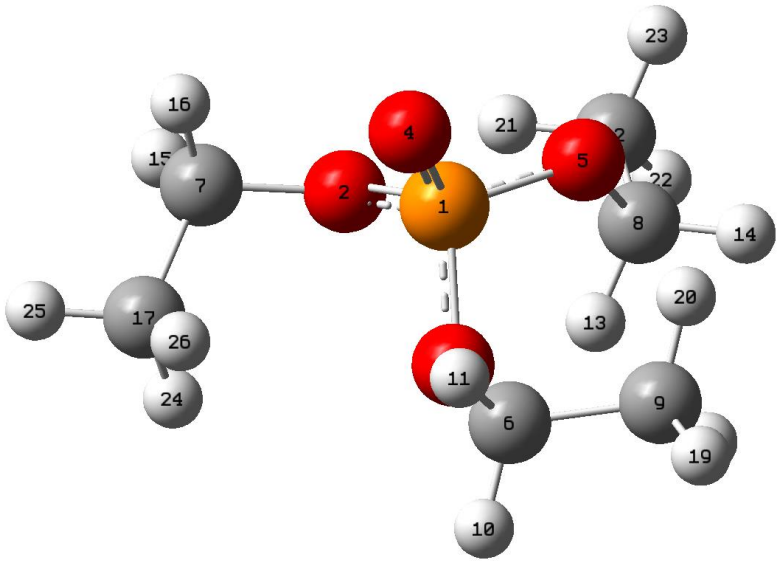

Figure S147: Output from the DFT modelling of **13** only.

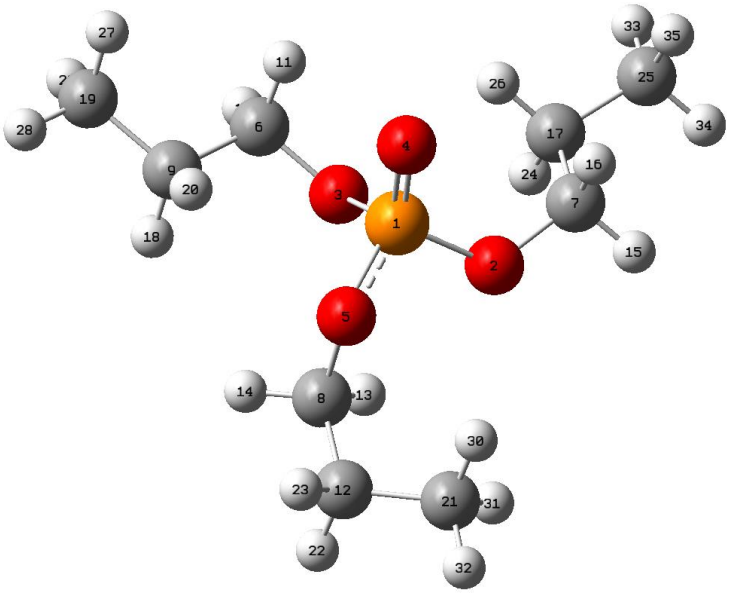

Figure S148: Output from the DFT modelling of **14** only.

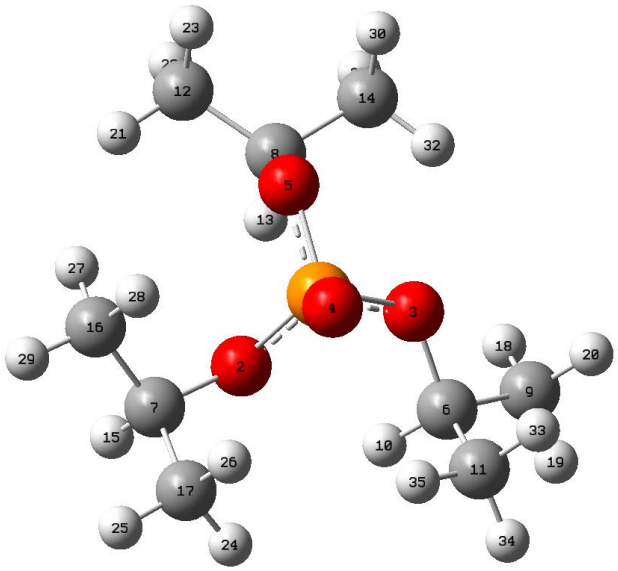

Figure S149: Output from the DFT modelling of **15** only.

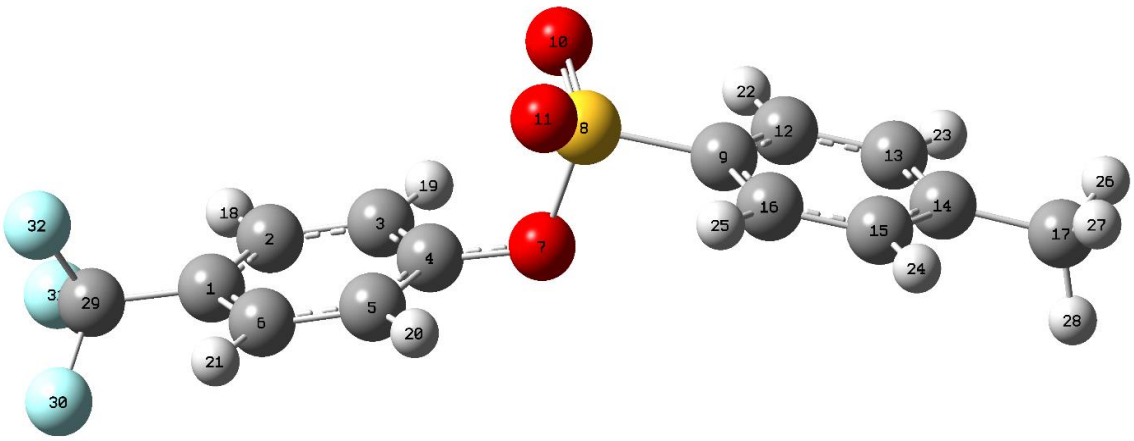

Figure S150: Output from the DFT modelling of **16** only. Total electronic energy (E(RM062X)): -1463.337306 Hartree. NBO Charges at Oxygen: O7 = -0.735, O10 = -0.939, O11 = -0.939 (see Table S12).

Table S12: Output from the DFT modelling of **16** only.

Center Number	Atomic Number	Atomic Type	Coordinates (Angstroms) X	Y	Z
1	6	0	0.386498	0.120093	5.251510
2	6	0	1.111040	-0.840967	4.556164
3	6	0	1.069173	-0.859171	3.167514
4	6	0	0.299080	0.089258	2.512622
5	6	0	-0.432662	1.052210	3.193992
6	6	0	-0.384499	1.065764	4.579798
7	8	0	0.292163	0.107880	1.116117
8	16	0	-0.832149	-0.838333	0.388067
9	6	0	-0.456595	-0.431445	-1.279041
10	8	0	-0.496829	-2.215771	0.670903
11	8	0	-2.135144	-0.336138	0.762016
12	6	0	0.489071	-1.190037	-1.958586
13	6	0	0.786887	-0.850704	-3.270523
14	6	0	0.159278	0.230509	-3.895301
15	6	0	-0.788197	0.969918	-3.179910
16	6	0	-1.102388	0.650281	-1.867883
17	6	0	0.510328	0.608726	-5.307884
18	1	0	1.709696	-1.566455	5.091063
19	1	0	1.624643	-1.589060	2.593499
20	1	0	-1.016995	1.773936	2.638557
21	1	0	-0.937609	1.812678	5.135770
22	1	0	0.967280	-2.032471	-1.474798
23	1	0	1.514900	-1.436584	-3.819241
24	1	0	-1.288032	1.803818	-3.658881
25	1	0	-1.841983	1.215308	-1.314481
26	1	0	0.907533	-0.244748	-5.857023
27	1	0	-0.360494	0.995824	-5.837744
28	1	0	1.273291	1.391833	-5.305928
29	6	0	0.389994	0.131469	6.751006
30	9	0	0.473026	1.377896	7.240160
31	9	0	1.410278	-0.566446	7.264572
32	9	0	-0.737368	-0.399071	7.254338

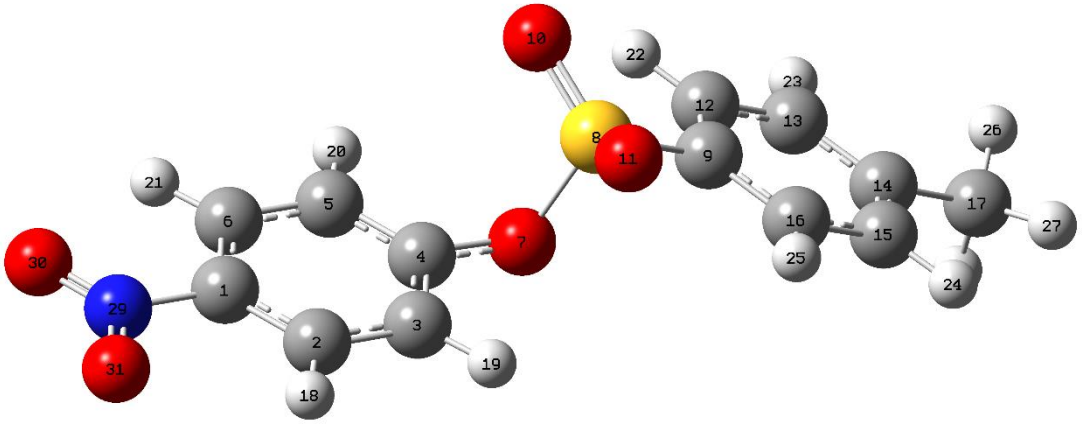

Figure S151: Output from the DFT modelling of **17** only. Total electronic energy (E(RM062X)): -1330.778537 Hartree. NBO Charges at Oxygen: O7 = -0.734, O10 = -0.937, O11 = -0.936, O30 = -0.413, O31 = -0.413 (see Table S13).

Table S13: Output from the DFT modelling of **17** only.

Center Number	Atomic Number	Atomic Type	Coordinates (Angstroms) X	Y	Z
1	6	0	0.421888	-0.144978	5.224473
2	6	0	1.051730	0.889088	4.547061
3	6	0	0.988616	0.905417	3.162070
4	6	0	0.303728	-0.112144	2.510952
5	6	0	-0.327324	-1.143347	3.194543
6	6	0	-0.266726	-1.162277	4.579559
7	8	0	0.282943	-0.118859	1.119015
8	16	0	-0.988659	0.647612	0.411669
9	6	0	-0.556567	0.350953	-1.263755
10	8	0	-2.185947	-0.075739	0.774468
11	8	0	-0.882016	2.052030	0.734340
12	6	0	-1.007583	-0.813317	-1.876586
13	6	0	-0.651954	-1.041583	-3.196812
14	6	0	0.145363	-0.130247	-3.897007
15	6	0	0.578986	1.028985	-3.247887
16	6	0	0.236684	1.279617	-1.926896
17	6	0	0.544599	-0.407372	-5.320067
18	1	0	1.576242	1.657732	5.096306
19	1	0	1.463190	1.687482	2.584657
20	1	0	-0.850259	-1.912357	2.641928
21	1	0	-0.740103	-1.945898	5.153532
22	1	0	-1.632598	-1.512231	-1.334981
23	1	0	-1.001560	-1.938491	-3.694684
24	1	0	1.188565	1.746440	-3.784509
25	1	0	0.563620	2.181146	-1.424105
26	1	0	-0.256300	-0.913481	-5.859947
27	1	0	0.797583	0.513631	-5.844815
28	1	0	1.422359	-1.058863	-5.341159
29	7	0	0.488562	-0.164648	6.697019
30	8	0	-0.064977	-1.074587	7.275670
31	8	0	1.093034	0.730287	7.247437

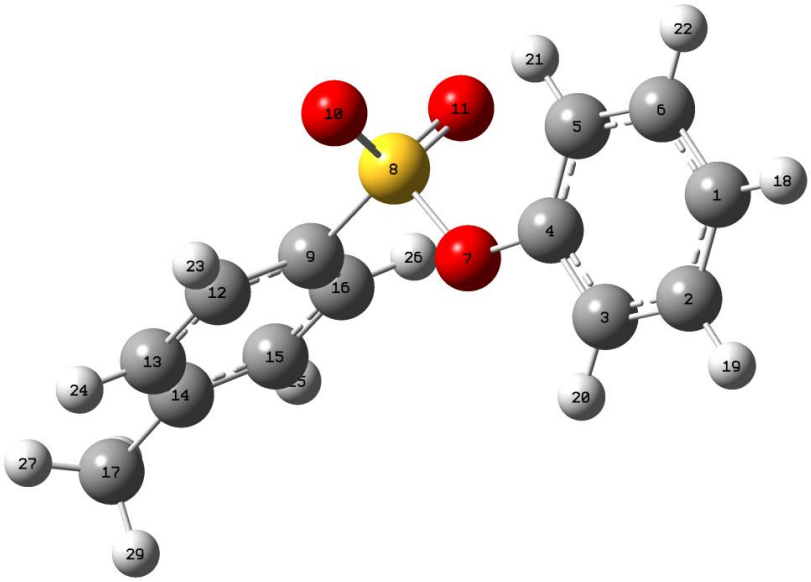

Figure S152: Output from the DFT modelling of **18** only. Total electronic energy (E(RM062X)): -1126.290819 Hartree. NBO Charges at Selected Atoms: O7 = -0.737, O10 = -0.942, O11 = -0.942 (see Table S14).

Table S14: Output from the DFT modelling of **18** only.

Center Number	Atomic Number	Atomic Type	Coordinates (Angstroms) X	Y	Z
1	6	0	0.546570	-0.000000	5.259903
2	6	0	1.636621	-0.000000	4.393108
3	6	0	1.439276	-0.000000	3.019022
4	6	0	0.142336	0.000000	2.521959
5	6	0	-0.960858	0.000000	3.365581
6	6	0	-0.742337	0.000000	4.741550
7	8	0	0.063395	0.000000	1.125332
8	16	0	-1.364887	0.000000	0.346196
9	6	0	-0.740755	0.000000	-1.297106
10	8	0	-2.034861	-1.248032	0.637028
11	8	0	-2.034861	1.248032	0.637028
12	6	0	-0.497870	-1.217178	-1.923080
13	6	0	0.000079	-1.204557	-3.217614
14	6	0	0.259288	-0.000000	-3.878239
15	6	0	0.000079	1.204557	-3.217614
16	6	0	-0.497870	1.217178	-1.923080
17	6	0	0.828005	-0.000000	-5.270453
18	1	0	0.702116	-0.000000	6.331241
19	1	0	2.646259	-0.000000	4.784916
20	1	0	2.269224	-0.000000	2.324013
21	1	0	-1.971070	0.000000	2.979763
22	1	0	-1.596931	0.000000	5.406748
23	1	0	-0.708963	-2.148197	-1.411993
24	1	0	0.186683	-2.143695	-3.725288
25	1	0	0.186683	2.143695	-3.725288
26	1	0	-0.708963	2.148197	-1.411993
27	1	0	0.516539	-0.887085	-5.822174
28	1	0	0.516539	0.887085	-5.822174
29	1	0	1.920534	0.000000	-5.227292

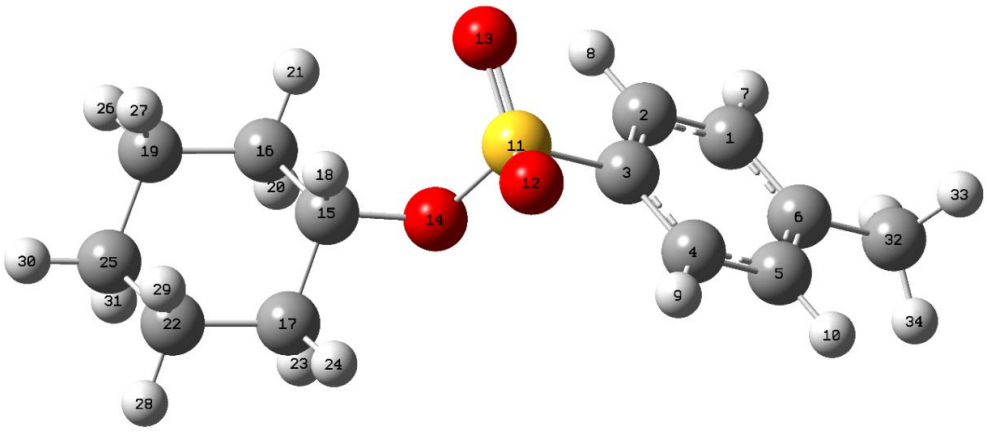

Figure S153: Output from the DFT modelling of **19** only. Total electronic energy (E(RM062X)): -1129.918714 Hartree. NBO Charges at Oxygen: O12 = -0.961, O13 = -0.962, O14 = -0.767 (see Table S15).

Table S15: Output from the DFT modelling of **19** only.

Center Number	Atomic Number	Atomic Type	Coordinates (Angstroms) X	Y	Z
1	6	0	-1.037574	-0.622530	-0.313373
2	6	0	0.332944	-0.639890	-0.098466
3	6	0	0.969687	0.553529	0.221568
4	6	0	0.276504	1.753819	0.324557
5	6	0	-1.093677	1.748001	0.105583
6	6	0	-1.767192	0.565777	-0.214818
7	1	0	-1.549564	-1.544874	-0.562248
8	1	0	0.899009	-1.560525	-0.168194
9	1	0	0.800094	2.666874	0.579028
10	1	0	-1.649514	2.675304	0.183817
11	16	0	2.714140	0.546911	0.469445
12	8	0	3.111195	1.699146	1.256166
13	8	0	3.156520	-0.764234	0.906230
14	8	0	3.182244	0.772366	-1.042096
15	6	0	4.626849	0.709485	-1.300965
16	6	0	4.949992	-0.629199	-1.940969
17	6	0	4.962318	1.884354	-2.200623
18	1	0	5.155301	0.812246	-0.346459
19	6	0	6.427782	-0.675818	-2.343138
20	1	0	4.318558	-0.741296	-2.829097
21	1	0	4.701595	-1.435216	-1.247764
22	6	0	6.439383	1.832256	-2.604556
23	1	0	4.329333	1.824345	-3.092602
24	1	0	4.725056	2.817032	-1.684256
25	6	0	6.783930	0.494211	-3.263256
26	1	0	6.643824	-1.628620	-2.830789
27	1	0	7.050338	-0.630155	-1.442200
28	1	0	6.662717	2.662026	-3.278253
29	1	0	7.063061	1.967428	-1.713515
30	1	0	7.845555	0.463323	-3.519133
31	1	0	6.223314	0.398905	-4.200323
32	6	0	-3.257460	0.567743	-0.419531
33	1	0	-3.767526	0.425245	0.536963
34	1	0	-3.594589	1.516524	-0.837706
35	1	0	-3.563853	-0.239771	-1.084638

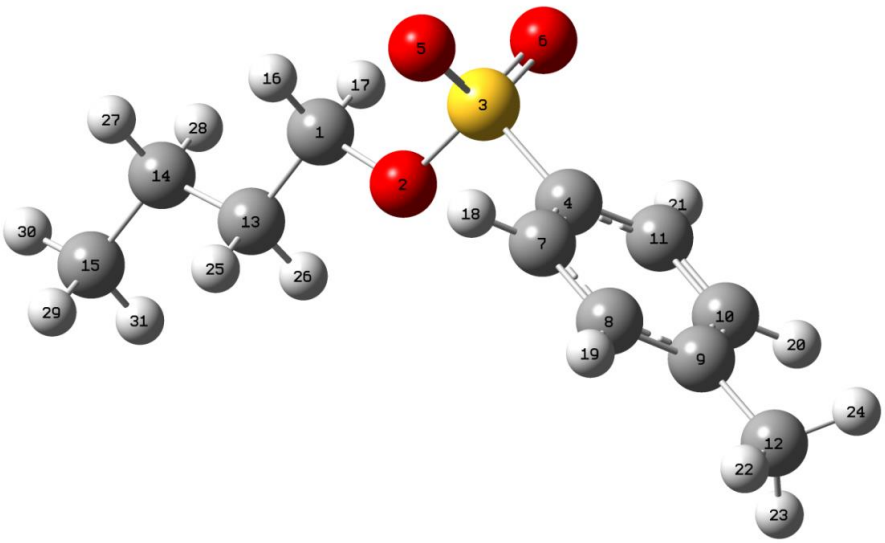

Figure S154: Output from the DFT modelling of **20** only. Total electronic energy (E(RM062X)): -1052.499642 Hartree. NBO Charges at Oxygen: O2 = -0.755, O5 = -0.959, O6 = -0.959 (see Table S16).

Table S16: Output from the DFT modelling of **20** only.

Center Number	Atomic Number	Atomic Type	Coordinates (Angstroms) X	Y	Z
1	6	0	-1.869619	-0.041811	-1.515264
2	8	0	-0.638178	0.136850	-0.759025
3	16	0	0.524511	0.964708	-1.489151
4	6	0	1.770653	0.834945	-0.251302
5	8	0	0.095129	2.342920	-1.626068
6	8	0	0.922788	0.244015	-2.682980
7	6	0	1.849674	1.813478	0.730312
8	6	0	2.827553	1.692511	1.709746
9	6	0	3.710835	0.611521	1.714503
10	6	0	3.601559	-0.356771	0.709630
11	6	0	2.634085	-0.256158	-0.277132
12	6	0	4.771687	0.480497	2.772979
13	6	0	-2.836972	-0.775554	-0.614236
14	6	0	-4.168540	-1.029766	-1.319699
15	6	0	-5.157347	-1.763360	-0.417274
16	1	0	-2.251441	0.942929	-1.795342
17	1	0	-1.640756	-0.617215	-2.414930
18	1	0	1.168570	2.655223	0.719563
19	1	0	2.905759	2.450835	2.479827
20	1	0	4.286155	-1.197445	0.702055
21	1	0	2.552941	-0.998921	-1.060936
22	1	0	4.724844	1.303764	3.484899
23	1	0	4.652759	-0.457661	3.319266
24	1	0	5.764992	0.471275	2.319049
25	1	0	-2.999973	-0.182484	0.290250
26	1	0	-2.387961	-1.725472	-0.309847
27	1	0	-4.598238	-0.075193	-1.639146
28	1	0	-3.992155	-1.615138	-2.227458
29	1	0	-5.365108	-1.180886	0.483622
30	1	0	-6.104025	-1.941491	-0.929861
31	1	0	-4.754187	-2.730144	-0.106048

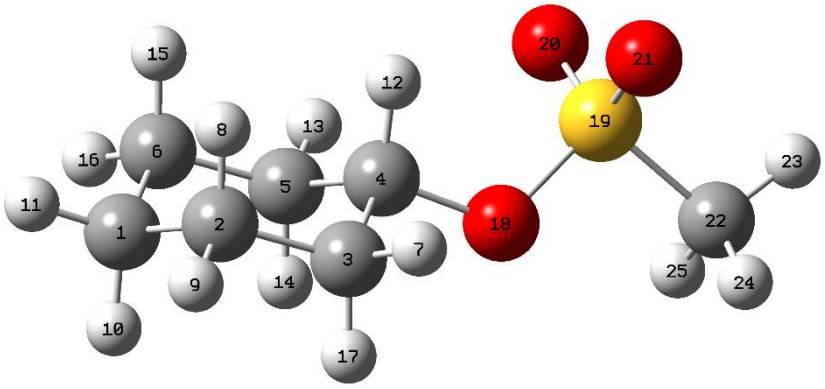

Figure S155: Output from the DFT modelling of **25** only. Total electronic energy (E(RM062X)): -898.910055 Hartree. NBO Charges at Oxygen: O18 = -0.771, O20 = -0.962, O21 = -0.961 (see Table S17).

Table S17: Output from the DFT modelling of **25** only.

Center Number	Atomic Number	Atomic Type	Coordinates (Angstroms) X	Y	Z
1	6	0	-2.501645	-1.051162	-0.077932
2	6	0	-0.977116	-1.181795	-0.117033
3	6	0	-0.302389	0.187621	0.012754
4	6	0	-0.776839	0.884364	1.274289
5	6	0	-2.287087	1.036466	1.325515
6	6	0	-2.956478	-0.335879	1.196226
7	1	0	0.785326	0.093071	0.036780
8	1	0	-0.648570	-1.826073	0.706499
9	1	0	-0.655134	-1.660958	-1.043831
10	1	0	-2.836772	-0.479379	-0.950979
11	1	0	-2.965527	-2.038119	-0.142701
12	1	0	-0.418684	0.337853	2.154085
13	1	0	-2.573816	1.532556	2.254647
14	1	0	-2.591065	1.679032	0.491961
15	1	0	-2.697984	-0.948923	2.067338
16	1	0	-4.041681	-0.215061	1.203524
17	1	0	-0.565783	0.816124	-0.844935
18	8	0	-0.162507	2.217259	1.276517
19	16	0	0.431207	2.731063	2.667345
20	8	0	-0.632869	2.791250	3.652740
21	8	0	1.605183	1.945920	3.001654
22	6	0	0.899870	4.356820	2.157341
23	1	0	1.340335	4.837762	3.028903
24	1	0	1.626201	4.264000	1.353815
25	1	0	0.004524	4.880773	1.832515

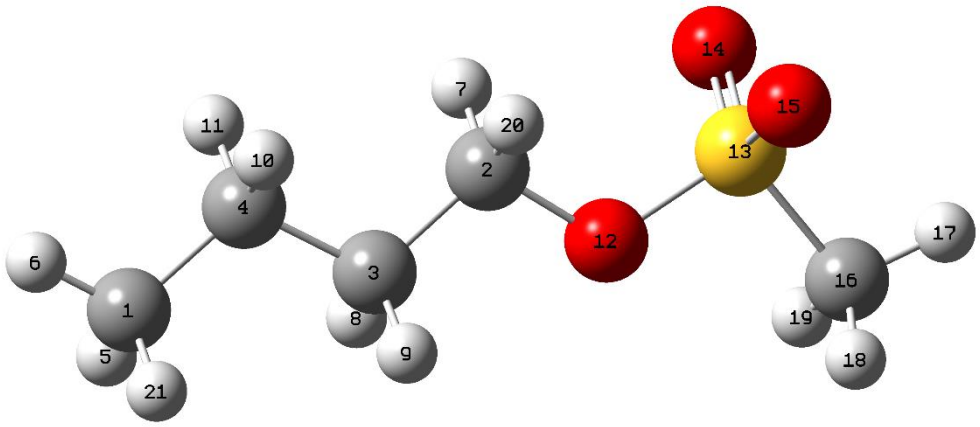

Figure S156: Output from the DFT modelling of **26** only. Total electronic energy (E(RM062X)): -821.490942 Hartree. NBO Charges at Oxygen: O12 = -0.759, O14 = -0.959, O15 = -0.958 (see Table S18).

Table S18: Output from the DFT modelling of **26** only.

Center Number	Atomic Number	Atomic Type	Coordinates (Angstroms) X	Y	Z
1	6	0	-2.127437	-1.117562	-1.772035
2	6	0	-0.695308	0.866798	1.225895
3	6	0	-1.095864	0.577392	-0.202843
4	6	0	-1.718288	-0.812188	-0.333441
5	1	0	-2.859579	-0.389291	-2.129339
6	1	0	-2.571302	-2.110924	-1.854842
7	1	0	-1.557527	0.848302	1.896362
8	1	0	-1.808913	1.338568	-0.532664
9	1	0	-0.212008	0.652935	-0.842806
10	1	0	-1.003615	-1.564345	0.014985
11	1	0	-2.592231	-0.880972	0.321808
12	8	0	-0.126921	2.206157	1.245299
13	16	0	0.381486	2.735143	2.669069
14	8	0	-0.750642	2.823446	3.571817
15	8	0	1.518970	1.940130	3.090954
16	6	0	0.902627	4.345604	2.164364
17	1	0	1.287692	4.837649	3.055695
18	1	0	1.681460	4.229848	1.414792
19	1	0	0.038118	4.873144	1.769358
20	1	0	0.062429	0.164332	1.580952
21	1	0	-1.261878	-1.077411	-2.437795

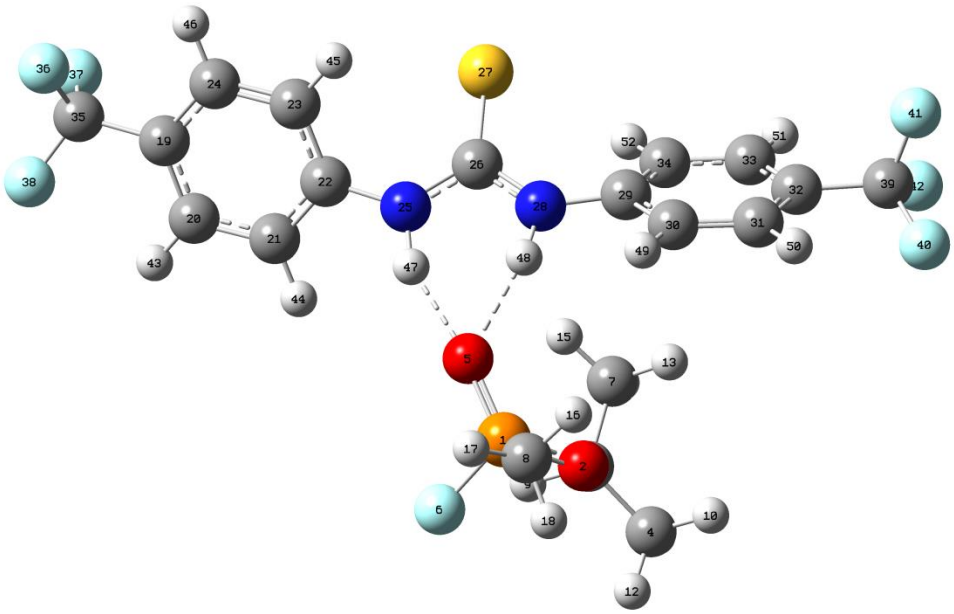

Figure S157: Output from the DFT modelling of **1**:sarin initiated with the P=O coordinated to the receptor through the formation of two hydrogen bonds. Total electronic energy (E(RM062X)): -2434.452868 Hartree. Binding mode 1 (see Table S19).

Table S19: Output from the DFT modelling of **1**:sarin initiated with the P=O coordinated to the receptor through the formation of two hydrogen bonds.

Center Number	Atomic Number	Atomic Type	Coordinates (Angstroms) X	Y	Z
1	15	0	-0.619303	0.332180	-0.857176
2	8	0	-0.270019	-0.871439	0.091237
3	6	0	-0.541020	-0.856085	1.536786
4	6	0	0.499898	-1.762565	2.154853
5	8	0	-2.015682	0.829554	-0.811880
6	9	0	0.351731	1.481520	-0.355122
7	6	0	-1.964589	-1.314774	1.780394
8	6	0	0.026349	-0.131747	-2.441786
9	1	0	-0.401367	0.171080	1.884677
10	1	0	0.381540	-2.778415	1.772262
11	1	0	0.372723	-1.779310	3.238270
12	1	0	1.504809	-1.409588	1.923101
13	1	0	-2.121451	-2.299818	1.333179
14	1	0	-2.144754	-1.384822	2.854679
15	1	0	-2.682156	-0.612672	1.354634
16	1	0	-0.555350	-0.970159	-2.824129
17	1	0	-0.067385	0.714496	-3.121545
18	1	0	1.071618	-0.420698	-2.345532
19	6	0	-6.204981	5.611300	0.174246
20	6	0	-4.999837	5.251209	0.764113
21	6	0	-4.534882	3.950307	0.632698
22	6	0	-5.270583	3.011550	-0.090806
23	6	0	-6.470330	3.384316	-0.700933
24	6	0	-6.937815	4.680586	-0.558258
25	7	0	-4.716608	1.724092	-0.244752
26	6	0	-5.345691	0.519761	-0.164277
27	16	0	-6.952164	0.314314	0.289757
28	7	0	-4.503916	-0.491654	-0.506826

29	6	0	-4.616143	-1.881040	-0.327702
30	6	0	-3.884188	-2.679362	-1.212926
31	6	0	-3.847855	-4.054436	-1.051059
32	6	0	-4.547161	-4.641742	-0.001558
33	6	0	-5.272166	-3.852653	0.885066
34	6	0	-5.304371	-2.474120	0.733032
35	6	0	-6.750257	6.993244	0.354475
36	9	0	-7.376894	7.435583	-0.746983
37	9	0	-7.652535	7.052226	1.350932
38	9	0	-5.794050	7.884309	0.651696
39	6	0	-4.555940	-6.130563	0.143593
40	9	0	-3.413627	-6.687455	-0.286742
41	9	0	-5.546663	-6.701715	-0.565889
42	9	0	-4.730559	-6.515597	1.416439
43	1	0	-4.426182	5.978344	1.324344
44	1	0	-3.600148	3.655281	1.094377
45	1	0	-7.020921	2.666286	-1.290614
46	1	0	-7.864199	4.974997	-1.036118
47	1	0	-3.701527	1.691903	-0.339448
48	1	0	-3.602700	-0.194053	-0.881396
49	1	0	-3.340844	-2.211967	-2.026272
50	1	0	-3.274663	-4.666200	-1.736400
51	1	0	-5.796828	-4.311728	1.713761
52	1	0	-5.841509	-1.863345	1.441921

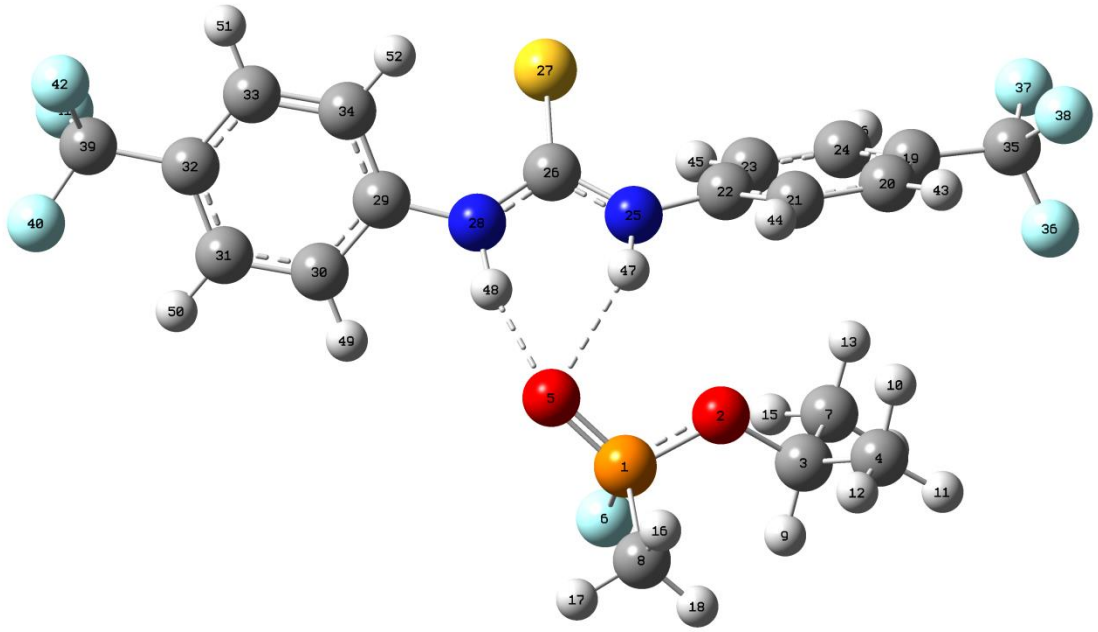

Figure S158: Output from the DFT modelling of **1**:sarin initiated with the O-P=O coordinated to the receptor through the formation of two hydrogen bonds, one to each oxygen atom. Total electronic energy (E(RM062X)): -2434.454821 Hartree. Binding mode 2 (see Table S20).

Table S20: Output from the DFT modelling of **1**:sarin initiated with the O-P=O coordinated to the receptor through the formation of two hydrogen bonds, one to each oxygen atom.

Center Number	Atomic Number	Atomic Type	Coordinates (Angstroms) X	Y	Z
1	15	0	-1.390437	1.007444	1.118029
2	8	0	-2.119294	2.376345	0.842181
3	6	0	-1.443118	3.563424	0.300437
4	6	0	-1.513319	4.643750	1.357726
5	8	0	-2.368702	-0.051319	1.440752
6	9	0	-0.647806	0.717377	-0.253156
7	6	0	-2.141283	3.927115	-0.992129
8	6	0	-0.051176	1.244038	2.262139
9	1	0	-0.402792	3.295333	0.094602
10	1	0	-2.557423	4.874098	1.579129
11	1	0	-1.024976	5.547996	0.990677
12	1	0	-1.016895	4.327904	2.276620
13	1	0	-3.174798	4.216280	-0.792883
14	1	0	-1.626161	4.768750	-1.458780
15	1	0	-2.133247	3.082785	-1.682812
16	1	0	-0.472300	1.507757	3.232172
17	1	0	0.511997	0.315397	2.350011
18	1	0	0.611624	2.039454	1.920323
19	6	0	-5.798634	5.100277	-0.538551
20	6	0	-5.435589	4.763851	0.761152
21	6	0	-5.200381	3.436012	1.083830
22	6	0	-5.321638	2.444311	0.108681
23	6	0	-5.678790	2.787699	-1.195845
24	6	0	-5.921054	4.115614	-1.514254
25	7	0	-4.982689	1.127206	0.476446

26	6	0	-5.593535	-0.042107	0.141708
27	16	0	-7.054608	-0.135331	-0.689829
28	7	0	-4.873838	-1.112740	0.566797
29	6	0	-5.200311	-2.480627	0.488127
30	6	0	-4.171309	-3.366467	0.163335
31	6	0	-4.409145	-4.732453	0.129207
32	6	0	-5.680177	-5.214864	0.417644
33	6	0	-6.706779	-4.336844	0.754787
34	6	0	-6.469876	-2.972161	0.800417
35	6	0	-5.959288	6.539999	-0.910813
36	9	0	-4.788330	7.086981	-1.290629
37	9	0	-6.808088	6.711085	-1.933856
38	9	0	-6.410324	7.282612	0.110517
39	6	0	-5.967243	-6.680483	0.326167
40	9	0	-4.865519	-7.426659	0.490396
41	9	0	-6.483909	-7.019211	-0.869322
42	9	0	-6.857801	-7.079365	1.247670
43	1	0	-5.340544	5.532566	1.518323
44	1	0	-4.916839	3.160312	2.092541
45	1	0	-5.748399	2.023134	-1.955396
46	1	0	-6.191737	4.385938	-2.527381
47	1	0	-4.196603	1.054542	1.115823
48	1	0	-3.918524	-0.910419	0.869737
49	1	0	-3.185796	-2.977821	-0.064798
50	1	0	-3.608430	-5.416355	-0.121665
51	1	0	-7.688626	-4.720963	1.003097
52	1	0	-7.256589	-2.291235	1.088600

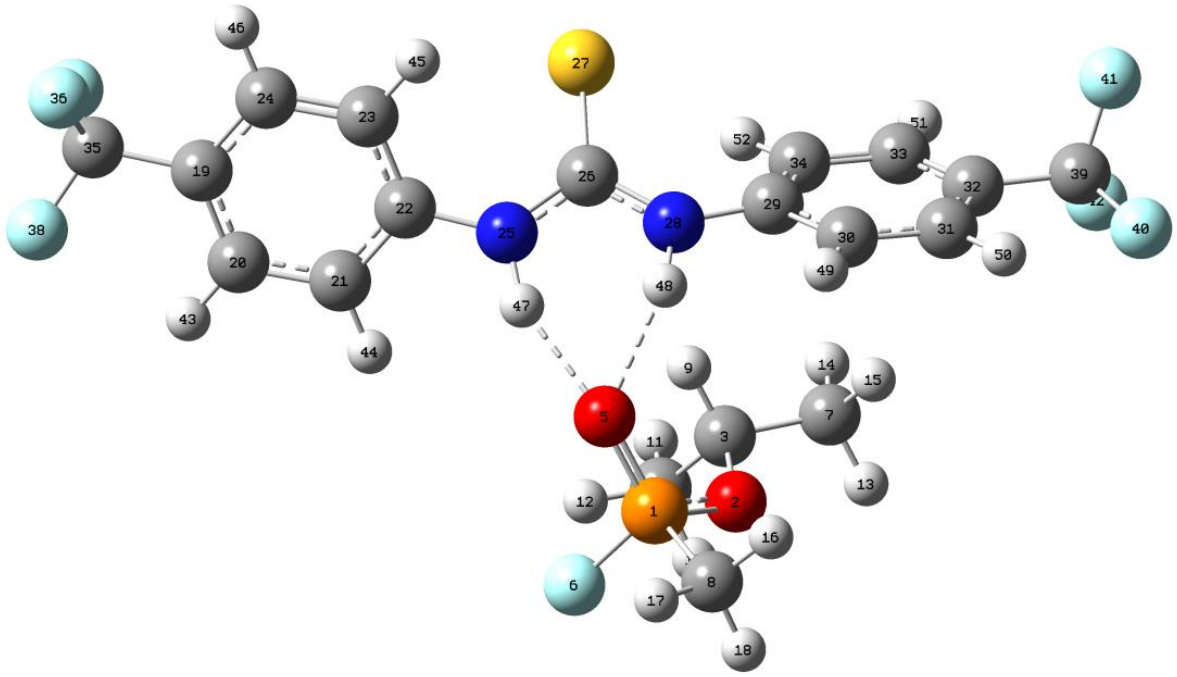

Figure S159: Output from the DFT modelling of **1**:sarin initiated with the F-P=O coordinated to the receptor through the formation of two hydrogen bonds, one to the oxygen and one to the fluorine atom. Total electronic energy (E(RM062X)): -2434.455439 Hartree. Binding mode 3 (see Table S21).

Table S21: Output from the DFT modelling of **1**:sarin initiated with the F-P=O coordinated to the receptor through the formation of two hydrogen bonds, one to the oxygen and one to the fluorine atom.

Center Number	Atomic Number	Atomic Type	Coordinates (Angstroms) X	Y	Z
1	15	0	-0.629546	0.675426	0.013940
2	8	0	-0.724123	-0.392551	1.164178
3	6	0	-1.780054	-0.389607	2.186169
4	6	0	-1.415514	0.606064	3.269514
5	8	0	-1.921432	1.091712	-0.584777
6	9	0	0.050283	1.930299	0.707791
7	6	0	-1.876563	-1.815556	2.680801
8	6	0	0.627471	0.068399	-1.078274
9	1	0	-2.708557	-0.093616	1.691163
10	1	0	-0.446735	0.347055	3.701422
11	1	0	-2.170504	0.575762	4.056845
12	1	0	-1.367849	1.623821	2.879457
13	1	0	-0.932239	-2.115655	3.139985
14	1	0	-2.670315	-1.889362	3.426173
15	1	0	-2.108339	-2.494265	1.858168
16	1	0	0.257297	-0.827832	-1.574743
17	1	0	0.848330	0.833412	-1.821847
18	1	0	1.525389	-0.168460	-0.509511
19	6	0	-6.243253	5.805755	-0.407677
20	6	0	-5.023791	5.559463	0.209636
21	6	0	-4.527830	4.263894	0.252966
22	6	0	-5.247009	3.216828	-0.323154

23	6	0	-6.461974	3.473132	-0.963250
24	6	0	-6.959571	4.765325	-0.995180
25	7	0	-4.661779	1.934640	-0.301782
26	6	0	-5.257824	0.739122	-0.045173
27	16	0	-6.855183	0.553706	0.443275
28	7	0	-4.387378	-0.289620	-0.244447
29	6	0	-4.448298	-1.633126	0.165325
30	6	0	-3.703308	-2.546973	-0.585491
31	6	0	-3.626924	-3.876804	-0.199507
32	6	0	-4.296713	-4.298787	0.942398
33	6	0	-5.034897	-3.391929	1.698127
34	6	0	-5.108853	-2.060482	1.321477
35	6	0	-6.824590	7.184674	-0.419897
36	9	0	-7.389314	7.481798	-1.601420
37	9	0	-7.790600	7.330911	0.505170
38	9	0	-5.907699	8.129140	-0.170331
39	6	0	-4.259037	-5.733043	1.365928
40	9	0	-3.284026	-6.421198	0.757390
41	9	0	-5.411675	-6.370336	1.092487
42	9	0	-4.066770	-5.858716	2.689461
43	1	0	-4.463187	6.370053	0.656872
44	1	0	-3.580861	4.058031	0.737849
45	1	0	-7.000921	2.668205	-1.440755
46	1	0	-7.898358	4.968535	-1.496289
47	1	0	-3.643274	1.915373	-0.371667
48	1	0	-3.502533	-0.027337	-0.676715
49	1	0	-3.183024	-2.208207	-1.473889
50	1	0	-3.045953	-4.578011	-0.784451
51	1	0	-5.535756	-3.720391	2.601184
52	1	0	-5.658071	-1.355337	1.926252

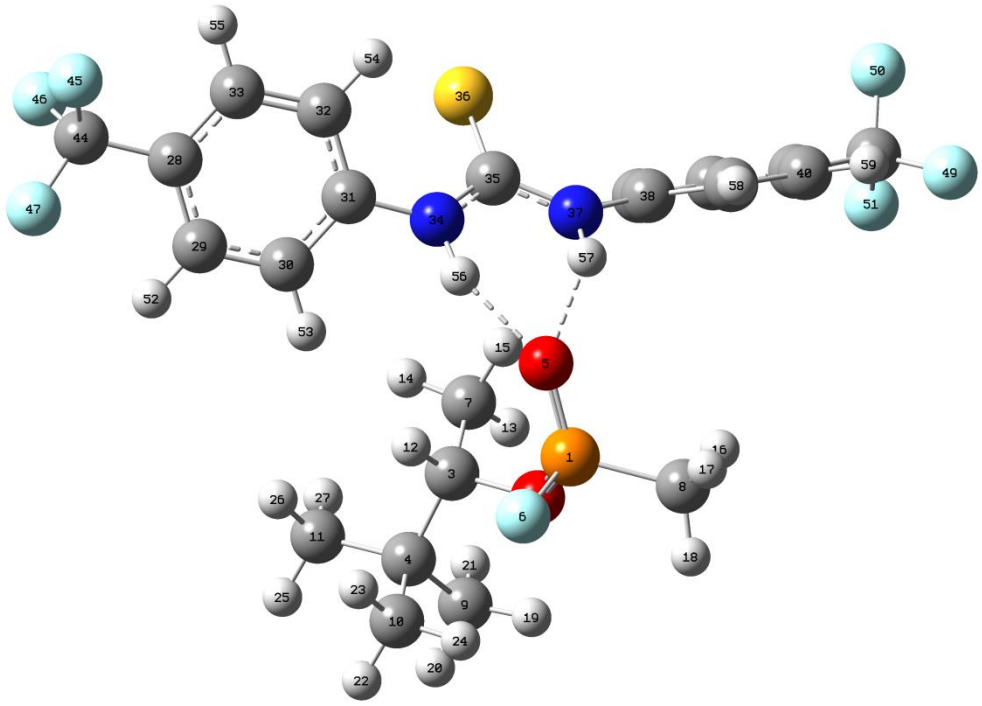

Figure S160: Output from the DFT modelling of **1**:soman initiated with the P=O coordinated to the receptor through the formation of two hydrogen bonds. Total electronic energy (E(RM062X)): -2552.369778 Hartree. Binding mode 1 (see Table S22).

Table S22: Output from the DFT modelling of **1**:soman initiated with the P=O coordinated to the receptor through the formation of two hydrogen bonds.

Center Number	Atomic Number	Atomic Type	Coordinates (Angstroms) X	Y	Z
1	15	0	0.002840	2.455866	-0.630580
2	8	0	0.060668	0.884377	-0.639550
3	6	0	-0.906466	0.078717	0.117251
4	6	0	-0.117216	-1.036687	0.818540
5	8	0	-1.358064	3.046659	-0.603377
6	9	0	0.760623	2.845888	0.706936
7	6	0	-1.991934	-0.350700	-0.850388
8	6	0	1.104954	2.971868	-1.918858
9	6	0	0.604177	-1.928431	-0.196608
10	6	0	0.911193	-0.391501	1.755088
11	6	0	-1.097779	-1.874307	1.648581
12	1	0	-1.337451	0.721642	0.893125
13	1	0	-1.585381	-0.988792	-1.636195
14	1	0	-2.783896	-0.886751	-0.325691
15	1	0	-2.431566	0.531748	-1.317154
16	1	0	0.664609	2.704223	-2.879036
17	1	0	1.234949	4.052056	-1.864534
18	1	0	2.066260	2.473669	-1.801405
19	1	0	1.259156	-1.336612	-0.839454
20	1	0	1.217277	-2.661370	0.333375

21	1	0	-0.099380	-2.477928	-0.825725
22	1	0	1.436530	-1.164715	2.320228
23	1	0	0.423851	0.279186	2.469209
24	1	0	1.650806	0.182321	1.193835
25	1	0	-0.541433	-2.596066	2.250843
26	1	0	-1.679971	-1.245381	2.329186
27	1	0	-1.790819	-2.432160	1.015774
28	6	0	-6.321528	2.365700	3.401157
29	6	0	-5.066349	1.778901	3.319294
30	6	0	-4.369056	1.819683	2.118711
31	6	0	-4.922546	2.450212	1.006443
32	6	0	-6.176748	3.058233	1.100631
33	6	0	-6.875946	3.006388	2.294395
34	7	0	-4.147784	2.520984	-0.172122
35	6	0	-4.554789	2.279227	-1.446207
36	16	0	-6.072723	1.677905	-1.858220
37	7	0	-3.581781	2.567672	-2.349253
38	6	0	-3.559398	2.277710	-3.731925
39	6	0	-3.081760	3.262282	-4.594937
40	6	0	-2.973404	3.004058	-5.955146
41	6	0	-3.348669	1.761237	-6.448136
42	6	0	-3.817034	0.770551	-5.587697
43	6	0	-3.914029	1.021672	-4.229026
44	6	0	-7.116249	2.294687	4.667619
45	9	0	-7.697737	3.469031	4.961401
46	9	0	-8.111391	1.393363	4.585607
47	9	0	-6.368435	1.948153	5.723483
48	6	0	-3.293148	1.482002	-7.917850
49	9	0	-2.459843	2.309004	-8.563730
50	9	0	-4.498050	1.617076	-8.500445
51	9	0	-2.888448	0.228570	-8.176501
52	1	0	-4.633106	1.289229	4.181694
53	1	0	-3.392779	1.356768	2.043136
54	1	0	-6.589008	3.574445	0.245677
55	1	0	-7.846024	3.482468	2.372553
56	1	0	-3.150952	2.703625	-0.044214
57	1	0	-2.746893	3.022830	-1.982195
58	1	0	-2.801059	4.229940	-4.196998
59	1	0	-2.601415	3.768605	-6.624919
60	1	0	-4.085349	-0.203918	-5.977334
61	1	0	-4.254570	0.250811	-3.552395

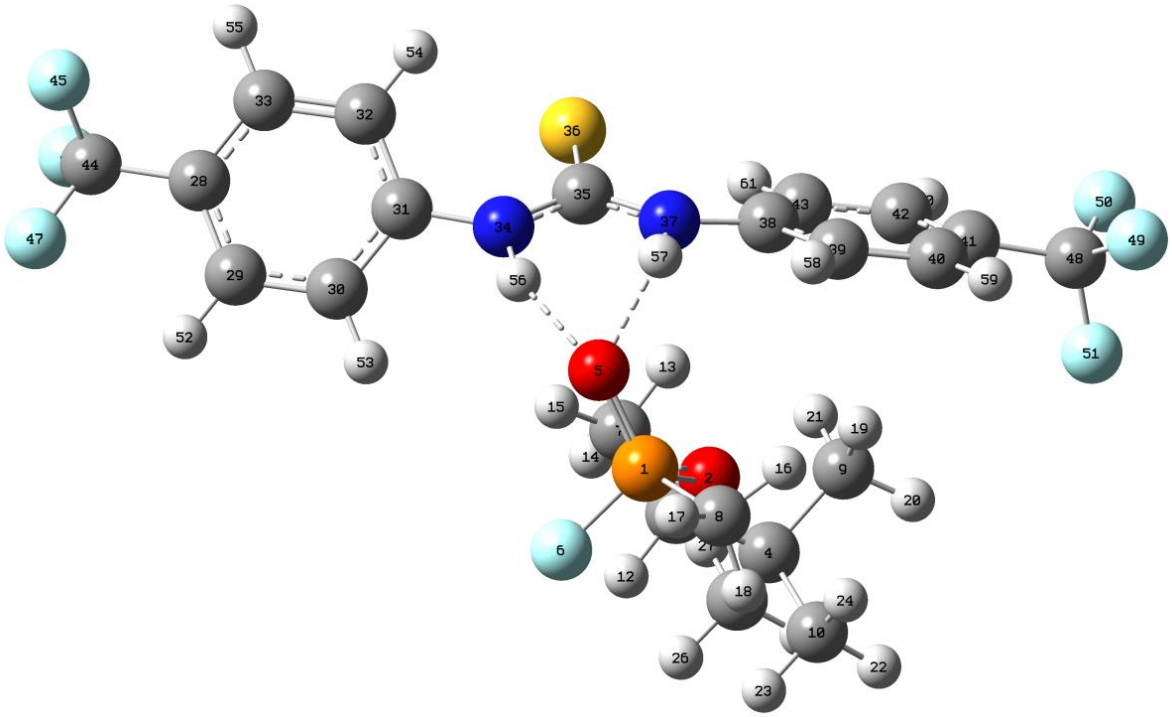

Figure S161: Output from the DFT modelling of **1**:soman initiated with the O-P=O coordinated to the receptor through the formation of two hydrogen bonds, one to each oxygen atom. Total electronic energy (E(RM062X)): -2552.371688 Hartree. Binding mode 2 (see Table S23).

Table S23: Output from the DFT modelling of **1**:soman initiated with the O-P=O coordinated to the receptor through the formation of two hydrogen bonds, one to each oxygen atom.

Center Number	Atomic Number	Atomic Type	Coordinates (Angstroms) X	Y	Z
1	15	0	-0.881646	2.587035	-0.911564
2	8	0	-1.153632	1.375080	-1.872446
3	6	0	-1.527253	0.009471	-1.484278
4	6	0	-1.059774	-0.903969	-2.628214
5	8	0	-2.041959	3.473041	-0.647844
6	9	0	-0.422804	1.887381	0.436074
7	6	0	-3.009150	-0.016968	-1.161565
8	6	0	0.582749	3.380096	-1.523716
9	6	0	-1.809711	-0.592049	-3.926757
10	6	0	0.444766	-0.692270	-2.838172
11	6	0	-1.305776	-2.360791	-2.216639
12	1	0	-0.944403	-0.235260	-0.591434
13	1	0	-3.604839	0.248434	-2.036402
14	1	0	-3.302406	-1.010742	-0.821781
15	1	0	-3.237600	0.686756	-0.356942
16	1	0	0.369963	3.783309	-2.513933
17	1	0	0.858576	4.193046	-0.853334
18	1	0	1.392064	2.654229	-1.590581
19	1	0	-1.749107	0.472209	-4.169108
20	1	0	-1.368996	-1.155904	-4.752972
21	1	0	-2.864301	-0.868608	-3.860744
22	1	0	0.820390	-1.405635	-3.575291
23	1	0	0.996181	-0.845399	-1.905328
24	1	0	0.652888	0.315656	-3.201172

25	1	0	-0.891493	-3.027074	-2.976774
26	1	0	-0.819397	-2.591690	-1.264290
27	1	0	-2.370553	-2.583808	-2.125081
28	6	0	-6.852193	2.934830	3.489884
29	6	0	-5.522841	2.541219	3.411380
30	6	0	-4.877683	2.550441	2.182076
31	6	0	-5.559165	2.956334	1.034908
32	6	0	-6.889518	3.373375	1.122856
33	6	0	-7.533669	3.352630	2.348516
34	7	0	-4.834559	3.008371	-0.173188
35	6	0	-5.224621	2.575076	-1.405526
36	16	0	-6.663486	1.760273	-1.697911
37	7	0	-4.283070	2.880673	-2.340771
38	6	0	-4.075088	2.462052	-3.662938
39	6	0	-3.022559	3.110876	-4.329395
40	6	0	-2.664589	2.746173	-5.612673
41	6	0	-3.358734	1.724438	-6.256604
42	6	0	-4.409278	1.087423	-5.612269
43	6	0	-4.776437	1.447824	-4.321298
44	6	0	-7.585262	2.884626	4.793655
45	9	0	-8.370551	3.959532	4.970073
46	9	0	-8.393352	1.812059	4.874909
47	9	0	-6.757010	2.822274	5.844875
48	6	0	-2.913223	1.256986	-7.603897
49	9	0	-2.371463	2.244785	-8.332268
50	9	0	-3.918485	0.736900	-8.322932
51	9	0	-1.973806	0.294747	-7.513549
52	1	0	-4.991703	2.226607	4.300348
53	1	0	-3.841396	2.241335	2.107630
54	1	0	-7.405025	3.721308	0.239628
55	1	0	-8.563248	3.681630	2.421785
56	1	0	-3.847192	3.252428	-0.079608
57	1	0	-3.501399	3.421126	-1.975748
58	1	0	-2.486413	3.909558	-3.828868
59	1	0	-1.849073	3.254152	-6.112251
60	1	0	-4.949635	0.293354	-6.113138
61	1	0	-5.589952	0.937420	-3.833878

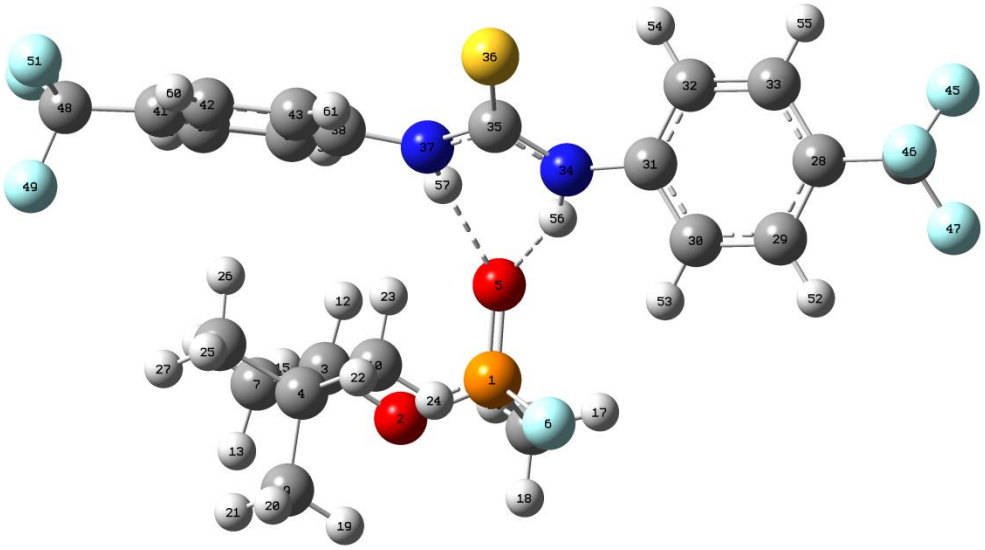

Figure S162: Output from the DFT modelling of **1**:soman initiated with the F-P=O coordinated to the receptor through the formation of two hydrogen bonds, one to the oxygen and one to the fluorine atom. Total electronic energy (E(RM062X)): -2552.373506 Hartree. Binding mode 3 (see Table S24).

Table S24: Output from the DFT modelling of **1**:soman initiated with the F-P=O coordinated to the receptor through the formation of two hydrogen bonds, one to the oxygen and one to the fluorine atom.

Center Number	Atomic Number	Atomic Type	Coordinates (Angstroms) X	Y	Z
1	15	0	-0.744860	2.373389	1.082010
2	8	0	0.040977	1.129997	0.531159
3	6	0	-0.265764	0.426559	-0.719816
4	6	0	-0.815094	-0.967562	-0.379521
5	8	0	-1.813416	2.900354	0.197472
6	9	0	-1.386566	1.818775	2.423281
7	6	0	0.994107	0.479652	-1.559522
8	6	0	0.469399	3.523138	1.673111
9	6	0	0.158928	-1.755313	0.500675
10	6	0	-2.149585	-0.798113	0.358323
11	6	0	-1.058788	-1.718159	-1.695476
12	1	0	-1.057990	0.988013	-1.221420
13	1	0	1.807312	-0.076468	-1.090936
14	1	0	0.803113	0.064172	-2.549840
15	1	0	1.307195	1.517549	-1.680586
16	1	0	1.000324	3.937845	0.816740
17	1	0	-0.029746	4.322939	2.218968
18	1	0	1.172107	3.008281	2.327011
19	1	0	0.358855	-1.225314	1.434095
20	1	0	-0.276196	-2.727325	0.745908
21	1	0	1.108526	-1.935911	-0.007881
22	1	0	-2.601546	-1.774793	0.545187
23	1	0	-2.855851	-0.206966	-0.234697
24	1	0	-2.011360	-0.307495	1.324638
25	1	0	-1.609607	-2.640277	-1.495502
26	1	0	-1.650275	-1.116469	-2.391424
27	1	0	-0.120953	-1.987301	-2.186123

28	6	0	-7.255319	4.066572	3.243249
29	6	0	-6.038037	3.475856	3.559628
30	6	0	-5.212606	3.021880	2.541246
31	6	0	-5.600500	3.160691	1.207645
32	6	0	-6.815051	3.774460	0.893706
33	6	0	-7.641778	4.217084	1.913931
34	7	0	-4.684559	2.739336	0.222818
35	6	0	-4.926040	2.064194	-0.932191
36	16	0	-6.436673	1.497715	-1.401145
37	7	0	-3.777379	1.913312	-1.652536
38	6	0	-3.482894	1.125576	-2.777299
39	6	0	-2.362536	1.520297	-3.522211
40	6	0	-1.917507	0.754787	-4.585658
41	6	0	-2.600741	-0.408582	-4.928237
42	6	0	-3.719561	-0.800090	-4.203646
43	6	0	-4.161745	-0.045597	-3.124975
44	6	0	-8.183137	4.511710	4.329837
45	9	0	-8.836422	5.638262	4.004583
46	9	0	-9.127904	3.590886	4.594017
47	9	0	-7.542470	4.744194	5.484002
48	6	0	-2.065785	-1.286855	-6.013165
49	9	0	-1.139982	-2.146243	-5.544385
50	9	0	-1.469469	-0.584866	-6.988145
51	9	0	-3.021165	-2.032310	-6.585335
52	1	0	-5.734150	3.368588	4.592968
53	1	0	-4.263255	2.553729	2.774590
54	1	0	-7.098706	3.914185	-0.138688
55	1	0	-8.580932	4.700490	1.673969
56	1	0	-3.700984	2.865685	0.465127
57	1	0	-2.971149	2.414474	-1.280148
58	1	0	-1.839874	2.432579	-3.255835
59	1	0	-1.046685	1.065051	-5.149903
60	1	0	-4.243141	-1.711229	-4.465623
61	1	0	-5.013417	-0.373637	-2.551541

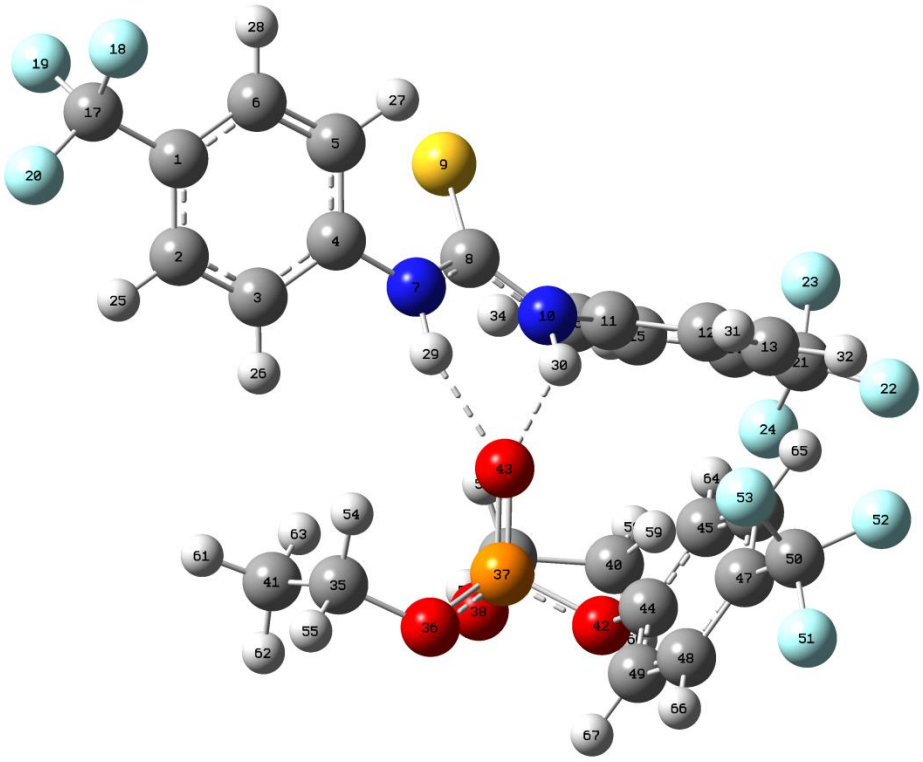

Figure S163: Output from the DFT modelling of **1**:**6** initiated with the P=O coordinated to the receptor through the formation of two hydrogen bonds. Total electronic energy (E(RM062X)): -3053.700646 Hartree. Binding mode 1 (see Table S25).

Table S25: Output from the DFT modelling of **1:6** initiated with the P=O coordinated to the receptor through the formation of two hydrogen bonds.

Center Number	Atomic Number	Atomic Type	Coordinates (Angstroms) X	Y	Z
1	6	0	5.238339	-0.196785	-0.707344
2	6	0	4.842873	0.366685	0.498277
3	6	0	3.494660	0.397102	0.828719
4	6	0	2.545263	-0.138448	-0.040107
5	6	0	2.950351	-0.722527	-1.242788
6	6	0	4.294313	-0.741755	-1.575680
7	7	0	1.198274	-0.138804	0.377228
8	6	0	0.095660	0.173517	-0.353325
9	16	0	0.128158	0.792139	-1.918403
10	7	0	-1.047766	-0.078613	0.337067
11	6	0	-2.362875	0.337194	0.034510
12	6	0	-3.397950	-0.567825	0.257046
13	6	0	-4.719342	-0.170505	0.094239
14	6	0	-4.997856	1.129546	-0.303686
15	6	0	-3.964831	2.036723	-0.536871
16	6	0	-2.648203	1.647240	-0.360228
17	6	0	6.679132	-0.199939	-1.112240
18	9	0	7.047891	-1.376042	-1.645341
19	9	0	6.940501	0.733233	-2.045172
20	9	0	7.501338	0.043471	-0.082958
21	6	0	-6.409470	1.584616	-0.507684
22	9	0	-7.305263	0.704278	-0.044378

23	9	0	-6.690523	1.780026	-1.807758
24	9	0	-6.648370	2.754666	0.107953
25	1	0	5.577049	0.783459	1.175481
26	1	0	3.171929	0.846458	1.760058
27	1	0	2.217002	-1.165849	-1.900580
28	1	0	4.612900	-1.200192	-2.504197
29	1	0	1.041733	-0.291646	1.374402
30	1	0	-0.937048	-0.566128	1.225327
31	1	0	-3.164816	-1.579084	0.568640
32	1	0	-5.523547	-0.871057	0.277349
33	1	0	-4.191855	3.054530	-0.831566
34	1	0	-1.842860	2.352989	-0.508523
35	6	0	2.222484	0.225564	4.881706
36	8	0	0.863052	-0.054437	5.319563
37	15	0	-0.332476	-0.061623	4.298387
38	8	0	-0.916018	1.398054	4.319481
39	6	0	-1.726382	1.909085	3.221477
40	6	0	-3.106577	1.288269	3.226535
41	6	0	2.377483	1.669570	4.455612
42	8	0	-1.449472	-0.900041	5.076589
43	8	0	-0.006758	-0.592521	2.951249
44	6	0	-1.312273	-2.277379	5.232306
45	6	0	-1.707663	-3.118622	4.201556
46	6	0	-1.609205	-4.489825	4.387033
47	6	0	-1.119410	-4.990445	5.590248
48	6	0	-0.723753	-4.135266	6.612597
49	6	0	-0.819973	-2.761282	6.434229
50	6	0	-0.975360	-6.473236	5.754954
51	9	0	-0.949920	-6.841719	7.042356
52	9	0	-1.978403	-7.142616	5.168001
53	9	0	0.161343	-6.928506	5.200302
54	1	0	2.468092	-0.469776	4.077218
55	1	0	2.834565	-0.005052	5.749752
56	1	0	-1.765427	2.981372	3.395371
57	1	0	-1.191817	1.719899	2.287943
58	1	0	-3.706151	1.727100	2.425369
59	1	0	-3.059739	0.209951	3.058327
60	1	0	-3.601516	1.472086	4.180889
61	1	0	3.425546	1.865707	4.221889
62	1	0	2.068236	2.339764	5.258355
63	1	0	1.780584	1.891699	3.567355
64	1	0	-2.088891	-2.699877	3.278871
65	1	0	-1.919795	-5.167207	3.601406
66	1	0	-0.348552	-4.536299	7.545203
67	1	0	-0.524201	-2.066426	7.209329

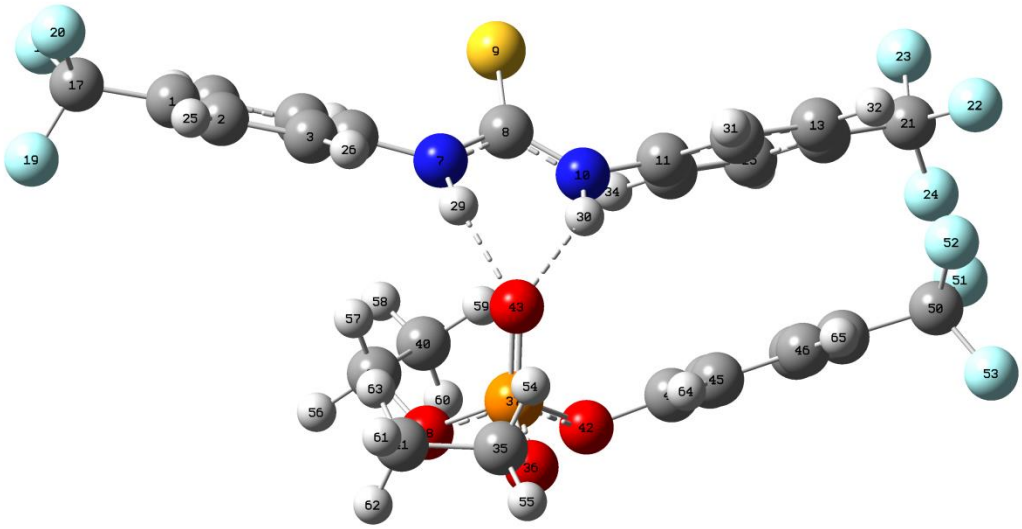

Figure S164: Output from the DFT modelling of **1**:**6** initiated with the P=O coordinated to the receptor through the formation of two hydrogen bonds, one to each oxygen atom. Total electronic energy (E(RM062X)): -3053.710781 Hartree. Binding mode 2 (see Table S26).

Table S26: Output from the DFT modelling of **1:6** initiated with the P=O coordinated to the receptor through the formation of two hydrogen bonds, one to each oxygen atom.

Center Number	Atomic Number	Atomic Type	Coordinates (Angstroms) X	Y	Z
1	6	0	4.992622	1.637690	-0.925855
2	6	0	5.042218	0.762561	0.155450
3	6	0	3.879662	0.154542	0.597959
4	6	0	2.659581	0.421331	-0.032681
5	6	0	2.611748	1.316953	-1.101849
6	6	0	3.781993	1.916235	-1.548291
7	7	0	1.512934	-0.171969	0.530631
8	6	0	0.386475	-0.634256	-0.071173
9	16	0	0.146788	-0.709033	-1.735393
10	7	0	-0.529588	-1.070776	0.834668
11	6	0	-1.803056	-1.616951	0.531740
12	6	0	-2.116425	-2.891682	0.985884
13	6	0	-3.378452	-3.425381	0.737575
14	6	0	-4.310503	-2.675728	0.037105
15	6	0	-4.001104	-1.391270	-0.412725
16	6	0	-2.750501	-0.858576	-0.159687
17	6	0	6.251977	2.314010	-1.369126
18	9	0	6.144444	2.845335	-2.593912
19	9	0	6.601180	3.316431	-0.542201
20	9	0	7.294383	1.467983	-1.392764
21	6	0	-5.672294	-3.221082	-0.264728
22	9	0	-5.879593	-4.426750	0.275599
23	9	0	-5.874838	-3.344935	-1.588691
24	9	0	-6.644667	-2.408630	0.185254
25	1	0	5.986004	0.546115	0.641053
26	1	0	3.908261	-0.537659	1.431457
27	1	0	1.669885	1.546273	-1.576242
28	1	0	3.745834	2.608576	-2.379648
29	1	0	1.547232	-0.281796	1.545055
30	1	0	-0.238717	-1.108129	1.810552

31	1	0	-1.373845	-3.466065	1.526666
32	1	0	-3.628395	-4.417455	1.089957
33	1	0	-4.742688	-0.808228	-0.946245
34	1	0	-2.497727	0.141826	-0.485759
35	6	0	1.735967	0.157908	6.163268
36	8	0	0.499982	0.741478	5.652967
37	15	0	0.264374	0.889976	4.106488
38	8	0	0.748760	2.341092	3.749119
39	6	0	1.096173	2.703074	2.380986
40	6	0	-0.089981	2.597285	1.446247
41	6	0	2.939468	1.008633	5.821524
42	8	0	-1.327683	1.017165	3.987391
43	8	0	0.833241	-0.201591	3.276540
44	6	0	-2.182331	-0.072476	3.918988
45	6	0	-1.938721	-1.243087	4.630168
46	6	0	-2.860945	-2.275588	4.548397
47	6	0	-4.004368	-2.126787	3.769832
48	6	0	-4.233793	-0.955370	3.058539
49	6	0	-3.311835	0.080235	3.128209
50	6	0	-4.998699	-3.246117	3.740916
51	9	0	-5.891450	-3.112647	2.751590
52	9	0	-4.402421	-4.440206	3.578451
53	9	0	-5.695754	-3.327992	4.886274
54	1	0	1.822273	-0.849561	5.754285
55	1	0	1.573900	0.098497	7.236242
56	1	0	1.453345	3.726419	2.461540
57	1	0	1.924515	2.066222	2.065251
58	1	0	0.218668	2.909278	0.446348
59	1	0	-0.460406	1.571349	1.379330
60	1	0	-0.902944	3.242768	1.780749
61	1	0	3.820385	0.591112	6.311311
62	1	0	2.797521	2.032497	6.169045
63	1	0	3.125845	1.020220	4.745204
64	1	0	-1.059007	-1.342805	5.253372
65	1	0	-2.687279	-3.195745	5.092926
66	1	0	-5.116192	-0.856567	2.438619
67	1	0	-3.453545	1.002293	2.578881

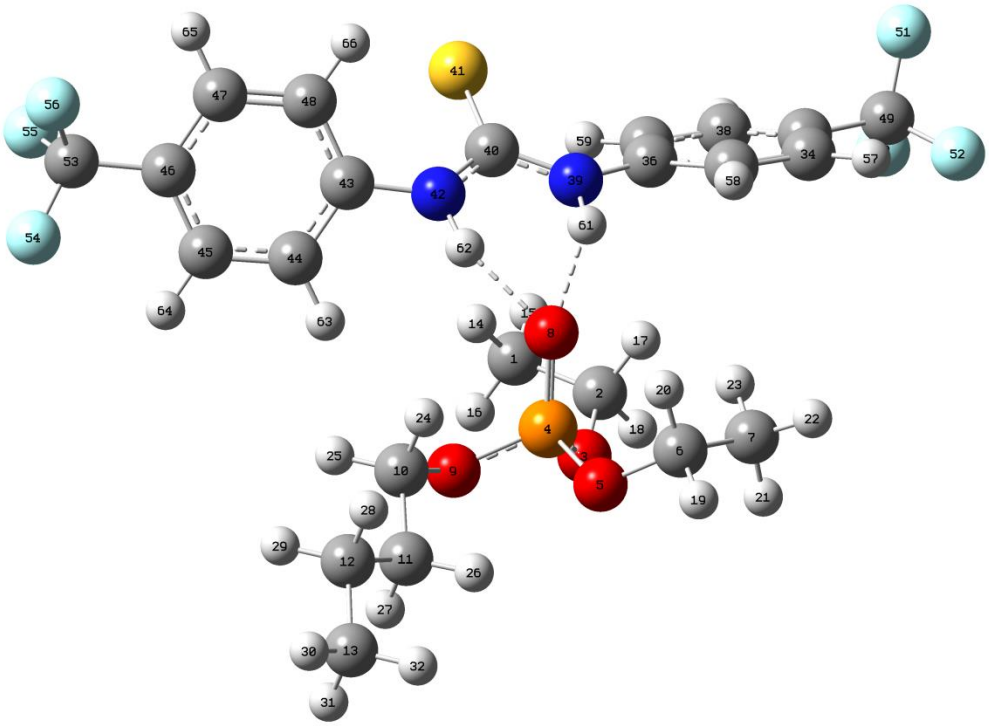

Figure S165: Output from the DFT modelling of **1**:**10** initiated with the P=O coordinated to the receptor through the formation of two hydrogen bonds. Total electronic energy (E(RM062X)): -2642.861038 Hartree. Binding mode 1 (see Table S27).

Table S27: Output from the DFT modelling of **1:10** initiated with the P=O coordinated to the receptor through the formation of two hydrogen bonds.

Center Number	Atomic Number	Atomic Type	Coordinates (Angstroms) X	Y	Z
1	6	0	0.783689	-1.744052	2.833526
2	6	0	1.666485	-0.769225	3.581599
3	8	0	0.940865	-0.099152	4.645567
4	15	0	-0.162826	0.990194	4.351733
5	8	0	0.041669	2.127624	5.428999
6	6	0	0.891341	3.270808	5.139843
7	6	0	2.333733	2.860190	4.929388
8	8	0	-0.162798	1.497962	2.951251
9	8	0	-1.490307	0.274644	4.813016
10	6	0	-2.741004	1.014466	4.876049
11	6	0	-3.046698	1.421377	6.302302
12	6	0	-4.394440	2.135445	6.397013
13	6	0	-4.725347	2.538906	7.831710
14	1	0	-0.044786	-1.230429	2.341359
15	1	0	1.372363	-2.248710	2.064299
16	1	0	0.379351	-2.494595	3.513703
17	1	0	2.088273	-0.011604	2.918071
18	1	0	2.482020	-1.276688	4.091404
19	1	0	0.780911	3.912619	6.010442
20	1	0	0.486005	3.778771	4.264013
21	1	0	2.695183	2.276272	5.776715
22	1	0	2.950806	3.754501	4.830746
23	1	0	2.449592	2.271336	4.016038

24	1	0	-2.684585	1.881546	4.211294
25	1	0	-3.499095	0.333414	4.489821
26	1	0	-2.248795	2.072670	6.669337
27	1	0	-3.054960	0.523661	6.927961
28	1	0	-4.380660	3.024077	5.757810
29	1	0	-5.180784	1.480913	6.007512
30	1	0	-5.688354	3.049030	7.888243
31	1	0	-4.769479	1.660555	8.480278
32	1	0	-3.962295	3.211844	8.230424
33	6	0	5.129620	0.295450	-0.056155
34	6	0	4.564523	1.477161	0.408962
35	6	0	3.188816	1.567956	0.550958
36	6	0	2.369639	0.480384	0.232195
37	6	0	2.944985	-0.712622	-0.214515
38	6	0	4.321346	-0.794425	-0.364197
39	7	0	0.995085	0.635650	0.491113
40	6	0	-0.087818	0.083485	-0.120341
41	16	0	-0.030480	-0.850396	-1.517360
42	7	0	-1.232252	0.379826	0.551981
43	6	0	-2.548557	-0.027969	0.245580
44	6	0	-3.316534	-0.556769	1.281823
45	6	0	-4.639770	-0.913558	1.059115
46	6	0	-5.187558	-0.746420	-0.205966
47	6	0	-4.425222	-0.213022	-1.243396
48	6	0	-3.108821	0.155621	-1.019747
49	6	0	6.607545	0.197726	-0.268997
50	9	0	7.080465	-1.021681	0.032240
51	9	0	6.948738	0.429023	-1.549708
52	9	0	7.288380	1.081923	0.473575
53	6	0	-6.595332	-1.170289	-0.488080
54	9	0	-7.313626	-1.338245	0.630158
55	9	0	-6.643267	-2.336074	-1.157365
56	9	0	-7.246353	-0.274572	-1.247488
57	1	0	5.191826	2.323101	0.659234
58	1	0	2.738289	2.486331	0.909493
59	1	0	2.324325	-1.567651	-0.432861
60	1	0	4.767968	-1.721134	-0.703628
61	1	0	0.785158	1.241722	1.284258
62	1	0	-1.111153	0.813461	1.469398
63	1	0	-2.868184	-0.696548	2.259091
64	1	0	-5.235471	-1.322774	1.864780
65	1	0	-4.867729	-0.067284	-2.221477
66	1	0	-2.518311	0.593489	-1.811404

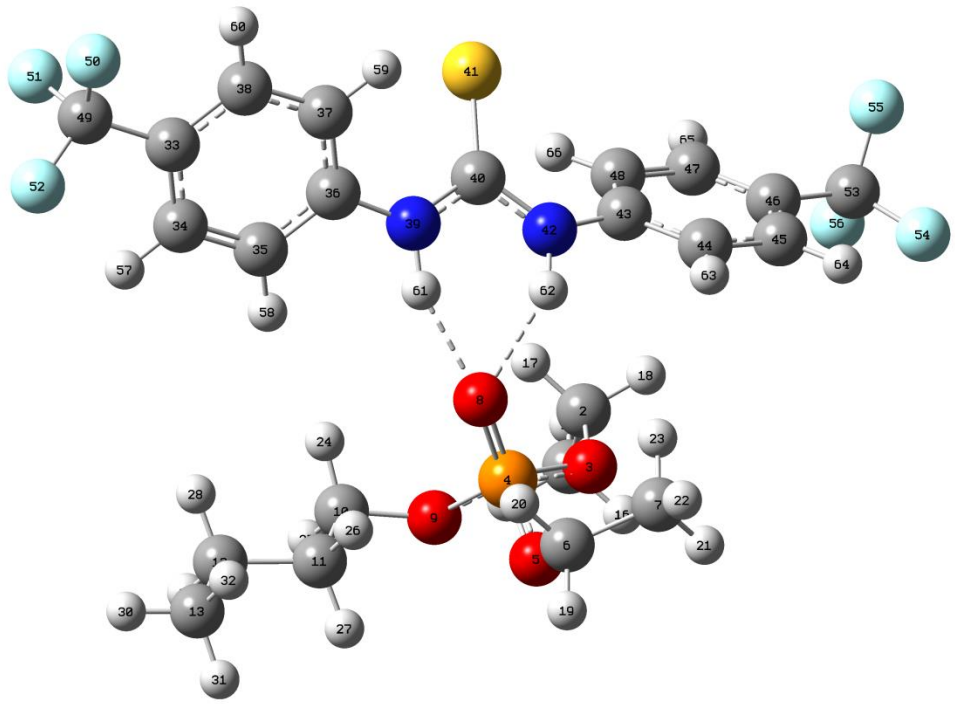

Figure S166: Output from the DFT modelling of **1**:**10** initiated with the P=O coordinated to the receptor through the formation of two hydrogen bonds, one to each oxygen atom. Total electronic energy (E(RM062X)): -2642.858794 Hartree. Binding mode 2 (see Table S28).

Table S28: Output from the DFT modelling of **1:10** initiated with the P=O coordinated to the receptor through the formation of two hydrogen bonds, one to each oxygen atom.

Center Number	Atomic Number	Atomic Type	Coordinates (Angstroms) X	Y	Z
1	6	0	-2.857173	2.151301	4.196413
2	6	0	-2.388341	1.008785	3.325136
3	8	0	-1.896175	-0.082668	4.154667
4	15	0	-0.348864	-0.281481	4.396444
5	8	0	-0.294138	-1.331016	5.572503
6	6	0	0.001780	-2.731396	5.323662
7	6	0	-1.161381	-3.424292	4.648857
8	8	0	0.434508	-0.684337	3.196147
9	8	0	0.102591	1.092932	5.032003
10	6	0	1.491017	1.511290	4.995600
11	6	0	2.400296	0.560745	5.750899
12	6	0	3.827421	1.101959	5.828796
13	6	0	4.757687	0.148954	6.574981
14	1	0	-2.027382	2.565993	4.768607
15	1	0	-3.279475	2.936053	3.566157
16	1	0	-3.629309	1.805790	4.884914
17	1	0	-1.600762	1.318948	2.632038
18	1	0	-3.205127	0.579980	2.745481
19	1	0	0.199707	-3.142968	6.310464
20	1	0	0.909783	-2.787833	4.721690
21	1	0	-2.071731	-3.303866	5.237344
22	1	0	-0.944007	-4.489183	4.552547
23	1	0	-1.329028	-3.019577	3.648782
24	1	0	1.789741	1.603332	3.949238
25	1	0	1.488322	2.500170	5.451058

26	1	0	2.408782	-0.415082	5.251802
27	1	0	1.999766	0.410079	6.758106
28	1	0	4.209441	1.272164	4.817010
29	1	0	3.817000	2.075642	6.328434
30	1	0	5.772441	0.546630	6.627452
31	1	0	4.405267	-0.014884	7.596237
32	1	0	4.800400	-0.821749	6.075026
33	6	0	5.518967	0.214417	-0.475976
34	6	0	5.046060	0.669086	0.750491
35	6	0	3.704139	0.524162	1.062371
36	6	0	2.827496	-0.077518	0.155321
37	6	0	3.312426	-0.553444	-1.064808
38	6	0	4.654319	-0.396521	-1.378443
39	7	0	1.494672	-0.247296	0.571323
40	6	0	0.348281	-0.173472	-0.157734
41	16	0	0.254019	0.318207	-1.764091
42	7	0	-0.725460	-0.556212	0.583515
43	6	0	-2.099225	-0.429565	0.296555
44	6	0	-2.937762	-1.460647	0.717196
45	6	0	-4.315224	-1.342065	0.581378
46	6	0	-4.849717	-0.192670	0.016160
47	6	0	-4.014750	0.839480	-0.410450
48	6	0	-2.642388	0.728715	-0.267134
49	6	0	6.954652	0.425656	-0.839737
50	9	0	7.400007	-0.493722	-1.708411
51	9	0	7.158057	1.624537	-1.416423
52	9	0	7.759733	0.381580	0.232859
53	6	0	-6.327661	-0.038452	-0.163667
54	9	0	-7.022896	-1.014237	0.433501
55	9	0	-6.677902	-0.046812	-1.461775
56	9	0	-6.772011	1.127233	0.335790
57	1	0	5.720526	1.133154	1.459340
58	1	0	3.325036	0.879248	2.013026
59	1	0	2.648568	-1.052929	-1.753769
60	1	0	5.031698	-0.770792	-2.321885
61	1	0	1.363151	-0.342306	1.580039
62	1	0	-0.511036	-0.954200	1.496876
63	1	0	-2.507568	-2.353322	1.154963
64	1	0	-4.963972	-2.141596	0.914305
65	1	0	-4.440352	1.740971	-0.835529
66	1	0	-1.993286	1.538685	-0.566539

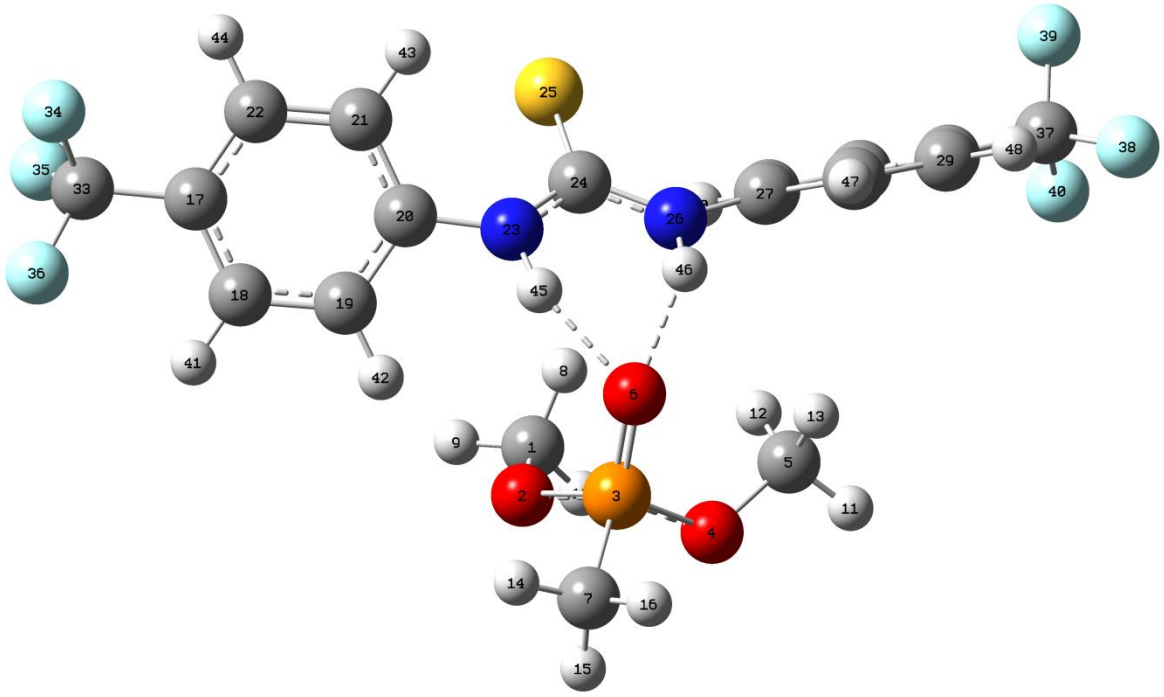

Figure S167: Output from the DFT modelling of **1**:**11** initiated with the P=O coordinated to the receptor through the formation of two hydrogen bonds. Total electronic energy (E(RM062X)): -2371.09972 Hartree. Binding mode 1 (see Table S29).

Table S29: Output from the DFT modelling of **1:11** initiated with the P=O coordinated to the receptor through the formation of two hydrogen bonds.

Center Number	Atomic Number	Atomic Type	Coordinates (Angstroms) X	Y	Z
1	6	0	0.866223	0.760742	2.191203
2	8	0	1.660222	-0.191590	1.458795
3	15	0	1.037399	-0.920706	0.178258
4	8	0	-0.393671	-1.449270	0.646278
5	6	0	-1.611142	-0.792775	0.245090
6	8	0	0.946134	-0.019542	-1.012065
7	6	0	2.047396	-2.371042	0.000503
8	1	0	0.414184	1.490090	1.514204
9	1	0	1.541665	1.270159	2.872802
10	1	0	0.090808	0.236652	2.750211
11	1	0	-2.422092	-1.451462	0.541756
12	1	0	-1.711119	0.167297	0.755125
13	1	0	-1.623945	-0.645606	-0.835227
14	1	0	3.081784	-2.065872	-0.155271
15	1	0	1.974099	-2.981058	0.899599
16	1	0	1.698221	-2.936520	-0.862585
17	6	0	5.355448	4.274899	0.511941
18	6	0	4.975829	3.000650	0.915010
19	6	0	3.725998	2.513912	0.557812
20	6	0	2.861264	3.299136	-0.205080
21	6	0	3.254871	4.570219	-0.626650
22	6	0	4.498609	5.057668	-0.258031
23	7	0	1.629335	2.724511	-0.586961
24	6	0	0.388167	3.272481	-0.505315
25	16	0	0.069510	4.829647	0.046633

26	7	0	-0.570372	2.393629	-0.906115
27	6	0	-1.973564	2.557406	-0.898933
28	6	0	-2.682058	2.118500	-2.016262
29	6	0	-4.069813	2.174501	-2.029061
30	6	0	-4.744675	2.675660	-0.924063
31	6	0	-4.041376	3.107683	0.198430
32	6	0	-2.657981	3.041514	0.218739
33	6	0	6.675067	4.839199	0.936911
34	9	0	7.235772	5.589091	-0.024706
35	9	0	6.557378	5.635017	2.015289
36	9	0	7.557997	3.884174	1.260725
37	6	0	-6.237268	2.792370	-0.932198
38	9	0	-6.804810	2.032417	-1.878059
39	9	0	-6.640195	4.055590	-1.157444
40	9	0	-6.774726	2.430471	0.243711
41	1	0	5.647517	2.391037	1.505629
42	1	0	3.412311	1.523947	0.871267
43	1	0	2.595469	5.160731	-1.245549
44	1	0	4.811934	6.040845	-0.587385
45	1	0	1.658989	1.723822	-0.794993
46	1	0	-0.234724	1.507450	-1.284886
47	1	0	-2.142338	1.736053	-2.874386
48	1	0	-4.618743	1.831644	-2.896467
49	1	0	-4.576664	3.474905	1.065733
50	1	0	-2.107492	3.349342	1.096036

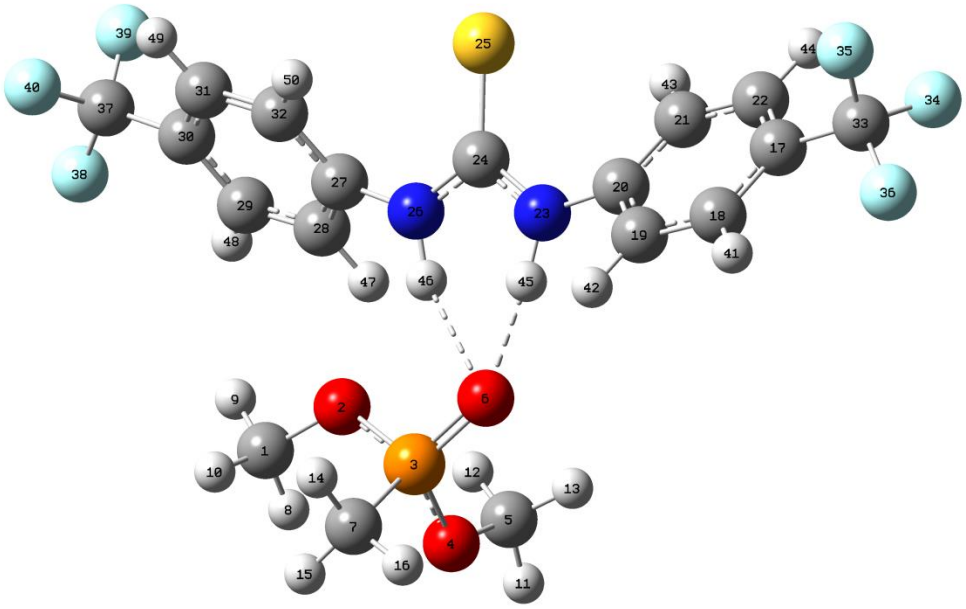

Figure S168: Output from the DFT modelling of **1**:**11** initiated with the P=O coordinated to the receptor through the formation of two hydrogen bonds, one to each oxygen atom. Total electronic energy (E(RM062X)): -2371.098193 Hartree. Binding mode 2 (see Table S30).

Table S30: Output from the DFT modelling of **1:11** initiated with the P=O coordinated to the receptor through the formation of two hydrogen bonds, one to each oxygen atom.

Center Number	Atomic Number	Atomic Type	Coordinates (Angstroms) X	Y	Z
1	6	0	-2.369719	-0.788938	0.859147
2	8	0	-1.156091	-0.033390	0.699994
3	15	0	0.287788	-0.721886	0.820974
4	8	0	0.276706	-1.928487	-0.218636
5	6	0	0.264422	-1.638195	-1.630757
6	8	0	1.298658	0.332928	0.541949
7	6	0	0.396124	-1.551272	2.392275
8	1	0	-2.349179	-1.678517	0.227845
9	1	0	-3.180448	-0.132959	0.553231
10	1	0	-2.498962	-1.069582	1.904932
11	1	0	0.221715	-2.596552	-2.139063
12	1	0	-0.614767	-1.042524	-1.883362
13	1	0	1.172457	-1.103126	-1.906593
14	1	0	0.266010	-0.816301	3.186300
15	1	0	-0.370952	-2.321339	2.471707
16	1	0	1.379417	-2.011997	2.481038
17	6	0	5.731584	4.412201	-0.229731
18	6	0	5.382645	3.424570	0.683964
19	6	0	4.061727	3.012145	0.774670
20	6	0	3.086547	3.583149	-0.046073
21	6	0	3.447279	4.557428	-0.980083
22	6	0	4.766721	4.974141	-1.061132
23	7	0	1.779945	3.069075	0.059537
24	6	0	0.595999	3.730588	0.022072
25	16	0	0.432444	5.403792	-0.109274
26	7	0	-0.454154	2.870214	0.108106

27	6	0	-1.834183	3.159083	0.134064
28	6	0	-2.672668	2.366623	-0.650801
29	6	0	-4.046532	2.560944	-0.621910
30	6	0	-4.581108	3.552382	0.192033
31	6	0	-3.749338	4.339313	0.984394
32	6	0	-2.377907	4.139934	0.965445
33	6	0	7.140550	4.910695	-0.298028
34	9	0	7.502096	5.234175	-1.549477
35	9	0	7.319923	6.018772	0.444469
36	9	0	8.023740	4.006091	0.148337
37	6	0	-6.054567	3.814894	0.194589
38	9	0	-6.761854	2.758379	-0.229782
39	9	0	-6.383508	4.844303	-0.606730
40	9	0	-6.507998	4.130678	1.417824
41	1	0	6.135145	2.979372	1.322252
42	1	0	3.775685	2.245724	1.485347
43	1	0	2.702872	4.972425	-1.642417
44	1	0	5.049725	5.724530	-1.789197
45	1	0	1.727166	2.072298	0.290844
46	1	0	-0.237330	1.878958	0.053818
47	1	0	-2.240294	1.597829	-1.280442
48	1	0	-4.694996	1.943918	-1.230930
49	1	0	-4.175179	5.094667	1.633563
50	1	0	-1.730626	4.729124	1.597944

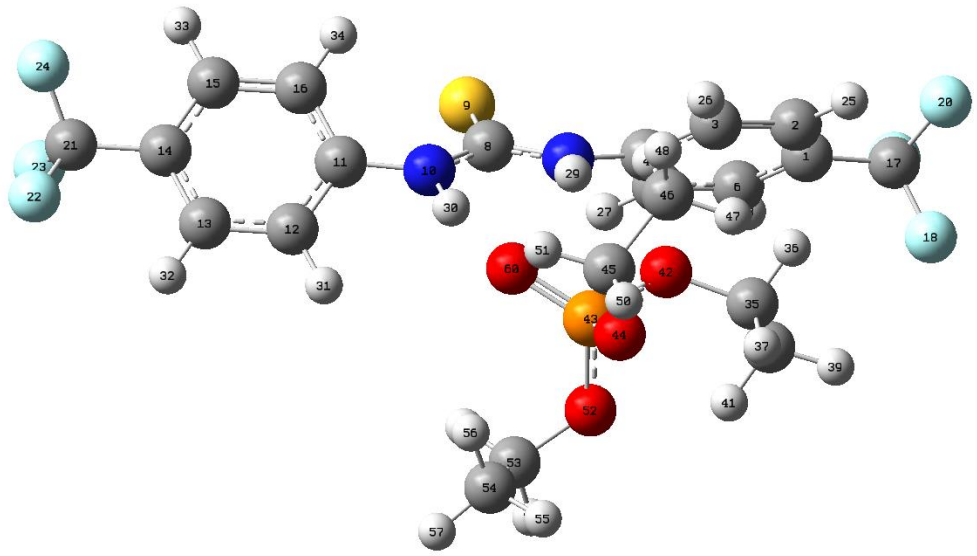

Figure S169: Output from the DFT modelling of **1**:**13** initiated with the P=O coordinated to the receptor.

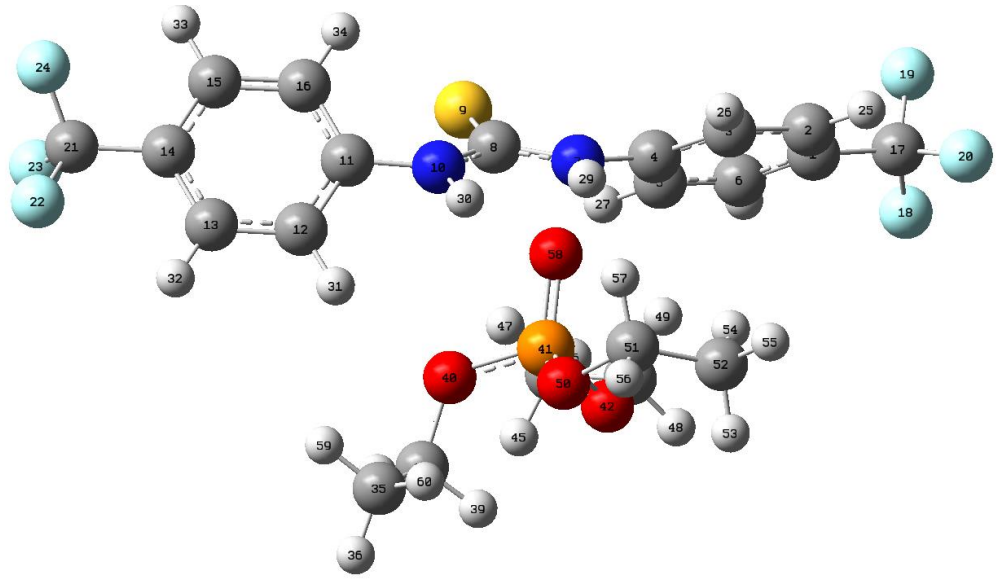

Figure S170: Output from the DFT modelling of **1**:**13** initiated with the P=O coordinated to the receptor.

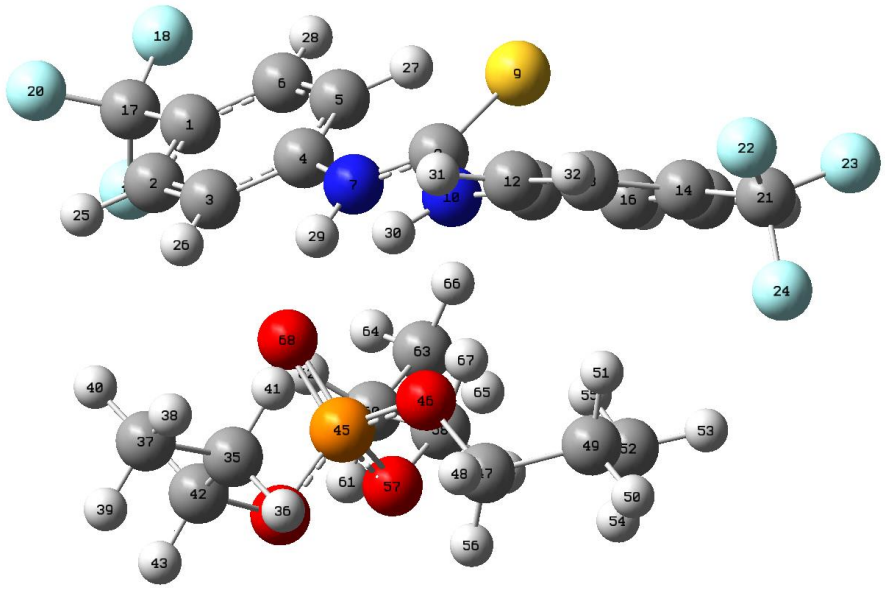

Figure S171: Output from the DFT modelling of **1**:**14** initiated with the P=O coordinated to the receptor.

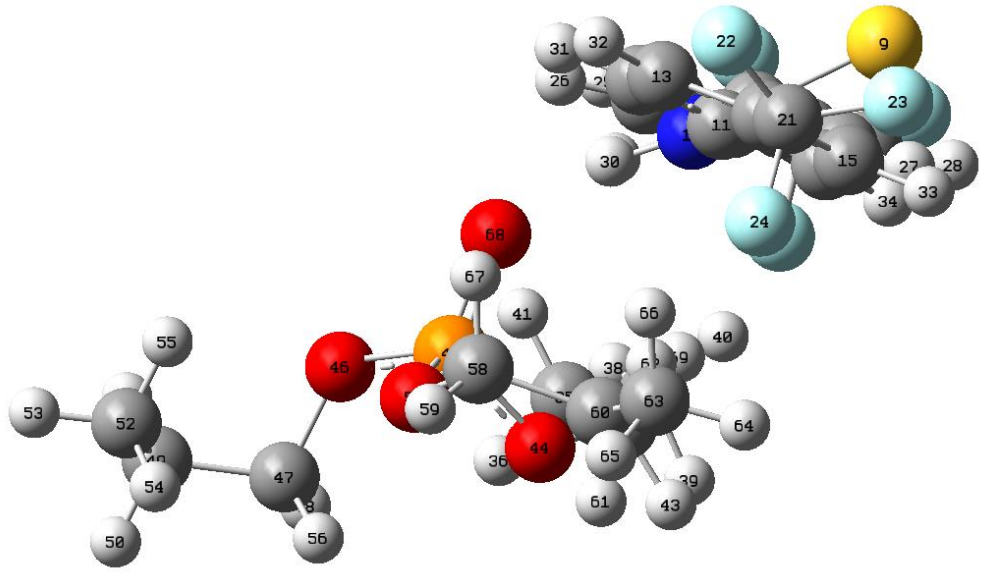

Figure S172: Output from the DFT modelling of **1**:**14** initiated with the P=O coordinated to the receptor.

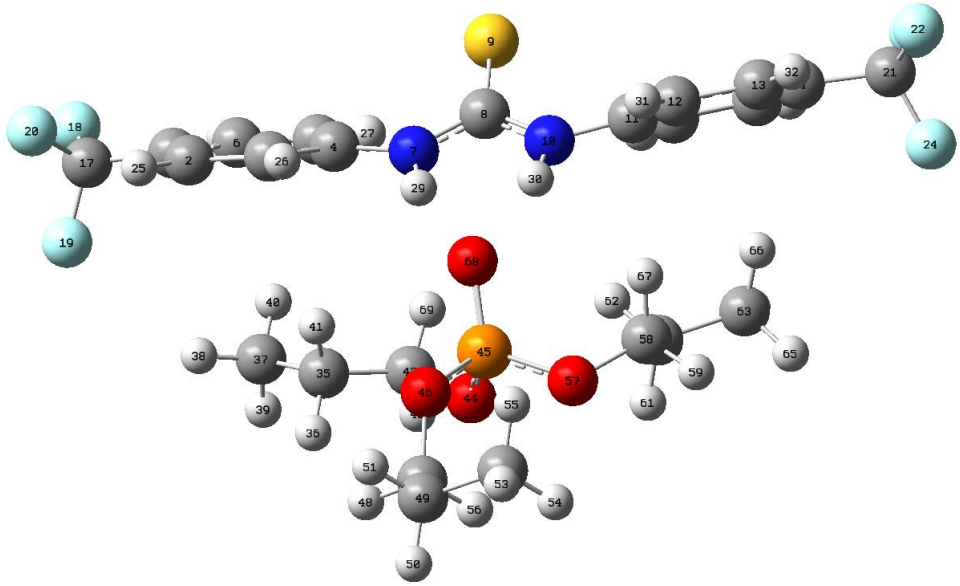

Figure S173: Output from the DFT modelling of **1**:**14** initiated with the P=O coordinated to the receptor.

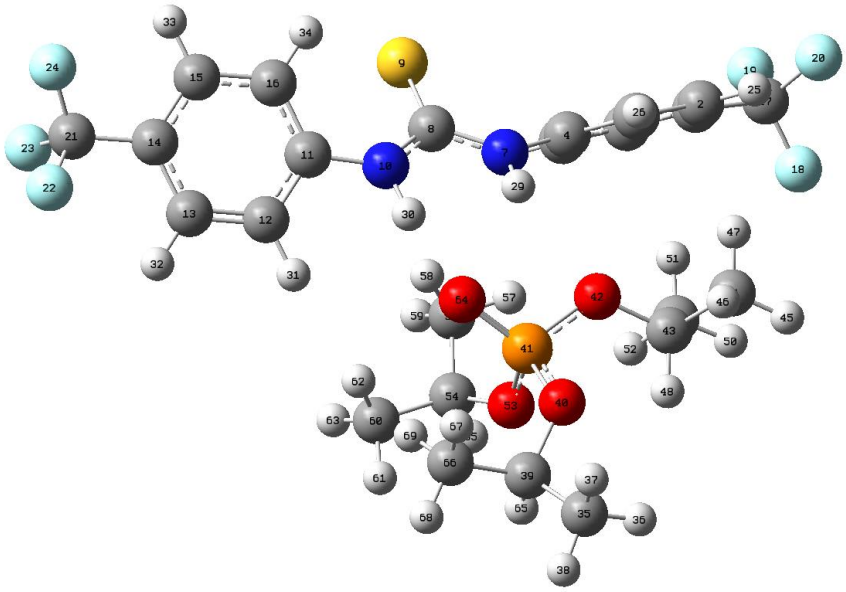

Figure S174*:* Output from the DFT modelling of **1**:**15** initiated with the P=O coordinated to the receptor.

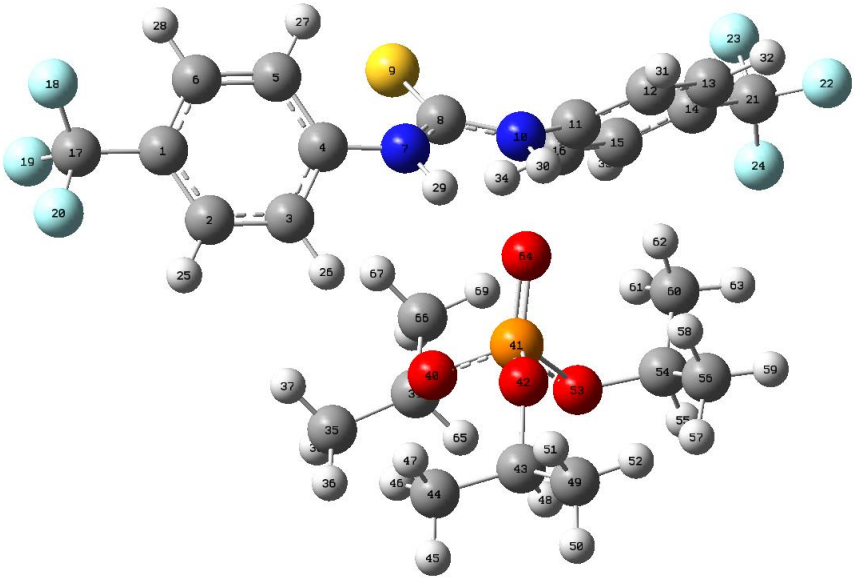

Figure S175: Output from the DFT modelling of **1**:**11** initiated with the P=O coordinated to the receptor.

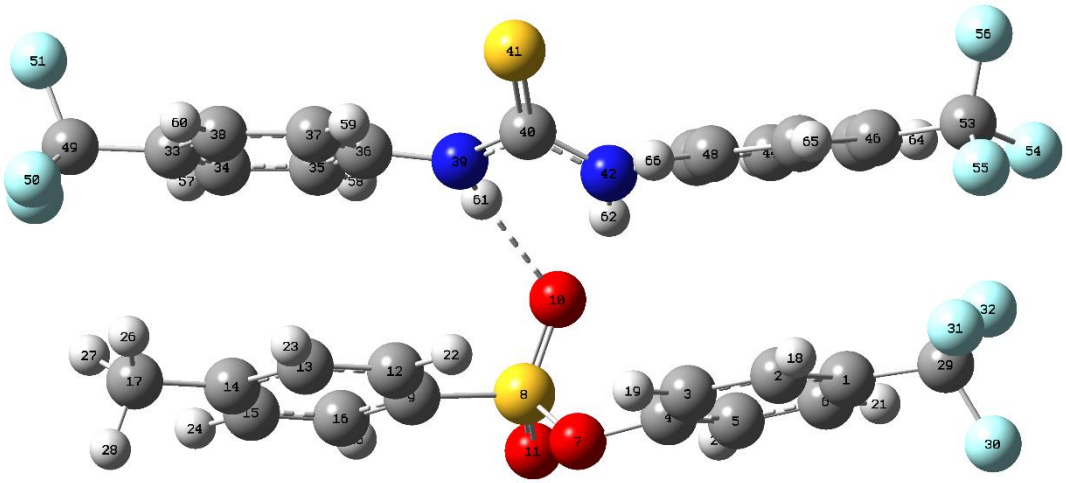

Figure S176: Output from the DFT modelling of **1**:**16** initiated with the S=O coordinated to the receptor through the formation of one hydrogen bonds, one to each oxygen atom. Total electronic energy (E(RM062X)): -3147.670507 Hartree. Binding mode 1 (see Table S31).

Table S31: Output from the DFT modelling of **1:16** initiated with the S=O coordinated to the receptor through the formation of one hydrogen bond.

Center Number	Atomic Number	Atomic Type	Coordinates (Angstroms) X	Y	Z
1	6	0	-4.433401	-0.508940	-0.408878
2	6	0	-3.562075	-1.504940	-0.828731
3	6	0	-2.224738	-1.449718	-0.450896
4	6	0	-1.804193	-0.408651	0.358886
5	6	0	-2.661505	0.599061	0.782790
6	6	0	-3.987835	0.546816	0.383983
7	8	0	-0.476041	-0.453156	0.797376
8	16	0	0.479822	0.848991	0.629275
9	6	0	2.026510	0.040290	0.428088
10	8	0	0.078833	1.510382	-0.609694
11	8	0	0.452864	1.630526	1.839102
12	6	0	2.124078	-1.057062	-0.421911
13	6	0	3.377665	-1.604860	-0.647198
14	6	0	4.519932	-1.060525	-0.053221
15	6	0	4.381788	0.039480	0.798606
16	6	0	3.138209	0.598927	1.051097
17	6	0	5.874562	-1.661127	-0.305668
18	1	0	-3.915811	-2.314598	-1.453965
19	1	0	-1.517535	-2.207752	-0.762873
20	1	0	-2.302287	1.395179	1.423207
21	1	0	-4.676632	1.320628	0.700110
22	1	0	1.243035	-1.476448	-0.893122
23	1	0	3.472312	-2.459726	-1.306413
24	1	0	5.260716	0.466685	1.267421
25	1	0	3.028563	1.447820	1.714300
26	1	0	5.885233	-2.228769	-1.236366
27	1	0	6.639968	-0.885460	-0.358173
28	1	0	6.142340	-2.338709	0.509631
29	6	0	-5.892706	-0.576308	-0.746949

30	9	0	-6.630723	-0.916872	0.322864
31	9	0	-6.158493	-1.475614	-1.702807
32	9	0	-6.363877	0.607934	-1.167175
33	6	0	5.546855	0.137987	-3.218494
34	6	0	4.961285	1.210135	-2.553873
35	6	0	3.584542	1.354581	-2.568803
36	6	0	2.778829	0.429321	-3.241700
37	6	0	3.371440	-0.649241	-3.904622
38	6	0	4.751937	-0.783203	-3.892917
39	7	0	1.393753	0.598652	-3.085288
40	6	0	0.333941	0.122794	-3.800150
41	16	0	0.440105	-0.545656	-5.336487
42	7	0	-0.832699	0.312055	-3.126760
43	6	0	-2.153895	0.051426	-3.552952
44	6	0	-3.116834	1.023058	-3.285420
45	6	0	-4.447964	0.791117	-3.603318
46	6	0	-4.811156	-0.415580	-4.187838
47	6	0	-3.853776	-1.393115	-4.446456
48	6	0	-2.525292	-1.167720	-4.122280
49	6	0	7.034918	-0.004187	-3.256610
50	9	0	7.420543	-1.290943	-3.244952
51	9	0	7.570663	0.539650	-4.363427
52	9	0	7.630104	0.594925	-2.212395
53	6	0	-6.231125	-0.658011	-4.597482
54	9	0	-7.098598	0.093060	-3.906901
55	9	0	-6.592514	-1.939625	-4.434725
56	9	0	-6.428505	-0.373214	-5.898531
57	1	0	5.573821	1.924531	-2.018064
58	1	0	3.122325	2.182438	-2.042312
59	1	0	2.762437	-1.387157	-4.401864
60	1	0	5.209014	-1.627157	-4.395675
61	1	0	1.149647	1.156400	-2.271928
62	1	0	-0.772261	0.815863	-2.245463
63	1	0	-2.819927	1.959227	-2.826820
64	1	0	-5.196572	1.543236	-3.390731
65	1	0	-4.149780	-2.339848	-4.881608
66	1	0	-1.781974	-1.932789	-4.291888

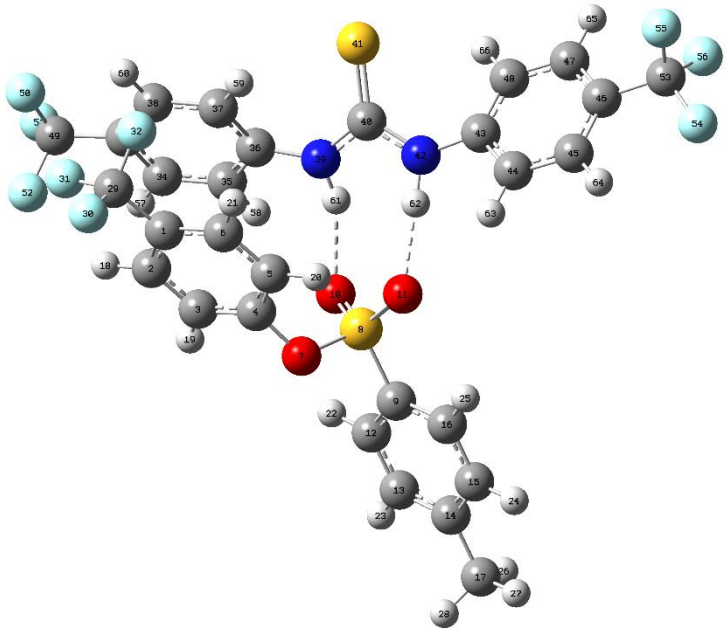

Figure S177: Output from the DFT modelling of **1**:**16** initiated with the O=S=O coordinated to the receptor through the formation of two hydrogen bonds, one to each oxygen atom. Total electronic energy (E(RM062X)): -3147.665792 Hartree. Binding mode 2 (see Table S32).

Table S32: Output from the DFT modelling of **1:16** initiated with the O=S=O coordinated to the receptor through the formation of two hydrogen bonds, one to each oxygen atom.

Center Number	Atomic Number	Atomic Type	Coordinates (Angstroms) X	Y	Z
1	6	0	-3.476662	-0.557210	-1.547362
2	6	0	-2.537005	-1.570726	-1.683480
3	6	0	-1.328520	-1.476972	-1.001966
4	6	0	-1.107014	-0.376490	-0.192908
5	6	0	-2.030187	0.652439	-0.055782
6	6	0	-3.228386	0.555999	-0.746761
7	8	0	0.078073	-0.343983	0.559844
8	16	0	1.249059	0.651773	0.041761
9	6	0	2.538734	0.181329	1.126710
10	8	0	1.550375	0.303676	-1.336124
11	8	0	0.827365	2.018973	0.297624
12	6	0	3.293729	-0.948301	0.819529
13	6	0	4.304574	-1.313983	1.691337
14	6	0	4.562354	-0.572235	2.851303
15	6	0	3.782703	0.553099	3.124338
16	6	0	2.761390	0.941401	2.267536
17	6	0	5.676277	-0.984652	3.772640
18	1	0	-2.737208	-2.420177	-2.324264
19	1	0	-0.569734	-2.244379	-1.084723
20	1	0	-1.812505	1.495283	0.587137
21	1	0	-3.969526	1.340944	-0.658565
22	1	0	3.098657	-1.515746	-0.082125
23	1	0	4.907239	-2.187504	1.470978
24	1	0	3.975864	1.135157	4.017388
25	1	0	2.157969	1.816545	2.472517
26	1	0	6.641728	-0.856510	3.277414
27	1	0	5.676339	-0.390083	4.685220

28	1	0	5.582560	-2.038738	4.040172
29	6	0	-4.812502	-0.666587	-2.221094
30	9	0	-5.777042	-1.010253	-1.352094
31	9	0	-4.824024	-1.586292	-3.195409
32	9	0	-5.195116	0.499011	-2.767825
33	6	0	-2.271048	-1.043819	-5.072848
34	6	0	-0.944527	-1.190895	-4.674252
35	6	0	-0.306497	-0.151872	-4.022448
36	6	0	-0.990628	1.041083	-3.752474
37	6	0	-2.319076	1.183381	-4.155385
38	6	0	-2.947677	0.142061	-4.825403
39	7	0	-0.291733	2.004333	-3.004622
40	6	0	-0.418109	3.362599	-2.968086
41	16	0	-1.316705	4.271791	-4.054441
42	7	0	0.291553	3.885483	-1.929313
43	6	0	0.524735	5.238665	-1.615941
44	6	0	0.478049	5.599598	-0.268919
45	6	0	0.759189	6.902964	0.115652
46	6	0	1.085227	7.846700	-0.849635
47	6	0	1.146682	7.487431	-2.194417
48	6	0	0.876224	6.185480	-2.581485
49	6	0	-2.963249	-2.208435	-5.704066
50	9	0	-4.194932	-1.910218	-6.132628
51	9	0	-2.283126	-2.694016	-6.756639
52	9	0	-3.089499	-3.236137	-4.839694
53	6	0	1.345720	9.269968	-0.468386
54	9	0	1.582930	9.414455	0.842264
55	9	0	0.303455	10.068307	-0.762729
56	9	0	2.403085	9.779248	-1.121357
57	1	0	-0.413424	-2.115821	-4.866870
58	1	0	0.720834	-0.260749	-3.695635
59	1	0	-2.866718	2.084827	-3.929427
60	1	0	-3.983088	0.247524	-5.121898
61	1	0	0.502007	1.616477	-2.501281
62	1	0	0.519201	3.241065	-1.174161
63	1	0	0.219975	4.853856	0.474060
64	1	0	0.721888	7.179454	1.161327
65	1	0	1.425805	8.222669	-2.939657
66	1	0	0.948864	5.898769	-3.620042

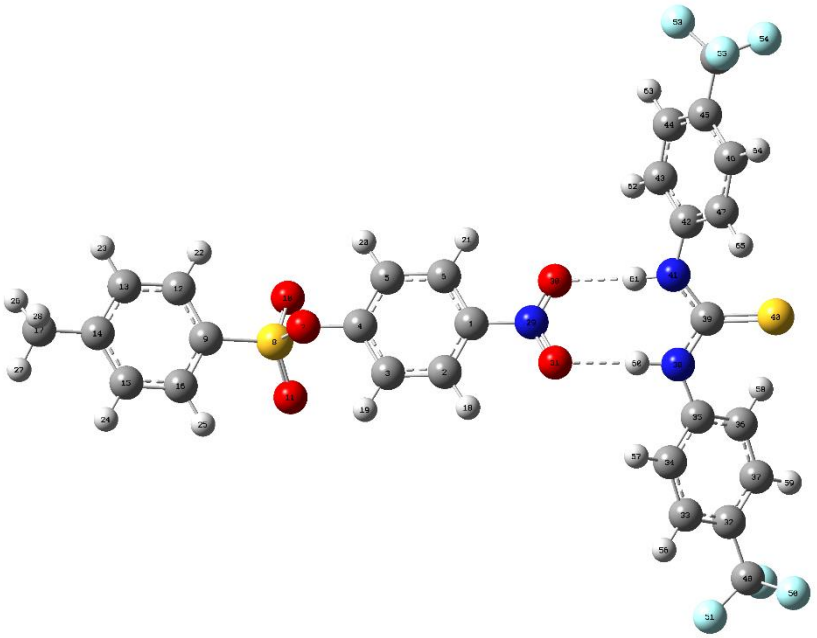

Figure S178: Output from the DFT modelling of **1**:**17** initiated with the nitro functionality coordinated to the receptor through the formation of two hydrogen bonds, one to each oxygen atom. Total electronic energy (E(RM062X)): -3015.094796 Hartree (see Table S33).

Table S33: Output from the DFT modelling of **1:17** initiated with the nitro functionality coordinated to the receptor through the formation of two hydrogen bonds, one to each oxygen atom.

Center Number	Atomic Number	Atomic Type	Coordinates (Angstroms) X	Y	Z
1	6	0	1.375935	3.769671	4.892242
2	6	0	2.355306	4.415728	4.149499
3	6	0	2.193498	4.488904	2.775581
4	6	0	1.069097	3.909616	2.200587
5	6	0	0.093404	3.264550	2.951178
6	6	0	0.247243	3.191907	4.326129
7	8	0	0.938380	3.945847	0.818253
8	16	0	0.057647	5.196864	0.205532
9	6	0	0.220420	4.802275	-1.496650
10	8	0	-1.305161	5.022428	0.651968
11	8	0	0.762276	6.415883	0.528533
12	6	0	-0.711118	3.948992	-2.078764
13	6	0	-0.565549	3.634674	-3.420990
14	6	0	0.493138	4.154764	-4.172864
15	6	0	1.408725	5.009885	-3.553172
16	6	0	1.285052	5.338792	-2.211094
17	6	0	0.652348	3.780424	-5.620480
18	1	0	3.215778	4.849075	4.638910
19	1	0	2.923119	4.981676	2.147194
20	1	0	-0.763932	2.828504	2.456438
21	1	0	-0.485055	2.698328	4.948897
22	1	0	-1.534720	3.555561	-1.496264
23	1	0	-1.286181	2.978635	-3.895191
24	1	0	2.226533	5.426257	-4.129399

25	1	0	1.988025	6.007323	-1.730147
26	1	0	-0.318170	3.660691	-6.102842
27	1	0	1.225647	4.532909	-6.161545
28	1	0	1.183962	2.828627	-5.703137
29	7	0	1.542575	3.692322	6.345944
30	8	0	0.649011	3.192375	7.000796
31	8	0	2.566719	4.132036	6.830845
32	6	0	4.473704	8.003412	10.921099
33	6	0	4.905931	7.280841	9.816555
34	6	0	4.276347	6.087917	9.489959
35	6	0	3.214035	5.619687	10.263545
36	6	0	2.767624	6.361278	11.359972
37	6	0	3.405420	7.545792	11.689291
38	7	0	2.574668	4.437294	9.840281
39	6	0	2.120726	3.398281	10.593219
40	16	0	2.361343	3.247556	12.249573
41	7	0	1.446362	2.497794	9.827387
42	6	0	0.918300	1.243998	10.194435
43	6	0	-0.324683	0.893393	9.665828
44	6	0	-0.872018	-0.352767	9.935091
45	6	0	-0.176006	-1.248206	10.737387
46	6	0	1.070157	-0.907222	11.257266
47	6	0	1.624902	0.332016	10.981766
48	6	0	5.169366	9.265648	11.324021
49	9	0	4.303178	10.213250	11.717467
50	9	0	6.007324	9.070099	12.358319
51	9	0	5.901481	9.786294	10.329883
52	6	0	-0.774041	-2.574908	11.086035
53	9	0	-1.716794	-2.955150	10.212532
54	9	0	-1.356965	-2.561189	12.298630
55	9	0	0.148719	-3.549109	11.123737
56	1	0	5.729234	7.642068	9.214062
57	1	0	4.607852	5.512347	8.633657
58	1	0	1.921812	6.017704	11.936604
59	1	0	3.057597	8.127045	12.534733
60	1	0	2.590890	4.289962	8.833557
61	1	0	1.154035	2.818277	8.906860
62	1	0	-0.860674	1.602278	9.045718
63	1	0	-1.835852	-0.622216	9.522799
64	1	0	1.618351	-1.619680	11.861598
65	1	0	2.602720	0.589112	11.360802

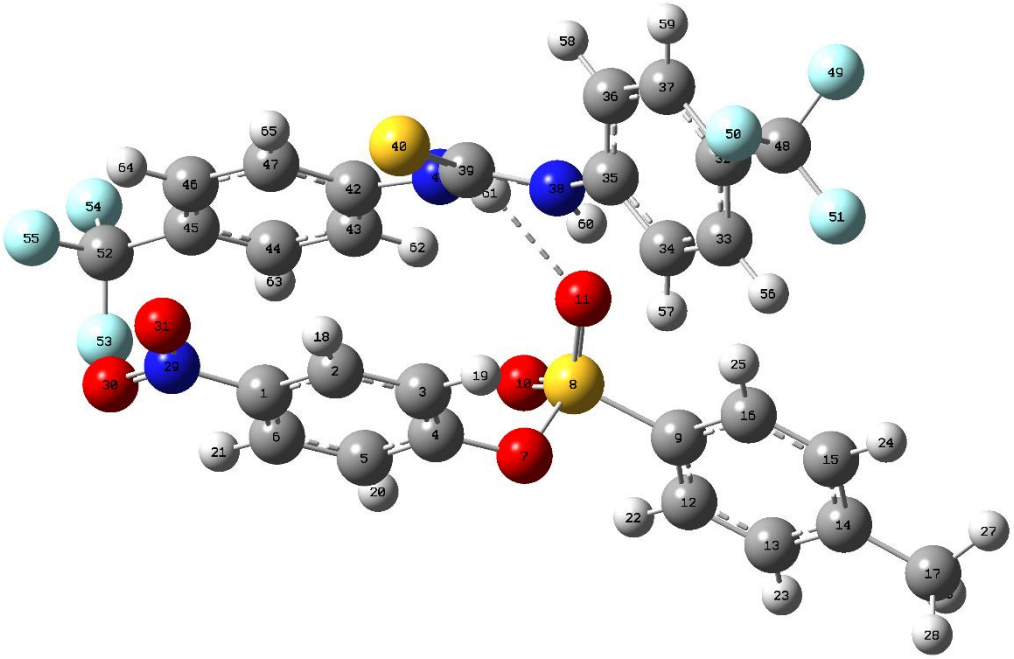

Figure S179: Output from the DFT modelling of **1**:**17** initiated with the S=O coordinated to the receptor through the formation of one hydrogen bond. Total electronic energy (E(RM062X)): -3015.109021 Hartree. Binding mode 1 (see Table S34).

Table S34: Output from the DFT modelling of **1:17** initiated with the S=O coordinated to the receptor through the formation of one hydrogen bonds.

Center Number	Atomic Number	Atomic Type	Coordinates (Angstroms) X	Y	Z
1	6	0	-2.883403	8.654768	0.134718
2	6	0	-2.477719	7.767496	1.122026
3	6	0	-1.612860	6.742145	0.771725
4	6	0	-1.200839	6.641281	-0.550503
5	6	0	-1.632996	7.512608	-1.541047
6	6	0	-2.489553	8.546461	-1.190528
7	8	0	-0.339258	5.595795	-0.894844
8	16	0	1.249979	5.972199	-0.960497
9	6	0	1.892608	4.404037	-1.398812
10	8	0	1.440368	6.941295	-2.013484
11	8	0	1.660217	6.338971	0.387239
12	6	0	1.985573	4.080047	-2.748463
13	6	0	2.481624	2.831379	-3.089421
14	6	0	2.874362	1.917957	-2.105906
15	6	0	2.769550	2.282573	-0.760085
16	6	0	2.275545	3.524651	-0.392029
17	6	0	3.382251	0.556103	-2.489605
18	1	0	-2.812368	7.895589	2.141570
19	1	0	-1.261387	6.027235	1.505363
20	1	0	-1.285712	7.388226	-2.558002
21	1	0	-2.829212	9.270208	-1.918591
22	1	0	1.690362	4.792925	-3.508187
23	1	0	2.570277	2.562615	-4.135397
24	1	0	3.083035	1.586371	0.008765
25	1	0	2.204466	3.812972	0.649037
26	1	0	3.880384	0.581236	-3.458797

27	1	0	4.077423	0.171441	-1.743392
28	1	0	2.546517	-0.145229	-2.561467
29	7	0	-3.743670	9.785192	0.522714
30	8	0	-4.078117	10.565472	-0.343437
31	8	0	-4.051389	9.887034	1.690750
32	6	0	1.100043	4.050410	6.442115
33	6	0	0.822117	3.605494	5.158262
34	6	0	0.780700	4.518810	4.110800
35	6	0	1.026651	5.867535	4.351009
36	6	0	1.325585	6.308534	5.642593
37	6	0	1.353386	5.400526	6.685501
38	7	0	1.041834	6.755727	3.252191
39	6	0	0.402294	7.958368	3.162925
40	16	0	-0.719167	8.487083	4.292565
41	7	0	0.773857	8.627978	2.036358
42	6	0	0.168817	9.682349	1.329680
43	6	0	0.508923	9.756974	-0.030080
44	6	0	-0.069199	10.707389	-0.847924
45	6	0	-1.000600	11.599019	-0.319643
46	6	0	-1.299132	11.568988	1.034651
47	6	0	-0.714853	10.621192	1.868534
48	6	0	1.132817	3.099823	7.598124
49	9	0	2.302753	3.155329	8.257412
50	9	0	0.180086	3.381437	8.503753
51	9	0	0.952386	1.827213	7.223941
52	6	0	-1.656696	12.577964	-1.240228
53	9	0	-2.208092	11.964466	-2.303523
54	9	0	-0.778277	13.466291	-1.740676
55	9	0	-2.624658	13.281389	-0.643158
56	1	0	0.630298	2.557103	4.971494
57	1	0	0.552140	4.184676	3.105796
58	1	0	1.540774	7.353514	5.817330
59	1	0	1.587063	5.737353	7.688616
60	1	0	1.427204	6.378234	2.390452
61	1	0	1.462609	8.138119	1.473435
62	1	0	1.208282	9.042897	-0.451989
63	1	0	0.178684	10.732710	-1.902874
64	1	0	-2.011481	12.271696	1.449229
65	1	0	-0.961366	10.604192	2.916430

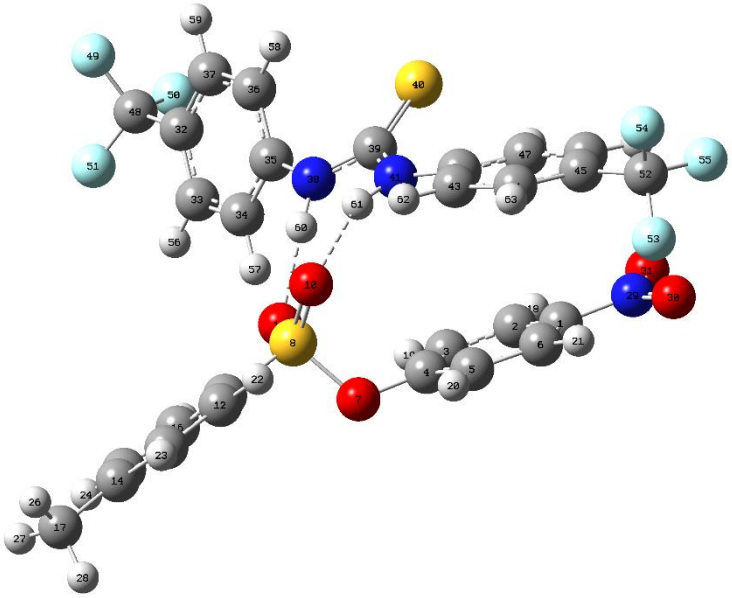

Figure S180: Output from the DFT modelling of **1**:**17** initiated with the O=S=O coordinated to the receptor through the formation of two hydrogen bonds, one to each oxygen atom. Total electronic energy (E(RM062X)): -3015.107536 Hartree. Binding mode 2 (see Table S35).

Table S35: Output from the DFT modelling of **1:17** initiated with the O=S=O coordinated to the receptor through the formation of two hydrogen bonds, one to each oxygen atom.

Center Number	Atomic Number	Atomic Type	Coordinates (Angstroms) X	Y	Z
1	6	0	-0.621739	3.281951	4.678722
2	6	0	-0.040539	4.492593	4.326415
3	6	0	0.377878	4.669129	3.017274
4	6	0	0.183896	3.629938	2.113973
5	6	0	-0.400765	2.424651	2.468654
6	6	0	-0.806938	2.240566	3.783041
7	8	0	0.627876	3.768367	0.794593
8	16	0	-0.227080	4.773243	-0.159521
9	6	0	0.462087	4.360506	-1.712745
10	8	0	-1.622768	4.383192	-0.061677
11	8	0	0.103200	6.138085	0.212619
12	6	0	0.009919	3.213537	-2.361107
13	6	0	0.567819	2.895491	-3.587087
14	6	0	1.561168	3.699912	-4.160020
15	6	0	1.984892	4.843178	-3.479700
16	6	0	1.443390	5.185026	-2.247965
17	6	0	2.165199	3.319963	-5.482974
18	1	0	0.078026	5.273442	5.064297
19	1	0	0.849623	5.588912	2.697081
20	1	0	-0.533144	1.652736	1.722107
21	1	0	-1.279437	1.323198	4.106479
22	1	0	-0.765148	2.597727	-1.921594
23	1	0	0.227395	2.011467	-4.113437
24	1	0	2.746032	5.477076	-3.918382
25	1	0	1.763871	6.073673	-1.719339
26	1	0	1.390215	3.024292	-6.191658
27	1	0	2.736683	4.143795	-5.908743
28	1	0	2.837336	2.467518	-5.355637

29	7	0	-1.092360	3.107837	6.062541
30	8	0	-1.524674	2.020914	6.381207
31	8	0	-1.044986	4.068806	6.800521
32	6	0	-1.219085	11.836188	0.675105
33	6	0	-0.189006	10.904228	0.649330
34	6	0	-0.456979	9.578600	0.958373
35	6	0	-1.753783	9.183726	1.290212
36	6	0	-2.790979	10.119016	1.292017
37	6	0	-2.517033	11.443715	0.993055
38	7	0	-1.970182	7.811853	1.527378
39	6	0	-2.747108	7.228115	2.483227
40	16	0	-3.509318	8.067169	3.718526
41	7	0	-2.817748	5.878578	2.292269
42	6	0	-3.322353	4.852455	3.108595
43	6	0	-3.665733	3.662792	2.450575
44	6	0	-4.082638	2.559023	3.170440
45	6	0	-4.169683	2.631677	4.558843
46	6	0	-3.856678	3.813614	5.215262
47	6	0	-3.421102	4.922970	4.500524
48	6	0	-0.938385	13.280016	0.399947
49	9	0	-1.936593	13.867085	-0.278698
50	9	0	-0.785609	13.988466	1.533738
51	9	0	0.182710	13.454753	-0.313656
52	6	0	-4.570204	1.405712	5.315632
53	9	0	-3.735064	0.378408	5.069514
54	9	0	-5.796427	0.976031	4.967262
55	9	0	-4.582639	1.594438	6.639384
56	1	0	0.817203	11.207785	0.390397
57	1	0	0.336991	8.840977	0.942379
58	1	0	-3.801303	9.807230	1.511654
59	1	0	-3.319907	12.170803	0.987070
60	1	0	-1.311562	7.204554	1.043846
61	1	0	-2.545202	5.547435	1.370049
62	1	0	-3.576677	3.607125	1.371903
63	1	0	-4.327843	1.638499	2.653408
64	1	0	-3.908300	3.864298	6.296095
65	1	0	-3.138462	5.820559	5.026659

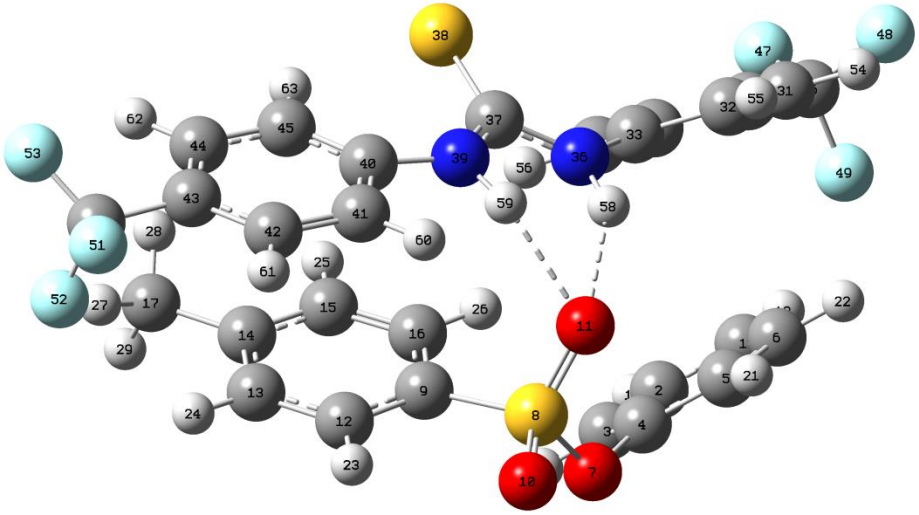

Figure S181: Output from the DFT modelling of **1**:**18** initiated with the S=O coordinated to the receptor through the formation of two hydrogen bonds. Total electronic energy (E(RM062X)): -2810.625018 Hartree. Binding mode 1 (see Table S36).

Table S36: Output from the DFT modelling of **1:18** initiated with the S=O coordinated to the receptor through the formation of two hydrogen bonds.

Center Number	Atomic Number	Atomic Type	Coordinates (Angstroms) X	Y	Z
1	6	0	4.678130	1.625594	3.580050
2	6	0	4.487505	0.285162	3.904676
3	6	0	3.354841	-0.111393	4.607632
4	6	0	2.428122	0.854738	4.970798
5	6	0	2.595247	2.196642	4.662514
6	6	0	3.733778	2.575581	3.957278
7	8	0	1.338397	0.446550	5.759663
8	16	0	-0.171621	0.440152	5.177414
9	6	0	-0.345959	-1.111047	4.363105
10	8	0	-1.013739	0.492002	6.342667
11	8	0	-0.264852	1.498682	4.179331
12	6	0	-1.383230	-1.946925	4.753837
13	6	0	-1.623994	-3.097200	4.011974
14	6	0	-0.836246	-3.416817	2.906891
15	6	0	0.221375	-2.566450	2.556643
16	6	0	0.466455	-1.404541	3.267080
17	6	0	-1.121571	-4.649790	2.096629
18	1	0	5.559299	1.929540	3.028518
19	1	0	5.221581	-0.455961	3.613624
20	1	0	3.185303	-1.144915	4.883835
21	1	0	1.855475	2.920953	4.977731
22	1	0	3.882476	3.618884	3.707819
23	1	0	-2.004280	-1.687087	5.601821
24	1	0	-2.453472	-3.740388	4.282548
25	1	0	0.836485	-2.801906	1.695086
26	1	0	1.258685	-0.731146	2.960334
27	1	0	-2.159616	-4.961672	2.218134
28	1	0	-0.929333	-4.470354	1.037454
29	1	0	-0.478005	-5.472959	2.418508
30	6	0	4.704026	2.408792	0.180310

31	6	0	3.803895	3.417753	0.496941
32	6	0	2.508340	3.083939	0.872469
33	6	0	2.130519	1.747191	0.943437
34	6	0	3.039136	0.736797	0.631802
35	6	0	4.326075	1.069601	0.242833
36	7	0	0.830722	1.431830	1.420968
37	6	0	-0.097856	0.660262	0.796077
38	16	0	0.146017	-0.005192	-0.726110
39	7	0	-1.235254	0.538337	1.539062
40	6	0	-2.276933	-0.404473	1.519340
41	6	0	-3.258702	-0.229219	2.506270
42	6	0	-4.270988	-1.156576	2.672277
43	6	0	-4.326428	-2.269612	1.839683
44	6	0	-3.385977	-2.427916	0.829920
45	6	0	-2.362616	-1.506277	0.661327
46	6	0	6.123159	2.748053	-0.155939
47	9	0	6.636956	1.921159	-1.077441
48	9	0	6.255669	3.996612	-0.620844
49	9	0	6.924179	2.654165	0.924553
50	6	0	-5.342027	-3.339811	2.071772
51	9	0	-6.418682	-2.893888	2.732548
52	9	0	-4.836177	-4.353430	2.807775
53	9	0	-5.774734	-3.891049	0.928135
54	1	0	4.105152	4.456192	0.444467
55	1	0	1.789510	3.856440	1.117134
56	1	0	2.736963	-0.299895	0.702362
57	1	0	5.039428	0.290797	0.002124
58	1	0	0.594770	1.821645	2.330316
59	1	0	-1.239829	1.095403	2.388666
60	1	0	-3.212021	0.634950	3.160510
61	1	0	-5.008902	-1.017028	3.452099
62	1	0	-3.437226	-3.287214	0.171510
63	1	0	-1.629208	-1.657986	-0.112113

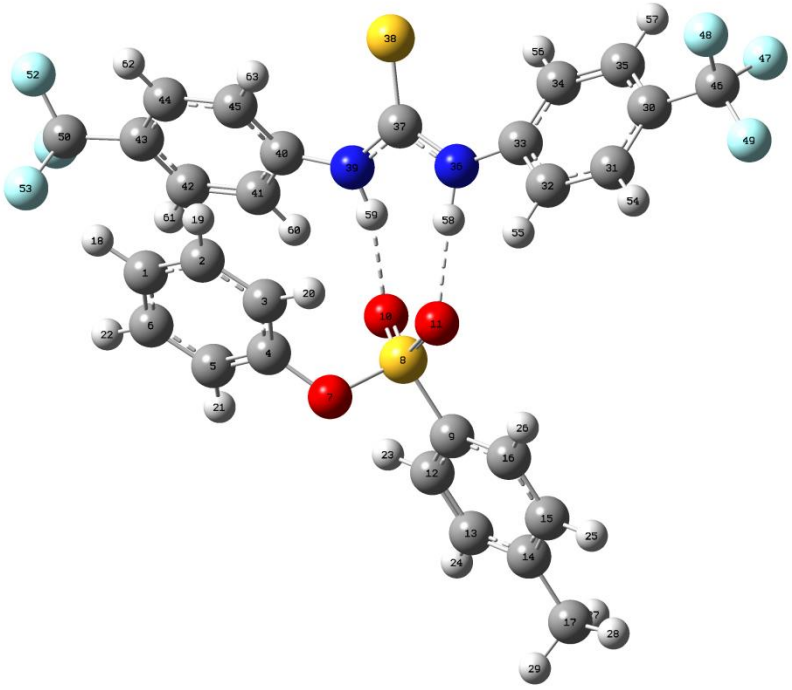

Figure S182: Output from the DFT modelling of **1**:**18** initiated with the O=S=O coordinated to the receptor through the formation of two hydrogen bonds, one to each oxygen atom. Total electronic energy (E(RM062X)): -2810.618042 Hartree. Binding mode 2 (see Table S37).

Table S37: Output from the DFT modelling of **1:18** initiated with the O=S=O coordinated to the receptor through the formation of two hydrogen bonds, one to each oxygen atom.

Center Number	Atomic Number	Atomic Type	Coordinates (Angstroms) X	Y	Z
1	6	0	-3.042031	3.073065	3.177894
2	6	0	-1.660989	3.113220	3.013253
3	6	0	-0.853721	2.142288	3.598733
4	6	0	-1.466877	1.139030	4.333100
5	6	0	-2.838984	1.070426	4.507484
6	6	0	-3.628548	2.056483	3.926190
7	8	0	-0.681626	0.162397	4.981351
8	16	0	0.072705	-0.916088	4.043868
9	6	0	0.426727	-2.149292	5.236476
10	8	0	-0.878195	-1.387974	3.049096
11	8	0	1.299306	-0.320306	3.539520
12	6	0	-0.621652	-2.934912	5.712077
13	6	0	-0.333889	-3.910031	6.649783
14	6	0	0.975099	-4.105788	7.110917
15	6	0	1.997704	-3.300271	6.609434
16	6	0	1.735276	-2.311582	5.668594
17	6	0	1.257133	-5.174902	8.129528
18	1	0	-3.665572	3.826772	2.713136
19	1	0	-1.205618	3.902355	2.427619
20	1	0	0.224593	2.162906	3.498235
21	1	0	-3.263983	0.261295	5.088044
22	1	0	-4.704807	2.021461	4.044567
23	1	0	-1.632063	-2.788694	5.349680
24	1	0	-1.133337	-4.533752	7.032744
25	1	0	3.013550	-3.445180	6.956934

26	1	0	2.525276	-1.685197	5.274454
27	1	0	0.961209	-6.153543	7.745669
28	1	0	2.314871	-5.208220	8.387118
29	1	0	0.682522	-4.993160	9.040304
30	6	0	5.567593	-0.654024	-0.514743
31	6	0	5.256027	-0.168126	0.749132
32	6	0	3.930081	0.057610	1.088468
33	6	0	2.914565	-0.203372	0.166899
34	6	0	3.230555	-0.714656	-1.094041
35	6	0	4.556724	-0.929566	-1.432164
36	7	0	1.587775	-0.012581	0.598326
37	6	0	0.533170	0.508026	-0.090814
38	16	0	0.649408	1.207325	-1.611774
39	7	0	-0.621380	0.376125	0.621921
40	6	0	-1.893739	0.938587	0.424139
41	6	0	-2.969207	0.232662	0.974456
42	6	0	-4.251186	0.749212	0.909437
43	6	0	-4.469616	1.975302	0.290881
44	6	0	-3.405737	2.680488	-0.259752
45	6	0	-2.117205	2.171269	-0.194913
46	6	0	6.995012	-0.848264	-0.919153
47	9	0	7.155946	-1.930816	-1.696434
48	9	0	7.464722	0.196084	-1.626009
49	9	0	7.809184	-0.992957	0.135682
50	6	0	-5.834222	2.581181	0.325062
51	9	0	-6.805805	1.658792	0.254745
52	9	0	-6.037353	3.451145	-0.674057
53	9	0	-6.046684	3.262830	1.471194
54	1	0	6.041143	0.034771	1.466128
55	1	0	3.673874	0.437694	2.070584
56	1	0	2.444161	-0.952912	-1.794524
57	1	0	4.804414	-1.332330	-2.406703
58	1	0	1.463166	-0.112267	1.604295
59	1	0	-0.608605	-0.321820	1.362585
60	1	0	-2.786273	-0.714231	1.469225
61	1	0	-5.077825	0.201690	1.345612
62	1	0	-3.577141	3.641227	-0.729496
63	1	0	-1.293419	2.736518	-0.600829

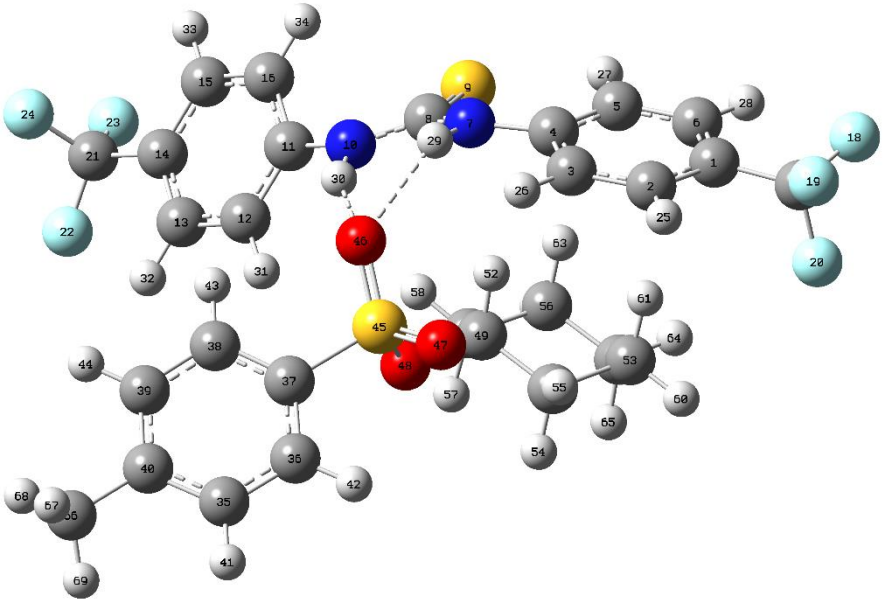

Figure S183: Output from the DFT modelling of **1**:**19** initiated with the S=O coordinated to the receptor through the formation of two hydrogen bonds. Total electronic energy (E(RM062X)): -2814.242885 Hartree. Binding mode 1 (see Table S38).

Table S38: Output from the DFT modelling of **1:19** initiated with the S=O coordinated to the receptor through the formation of two hydrogen bonds.

Center Number	Atomic Number	Atomic Type	Coordinates (Angstroms) X	Y	Z
1	6	0	5.406743	-0.478411	1.046336
2	6	0	4.811977	0.624079	0.436641
3	6	0	3.545051	0.504925	-0.101301
4	6	0	2.851441	-0.715596	-0.040344
5	6	0	3.468765	-1.827089	0.537349
6	6	0	4.739946	-1.694570	1.086017
7	7	0	1.548934	-0.687526	-0.573243
8	6	0	0.433393	-1.421536	-0.269922
9	16	0	0.427456	-2.950170	0.412120
10	7	0	-0.698545	-0.730397	-0.583597
11	6	0	-2.034037	-1.173435	-0.460402
12	6	0	-2.938882	-0.331297	0.182325
13	6	0	-4.277722	-0.690139	0.277312
14	6	0	-4.700452	-1.897047	-0.261877
15	6	0	-3.798502	-2.738805	-0.911538
16	6	0	-2.466569	-2.377473	-1.019128
17	6	0	6.729545	-0.316799	1.723655
18	9	0	7.384677	-1.478439	1.852768
19	9	0	7.537379	0.525798	1.062283
20	9	0	6.593738	0.187095	2.965633
21	6	0	-6.141009	-2.299774	-0.197654
22	9	0	-6.843096	-1.557331	0.667873
23	9	0	-6.286102	-3.582874	0.170517
24	9	0	-6.747624	-2.181228	-1.392392
25	1	0	5.330647	1.573904	0.392559
26	1	0	3.072109	1.369326	-0.556949
27	1	0	2.967838	-2.780065	0.562405
28	1	0	5.211667	-2.556080	1.541963

29	1	0	1.345630	0.196825	-1.030565
30	1	0	-0.592575	0.275243	-0.703957
31	1	0	-2.589216	0.600543	0.613223
32	1	0	-4.980337	-0.038238	0.779620
33	1	0	-4.140277	-3.674067	-1.338660
34	1	0	-1.763384	-3.015161	-1.535881
35	6	0	-1.857367	6.293514	0.815815
36	6	0	-0.812381	5.388243	0.911811
37	6	0	-0.924236	4.175079	0.239500
38	6	0	-2.041636	3.850170	-0.519876
39	6	0	-3.074016	4.774301	-0.603028
40	6	0	-2.997975	6.001440	0.060291
41	1	0	-1.788046	7.242905	1.333876
42	1	0	0.074171	5.618134	1.490043
43	1	0	-2.096605	2.902802	-1.041228
44	1	0	-3.951952	4.538243	-1.192800
45	16	0	0.391293	3.018543	0.379820
46	8	0	0.268189	2.001651	-0.665706
47	8	0	1.669294	3.690790	0.484508
48	8	0	0.019673	2.344086	1.774587
49	6	0	0.932245	1.294436	2.265223
50	6	0	1.985181	1.898706	3.177586
51	6	0	0.070606	0.255584	2.957518
52	1	0	1.412988	0.841757	1.394891
53	6	0	2.866556	0.782010	3.749385
54	1	0	1.475498	2.428370	3.989754
55	1	0	2.583323	2.623732	2.622641
56	6	0	0.960861	-0.842499	3.551530
57	1	0	-0.501141	0.749642	3.750418
58	1	0	-0.641173	-0.168236	2.242886
59	6	0	2.021962	-0.259260	4.485492
60	1	0	3.619393	1.214157	4.412008
61	1	0	3.406930	0.292557	2.929143
62	1	0	0.336737	-1.571031	4.073591
63	1	0	1.457440	-1.378930	2.735274
64	1	0	2.659594	-1.058066	4.871541
65	1	0	1.534594	0.211280	5.347263
66	6	0	-4.108808	7.007864	-0.060226
67	1	0	-3.892225	7.707782	-0.871712
68	1	0	-5.058388	6.521197	-0.282389
69	1	0	-4.214139	7.586629	0.857781

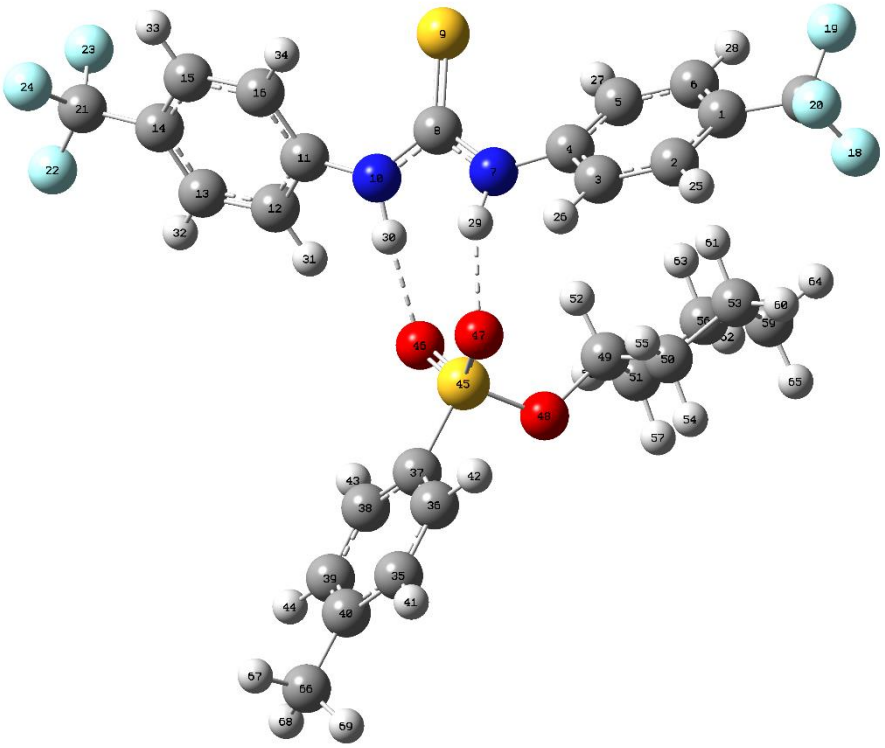

Figure S184: Output from the DFT modelling of **1**:**19** initiated with the O=S=O coordinated to the receptor through the formation of two hydrogen bonds, one to each oxygen atom. Total electronic energy (E(RM062X)): -2814.243328 Hartree. Binding mode 2 (see Table S39).

Table S39: Output from the DFT modelling of **1:19** initiated with the O=S=O coordinated to the receptor through the formation of two hydrogen bonds, one to each oxygen atom.

Center Number	Atomic Number	Atomic Type	Coordinates (Angstroms) X	Y	Z
1	6	0	5.330103	-1.411139	0.767772
2	6	0	4.990278	-0.419689	-0.145353
3	6	0	3.656226	-0.195010	-0.448875
4	6	0	2.656028	-0.954862	0.165163
5	6	0	3.001566	-1.931488	1.103825
6	6	0	4.338369	-2.161747	1.391876
7	7	0	1.324279	-0.626246	-0.145676
8	6	0	0.228924	-1.437694	-0.242881
9	16	0	0.282676	-3.113783	-0.240237
10	7	0	-0.909168	-0.698546	-0.346424
11	6	0	-2.223684	-1.138013	-0.594345
12	6	0	-3.251195	-0.508005	0.108835
13	6	0	-4.574288	-0.850366	-0.131445
14	6	0	-4.869091	-1.825646	-1.075246
15	6	0	-3.847156	-2.446762	-1.790091
16	6	0	-2.525866	-2.101595	-1.559998
17	6	0	6.758240	-1.603132	1.166079
18	9	0	7.072781	-0.878207	2.257843
19	9	0	7.034132	-2.879917	1.470149
20	9	0	7.612193	-1.228933	0.203137
21	6	0	-6.283208	-2.248993	-1.319571
22	9	0	-7.172238	-1.373352	-0.832032
23	9	0	-6.558054	-3.436607	-0.750040

24	9	0	-6.545381	-2.392781	-2.628987
25	1	0	5.761414	0.171096	-0.623715
26	1	0	3.379198	0.572657	-1.162085
27	1	0	2.233208	-2.499713	1.605380
28	1	0	4.607388	-2.920549	2.116597
29	1	0	1.213077	0.323142	-0.496933
30	1	0	-0.846660	0.262194	-0.010202
31	1	0	-3.006581	0.250035	0.843867
32	1	0	-5.368978	-0.360267	0.415867
33	1	0	-4.085706	-3.188918	-2.542527
34	1	0	-1.733983	-2.563048	-2.130954
35	6	0	0.298931	6.514845	-1.171984
36	6	0	0.744036	5.256171	-0.801174
37	6	0	-0.111672	4.445785	-0.061294
38	6	0	-1.384277	4.856727	0.314987
39	6	0	-1.807008	6.121827	-0.069242
40	6	0	-0.976967	6.963807	-0.813111
41	1	0	0.949874	7.160526	-1.749904
42	1	0	1.727984	4.903765	-1.085302
43	1	0	-2.026735	4.199033	0.886784
44	1	0	-2.797083	6.459519	0.213505
45	16	0	0.449255	2.858166	0.432615
46	8	0	-0.680524	2.005041	0.783934
47	8	0	1.380820	2.306338	-0.545129
48	8	0	1.246126	3.227989	1.750936
49	6	0	2.033632	2.144630	2.375893
50	6	0	3.502092	2.394020	2.090166
51	6	0	1.707678	2.159981	3.856440
52	1	0	1.717128	1.190345	1.937136
53	6	0	4.349336	1.351114	2.825325
54	1	0	3.752498	3.400681	2.441989
55	1	0	3.678155	2.356496	1.012506
56	6	0	2.566870	1.121201	4.586021
57	1	0	1.921353	3.161247	4.245329
58	1	0	0.642635	1.964429	3.997940
59	6	0	4.056501	1.359535	4.326830
60	1	0	5.408820	1.531313	2.631049
61	1	0	4.118213	0.358508	2.425186
62	1	0	2.348480	1.154832	5.655155
63	1	0	2.296543	0.118372	4.234496
64	1	0	4.652572	0.593911	4.829029
65	1	0	4.347969	2.327057	4.751332
66	6	0	-1.453174	8.321475	-1.250354
67	1	0	-1.824196	8.274345	-2.277635
68	1	0	-2.264124	8.678236	-0.615864
69	1	0	-0.639510	9.047130	-1.225596

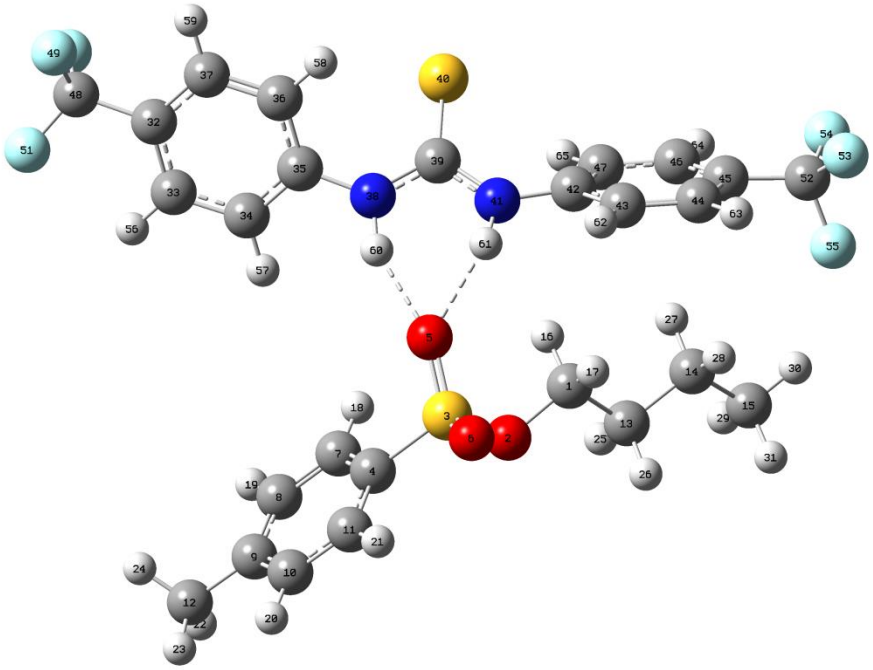

Figure S185: Output from the DFT modelling of **1**:**20** initiated with the S=O coordinated to the receptor through the formation of two hydrogen bonds. Total electronic energy (E(RM062X)): -2736.820519 Hartree. Binding mode 1 (see Table S40).

Table S40: Output from the DFT modelling of **1:20** initiated with the S=O coordinated to the receptor through the formation of two hydrogen bonds.

Center Number	Atomic Number	Atomic Type	Coordinates (Angstroms) X	Y	Z
1	6	0	-1.657252	0.753602	4.165715
2	8	0	-0.679808	0.109686	5.037747
3	16	0	-0.033967	-1.250056	4.507392
4	6	0	1.421335	-1.303039	5.490394
5	8	0	0.318988	-1.048246	3.102686
6	8	0	-0.903506	-2.361547	4.819549
7	6	0	2.424625	-0.365449	5.253190
8	6	0	3.573149	-0.422416	6.022426
9	6	0	3.729908	-1.399247	7.015385
10	6	0	2.704983	-2.321584	7.223475
11	6	0	1.540131	-2.282448	6.464934
12	6	0	4.992940	-1.443369	7.830389
13	6	0	-2.305914	1.868437	4.951394
14	6	0	-3.329026	2.605897	4.086635
15	6	0	-3.943282	3.795369	4.819020
16	1	0	-1.121121	1.142196	3.297846
17	1	0	-2.393451	0.010525	3.845740
18	1	0	2.305494	0.389288	4.484852
19	1	0	4.364496	0.299068	5.853949
20	1	0	2.814959	-3.081558	7.987831
21	1	0	0.742343	-2.997123	6.622120
22	1	0	5.174639	-0.478199	8.307420
23	1	0	4.939374	-2.209224	8.603154
24	1	0	5.850847	-1.658485	7.189209
25	1	0	-1.530237	2.562439	5.288265
26	1	0	-2.789223	1.452768	5.839707

27	1	0	-2.845498	2.947430	3.164715
28	1	0	-4.118033	1.911250	3.781014
29	1	0	-3.172610	4.517071	5.100809
30	1	0	-4.673847	4.305647	4.190183
31	1	0	-4.448308	3.470299	5.732076
32	6	0	5.439508	-1.090094	-0.859790
33	6	0	5.269863	-0.682989	0.456967
34	6	0	3.998437	-0.370330	0.919206
35	6	0	2.899991	-0.470388	0.067216
36	6	0	3.072382	-0.902170	-1.249582
37	6	0	4.342944	-1.201713	-1.711809
38	7	0	1.619416	-0.203449	0.599791
39	6	0	0.621234	0.530721	0.038758
40	16	0	0.783511	1.425658	-1.374954
41	7	0	-0.527888	0.442983	0.763539
42	6	0	-1.728200	1.169141	0.628641
43	6	0	-2.919824	0.482512	0.877164
44	6	0	-4.130172	1.157107	0.859789
45	6	0	-4.153223	2.519623	0.582793
46	6	0	-2.971180	3.207241	0.330388
47	6	0	-1.755643	2.538687	0.360246
48	6	0	6.808936	-1.375047	-1.392812
49	9	0	6.811803	-2.412961	-2.243844
50	9	0	7.310682	-0.328317	-2.072849
51	9	0	7.687025	-1.656928	-0.420524
52	6	0	-5.452484	3.256640	0.654100
53	9	0	-6.477586	2.524736	0.193265
54	9	0	-5.432670	4.399998	-0.042976
55	9	0	-5.766205	3.586788	1.923287
56	1	0	6.121805	-0.607072	1.120246
57	1	0	3.856030	-0.044286	1.942330
58	1	0	2.214350	-1.012676	-1.896718
59	1	0	4.479808	-1.543437	-2.730473
60	1	0	1.469070	-0.516935	1.556067
61	1	0	-0.544729	-0.279977	1.479093
62	1	0	-2.890775	-0.581730	1.080999
63	1	0	-5.051846	0.622755	1.055274
64	1	0	-2.994239	4.270634	0.127608
65	1	0	-0.834639	3.076105	0.191161

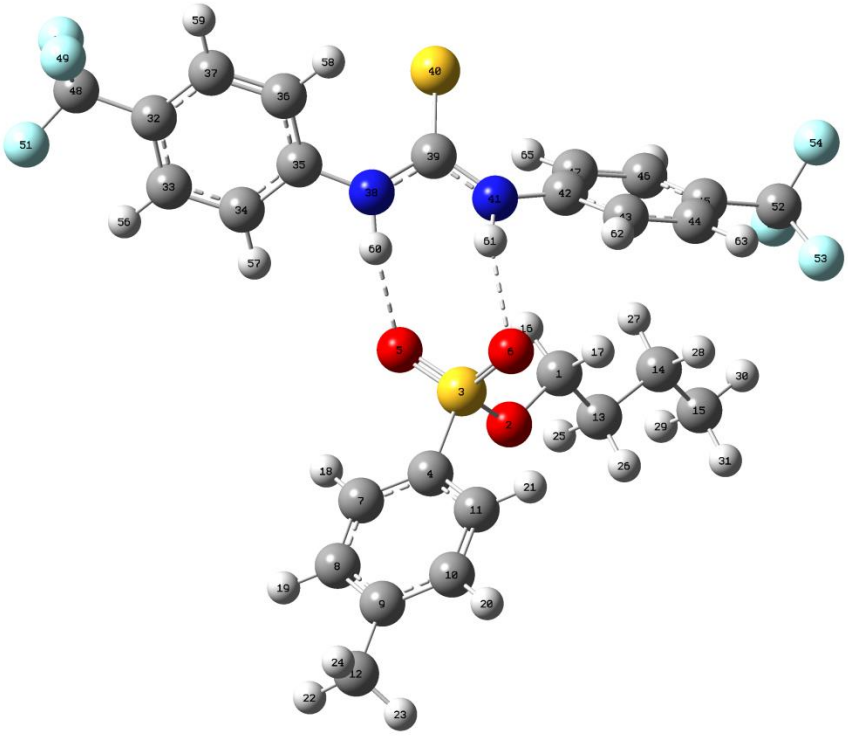

Figure S186: Output from the DFT modelling of **1**:**20** initiated with the O=S=O coordinated to the receptor through the formation of two hydrogen bonds, one to each oxygen atom. Total electronic energy (E(RM062X)): -2736.821915 Hartree. Binding mode 2 (see Table S41).

Table S41: Output from the DFT modelling of **1:20** initiated with the O=S=O coordinated to the receptor through the formation of two hydrogen bonds, one to each oxygen atom.

Center Number	Atomic Number	Atomic Type	Coordinates (Angstroms) X	Y	Z
1	6	0	-1.721592	1.759875	3.637641
2	8	0	-0.880823	1.016306	4.576316
3	16	0	-0.109933	-0.249629	3.995356
4	6	0	0.376090	-1.032806	5.489566
5	8	0	1.063398	0.200137	3.257688
6	8	0	-1.059270	-1.073763	3.259135
7	6	0	1.647042	-0.792641	5.995174
8	6	0	2.009303	-1.409575	7.185459
9	6	0	1.121271	-2.249212	7.860766
10	6	0	-0.151703	-2.466247	7.320259
11	6	0	-0.536608	-1.862583	6.134625
12	6	0	1.526624	-2.935657	9.135841
13	6	0	-2.366194	2.889012	4.408190
14	6	0	-3.381932	3.622030	3.531082
15	6	0	-4.033432	4.794411	4.257858
16	1	0	-1.089508	2.129049	2.825574
17	1	0	-2.469545	1.072374	3.237793
18	1	0	2.335257	-0.145684	5.465988
19	1	0	2.997442	-1.235484	7.594564
20	1	0	-0.847203	-3.117575	7.836792
21	1	0	-1.517856	-2.036090	5.710341
22	1	0	2.400609	-2.460397	9.580177
23	1	0	0.711130	-2.922309	9.860239

24	1	0	1.773495	-3.981605	8.936050
25	1	0	-1.595339	3.581280	4.757631
26	1	0	-2.866084	2.475008	5.288711
27	1	0	-2.890199	3.978177	2.619910
28	1	0	-4.152961	2.913779	3.210126
29	1	0	-3.285406	5.534133	4.552937
30	1	0	-4.766731	5.289384	3.618882
31	1	0	-4.545469	4.454793	5.161525
32	6	0	5.478874	-1.112665	-0.871789
33	6	0	5.233644	-0.525837	0.362729
34	6	0	3.924911	-0.295061	0.763356
35	6	0	2.864047	-0.653312	-0.067931
36	6	0	3.114031	-1.262777	-1.299841
37	6	0	4.421071	-1.482687	-1.700135
38	7	0	1.557577	-0.451220	0.416622
39	6	0	0.479509	0.039751	-0.256281
40	16	0	0.524104	0.685064	-1.803219
41	7	0	-0.652257	-0.070144	0.496080
42	6	0	-1.871677	0.619969	0.375191
43	6	0	-3.027884	-0.042293	0.792817
44	6	0	-4.236492	0.636529	0.851645
45	6	0	-4.291192	1.975613	0.482925
46	6	0	-3.146312	2.630853	0.037437
47	6	0	-1.935068	1.961014	-0.011961
48	6	0	6.880470	-1.328300	-1.349253
49	9	0	7.034188	-2.529979	-1.928928
50	9	0	7.243131	-0.418228	-2.271526
51	9	0	7.777715	-1.249849	-0.357400
52	6	0	-5.584900	2.724057	0.557630
53	9	0	-6.408372	2.214816	1.486606
54	9	0	-6.258537	2.705434	-0.604792
55	9	0	-5.396353	4.018102	0.866568
56	1	0	6.055586	-0.247394	1.009389
57	1	0	3.719109	0.166626	1.722189
58	1	0	2.290206	-1.570307	-1.927439
59	1	0	4.619430	-1.960990	-2.651798
60	1	0	1.476161	-0.427752	1.432150
61	1	0	-0.630737	-0.734797	1.265193
62	1	0	-2.966330	-1.079152	1.100932
63	1	0	-5.126491	0.128200	1.200662
64	1	0	-3.192154	3.678473	-0.234163
65	1	0	-1.037594	2.481036	-0.313916

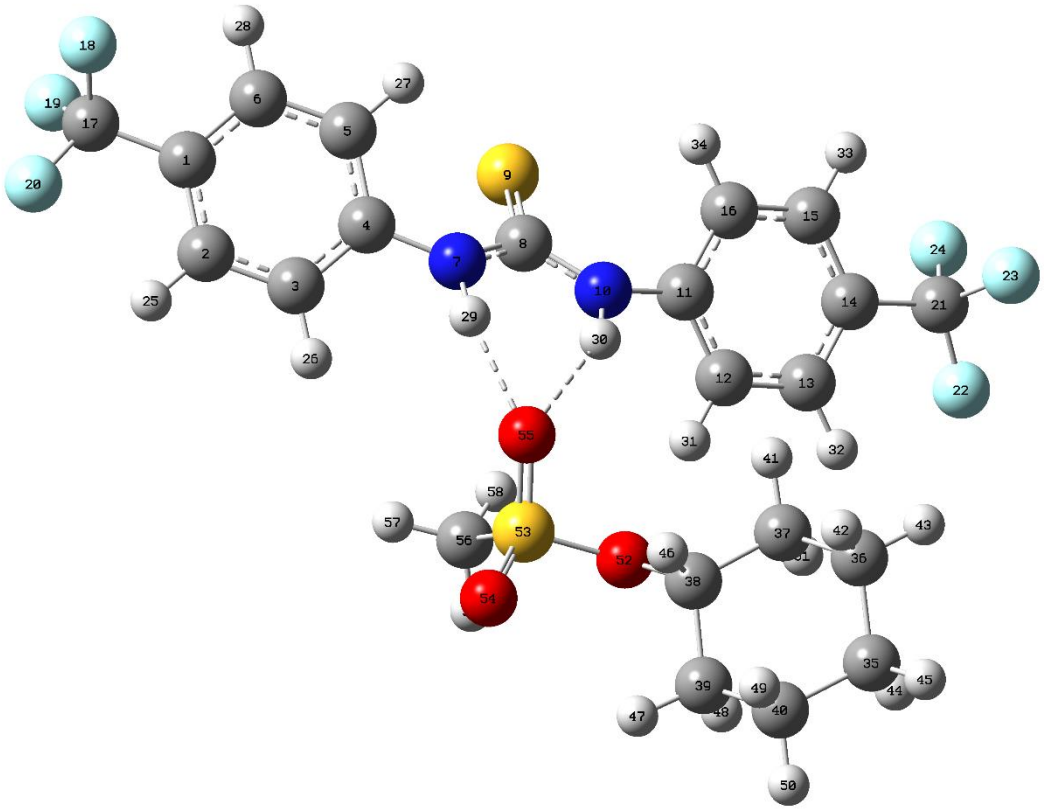

Figure S187: Output from the DFT modelling of **1**:**25** initiated with the S=O coordinated to the receptor through the formation of two hydrogen bonds. Total electronic energy (E(RM062X)): -2583.227849 Hartree. Binding mode 1 (see Table S42).

Table S42: Output from the DFT modelling of **1:25** initiated with the S=O coordinated to the receptor through the formation of two hydrogen bonds.

Center Number	Atomic Number	Atomic Type	Coordinates (Angstroms) X	Y	Z
1	6	0	4.587660	4.474057	-1.742846
2	6	0	4.302453	4.660770	-0.396992
3	6	0	3.079903	4.239788	0.107943
4	6	0	2.145205	3.630734	-0.728952
5	6	0	2.446451	3.423094	-2.077502
6	6	0	3.662855	3.853408	-2.580179
7	7	0	0.950919	3.164861	-0.141944
8	6	0	-0.318972	3.249992	-0.623846
9	16	0	-0.743561	4.035856	-2.049751
10	7	0	-1.215836	2.667057	0.216755
11	6	0	-2.622026	2.612753	0.077108
12	6	0	-3.403123	2.967691	1.174508
13	6	0	-4.787354	2.867150	1.106829
14	6	0	-5.383706	2.423209	-0.064904
15	6	0	-4.605010	2.059009	-1.162324
16	6	0	-3.224894	2.144392	-1.092101
17	6	0	5.879381	4.954312	-2.326124
18	9	0	6.445222	4.030047	-3.119881
19	9	0	5.709847	6.049477	-3.088706
20	9	0	6.779408	5.273251	-1.386735
21	6	0	-6.871241	2.285162	-0.162984

22	9	0	-7.509969	2.871556	0.857509
23	9	0	-7.254829	0.996076	-0.172814
24	9	0	-7.350293	2.826829	-1.294622
25	1	0	5.024879	5.132846	0.255928
26	1	0	2.846509	4.382265	1.156407
27	1	0	1.738458	2.918567	-2.717821
28	1	0	3.901962	3.687757	-3.623917
29	1	0	1.040053	2.883142	0.831670
30	1	0	-0.861616	2.385574	1.127693
31	1	0	-2.927788	3.319217	2.083194
32	1	0	-5.393686	3.145078	1.959269
33	1	0	-5.077882	1.700276	-2.068888
34	1	0	-2.612344	1.843884	-1.929773
35	6	0	-3.619825	0.426064	6.559241
36	6	0	-3.344276	0.062633	5.098391
37	6	0	-2.931048	1.296664	4.288604
38	6	0	-1.735915	1.963522	4.941577
39	6	0	-1.990174	2.345633	6.387930
40	6	0	-2.403620	1.107533	7.190382
41	1	0	-2.684605	1.025398	3.259314
42	1	0	-2.541194	-0.681818	5.056031
43	1	0	-4.224858	-0.392181	4.640609
44	1	0	-4.478771	1.105183	6.606417
45	1	0	-3.886144	-0.469645	7.124851
46	1	0	-0.859390	1.311198	4.866674
47	1	0	-1.094477	2.808208	6.806952
48	1	0	-2.795368	3.087938	6.406307
49	1	0	-1.567356	0.399897	7.222224
50	1	0	-2.615432	1.396590	8.221634
51	1	0	-3.756830	2.016679	4.257802
52	8	0	-1.457713	3.196469	4.177205
53	16	0	0.063437	3.495669	3.822765
54	8	0	0.885927	3.394005	5.008471
55	8	0	0.434227	2.644726	2.691223
56	6	0	-0.093749	5.172727	3.291595
57	1	0	0.906328	5.503712	3.016446
58	1	0	-0.764433	5.206088	2.435497
59	1	0	-0.479964	5.751942	4.126845

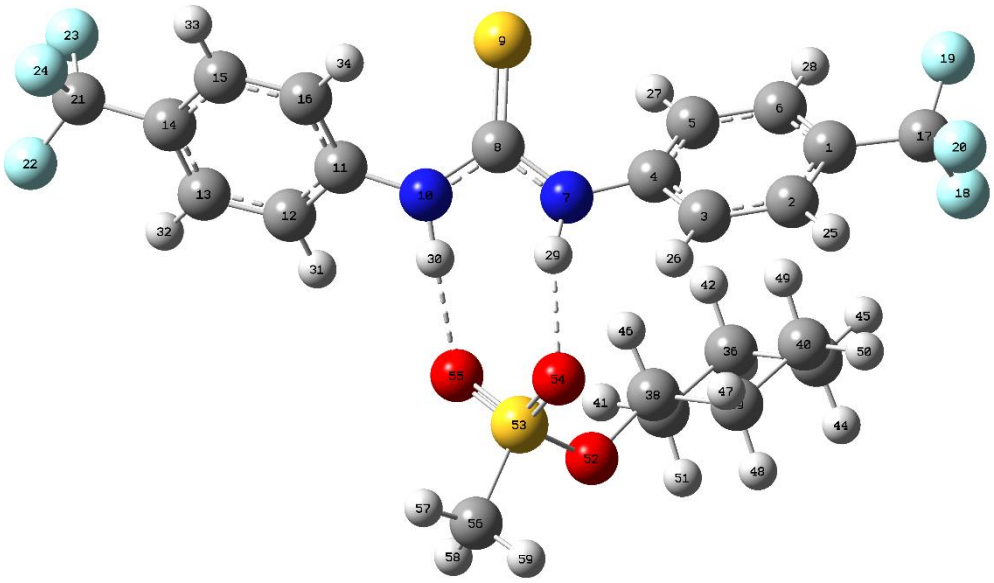

Figure S188: Output from the DFT modelling of **1**:**25** initiated with the O=S=O coordinated to the receptor through the formation of two hydrogen bonds, one to each oxygen atom. Total electronic energy (E(RM062X)): -2583.235441 Hartree. Binding mode 2 (see Table S43).

Table S43: Output from the DFT modelling of **1:25** initiated with the O=S=O coordinated to the receptor through the formation of two hydrogen bonds, one to each oxygen atom.

Center Number	Atomic Number	Atomic Type	Coordinates (Angstroms) X	Y	Z
1	6	0	3.558243	1.463774	0.179305
2	6	0	3.358702	2.805926	0.481451
3	6	0	2.076604	3.332917	0.447012
4	6	0	0.988968	2.518230	0.119117
5	6	0	1.191969	1.163618	-0.159082
6	6	0	2.478077	0.645608	-0.137693
7	7	0	-0.288458	3.104572	0.170438
8	6	0	-1.380546	2.868926	-0.615901
9	16	0	-1.358634	1.960388	-2.025876
10	7	0	-2.484211	3.476423	-0.101272
11	6	0	-3.768696	3.593219	-0.665377
12	6	0	-4.858505	3.465476	0.197708
13	6	0	-6.150194	3.630746	-0.279805
14	6	0	-6.353004	3.922726	-1.623224
15	6	0	-5.268132	4.064470	-2.484713
16	6	0	-3.975754	3.909469	-2.010019
17	6	0	4.923169	0.866286	0.302163
18	9	0	5.135433	0.359398	1.532990
19	9	0	5.116232	-0.143251	-0.559100
20	9	0	5.895420	1.764004	0.089121
21	6	0	-7.741126	4.048612	-2.167417
22	9	0	-8.635969	4.353512	-1.216975
23	9	0	-8.163921	2.906507	-2.739705
24	9	0	-7.827735	4.997261	-3.113207
25	1	0	4.198672	3.439945	0.736660
26	1	0	1.907723	4.378810	0.676128
27	1	0	0.352126	0.523537	-0.383546
28	1	0	2.637592	-0.403540	-0.354701

29	1	0	-0.337835	3.920638	0.778315
30	1	0	-2.442317	3.705972	0.891768
31	1	0	-4.685723	3.236887	1.243038
32	1	0	-6.993238	3.532213	0.391955
33	1	0	-5.431932	4.316654	-3.525293
34	1	0	-3.132309	4.045706	-2.670302
35	6	0	2.019478	0.240383	4.411682
36	6	0	0.508435	0.014119	4.319666
37	6	0	-0.263931	1.268225	4.744341
38	6	0	0.182003	2.452014	3.908796
39	6	0	1.674865	2.707097	3.994394
40	6	0	2.434030	1.447191	3.568213
41	1	0	-1.341135	1.128001	4.632955
42	1	0	0.245240	-0.238891	3.285737
43	1	0	0.203161	-0.828840	4.942616
44	1	0	2.297597	0.411623	5.457903
45	1	0	2.554142	-0.651809	4.077242
46	1	0	-0.121613	2.303313	2.865092
47	1	0	1.939023	3.559212	3.363894
48	1	0	1.918150	2.961999	5.031547
49	1	0	2.212947	1.236610	2.516789
50	1	0	3.509878	1.622538	3.635593
51	1	0	-0.060235	1.493916	5.796493
52	8	0	-0.527085	3.636613	4.433187
53	16	0	-1.174255	4.610576	3.367699
54	8	0	-0.161029	5.027238	2.404203
55	8	0	-2.355887	3.979113	2.789307
56	6	0	-1.631845	5.939538	4.430520
57	1	0	-2.121118	6.681432	3.802131
58	1	0	-2.314740	5.546956	5.180311
59	1	0	-0.724668	6.337170	4.878998

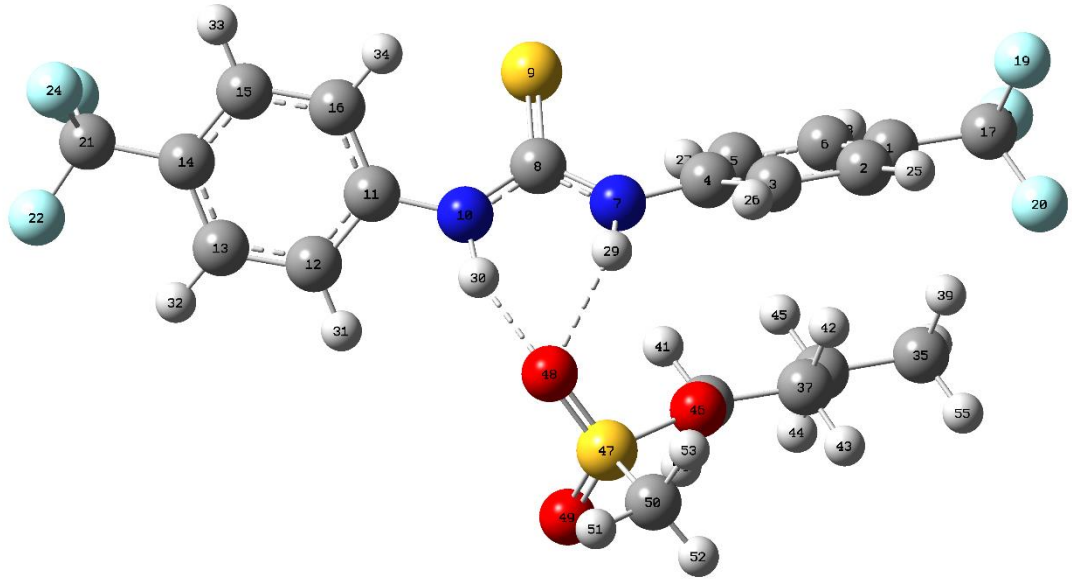

Figure S189: Output from the DFT modelling of **1**:**26** initiated with the S=O coordinated to the receptor through the formation of two hydrogen bonds. Total electronic energy (E(RM062X)): -2505.815519 Hartree. Binding mode 1 (see Table S44).

Table S44: Output from the DFT modelling of **1:26** initiated with the O=S=O coordinated to the receptor through the formation of two hydrogen bonds.

Center Number	Atomic Number	Atomic Type	Coordinates (Angstroms) X	Y	Z
1	6	0	4.112487	2.182030	0.312863
2	6	0	3.937873	3.453413	0.854444
3	6	0	2.658344	3.933747	1.076707
4	6	0	1.547390	3.145322	0.761444
5	6	0	1.727775	1.868005	0.230925
6	6	0	3.012239	1.393169	0.000615
7	7	0	0.276275	3.654541	1.091767
8	6	0	-0.898696	3.545260	0.407731
9	16	0	-1.036290	2.908166	-1.141076
10	7	0	-1.941839	4.019219	1.137788
11	6	0	-3.285723	4.169354	0.731538
12	6	0	-4.282737	3.754108	1.612142
13	6	0	-5.620452	3.936290	1.286664
14	6	0	-5.955986	4.529721	0.077181
15	6	0	-4.961871	4.956459	-0.801186
16	6	0	-3.627286	4.786373	-0.473923
17	6	0	5.506660	1.680456	0.102008
18	9	0	5.536101	0.433443	-0.385584
19	9	0	6.200768	2.454164	-0.747484
20	9	0	6.205178	1.665862	1.252651
21	6	0	-7.389948	4.691152	-0.320693
22	9	0	-8.227002	4.567418	0.717695
23	9	0	-7.764101	3.773954	-1.230942
24	9	0	-7.624151	5.889955	-0.878665
25	1	0	4.796864	4.065660	1.102395
26	1	0	2.510660	4.921820	1.495936
27	1	0	0.872508	1.245037	0.013499
28	1	0	3.152446	0.398035	-0.402452

29	1	0	0.252057	4.239622	1.922324
30	1	0	-1.764293	4.171067	2.129098
31	1	0	-4.007584	3.284754	2.549108
32	1	0	-6.394018	3.613955	1.971441
33	1	0	-5.231715	5.440499	-1.732056
34	1	0	-2.851047	5.138556	-1.137638
35	6	0	3.862396	-0.882332	2.800719
36	6	0	1.060493	1.604317	3.760383
37	6	0	2.463817	1.084878	3.544984
38	6	0	2.449193	-0.356507	3.038015
39	1	0	4.388789	-0.263039	2.070072
40	1	0	3.847265	-1.906988	2.425883
41	1	0	0.463473	1.561611	2.845640
42	1	0	2.978252	1.725644	2.823397
43	1	0	3.012355	1.145683	4.489504
44	1	0	1.932936	-0.995003	3.761747
45	1	0	1.875118	-0.406813	2.107036
46	8	0	1.190393	3.007361	4.151181
47	16	0	-0.065175	3.753547	4.796492
48	8	0	-0.721313	4.518862	3.738860
49	8	0	-0.874447	2.809709	5.535763
50	6	0	0.779663	4.868415	5.872342
51	1	0	0.017054	5.496676	6.328891
52	1	0	1.306234	4.278766	6.618725
53	1	0	1.465170	5.459518	5.269451
54	1	0	0.546643	1.068642	4.559490
55	1	0	4.441939	-0.868157	3.726996

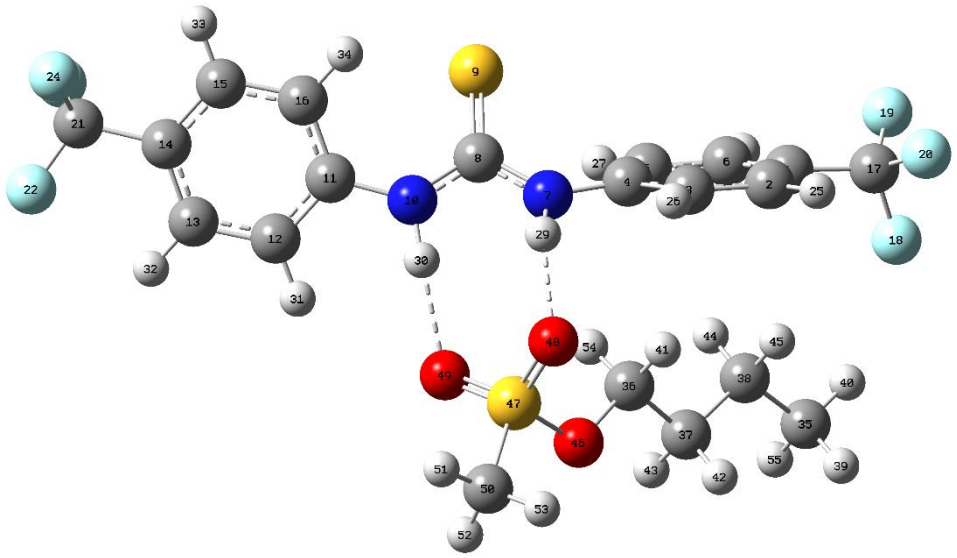

Figure S190: Output from the DFT modelling of **1**:**26** initiated with the O=S=O coordinated to the receptor through the formation of two hydrogen bonds, one to each oxygen atom. Total electronic energy (E(RM062X)): -2505.814231 Hartree. Binding mode 2 (see Table S45).

Table S45: Output from the DFT modelling of **1:26** initiated with the O=S=O coordinated to the receptor through the formation of two hydrogen bonds, one to each oxygen atom.

Center Number	Atomic Number	Atomic Type	Coordinates (Angstroms) X	Y	Z
1	6	0	4.054197	2.119673	0.307702
2	6	0	3.922147	3.298130	1.031698
3	6	0	2.664335	3.859456	1.204170
4	6	0	1.537315	3.235057	0.666524
5	6	0	1.674624	2.044615	-0.052522
6	6	0	2.933437	1.497194	-0.236073
7	7	0	0.278816	3.782345	0.977501
8	6	0	-0.839920	3.851050	0.197087
9	16	0	-0.850535	3.596670	-1.460241
10	7	0	-1.934690	4.156486	0.946508
11	6	0	-3.240153	4.449886	0.509137
12	6	0	-4.297596	3.924223	1.252494
13	6	0	-5.608307	4.224588	0.910232
14	6	0	-5.860663	5.050380	-0.177834
15	6	0	-4.807219	5.588072	-0.914200
16	6	0	-3.497269	5.298187	-0.570732
17	6	0	5.387137	1.453823	0.177197
18	9	0	5.531931	0.451138	1.067317
19	9	0	5.562515	0.905593	-1.034491
20	9	0	6.405750	2.298234	0.384398
21	6	0	-7.265272	5.349204	-0.597925
22	9	0	-8.155994	5.084018	0.367237
23	9	0	-7.633901	4.627320	-1.671919
24	9	0	-7.424048	6.637908	-0.940974
25	1	0	4.793673	3.780712	1.455234
26	1	0	2.547872	4.778824	1.766232
27	1	0	0.800964	1.546567	-0.447101
28	1	0	3.041337	0.571283	-0.788366

29	1	0	0.242973	4.269447	1.871089
30	1	0	-1.869202	3.914869	1.934988
31	1	0	-4.085316	3.279709	2.097806
32	1	0	-6.426724	3.815672	1.488443
33	1	0	-5.010761	6.250604	-1.746861
34	1	0	-2.678307	5.733140	-1.124325
35	6	0	3.553361	-1.376263	3.389512
36	6	0	1.125288	1.613273	3.625251
37	6	0	1.826875	0.353477	4.072411
38	6	0	2.778895	-0.128351	2.977104
39	1	0	4.144818	-1.185991	4.288514
40	1	0	4.235056	-1.690673	2.597536
41	1	0	1.843674	2.397362	3.379271
42	1	0	2.387142	0.566197	4.987572
43	1	0	1.087973	-0.418329	4.303932
44	1	0	2.210348	-0.329817	2.063286
45	1	0	3.481084	0.674908	2.731952
46	8	0	0.306187	2.090068	4.738625
47	16	0	-0.528038	3.415317	4.464299
48	8	0	0.350154	4.419870	3.877793
49	8	0	-1.714708	3.086575	3.683509
50	6	0	-0.965605	3.831514	6.119339
51	1	0	-1.581342	4.726907	6.057088
52	1	0	-1.526033	2.997885	6.536120
53	1	0	-0.048448	4.019049	6.672093
54	1	0	0.470178	1.431113	2.768197
55	1	0	2.873984	-2.205087	3.602839

Exhaustive parameter search

R Studio was used to compile all possible parameter combinations for of both two (models 1-10) and three (models 11–20) parameter combinations. The top 10 models for both parameters combinations are shown in Figures S191 – S210. Where K_{ass} < 10, these data were excluded from this exhaustive parameter search as these values were defined to be beyond the limitations of our experimental ^{1}H NMR titration methodology.

Table S46: Table of all the parameters used within this study. [a] SWF is determined by the area that is within 1/8th of the E_{min}, [b] SAF is determined by the area that is within 1/8th of the E_{max} at the electrophilic centre, [c] The positive surface area is the area within 1/8th of the E_{max} across the whole molecule.

Parameter	Parameter description	Parameter definition
P0	Association constant (M^{-1})	Association constant derived using a 1:1 binding isotherm.
P1	E_{min} (kJ/mol)	Electrostatic surface energy minimum
P2	E_{max} (kJ/mol)	Electrostatic surface energy maximum
P3	Molecular Volume ($Å^3$)	Total volume the molecule occupies
P4	Molecular Area ($Å^2$)	Total molecular area of the molecule.
P5	Solvent accessible area ($Å^2$)	Area accessible with a 1.4 Å radius probe.
P6	Polar surface area ($Å^2$)	The area due to nitrogen and oxygen and any attached hydrogens.
P7	% Polar surface area ($Å^2$)	The percentage polar surface area of the total surface area.
P8	Polarizability	How easily an electron cloud is distorted by an electric field
P9	Steric weighting factor (SWF) ($Å^2$)	Area within 1/8th of the E_{min}
P10	Steric accessibility factor (SAF) ($Å^2$)	Area within 1/8th of the E_{max}
P11	HOMO (eV)	Highest occupied molecular orbital
P12	LUMO (eV)	Lowest unoccupied molecular orbital
P13	Energy (kJ)	Total energy
P14	Electrostatic charge	The electrostatic charge of the HBA oxygen atom of the simulant.
P15	Additive N..O Bond length (Å)	The N..O bond lengths from both N atoms of the receptor added together.
P16	Log P	Octanol water partition coefficient
P17	Dipole moment (D)	Separation of charge across the molecule.
P18	Additive NH..O bond length	Sum of both NH..O bond lengths between receptor and simulant.
P19	Additive angle difference from 180°	Sum of the N.H..O angles difference from 180° between receptor and simulant.

Two Parameter Fits

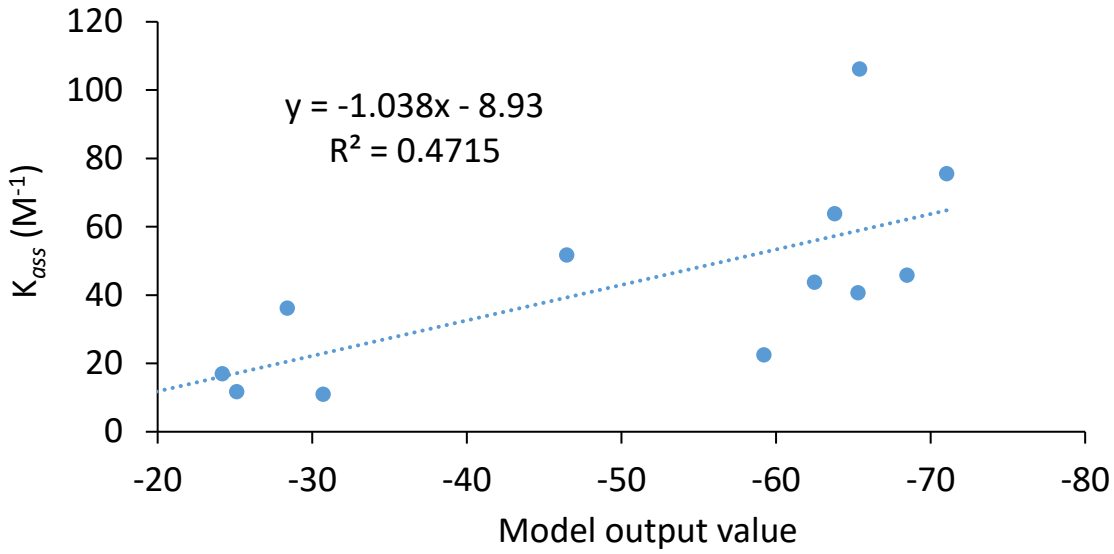

Figure S191: Model 1 vs K_{ass}. Model: P0 = P10 * P11. Linear trend line: R^2 = 0.4715, intercept = -8.9333 and slope = -1.0380.

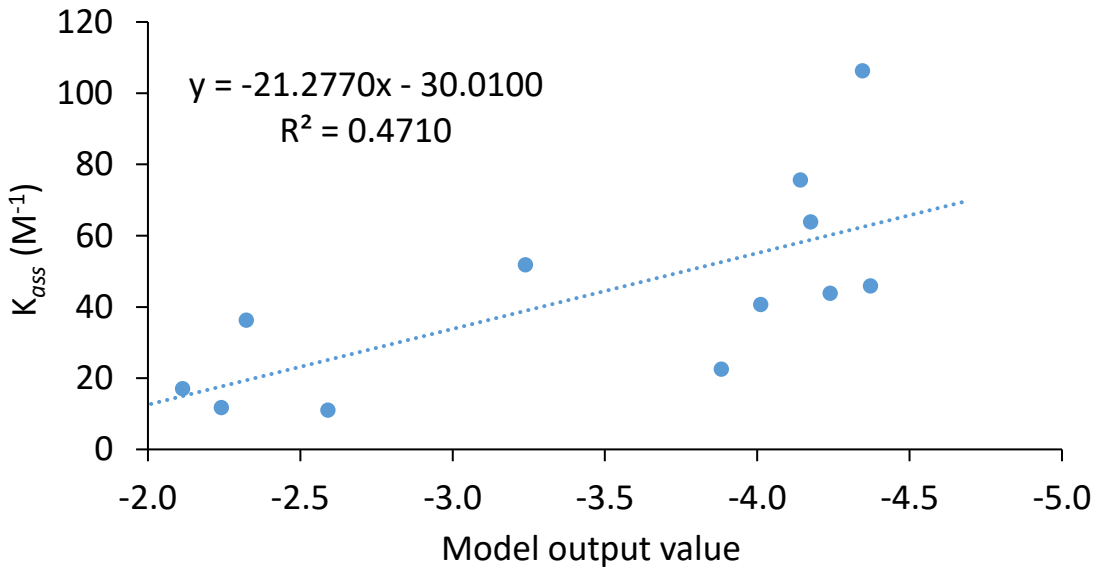

Figure S192: Model 2 vs K_{ass}. Model: P0 = P10 * P14. Linear trend line: R^2 = 0.4710, intercept = -30.0112 and slope = -21.2774.

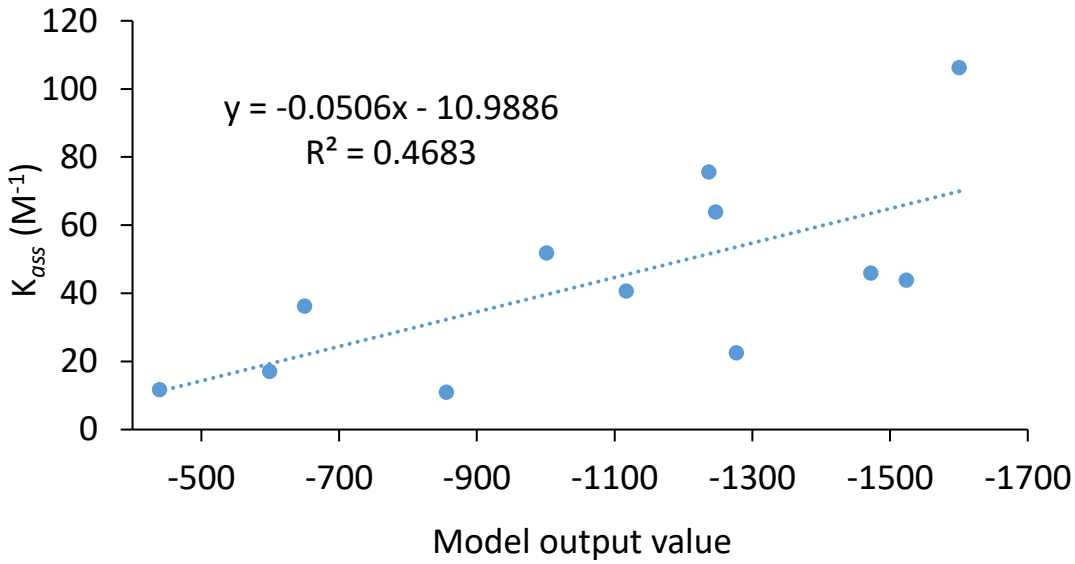

Figure S193: Model 3 vs K_{ass}. Model: P0 = P1 * P10. Linear trend line: R^2 = 0.4683, intercept = -10.9886 and slope = -0.0506.

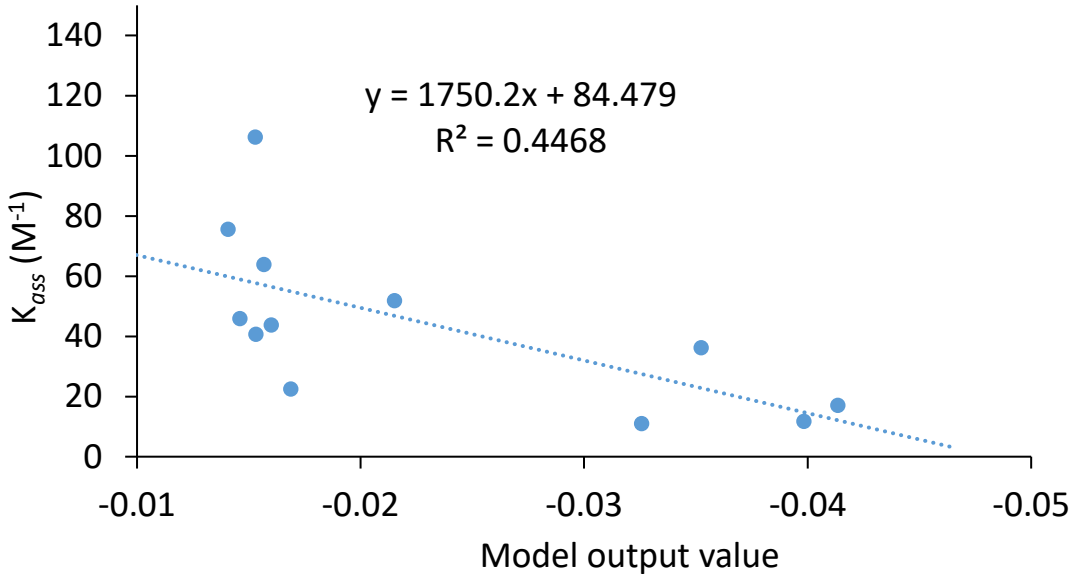

Figure S194: Model 4 vs K_{ass}. Model: P0 = $(P11 * P10)^{-1}$. Linear trend line: R^2 = 0.4468, intercept = 84.4793 and slope = 1750.1617

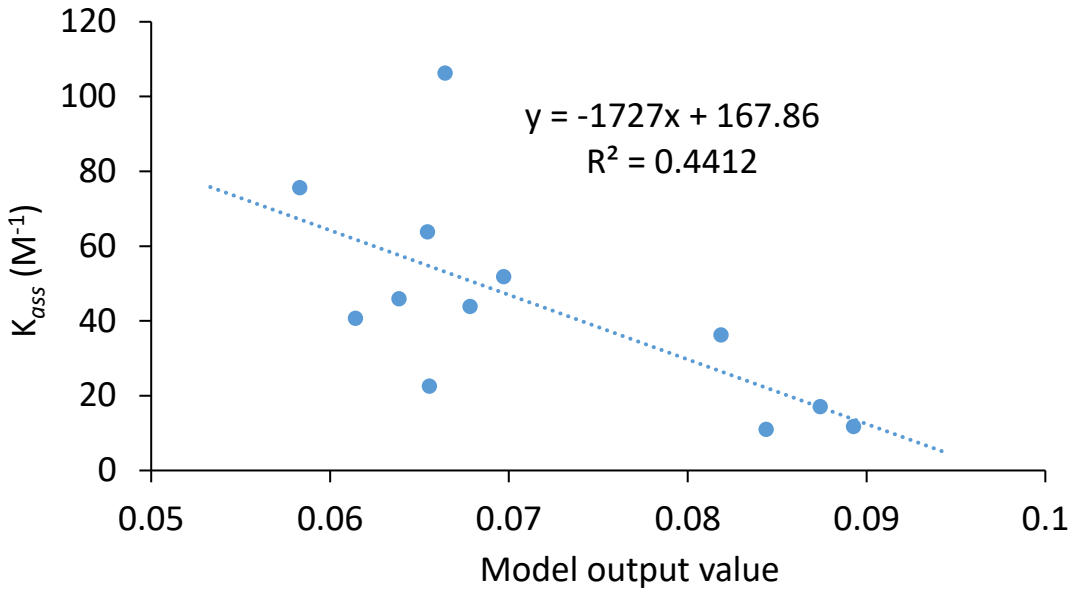

Figure S195: Model 5 vs K_{ass}. Model: P0 = P14 * $(P11)^{-1}$. Linear trend line: R^2 = 0.4412, intercept = 167.8598 and slope = -1726.9849.

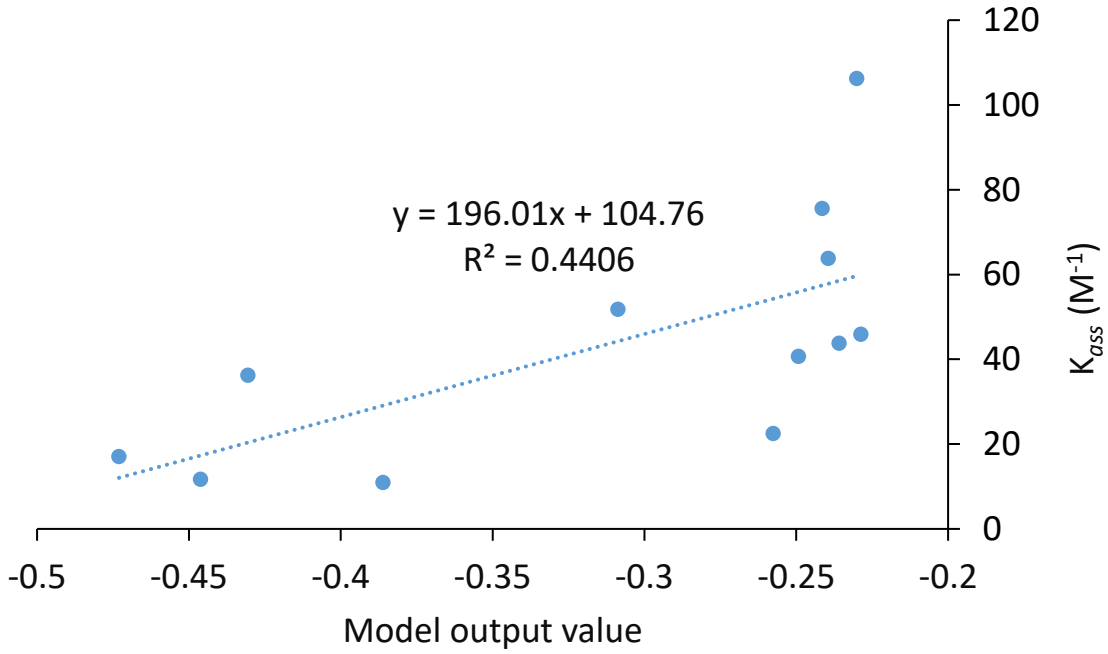

Figure S196: Model 6 vs K_{ass}. Model: P0 = $(P14 * P10)^{-1}$. Linear trend line: R^2 = 0.4406, intercept = 104.7600 and slope = 196.0087.

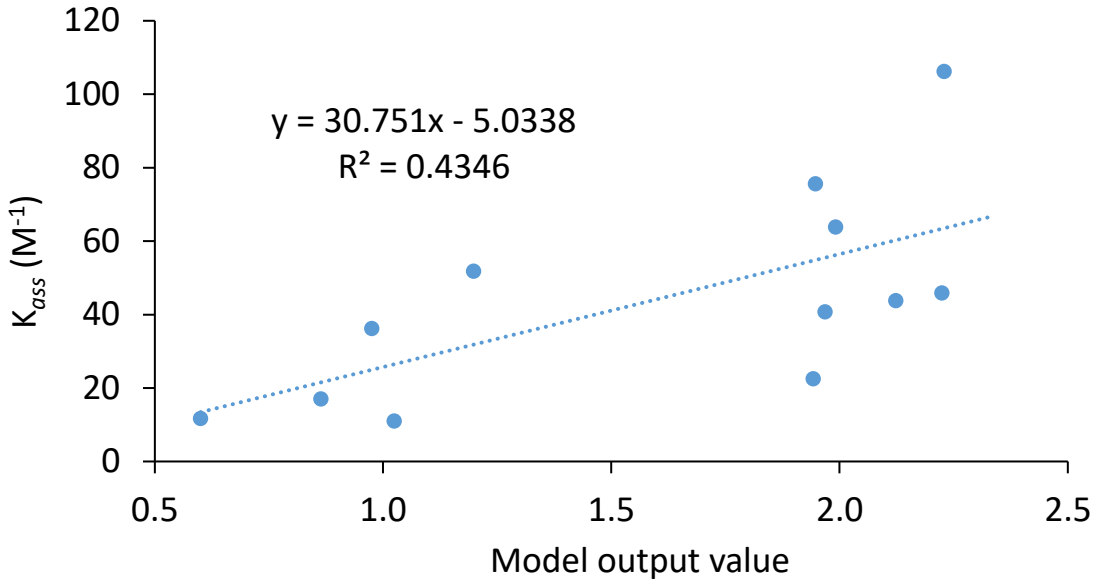

Figure S197: Model 7 vs K_{ass}. Model: P0 = P10 * $(P18)^{-1}$. Linear trend line: R^2 = 0.4346, intercept = -5.0338 and slope = 30.7510.

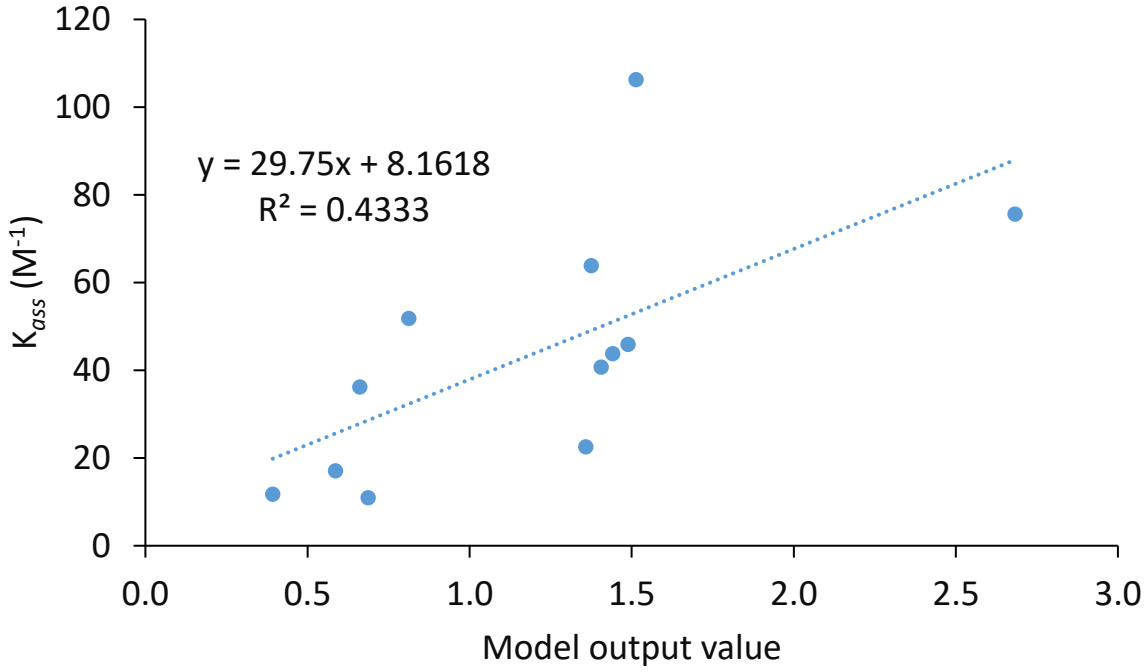

Figure S198: Model 8 vs K_{ass}. Model: P0 = P10 * $(P15)^{-1}$. Linear trend line: R^2 = 0.4333, intercept = 8.1618 and slope = 29.7500.

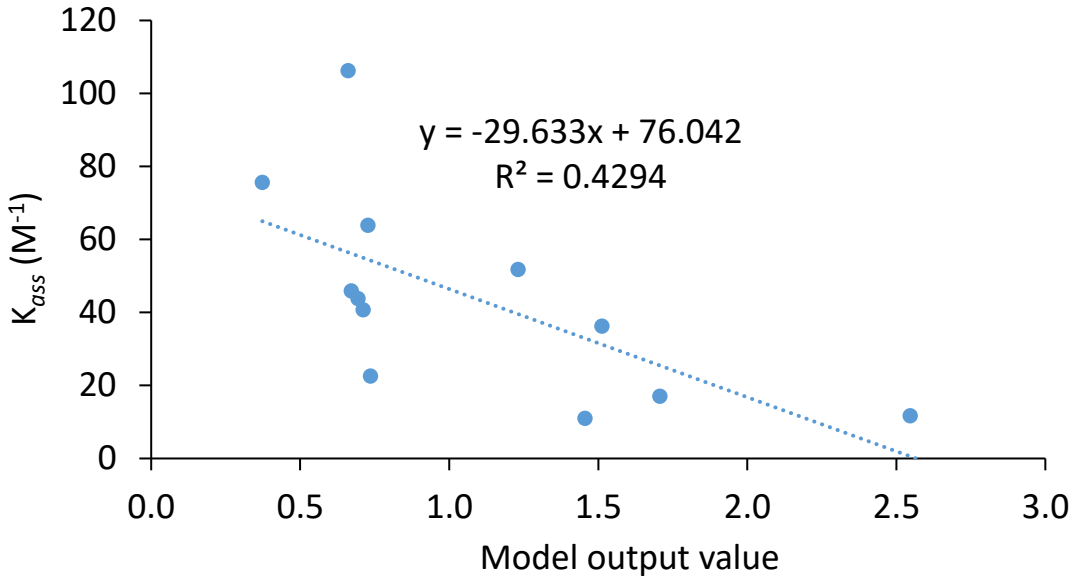

Figure S199: Model 9 vs K_{ass}. Model: P0 = P15 * $(P10)^{-1}$. Linear trend line: R^2 = 0.4294, intercept = 76.0419 and slope = -29.6332.

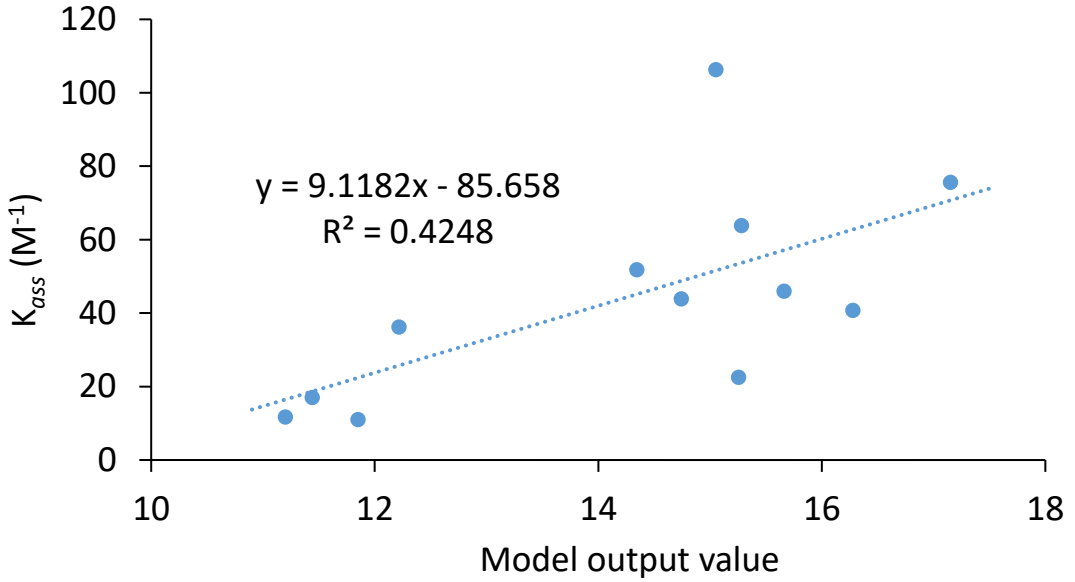

Figure S200: Model 10 vs K_{ass}. Model: P0 = P11 * $(P14)^{-1}$. Linear trend line: R^2 = 0.4248, intercept = -85.6579 and slope = 9.1182.

Table S47: Summary of the parameters and equations used within the top 10 models, identified through ranking of R^2 values, for the two parameter fits.

Parameter	Model Number										Total
	1	2	3	4	5	6	7	8	9	10	
R^2	0.4714	0.4710	0.4683	0.4468	0.4412	0.4406	0.4346	0.4333	0.4294	0.4248	
Equation	$P0 = P_X * P_y^{-1}$	$P0 = P_X * P_y$	$P0 = P_X * P_y$	$P0 = (P_X * P_y)^{-1}$	$P0 = P_X * (P_y)^{-1}$	$P0 = (P_X * P_y)^{-1}$	$P0 = P_X * (P_y)^{-1}$	$P0 = P_X * (P_y)^{-1}$	$P0 = P_X * (P_y)^{-1}$	$P0 = P_X * (P_y)^{-1}$	
Slope	-1.0380	-21.2774	-0.0506	1750.1617	-1726.9849	196.0087	30.7510	29.7500	-29.6332	9.1182	
Intercept	-8.9333	-30.0112	-10.9886	84.4793	167.8598	104.7600	-5.0338	8.1618	76.04120	-85.6579	
P_1			×								1
P_2											0
P_3											0
P_4											0
P_5											0
P_6											0
P_7											0
P_8											0
P_9											0
P_{10}	×	×	×	×		×	×	×	×		8
P_{11}	×			×	×					×	4
P_{12}											0
P_{13}											0
P_{14}		×			×	×				×	4
P_{15}								×	×		2
P_{16}											0
P_{17}											0
P_{18}							×				1
P_{19}											0

It can be seen that several fits are reciprocal e.g. Model 8 is 1/(Model 9); the gradients change sign as a result. This is understandable as, when fitting to a simplistic linear model, both linear and inverse fits will be found.

Three Parameter Fits

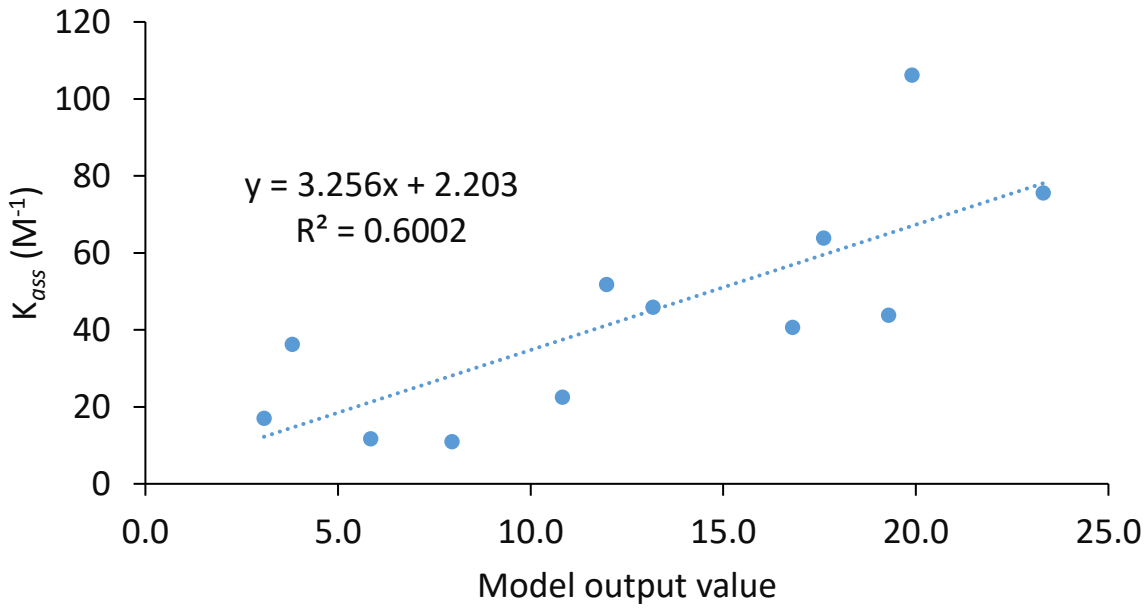

Figure S201: Model 11 vs K_{ass}. Model: P0 = P10 * P10 * $(P17)^{-1}$. Linear trend line: R^2 = 0.6002, intercept = 2.2030 and slope = 3.2560.

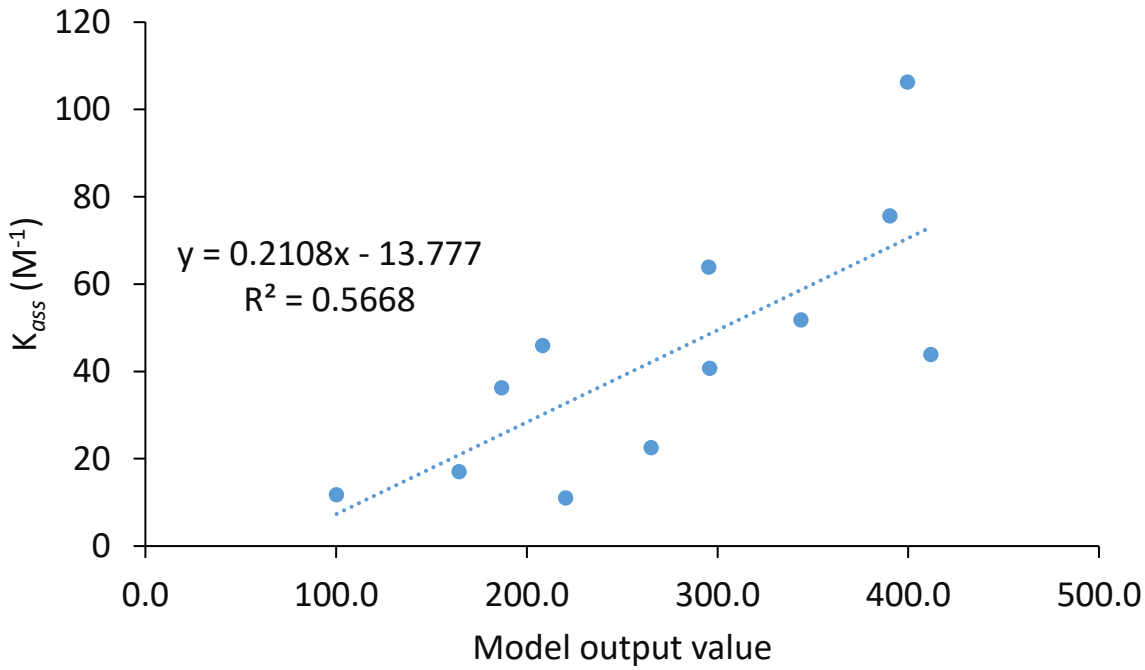

Figure S202: Model 12 vs K_{ass}. Model: P0 = P6 * P10 * $(P17)^{-1}$. Linear trend line: R^2 = 0.5668, intercept = -13.7771 and slope = 0.2108.

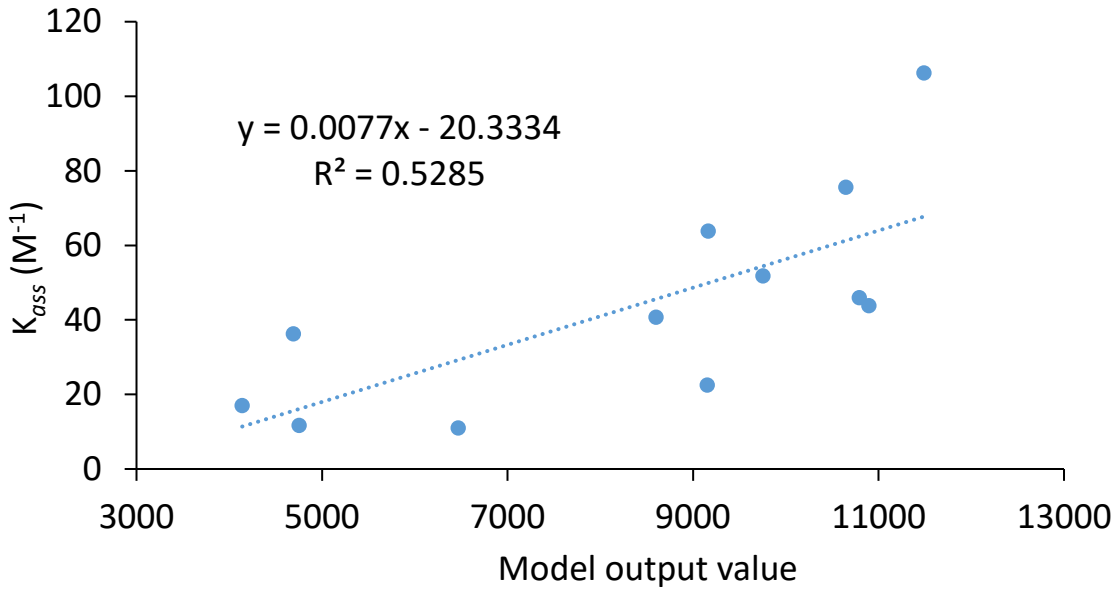

Figure S203: Model 13 vs K_{ass}. Model: P0 = P1 * P10 * P11. Linear trend line: R^2 = 0.5285, intercept = -20.3334 and slope = 0.0077.

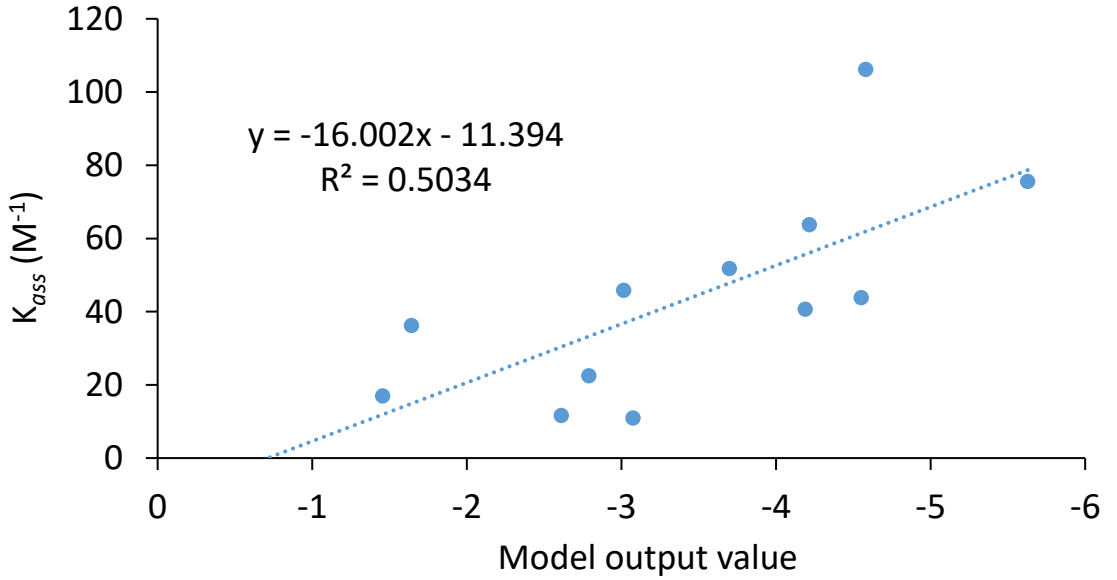

Figure S204: Model 14 vs K_{ass}. Model: P0 = P10 * (P14 * P17)$^{-1}$. Linear trend line: R^2 = 0.5034, intercept = -11.3939 and slope = -16.0023.

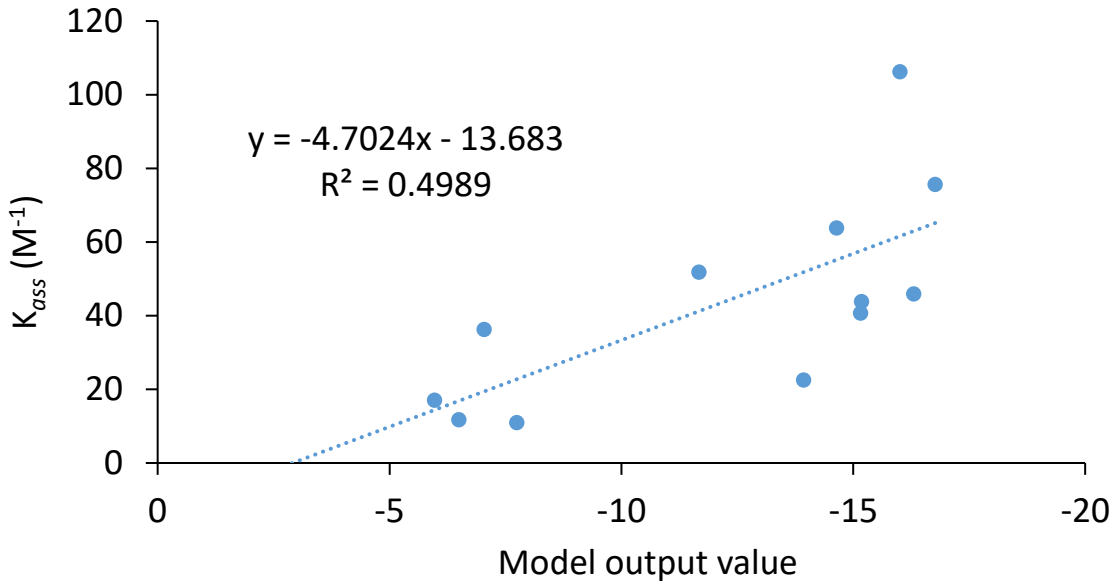

Figure S205: Model 15 vs K_{ass}. Model: P0 = P10 * P11 * $(P18)^{-1}$. Linear trend line: R^2 = 0.4989, intercept = -13.6827 and slope = -4.7024.

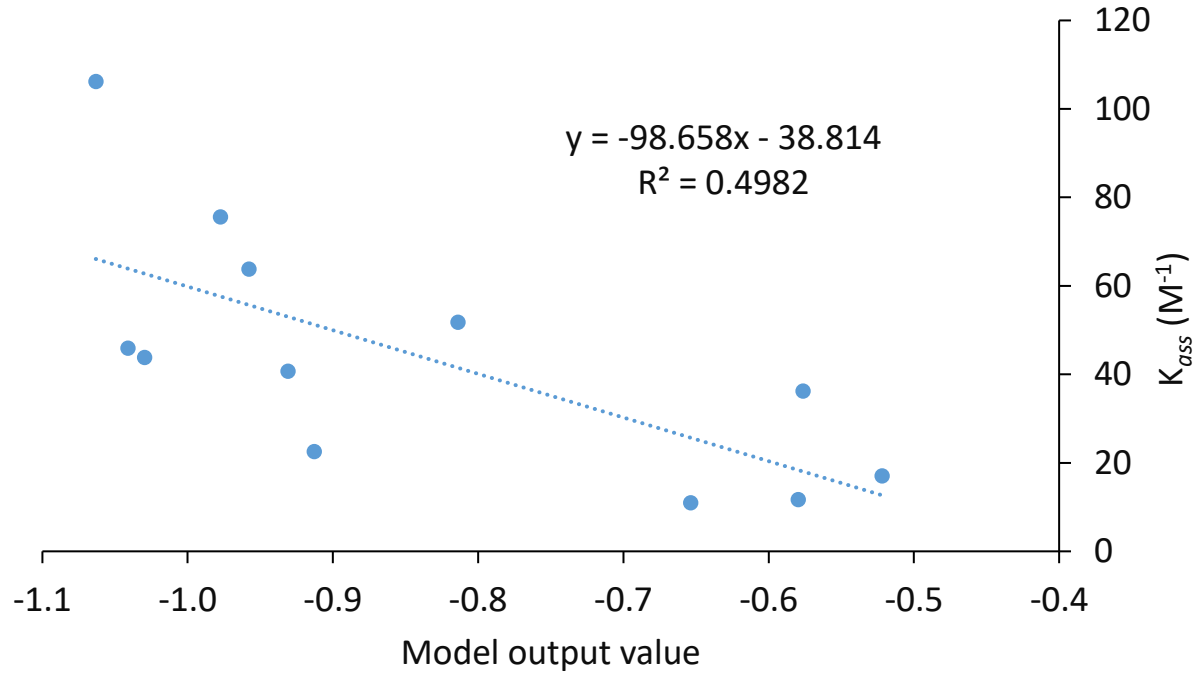

Figure S206: Model 16 vs K_{ass}. Model: P0 = P10 * P14 * $(P18)^{-1}$. Linear trend line: R^2 = 0.4982, intercept = -38.8140 and slope = -98.6581.

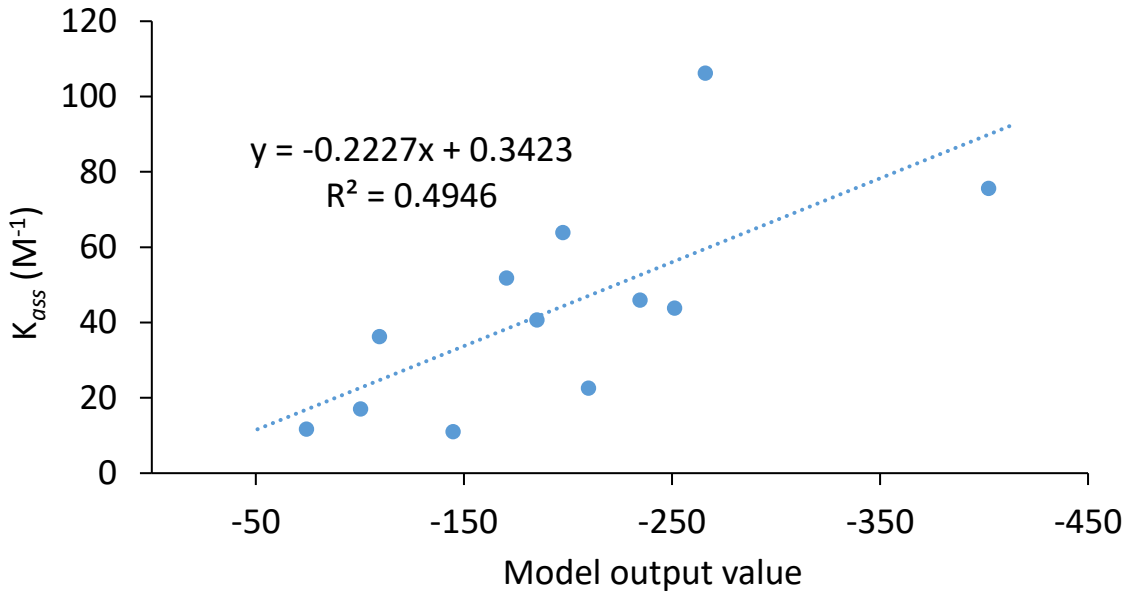

Figure S207: Model 17 vs K_{ass}. Model: P0 = P1 * P10 * $(P15)^{-1}$. Linear trend line: R^2 = 0.4946, intercept = 0.3424 and slope = -0.2227.

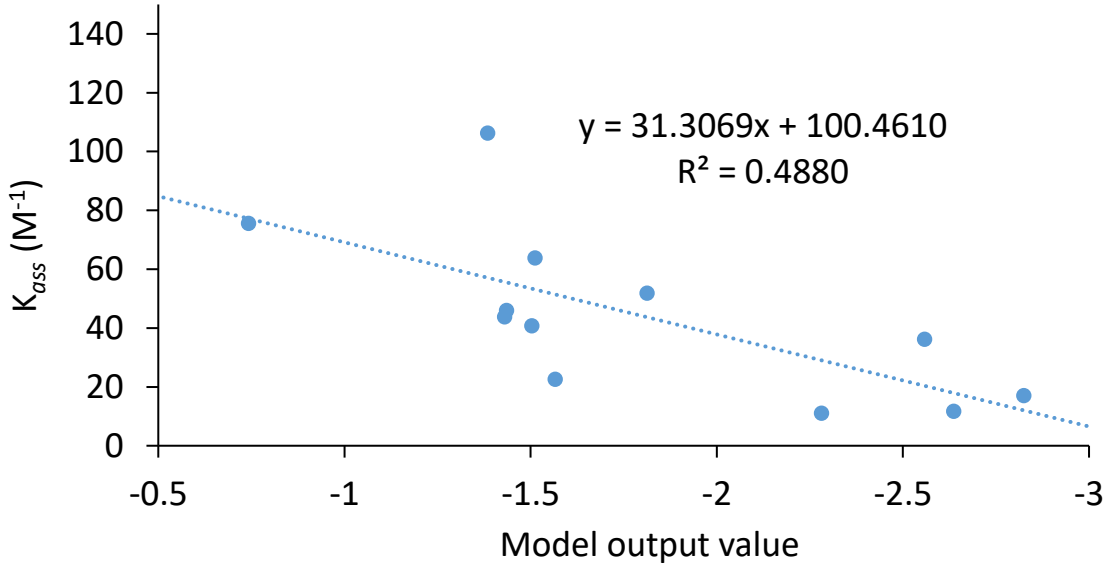

Figure S208: Model 18 vs K_{ass}. Model: P0 = P15 * $(P14 * P10)^{-1}$. Linear trend line: R^2 = 0.4880, intercept = 100.4610 and slope = 31.3069.

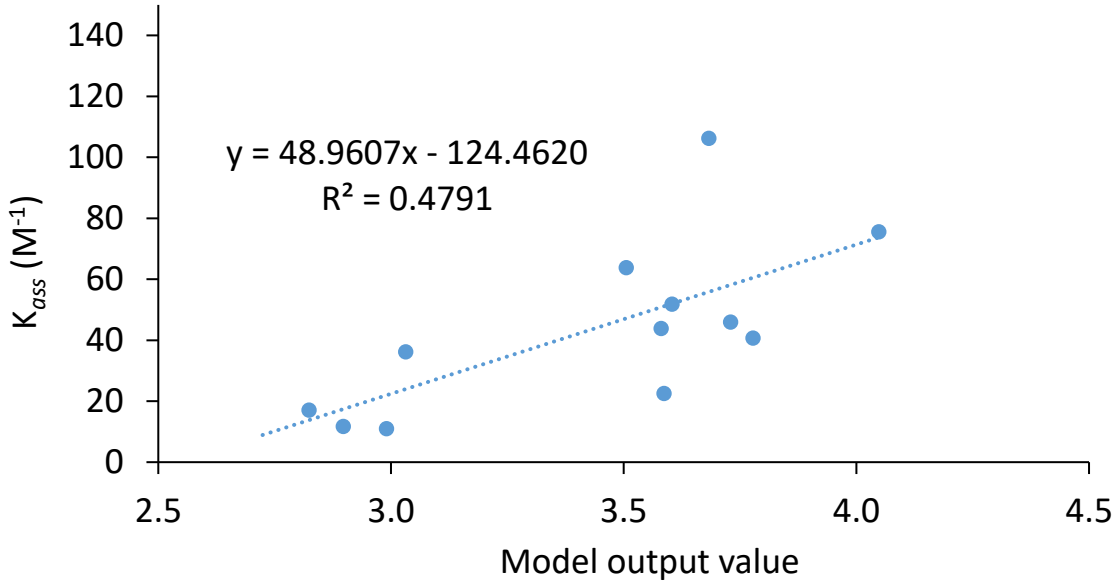

Figure S209: Model 19 vs K_{ass}. Model: P0 = P11 * (P14 * P18)$^{-1}$. Linear trend line: R^2 = 0.4791, intercept = -124.4620 and slope = 48.9607.

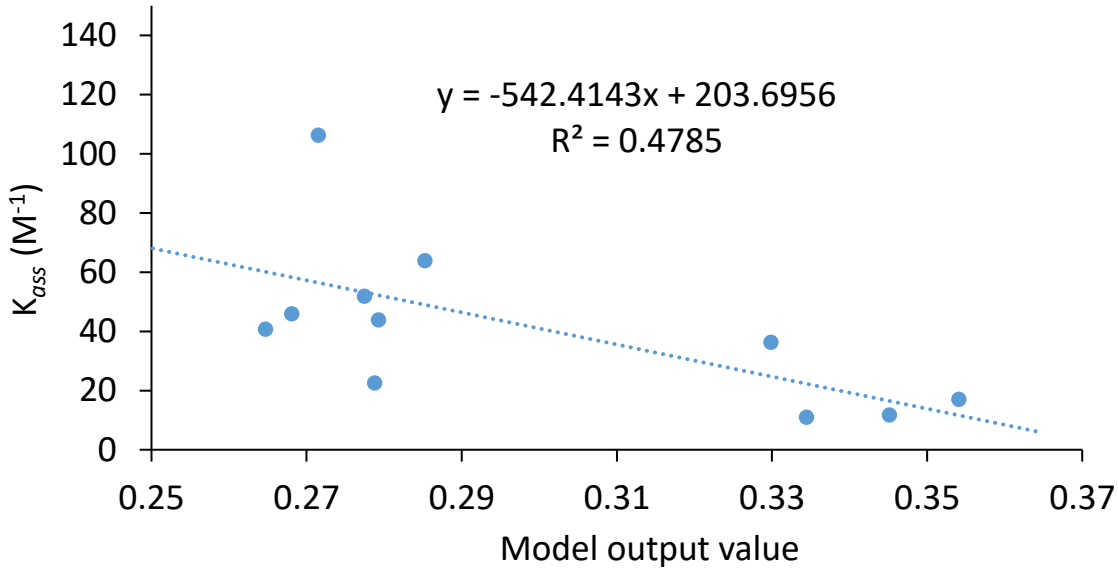

Figure S210: Model 20 vs K_{ass}. Model: P0 = P18 * P14 * (P11)$^{-1}$. Linear trend line: R^2 = 0.4785, intercept = 203.6956 and slope = -542.4144.

Table S48: Summary of the parameters and equations used within the top 10 models, identified through ranking of R^2 values, for the three parameter fits.

Parameter	Model Number										Total
	11	12	13	14	15	16	17	18	19	20	
R^2	0.6002	0.5667	0.5286	0.5034	0.4989	0.4982	0.4946	0.4880	0.4790	0.4785	
Equation	$P0 = P_X*P_X*(P_Y)^{-1}$	$P0 = P_X*P_Y*(P_Z)^{-1}$	$P0 = P_X*P_Y*P_Z$	$P0 = P_X*(P_Y*P_Z)^{-1}$	$P0 = P_X*P_Y*(P_Z)^{-1}$	$P0 = P_X*P_Y*(P_Z)^{-1}$	$P0 = P_X*P_Y*(P_Z)^{-1}$	$P0 = P_X*(P_Y*P_Z)^{-1}$	$P0 = P_X*(P_Y*P_Z)^{-1}$	$P0 = P_X*P_Y*(P_Z)^{-1}$	
Slope	3.2560	0.2108	-20.3334	-16.0023	-4.7024	-98.6581	-0.2227	31.3069	48.9607	-542.4140	
Intercept	2.2030	-13.7771	0.0077	-11.3939	-13.6827	-38.8140	0.3424	100.4610	-124.4620	203.6956	
P_1			×				×				2
P_2											0
P_3											0
P_4											0
P_5											0
P_6		×									1
P_7											0
P_8											0
P_9											0
P_{10}	××	×	×	×	×	×	×	×			9
P_{11}			×		×				×	×	4
P_{12}											0
P_{13}											0
P_{14}				×		×		×	×	×	5
P_{15}							×	×			2
P_{16}											0
P_{17}	×	x		×							3
P_{18}					×	×			×	×	4
P_{19}											0

Free energy contributions and Parametric fitting

The well-known relationship between free energy and equilibrium constant is given by:

$$\Delta G = -RT \ln K$$

As a result of this, additive contributions to free energy will have a multiplicative contribution to equilibrium constant. Thus for any given contribution to *K*, such that:

$$\text{Equation 1: } K_{ass} = P_x^a \times P_y^b$$

$$|a| + |b| = 2$$

$$\text{Equation 2: } K_{ass} = P_x^a \times P_y^b \times P_z^c$$

$$|a| + |b| + |c| = 3$$

It can be seen that:

$$\begin{aligned} \Delta G &= -RT \ln K \\ &= -RT \ln P_x - RT \ln P_y - RT \ln P_z \end{aligned}$$

Crucially, the same is true for any constants of proportionality required to relate a given parameter to the energetic contribution (*e.g.* charge and energy linked *via* Coulomb's law) as these give rise to constant contributions to energy and so do not affect the gradient of the correlation.

References

1. P. Job, *Anal. Chim. Appl.*, 1928, **9**, 113–203.

2 N. Busschaert, I. L. Kirby, S. Young, S. J. Coles, P. N. Horton, M. E. Light and P. A. Gale, *Angew. Chemie - Int. Ed.*, 2012, **51**, 4426–4430.

3 C. M. Chau, T. J. Chuan and K. M. Liu, *RSC Adv.*, 2014, **4**, 1276–1282.

4 S. M. S. Chauhan, B. Garg and T. Bisht, *Molecules*, 2007, **12**, 2458–2466.

5 Y. F. Chen, C. L. Kao, W. K. Lee, P. C. Huang, C. Y. Hsu and C. H. Kuei, *J. Chinese Chem. Soc.*, 2016, **63**, 751–757.

6 D. S. Panmand, A. D. Tiwari, S. S. Panda, J. C. M. Monbaliu, L. K. Beagle, A. M. Asiri, C. V. Stevens, P. J. Steel, C. D. Hall and A. R. Katritzky, *Tetrahedron Lett.*, 2014, **55**, 5898–5901.

7 H. Huang and J. Y. Kang, *Org. Lett.*, 2018, **20**, 4938–4941.

8 S. Feng, J. Li and J. Wei, *New J. Chem.*, 2017, **41**, 4743–4746.

9 D. V. Schoonover and H. W. Gibson, *Tetrahedron Lett.*, 2017, **58**, 242–244.

10 J. W. W. Chang, E. Y. Chia, C. L. L. Chai and J. Seayad, *Org. Biomol. Chem.*, 2012, **10**, 2289–2299.

11 T. Noji, H. Fujiwara, K. Okano and H. Tokuyama, *Org. Lett.*, 2013, **15**, 1946–1949.

12 N. Ortega, A. Feher-Voelger, M. Brovetto, J. I. Padrón, V. S. Martín and T. Martín, *Adv. Synth. Catal.*, 2011, **353**, 963–972.

13 J. Wang, Y. Zhao, W. Zhao, P. Wang and J. Li, *J. Carbohydr. Chem.*, 2017, **35**, 445–454.

14 C. A. Hunter, *Angew. Chem. Int. Ed*, 2004, **43**, 5310–5324.

15 J. J. P. Stewart, *J Mol Model*, 2007, **13**, 1173–1213.

16 Y. Zhao and D. G. Truhlar, *Theor. Chem. Acc.*, 2008, **120**, 215–241.

17 A. D. McLean and G. S. Chandler, *J. Chem. Phys.*, 1980, **72**, 5639–5648.

18 M. J. Frisch, G. W. Trucks, H. B. Schlegel, G. E. Scuseria, M. A. Robb, J. R. Cheeseman, G. Scalmani, V. Barone, G. A. Petersson, H. Nakatsuji, X. Li, M. Caricato, A. V. Marenich, J. Bloino, B. G. Janesko, R. Gomperts, B. Mennucci, H. P. Hratchian, J. V. Ortiz, A. F. Izmaylov, J. L. Sonnenberg, Williams, F. Ding, F. Lipparini, F. Egidi, J. Goings, B. Peng, A. Petrone, T. Henderson, D. Ranasinghe, V. G. Zakrzewski, J. Gao, N. Rega, G. Zheng, W. Liang, M. Hada, M. Ehara, K. Toyota, R. Fukuda, J. Hasegawa, M. Ishida, T. Nakajima, Y. Honda, O. Kitao, H. Nakai, T. Vreven, K. Throssell, J. A. Montgomery Jr., J. E. Peralta, F. Ogliaro, M. J. Bearpark, J. J. Heyd, E. N. Brothers, K. N. Kudin, V. N. Staroverov, T. A. Keith, R. Kobayashi, J. Normand, K. Raghavachari, A. P. Rendell, J. C. Burant, S. S. Iyengar, J. Tomasi, M. Cossi, J. M. Millam, M. Klene, C. Adamo, R. Cammi, J. W. Ochterski, R. L. Martin, K. Morokuma, O. Farkas, J. B. Foresman and D. J. Fox, Gaussian 16; Revision A.03; Gaussian Inc.; Wallingford CT; 2016.

19 M. Walker, A. J. A. Harvey, A. Sen and C. E. H. Dessent, *J. Phys. Chem. A*, 2013, **117**, 12590–12600.